US Army Corps
of Engineers ®

PDC TR-06-01 Rev 1
September 2008

U.S. ARMY CORPS OF ENGINEERS
PROTECTIVE DESIGN CENTER TECHNICAL REPORT

Methodology Manual for the Single-Degree-of-Freedom Blast Effects Design Spreadsheets (SBEDS)

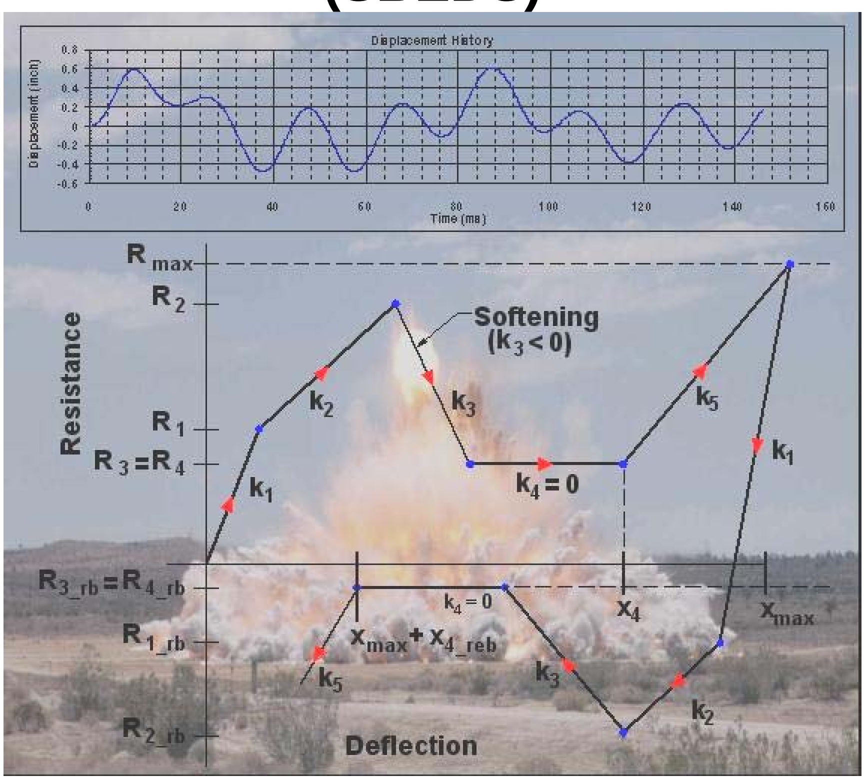

DISTRIBUTION STATEMENT A: Approved for Public Release; Distribution is unlimited.

Methodology Manual TOC

This page intentionally blank

FOREWORD

This document was prepared for the U.S. Army Corps of Engineers Protective Design Center by Protection Engineering Consultants, LLC (PEC) and Baker Engineering and Risk Consultants, Inc. (BakerRisk). PEC and BakerRisk made every reasonable effort to perform the work contained herein in a manner consistent with high professional standards.

The work was conducted on the basis of information made available to PEC and BakerRisk. Neither PEC, BakerRisk, nor any person acting on its behalf makes any warranty or representation, expressed or implied, with respect to the accuracy, completeness, or usefulness of this information. All observations, conclusions and recommendations contained herein are relevant only to the project, and should not be applied to any other facility or operation.

Any third party use of this Report or any information or conclusions contained therein shall be at the user's sole risk. Such use shall constitute an agreement by the user to release, defend and indemnify BakerRisk from and against any and all liability in connection therewith (including any liability for special, indirect, incidental or consequential damages), regardless of how such liability may arise.

PEC and BakerRisk regard the work that it has done as being advisory in nature. The responsibility for use and implementation of the conclusions and recommendations contained herein rests entirely with the client.

This information is furnished by the United States Government and is accepted and used by the recipient with the express understanding that the United States Government makes no warranties, expressed or implied, concerning the accuracy, completeness, reliability, usability, or suitability for any particular purpose of the information and data contained in this document, and the United States Government shall be under no liability whatsoever to any person by reason of any use made thereof.

Methodology Manual TOC

This page intentionally blank

CONTENTS

FIGURES

TABLES

CHAPTER 1 - INTRODUCTION

1-1 PURPOSE AND SCOPE

This Technical Report explains the methodology for the SBEDS workbook. The SBEDS workbook is an Excel-based tool for design of structural components subjected to dynamic loads using single degree of freedom (SDOF) methodology. It was developed by for the U.S. Army Corps of Engineers Protective Design Center as a tool for designers to use in satisfying Department of Defense (DoD) antiterrorism standards.

The SBEDS workbook is intended for structural engineers with some experience in structural dynamics and blast effects. It is not for the non-structural engineer. SBEDS is suited for preliminary design or final design when used by a skilled engineer. SBEDS will aid the engineer in design of the member, but the actual design of members and connections is the full responsibility of the engineer.

1-2 APPLICABILITY

The SBEDS workbook and the methodology in this report applies to new construction, major renovations, and leased buildings and must be utilized in accordance with the applicability requirements of UFC 4-010-01 *Minimum Antiterrorism Standards for Buildings* (UFC 4-010-01) or as directed by Service Guidance. See UFC 4-010-01 for additional detail on the structures that must be considered.

This page intentionally blank

CHAPTER 2 - FREE-FIELD AIRBLAST LOAD

2-1 GENERAL DISCUSSION OF EXPLOSIONS

Generally speaking, an explosion is a release of energy that occurs so rapidly that there is a local accumulation of energy at the site of the explosion. The accumulated energy dissipates violently through blast waves, propulsion of fragments, and thermal radiation. Explosions include detonation or deflagration of solid explosives and dust or vapor clouds, pressure vessel bursts, rapid electric energy discharge in a spark gap, rapid vaporization of a fine wire or thin metal strip, and molten metal contacting liquid. Depending on the configuration and location of the explosive source, the released energy may cause a pressure wave in air (airblast), groundshock, fragmentation, cratering, thermal radiation, or any combination of these effects. This manual focuses on airblast loading because SBEDS is intended primarily for determining structural component response to airblast loads. However, SBEDS can be used to determine response from any input dynamic load.

2-1.1 DEFLAGRATION VS. DETONATION

Deflagration and detonations are the two most common types of explosions. They differ primarily in the speed of the reaction process causing energy release. If the reaction speed is less than the speed of sound in the explosive material, the explosion is considered a deflagration. If the reaction speed is equal to, or greater than, the speed of sound in the explosive material, it is considered a detonation. High explosives, such as TNT and C4, are manufactured so that their reaction process will cause a detonation. Vapor and dust clouds, which are usually caused by accidental conditions that do not result an optimal fuel-air mixing and reactant proportions, typically deflagrate. The sudden release of energy from a detonation causes a “shock” wave, which is a pressure disturbance that propagates radially outward in all directions from the source and causes an immediate rise to peak pressure as it moves through surrounding air. A deflagration creates a “pressure” wave, which causes a more gradual rise to peak pressure as it moves through surrounding air and typically has a lower peak pressure than a shock wave from an equivalent energy release. In both cases the pressures are usually much larger than any hurricane or tornado pressures, but have total durations that are only hundreds or tenths of a second. The instantaneous rise time to a given peak pressure from a shock can cause significantly more damage to a structural component than the more gradual rise to the same peak pressure from a pressure wave.

In the far field, a process known as “shocking up” occurs to pressure waves, where the central and latter parts of the pressure wave move faster through air that is densified by the leading edge of the wave and “catch up” to the front of the wave to create a shock wave, where the peak pressure is applied nearly instantaneously. It is possible that blast pressures from the detonation and deflagration of explosive sources with equivalent energies can be almost the same in the far field, particularly if the reaction speed for the deflagration is near the speed of sound in the explosive material. Shocking up is a gradual process and the distance over which it occurs depends on a number of different variables (Baker et al 1983).

It is always conservative to treat an explosion as a detonation, particularly if it involves the rapid reaction of a solid material. For that reason, this methodology manual will focus on airblast pressures created by detonation of high explosives. Calculation of airblast loads from deflagrations is a more complicated process that is outside the scope of this manual (Baker et al 1983).

2-2 BLAST LOAD PARAMETERS

A shock wave creates a pressure pulse, or disturbance as it passes through a point in the atmosphere with characteristics that can be related to the detonated charge energy and the standoff distance from the center of the energy source to the point of interest. Figure 2-1 shows the idealized shape of a pressure pulse at a point caused by the shock wave from a high explosive detonation. The pressure pulse, or blast load shape, in Figure 2-1 shows that as the shock wave passes through the point of interest, the pressure at the point suddenly rises and then decays as the shock front moves past the point. Following this, there is a negative, suction pressure at the point with a much lower intensity, but longer duration, than the positive phase pressure. The blast load shape in Figure 2-1 is characterized by the parameters shown in the figure, where the impulse is the area under the pressure vs. time curve. The subscripts on these parameters refer to a side-on pressure pulse, which occurs in free-air (i.e. not on a building surface), but the shape of a pressure pulse applied to a building surface is generally very similar. The positive phase and negative phase peak pressures, impulses, and durations are typically determined from empirical relationships that are discussed in the next sections of this chapter.

Figure 2-1 Typical Pressure-Time History of an Airblast in Free Air

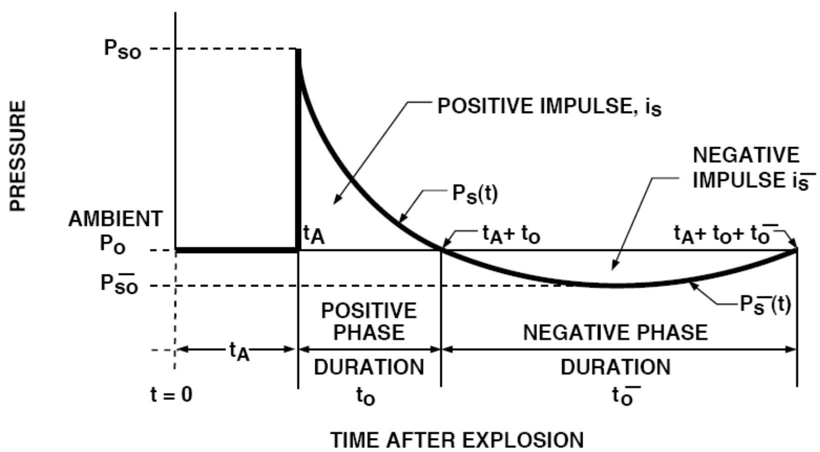

The shape of the positive phase blast load from an open air explosion in Figure 2-1 can be represented mathematically with Equation 2-1, which is known as the modified Friedlander equation. The decay coefficient θ can be determined from the integral of Equation 2-1 if the positive phase peak pressure and impulse are known. Blast loads inside confined areas, or near surrounding buildings that can reflect the blast load, will cause blast load histories with different shapes as discussed later in this manual. Figure 2-2 shows the approximate equation used in SBEDS to model the shape of the negative phase blast load (Granstrom, 1956), which has not been studied or understood as well as the positive phase. The integral of the negative phase blast load equation in Figure 2-2 sometimes differs from the impulse determined from available empirical prediction equations unless a correction term Cp^- is calculated and applied to the time variable, as stated in Equation 2-2. A number of trials have shown that Cp^- is usually within the range of 0.9 to 1.1.

Equation 2-1

$$P_s(t) = P_{so}\left[1 - \left(\frac{t - t_A}{t_o}\right)\right]e^{-\left(\frac{t - t_A}{\theta}\right)}$$

$$t_A \le t \le t_A + t_o$$

where: $P_s(t)$= shock overpressure as a function of time (MPa)
P_{so} = peak side-on overpressure (MPa)
t =detonation time (ms)
t_A = arrival time of initial shock front (ms)
t_o = positive phase duration (ms)
θ = shape constant of pressure waveform

Figure 2-2 Pressure History Shape Used in SBEDS for Negative Phase of Load

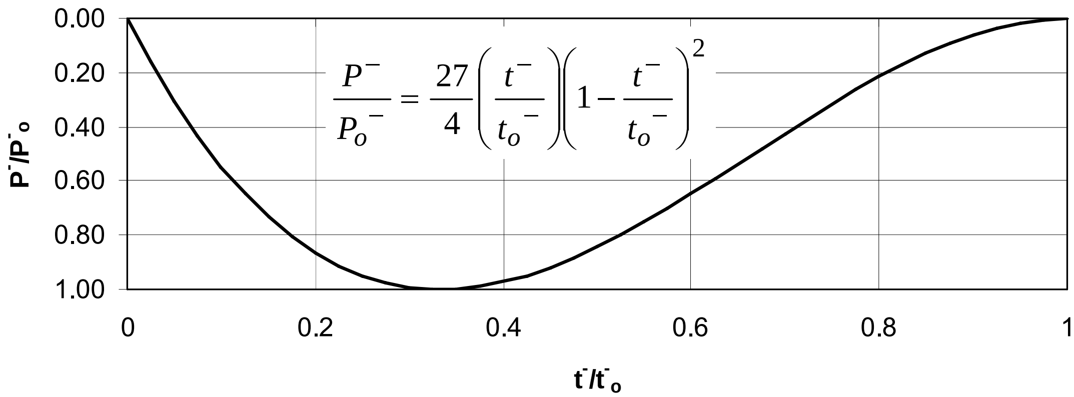

where: P^-_o = peak negative pressure
t^-_o = negative phase duration
t^- = corrected time after first negative pressure determined from Equation 2-2

Equation 2-2

$$t^- = t'^- \, Cp^-$$

$$Cp^- = \frac{i^-}{i'^-}$$

where: t'^- = time after first negative pressure
C_p^- = correction factor for time after first negative pressure preserving actual impulse i^-
i'^- = negative phase impulse calculated initially with integral of equation in Figure 2-2 with $t^- = t'^-$
i^- = actual negative phase impulse from empirical prediction method such as Figure 2-5 or Figure 2-9

Typically, the most important blast load parameters used to calculate the response of structural components to blast load are the positive phase peak pressure and impulse. The shape of the positive phase blast load in Figure 2-1 is often simplified for design or analysis purposes as a right triangle that preserves the same peak pressure and impulse and has a fictitious “equivalent” duration that is shorter than the actual duration. This blast load, which is illustrated in Figure 2-3, is a conservative simplification in that it will cause similar or somewhat more structural response than the actual blast load, depending on the ratio of the blast load duration to the natural period of the structural component. Note that fictitious duration t_d in Figure 2-3 is less than the actual positive blast load duration, t_o, in Figure 2-1.

Figure 2-3 Simplified Right Triangular Blast Pressure History for Positive Phase Blast Load

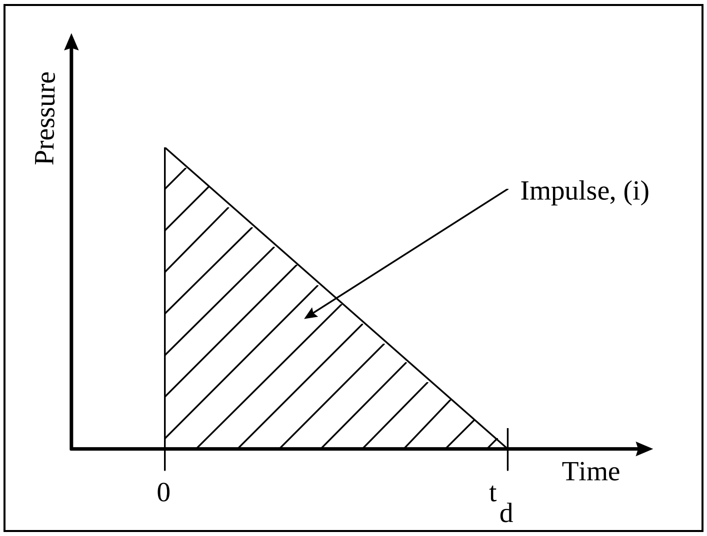

2-3 CUBE ROOT SCALING

Blast load parameters for unconfined, open-air explosions can be calculated from empirical curves based on Hopkinson (cube-root) scaling. Cube root scaling, which can be derived from dimensional analysis, generalizes the measured blast load parameters measured in a limited number of tests so that they can be used to predict blast load parameters for a wide range of geometrically similar charge weight and standoff configurations. According to cube-root scaling, blast load parameters in Figure 2-1 for two different explosion cases will be equal if the two cases are “geometrically similar”. For the simple case of two spherical or hemispherical charges of the same explosive type, the cases are geometrically similar if the two explosive charge radii are in the same proportion as the two standoff distances to the point of interest, so that the two cases have equal scaled standoffs as defined in Equation 2-3.

Note that the charge radius is proportional to the cube root of the charge mass. In this case, the blast load parameters with dimensions of pressure and velocity will be equal for both cases at the equal “scaled” times. The scaled time is time divided by the cube root of the charge mass (i.e., $t/W^{1/3}$). Therefore, the peak pressures at time zero will be equal for two explosion scenario cases with the same scaled standoffs and the pressure will decay to zero over different duration times t_0 for the two cases, where $t_0/W^{1/3}$ is the same for both cases. Blast parameters with units of time, such as duration, arrival time, and impulse are equal for two geometrically similar explosion cases (i.e., having the same scaled standoff) only in terms of their scaled values (i.e., $t/W^{1/3}$, $i/W^{1/3}$), rather than in absolute values of i and t.

Equation 2-3

$$\frac{R_1}{R_2} = \left(\frac{W_1}{W_2}\right)^{\frac{1}{3}} \quad or \quad Z_1 = Z_2 \quad where \quad Z = \frac{R}{W^{\frac{1}{3}}}$$

where: W_i = explosive mass (kg) for case i
R_i = standoff distance from detonation point of W_i (m)
Z_i = scaled standoff for case i

Cube-root scaling relationships have been proven experimentally for explosive masses ranging from several grams to tens of thousands of kilograms. Measured blast load parameters from a given type of explosion scenario, such as hemispherical or spherical TNT explosions, can be plotted in terms of the scaled standoff to measurement points and measured pressures, velocities, scaled blast load durations, and scaled blast load impulses at those points to create relatively simple plots in terms of scaled standoff distance and scaled blast parameters. The scaling relations apply when there are: (1) identical ambient conditions, (2) identical charge shapes, and (3) identical charge-to-surface geometries to those in the experiments used to develop the plots. However, reasonable values can be obtained using the scaling relations even when these conditions are not exactly the same.

2-4 PREDICTION EQUATIONS FOR BLAST LOAD PARAMETERS FROM A FREE-AIR BURST OF SPHERICAL TNT

Figure 2-4 through Figure 2-7 show relationships for a spherical free-air burst of TNT between the scaled standoff and parameters for the positive and negative phase blast load based on cube root scaling. These relationships are applicable when the energy from the explosive charge can expand spherically to the point of interest. Modified procedures to calculate blast loads from other high explosive types and charge geometries are described later in this chapter. The terms in Figure 2-4 through Figure 2-7 are defined in Figure 2-1 and Equation 2-1, except that L_w is the shock wavelength and U_s is the shock front velocity. Also, blast load parameters are shown in the figures for side-on (subscript "s_o") and reflected (subscript "r") blast loads. A side-on blast load is equal to the free-field blast load, which is the blast load at a point in the open. A higher reflected blast load is applied to a point on a rigid surface facing the explosive source. This is illustrated in Figure 2-8. Only the worst case of a "fully" reflected blast load caused by a shock wave that propagates normal to the surface with the point of interest is considered in this chapter. Other cases are considered in Chapter 3. All terms involving time, including impulse, are scaled by the cube root of the charge mass. Time and impulse values are equal to the scaled values from Figure 2-4 through Figure 2-7 multiplied by the cube root of the charge mass causing the blast load.

Figure 2-4 Positive Phase Shock Wave Parameters for a Spherical TNT Explosion in Free Air at Sea Level (Metric)

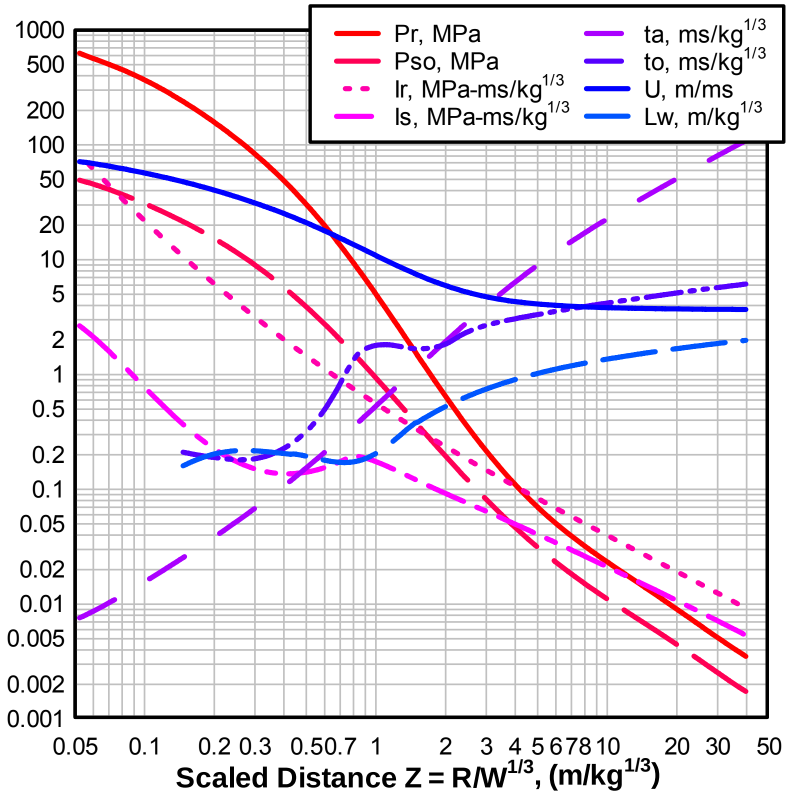

Figure 2-5 Positive Phase Shock Wave Parameters for a Spherical TNT Explosion in Free Air at Sea Level (English)

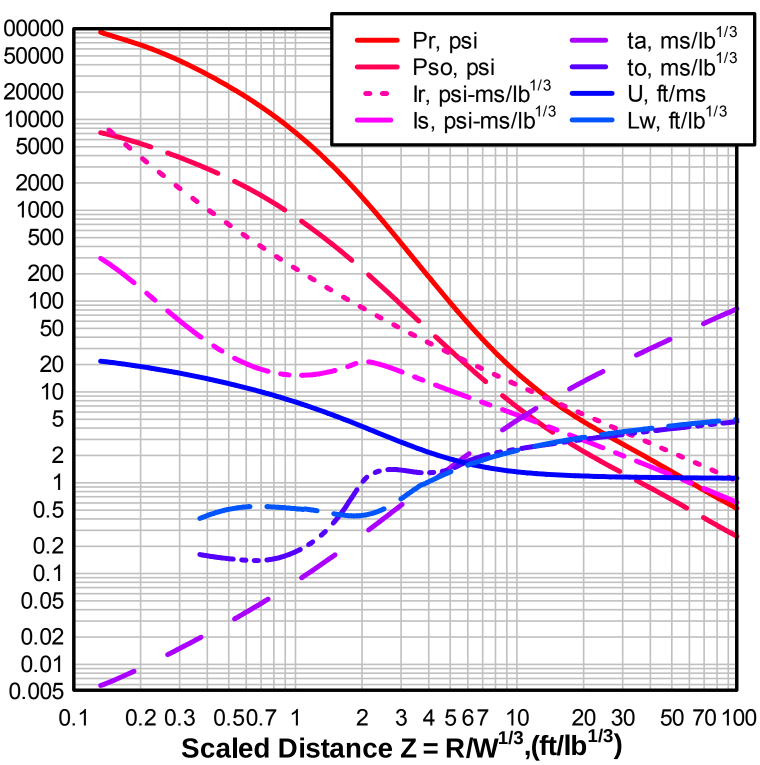

Methodology Manual TOC

Figure 2-6 Negative Phase Shock Wave Parameters for a Spherical TNT Explosion in Free Air at Sea Level (Metric)

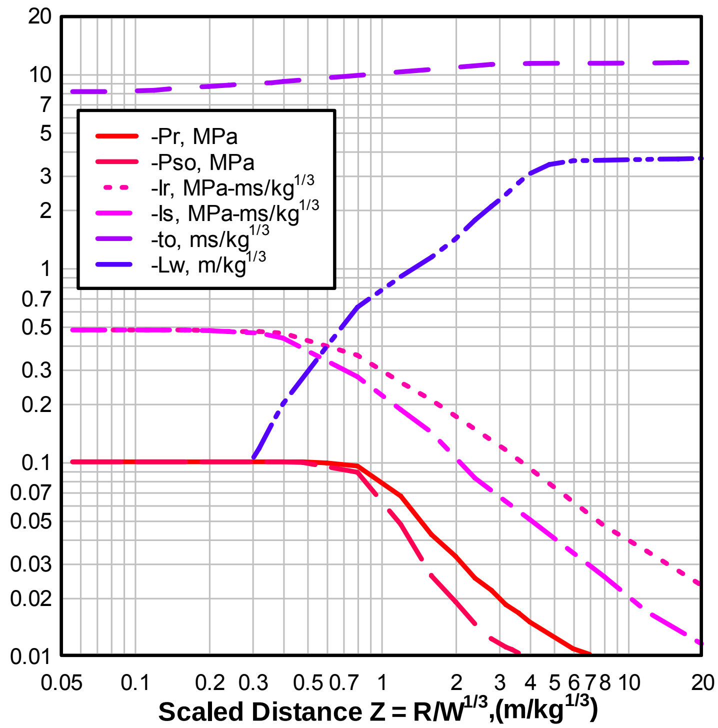

Figure 2-7 Negative Phase Shock Wave Parameters for a Spherical TNT Explosion in Free Air at Sea Level (English)

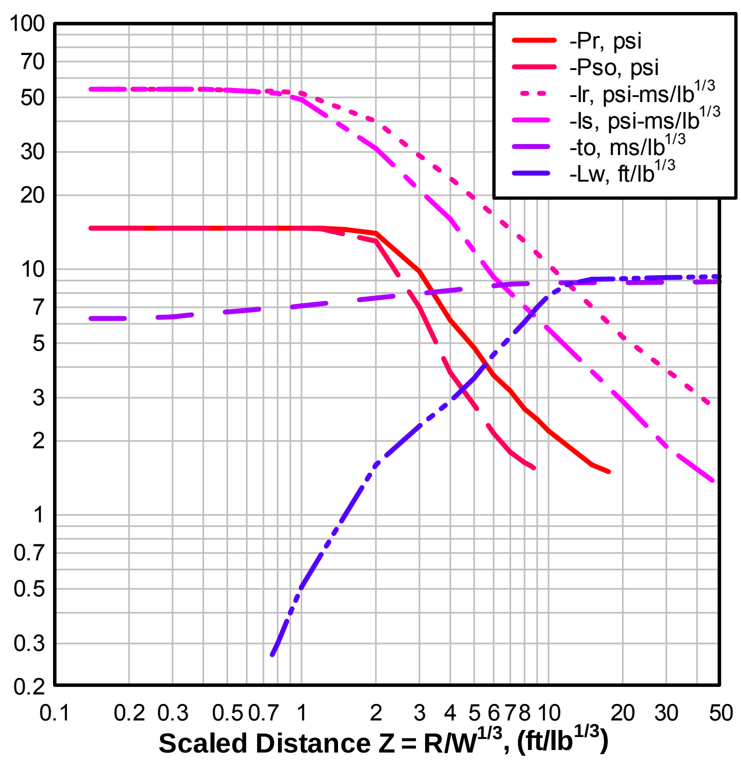

Figure 2-8 Typical Reflected and Side-on Pressure-Time Histories

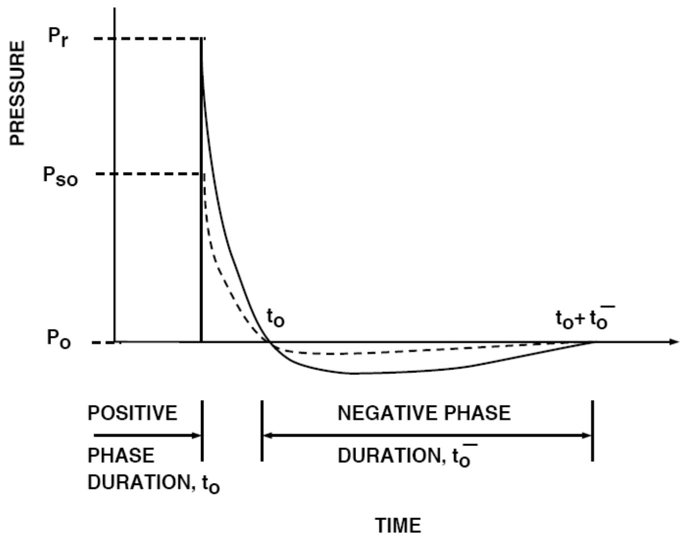

The general trends in Figure 2-4 and Figure 2-6 are that the pressure and impulse of the blast load decrease as the standoff increases and duration terms increase with increasing standoff distance. This is consistent with the fact that the energy in the shock wave dissipates as it propagates through a larger volume of air and is distributed over a longer wavelength. These figures apply for a spherical free-air burst, which is the simplest blast loading case and the basis of many tests. However, this case only applies when both the charge and the point of interest are “far” from any large surface that impedes blast wave propagation and prevent spherical expansion (other than a surface containing the point of interest). From a practical perspective, this means that the point of interest, which may be on a surface or in the free-field, must be significantly closer to the charge than to the ground or to any other surrounding building or walls. An example of this is an elevated explosion above a building roof with points of interest on the roof.

A more typical case is an explosion that occurs much nearer to the ground than to the point of interest, which may be a distant building. In this case the blast load consists of the pressure pulse for a free-air explosion of the charge mass plus the shock wave reflection off the ground, which also propagates to the point of interest. This is discussed further in the next section. Thus, the total blast load for most practical cases includes load from the shock wave reflection off the ground, and is therefore greater than the blast loads predicted for a free-air burst explosion.

2-5 SURFACE BURST FOR HEMISPHERICAL TNT

Figure 2-9 through Figure 2-12 show relationships between the scaled standoff and parameters for positive and negative phase blast loads for a hemispherical surface TNT detonation based on cube-root scaling. Modified procedures to calculate blast loads from other shapes and types of high explosive are described later in this chapter. The figures show parameters for side-on and fully reflected blast loads, as described in Section 2-4. Figure 2-9 through Figure 2-12 are applicable for a hemispherically shaped charge with the flat surface against the ground. In practice, however, they are

Methodology Manual TOC

used for charge masses with spherical shapes and other shapes at, or near the surface. The effect of non-hemispherical charge shape is discussed in Section 2-6.3.
Blast loads from a surface burst of a given charge mass are more intense than from a free-air explosion because the energy in the shock wave is confined by the ground surface so that, at any standoff distance, it only expands into one-half the volume as a free-air explosion (i.e., hemispherically instead of spherically). As a rough approximation based on test data, the blast loads from a surface burst with a given charge mass W are the same as those from a free-air explosion with a charge mass of 1.8W. The multiplication factor would be closer to 2.0 if the ground were perfectly rigid.

Figure 2-13 shows relationships between several other blast load parameters and the peak side-on blast pressure, which should be determined from Figure 2-4 or Figure 2-9 as applicable. Typically, it is conservative to use Figure 2-9. The dynamic pressure is the “wind” pressure from air particles accelerated by the shock wave. It dynamic pressure history can be approximated as having the same shape and duration as the positive shock pressure history and a peak pressure, q_s, from Figure 2-13. The dynamic pressure is included in the predicted reflected blast loads and it is included in the blast load after clearing of the reflected blast load, as discussed in Section 3-2. The dynamic pressure creates suction on components not facing the explosive source, similar to wind loads, and therefore reduces blast pressures on these components. This effect is usually secondary and is often ignored, although it is included in some cases as described in Section 3-4. The peak particle velocity and density of air particles caused by the shock wave is also shown in Figure 2-13.

Figure 2-9 Positive Phase Shock Wave Parameters for a Hemispherical Surface Burst of TNT at Sea Level (Metric)

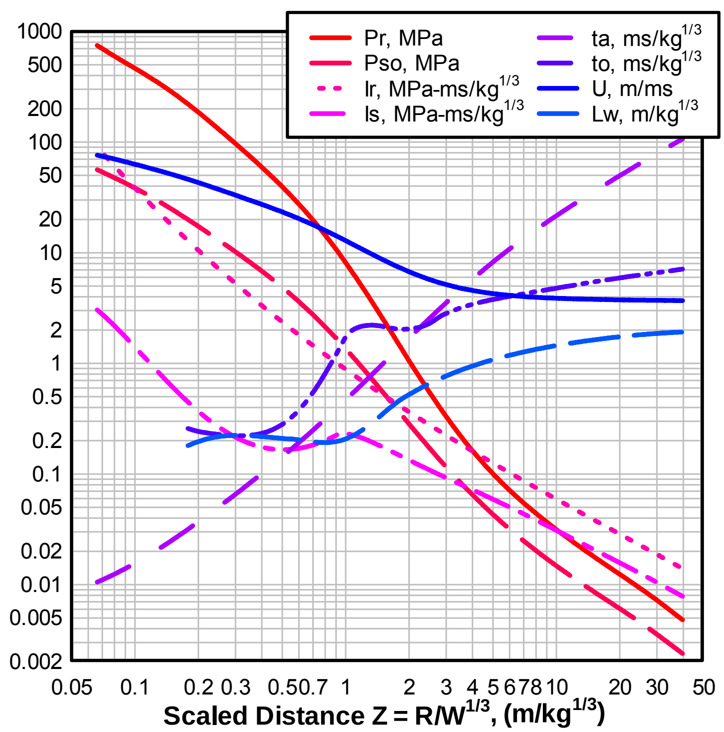

Methodology Manual TOC

Figure 2-10 Positive Phase Shock Wave Parameters for a Hemispherical Surface Burst of TNT at Sea Level (English)

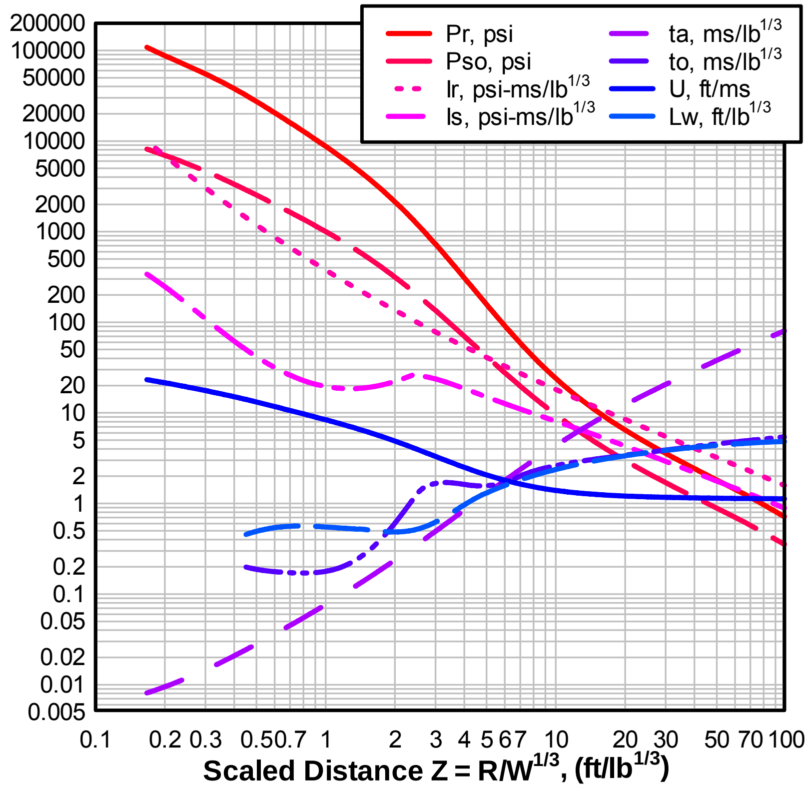

Figure 2-11 Negative Phase Shock Wave Parameters for a Hemispherical Surface Burst of TNT at Sea Level (Metric)

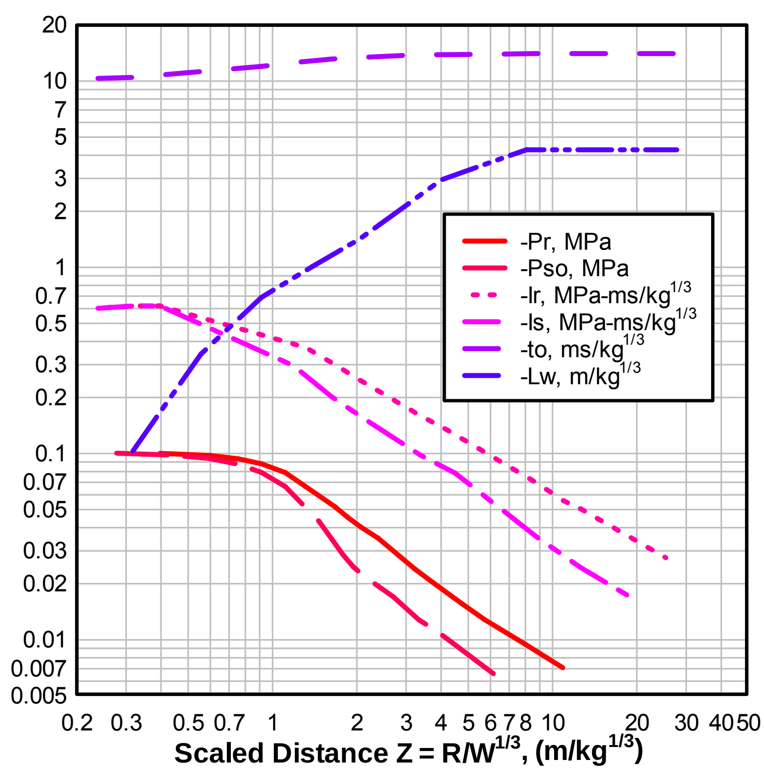

Methodology Manual TOC

Figure 2-12 Negative Phase Shock Wave Parameters for a Hemispherical Surface Burst of TNT at Sea Level (English)

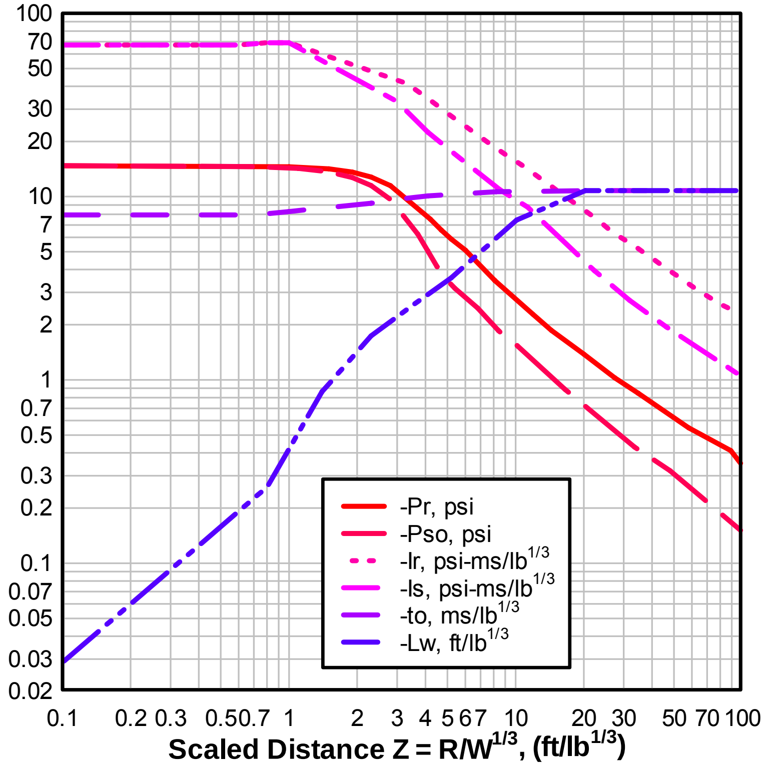

Figure 2-13 Peak Side-On Overpressure Versus Peak Dynamic Pressure, Density of Air Behind Shock Front, and Particle Velocity

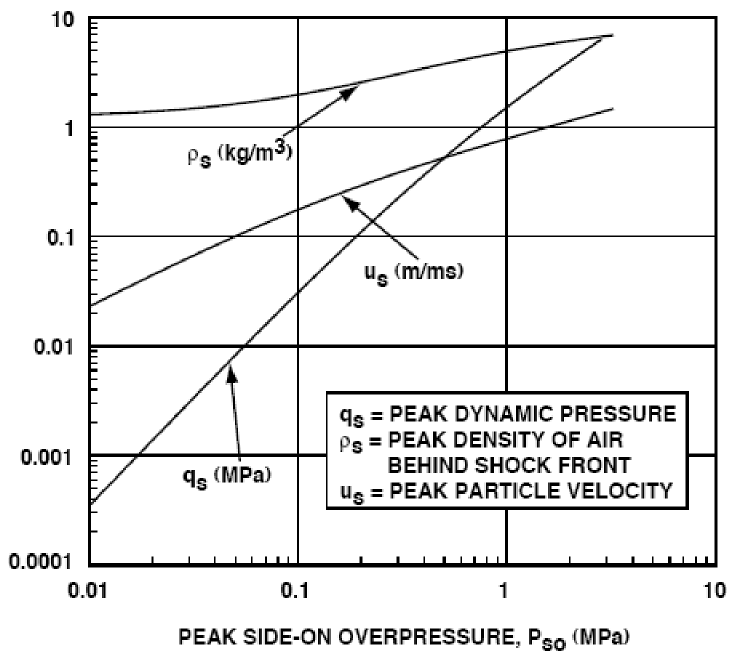

Methodology Manual TOC

2-5.1 NEAR SURFACE BURST

Figure 2-14 shows the case of a near surface explosion, where the height of burst H is small relative to the standoff to the points of interest on the building, R_G. In this case, both the incident shock wave (solid lines) and the ground reflection of the shock wave (dashed lines) propagate towards the building. It can be assumed simplistically that the shock wave's angle of reflection off the ground at each point is approximately equal to its angle of incidence, as for an elastic wave. The ground reflection wave moves through air that was densified by the incident shock wave, which allows it to travel faster than the incident shock wave, catch up to it, and merge to form a Mach front.

The Mach front includes the energy of both the incident and ground reflection and has essentially the same intensity as the shock wave from a surface burst, even though the charge exploded some distance above the surface. The height of the Mach front increases as the wave propagates away from the center of the detonation. The height of the triple point at radial distances from the explosive source is referred to as the path of the triple point and is formed by the intersection of the initial, reflected, and Mach waves as shown in Figure 2-14. The blast load from the Mach front below the triple point has a single pressure pulse, as shown in Figure 2-15. This figure also shows that the blast load above the triple point consists of two pressure pulses, one from the incident shock wave and one from the ground reflection, that superimpose in time. Figure 2-16 gives the scaled height of the triple point as a function of the scaled horizontal distance from the charge and the scaled charge height.

Figure 2-14 Mach Stem Effect from Near Surface Burst

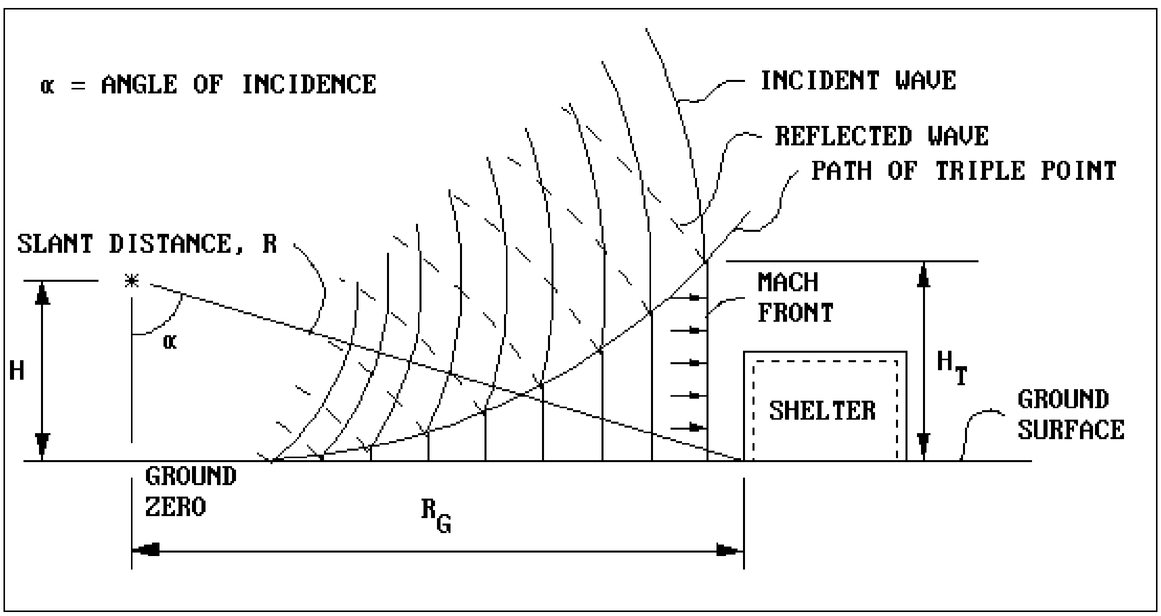

The near surface explosion in Figure 2-14 is the most common case for terrorist threats and accidental explosions. It is generally conservative to assume the blast load for this case is caused by the Mach front and equals that from a surface burst of the given charge mass. If the point of interest is above the triple point, the blast load will have less peak pressure and about the same impulse, so that it is a less severe case. If a detailed analysis of the blast load is merited, the BLASTX computer program (Britt et al, 2001) can be used to explicitly account for the ground reflection and calculate a multi-pulse blast load similar to Case b in Figure 2-15. Computational fluid dynamics (CFD) computer programs can also be used for this purpose.

Figure 2-15 Shock Profile Above and Below the Triple Point

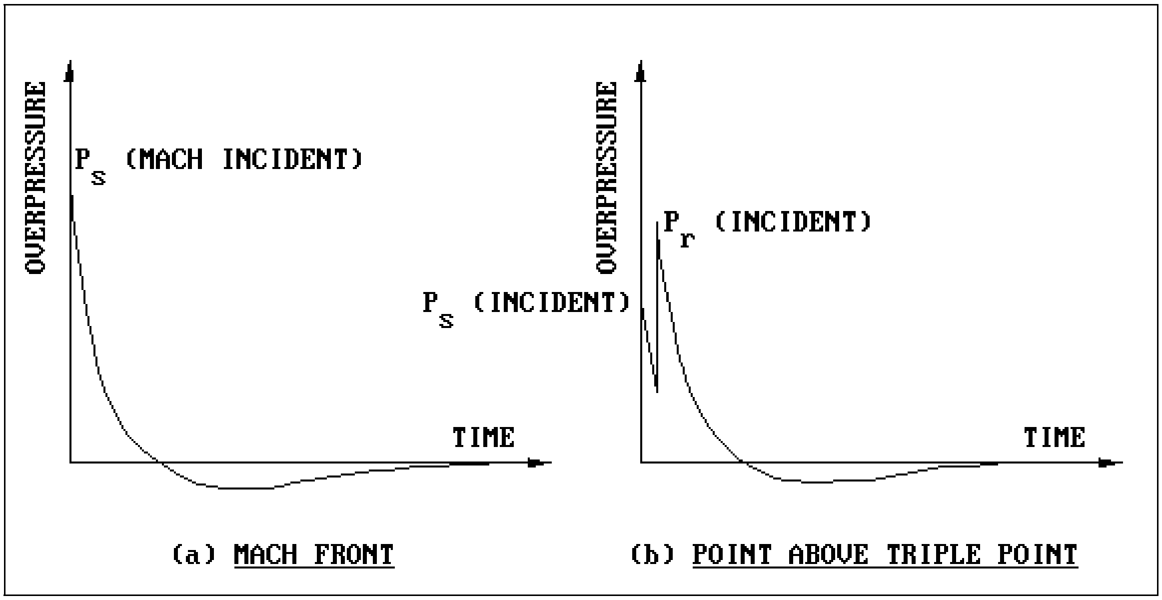

Figure 2-16 Scaled Height of Triple Point

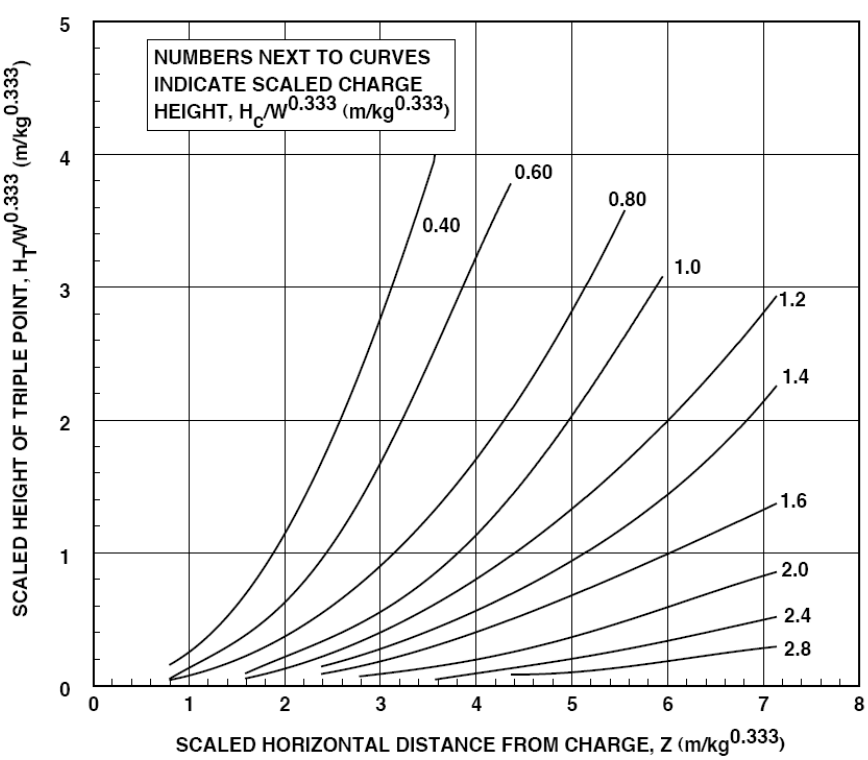

2-6 CHARGE MASS EQUIVALENCY FACTORS

The prediction methods to determine blast load parameters for TNT explosions presented previously in this chapter can be extended to include other explosives, charge shapes, and casing effects by multiplying the charge mass by an equivalency factor. This factor is equal to ratio of mass of the given explosive necessary to produce the same blast effects as a unit mass of bare spherical TNT for the same explosion conditions (i.e., free-air, surface burst, etc.) In general, the equivalency factor is not a constant for all blast parameters (such as peak pressure and impulse) and for all scaled distances from the explosion. Ideally, equivalency factors are determined by testing or based on factors determined from previous test results.

2-6.1 TNT EQUIVALENCY FACTOR FOR HIGH EXPLOSIVE TYPE

Equivalency factors that account for a different explosive material than TNT are generally referred to as TNT equivalency factors. The equivalent TNT mass for a given explosive is equal the actual mass multiplied by the TNT equivalency factor for the explosive. Table 2-1 and Table 2-2 show TNT equivalency factors for a wide range of different high explosive types. These values are based on testing in a free-air condition where the positive phase peak pressure and impulse were measured over a given range of scaled standoffs from the charge corresponding to the side-on peak pressure ranges shown in the tables. In practice, the values in Table 2-1 and Table 2-2 are usually applied to surface burst cases and to pressure ranges outside those shown in the table unless applicable test data for these cases is available.

As shown in Table 2-1 and Table 2-2, the TNT equivalency values for peak pressure and impulse are not always the same. This presents a potential problem since structural component response to blast load is generally sensitive to both the peak pressure and impulse and inaccurate response can be calculated if either value is incorrect. Fortunately, TNT equivalency values for peak pressure and impulse are almost always within 15%. In practice, the TNT equivalency factors for peak pressure and impulse are typically averaged and the average value applied to the charge mass. The resulting error is almost always within the range of other uncertainties associated with the blast load prediction methods.

If a large discrepancy exists between the TNT equivalency factors for peak pressure and impulse, an assessment can be made of whether the peak pressure or impulse has more affect on the structural response for which the blast load is calculated, and the TNT equivalency factor selected accordingly. In almost all cases of conventional, non-hardened construction, structural component response is more sensitive the impulse of the blast load than the peak pressure for loading by explosions outside the building. In this case, the TNT equivalency factor for the impulse would be used. The sensitivity of structural component response to the peak pressure and the impulse from a blast load is discussed more in Section 9-1. The TNT equivalency factor can be estimated from its heat of detonation relative to that of TNT, as shown in Equation 2-4, if the explosive is not listed in Table 2-1 and Table 2-2 and there is no available blast measurements that can be used to empirically determine the TNT equivalency factor.

Table 2-1 TNT Equivalency Factors for Free-Air Explosions

Explosive	Density Mg/m3	Equivalent Mass for Pressure	Equivalent Mass for Impulse	Pressure Range MPa
Amatol (50/50)	1.59	0.97	0.87	NA[1]
Ammonia Dynamite (50 percent Strength)	NA[1]	0.90	0.90[2]	NA[1]
Ammonia Dynamite (20 percent Strength)	NA[1]	0.70	0.70[2]	NA[1]
ANFO (94/6 Ammonium Nitrate/Fuel Oil)	NA[1]	0.87	0.87[2]	0.03 to 6.90
AFX-644	1.75	0.73[2]	0.73[2]	NA[1]
AFX-920	1.59	1.01[2]	1.01[2]	NA[1]
AFX-931	1.61	1.04[2]	1.04[2]	NA[1]
Composition A-3	1.65	1.09	1.07	0.03 to 0.35
Composition B	1.65	1.11 1.20	0.98 1.30	0.03 to 0.35 0.69 to 6.90
Composition C-3	1.60	1.05	1.09	NA[1]
Composition C-4	1.59	1.20 1.37	1.19 1.19	0.07 to 1.38 1.38 to 20.70
Cyclotol (75/25 RDX/TNT) (70/30) (60/40)	1.71 1.73 1.74	1.11 1.14 1.04	1.26 1.09 1.16	NA[1] 0.03 to 0.35 NA[1]
DATB	1.80	0.87	0.96	NA[1]
Explosive D	1.72	0.85[2]	0.81	0.01 to 0.30
Gelatin Dynamite (50 percent Strength)	NA[1]	0.80	0.80[2]	NA[1]
Gelatin Dynamite (20 percent Strength)	NA[1]	0.70	0.70[2]	NA[1]
H-6	1.76	1.38	1.15	0.03 to 0.70
HBX-1	1.76	1.17	1.16	0.03 to 0.14
HBX-3	1.85	1.14	0.97	0.03 to 0.17
HMX	NA[1]	1.25	1.25[2]	NA[1]
LX-14	NA[1]	1.80	1.80[2]	NA[1]
MINOL II	1.82	1.20	1.11	0.02 to 0.14
Nitrocellulose	1.65 to 1.70	0.50	0.50[2]	NA[1]
Nitroglycerine Dynamite (50 percent Strength)	NA[1]	0.90	0.90[2]	NA[1]
Nitroguanidine (NQ)	1.72	1.00	1.00[2]	NA[1]
Nitromethane	NA[1]	1.00	1.00[2]	NA[1]

[1]NA - Data not available. [2]Value is estimated.

Table 2-2 TNT Equivalency Factors for Free-Air Explosions (Continued)

Explosive	Density Mg/m3	Equivalent Mass for Pressure	Equivalent Mass for Impulse	Pressure Range MPa
Octol (75/25 HMX/TNT)	1.81	1.02	1.06	NA[1]
(70/30)	1.14	1.09	1.09[2]	0.01 to 0.30
PBX-9010	1.80	1.29	1.29[2]	0.03 to 0.21
PBX-9404	1.81	1.13	1.13[2]	0.03 to 0.69
		1.70	1.70	0.69 to 6.90
PBX-9502	1.89	1.00	1.00	NA[1]
PBXC-129	1.71	1.10	1.10[2]	NA[1]
PBXN-4	1.71	0.83	0.85	NA[1]
PBXN-107	1.64	1.05[2]	1.05[2]	NA[1]
PBXN-109	1.67	1.05[2]	1.05[2]	NA[1]
PBXW-9	NA[1]	1.30	1.30[2]	NA[1]
PBXW-125	1.80	1.02[2]	1.02[2]	NA[1]
Pentolite (Cast)	1.64	1.42	1.00	0.03 to 0.69
	1.68	1.38	1.14	0.03 to 4.14
	NA[1]	1.50	1.00	0.69 to 6.90
PETN	1.77	1.27	1.27[2]	0.03 to 0.69
Picrotol (52/48 Ex D/TNT)	1.63	0.90	0.93	0.03 to 4.10
RDX	NA[1]	1.10	1.10[2]	NA[1]
RDX/Wax (98/2)	1.92	1.16	1.16[2]	NA[1]
RDX/AL/Wax (74/21/5)	NA[1]	1.30	1.30[2]	NA[1]
TATB	NA[1]	1.00	1.00[2]	NA[1]
Tetryl	1.73	1.07	1.07[2]	0.02 to 0.14
Tetrytol (75/25 Tetryl/TNT)	1.59	1.06	1.06[2]	NA[1]
TNETB	1.69	1.13	0.96	0.03 to 0.69
TNETB/AL (90/10)	1.75	1.23	1.11	0.03 to 0.69
(78/22)	1.18	1.32	1.32[2]	NA[1]
(65/35)	1.23	1.38	1.38[2]	NA[1]
TNT	1.63	1.00	1.00	Standard
Torpex	1.85	1.23	1.28	0.01 to 0.30
Tritonal (80/20 TNT/AL)	1.72	1.07	0.96	0.03 to 0.69

[1]NA - Data not available. [2]Value is estimated.

Equation 2-4

$$W_E = \left[\frac{H^d_{EXP}}{H^d_{TNT}}\right] W_{EXP}$$

where: W_E = equivalent TNT mass of explosive in question (kg)
W_{EXP} = mass of the explosive in question (kg)
H^d_{TNT} = heat of detonation of TNT (MJ/kg)
H^d_{EXP} = heat of detonation of explosive in question (MJ/kg)

2-6.2 EQUIVALENCY FACTOR FOR CASED EXPLOSIVES

Experimental data indicate that the blast parameters of cased high-explosive (HE) charges are significantly different from those determined for bare charges. Most of the effects due to casing remain unexplained and have not been reduced to a working functional form. Variables that can influence the blast are: (1) case mass, (2) case material properties such as toughness and density, (3) case thickness, and (4) explosive properties such as detonation velocity and density. With such a large number of variables, assumptions have been made by various investigators to simplify calculations. One approach is to assume that the casing mass is the only variable significantly contributing to the blast parameters other than charge mass and standoff. Equation 2-5 shows an empirical equation for steel cased charges that determines an equivalent bare charge mass, W', that can be multiplied by any applicable equivalency factors and used to predict blast load parameters.

Equation 2-5

$$W' = \left[.2 + \frac{.8}{\left(1 + \frac{m_c}{W}\right)}\right] W$$

where: W' = equivalent bare charge mass (kg)
W = mass of charge inside casing (kg)
m_c = mass of casing (kg)

Figure 2-17 is a plot of Equation 2-5, with experimental data plotted as points. The plot shows considerable scatter between Equation 2-5 and the experimental data, especially for materials other than steel. The legend in Figure 2-17 indicates that a variety of materials were used as casings, and W´ is generally greater than W. All casing materials were highly brittle or were held together with a brittle matrix material. Equation 2-5 is not recommended for GP bombs, since data shows that peak pressure and impulse from these weapons correlates better when no casing effects are considered.

Figure 2-17 Equivalent Experimental Charge Masses for Various Casing Materials

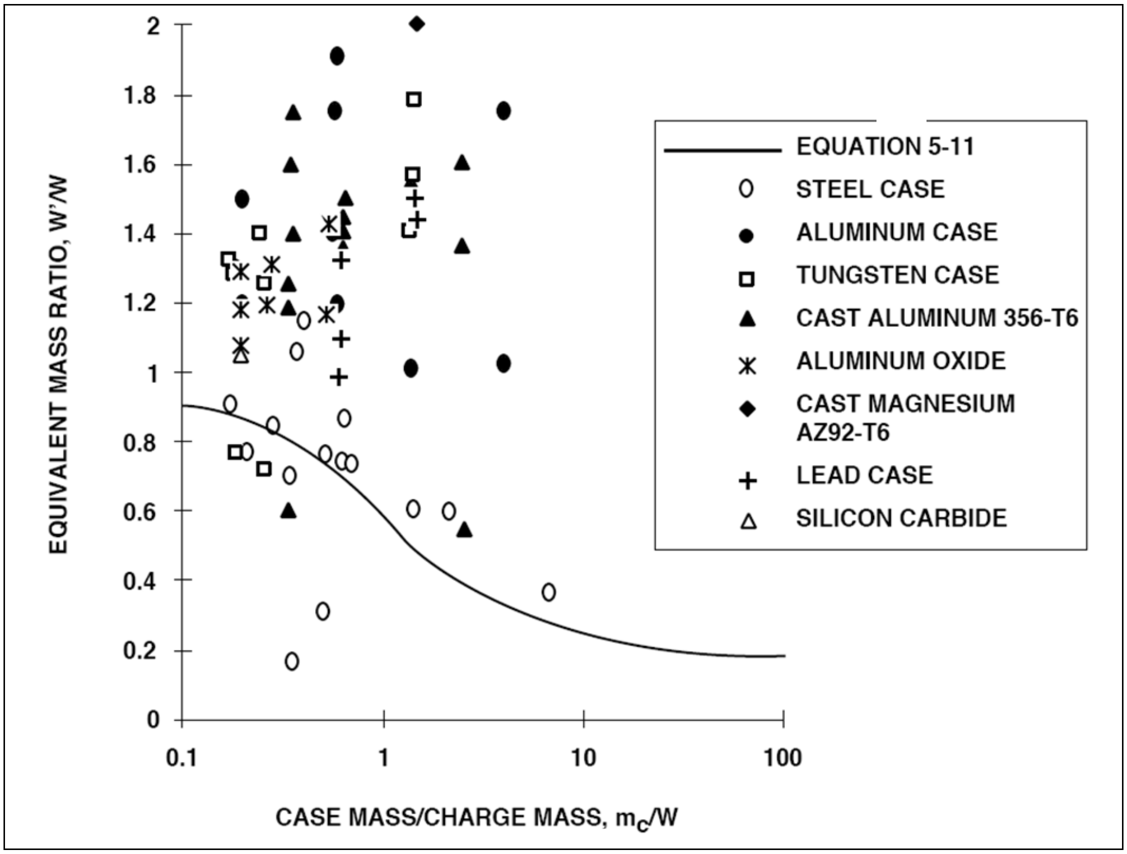

2-6.3 **NON-HEMISPHERICAL CHARGE GEOMETRY**

Numerous experimental measurements have been obtained on airblast from cylindrical charges detonated in free-air from Composition B cylinders with L/D from 1/4 to 10/1 and peak side-on overpressure from 0.014 to 0.690 MPa. The data can be curve fit to an equation of the form shown in Equation 2-6. Curve-fits are shown in Chapter 5 of UFC 3-340-01 for a variety of L/D ratios and for free-air and surface burst detonations. These curve-fits show that blast loads along the azimuth angles defined in Figure 2-18 that are perpendicular to the long dimension of the cylindrical charge have significantly greater blast loads than blast loads along other azimuth angles for scaled standoffs up to approximately 5.0 m/kg$^{1/3}$ (12 ft/lb$^{1/3}$). Therefore, cylindrical charges with L/D < 1 (i.e., disk-shaped charges) cause the highest blast loads at azimuth angles of 0 and 180 degrees (as defined in Figure 2-18), while charges with L/D > 1 cause the highest blast loads at azimuth angles near 90 degrees.

Equation 2-6

$$P_{SO} = f(Z, L/D, \theta)$$

where:

P_{so} = peak side-on overpressure
Z =scaled radial standoff from the cylinder
L/D = cylinder length-to-diameter ratio
θ= azimuth angle (Figure 2-18)

Figure 2-18 Azimuth Angles, θ, For Blast Relative to Longitudinal Axis of Cylindrical Shaped Charge (Initiation Point at θ= 0)

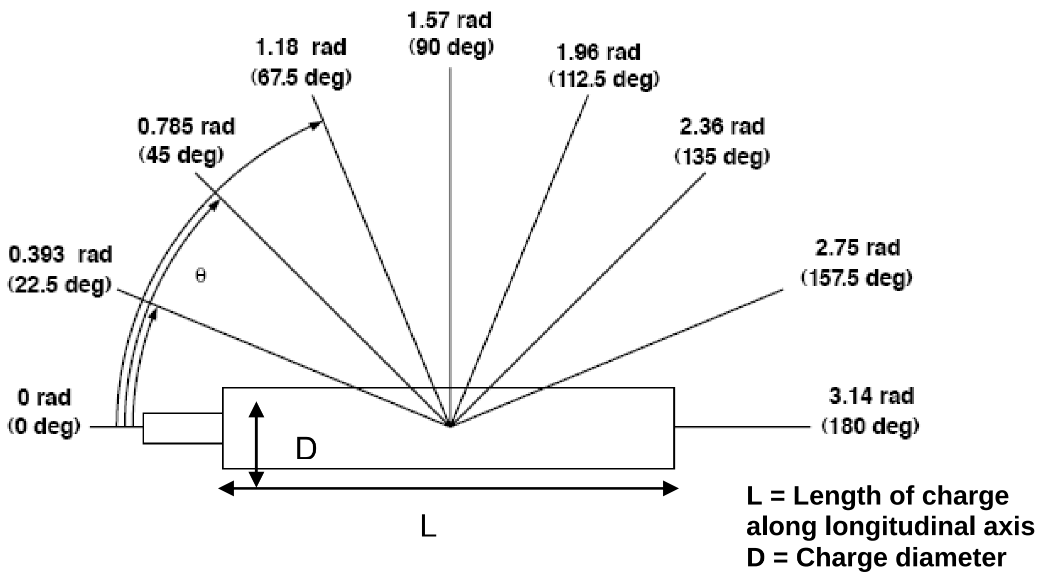

Figure 2-19 Peak Pressure at 0, 90, 180 Degree Azimuth Angles from Cylindrical Charge with L/D=5

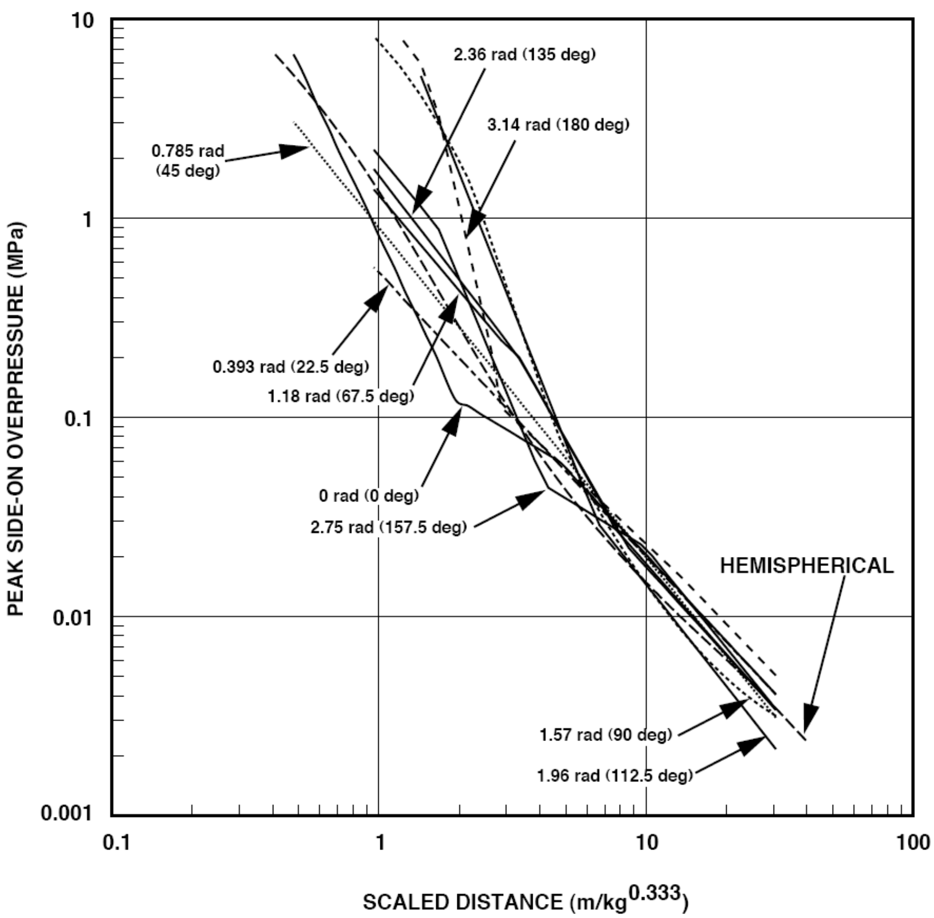

Figure 2-20 Impulse at 0, 90, 180 Degree Azimuth Angles from Cylindrical Charge with L/D=5

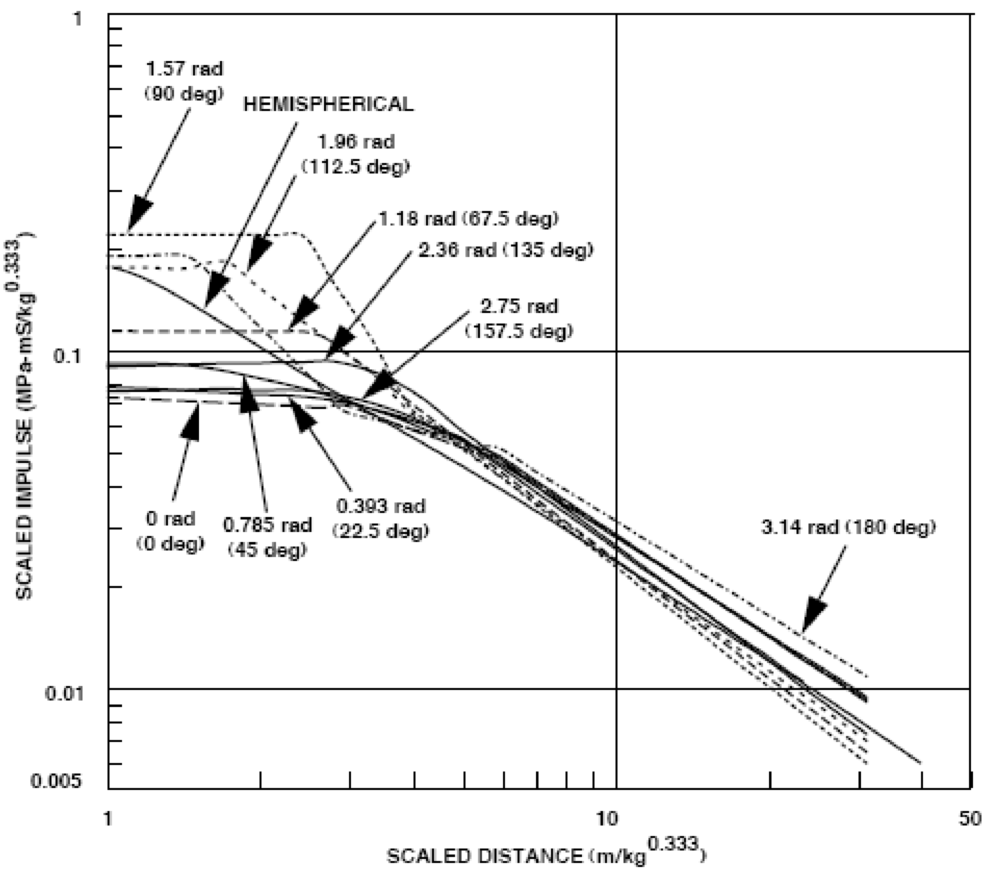

At scaled standoffs greater than 5.0 m/kg$^{1/3}$, the blast loads from a cylindrical charge are relatively equal at all azimuth angles to the blast loads from a spherical or hemispherical shaped charge of equal mass. Figure 2-19 and Figure 2-20 show the magnitudes of positive phase peak pressure and scaled impulse from the surface burst of a long cylindrical charge with L/D=5 relative to those from a hemispherical surface burst. The BLASTX computer program (Britt et al, 2001) can also be used to calculate the blast loads from cylindrical high explosive charges.

2-7 CONFINED DETONATIONS

A detonation within a structure produces shock and quasistatic blast loads. Shock loads are caused by the shock wave as it reverberates within the structure and gas, or quasistatic pressure loads, are caused by confinement of the heat and products of the detonation by the surrounding structure. The shock loads, $P_r(t)$, include the initial incident wave and the reflections from adjacent surfaces. The gas pressure, $P_g(t)$, rises relatively quickly to a peak value and then decays relatively slowly based on the amount of venting of the confined gases to the atmosphere allowed by the surrounding structure. This is illustrated in Figure 2-21.

The airblast pulses from a reverberating shock wave can be predicted using the image charge method, where the pulse from the shock wave reflection off each surface of the room is equal to the pressure pulse from a spherical free-air burst of an “image” charge with the same weight as the actual charge, located at a standoff from the point of interest equal to the full path length of the shock wave to the reflecting wall and then to the point of interest (such as paths B and C in Figure 2-21), impacting the point of interest with an angle of incidence equal to that of the reflected wave. The calculated pressure pulses from all surfaces can be linearly superimposed in time as a first approximation, or they can be combined more accurately using non-linear superposition laws based on computational fluid dynamics principles such as the LAMB nonlinear shock wave addition equations (Needam and Wittwer, 1977).

Figure 2-21 Blast Pressure From Confined Explosion

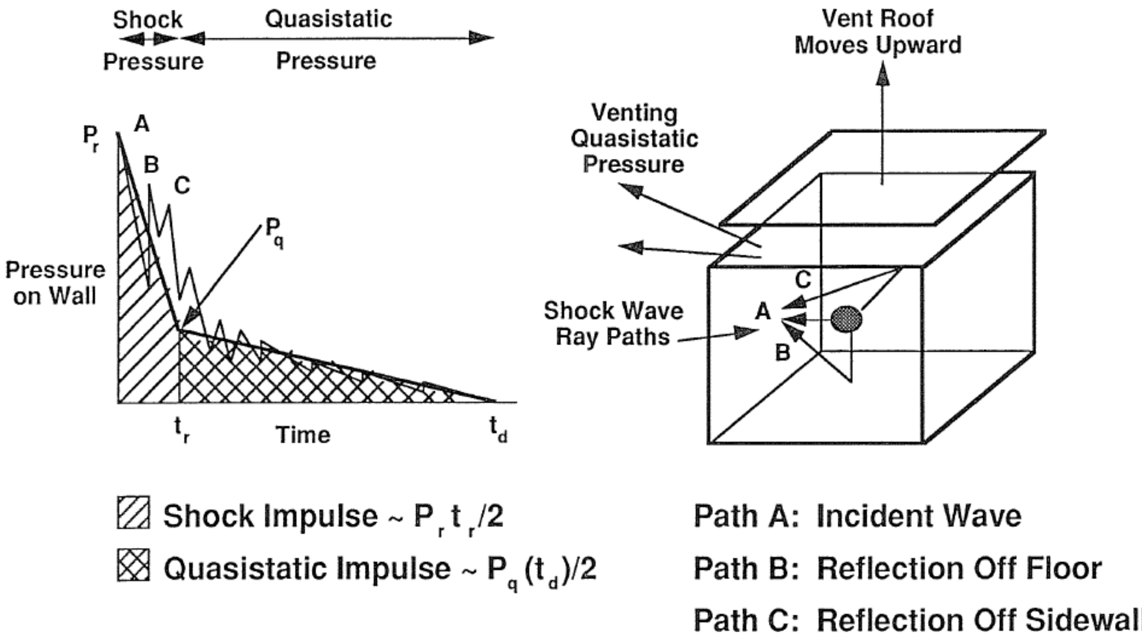

The peak quasistatic pressure is primarily a function of the charge weight relative to the confined volume. Simplistically, the rise time to peak quasistatic pressure is often assumed to coincide with the duration of the shock pulses, so that there is a direct transition from shock loading to the peak quasistatic pressure. The duration of the gas pressure load is a function of the vent area, including open vent areas and vent area covered by frangible surfaces failed by the blast loading during the duration of the quasistatic pressure. The decay time of the quasistatic pressure can be very long relative to the blast load from the shock wave.

The relative importance of the shock and quasistatic parts of an internal blast load depends on many factors and may not be apparent until a complete response analysis is performed. For example, even though the peak gas pressure may be much lower than the peak shock pressure, the gas pressure impulse could be many times greater than the shock impulse and could control the response of a structural component of interest. Therefore, both loadings must be considered when evaluating the effects of an internal explosion. Detailed discussion of methods to determine confined blast loads is outside the scope of this manual. This discussion is provided in UFC 3-340-01, TM 5-1300, and DOE/TIC 11628.

2-8 BLAST WALLS AND REVETMENTS

In general, blast walls and revetments are only effective for reducing blast loads in the immediate vicinity behind the wall or revetment (i.e., within one or two wall or revetment heights). They are much more effective at stopping fragments. Figure 2-22 shows the process by which a blast wave propagates above and around a wall, which involves a turbulent area of vortices immediately behind the wall. The shock wave “fills in” the area behind the wall in a relatively efficient manner so that pressure reduction only occurs over a limited area behind the wall. More detailed methods to calculate the blast load behind a wall are discussed in UFC 3-340-01.

Figure 2-22 Wave Diffraction Around Walls

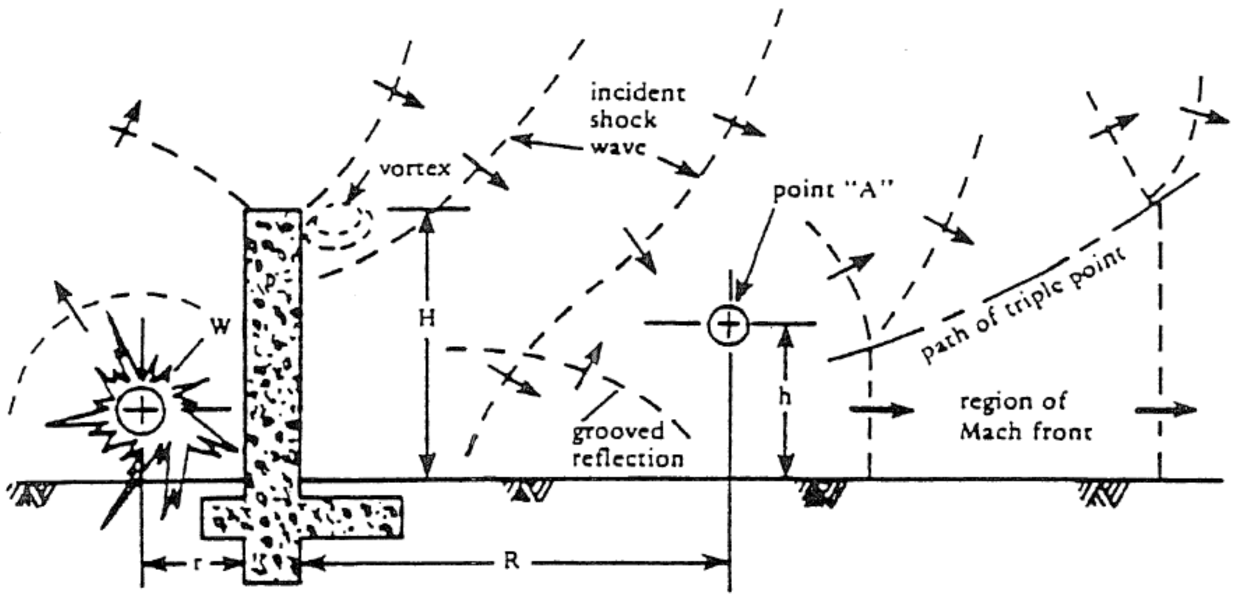

Figure 2-23 shows how a shock wave fills in the area within an L-shaped shield wall projecting out from a building wall in front of a door, and reflects off interior surfaces of the shield wall, based on computational fluid dynamics (CFD) modeling results. The wall is impacted by a shock wave propagating normal to the wall surface, which has reflected off the wall and is propagating around the edges of the wall. This analysis illustrates how a shock wave can fill into, and reverberate within, an enclosure to cause enhanced blast loading. The relatively high pressures caused by multiple reflections of the shock wave occurring within the L-shaped shield in the CFD model was validated with shock tube testing (Thomas et al, 2004).

Figure 2-23 High Calculated Shock Pressures (in Red) Within L-Shaped Enclosure In Front of Door

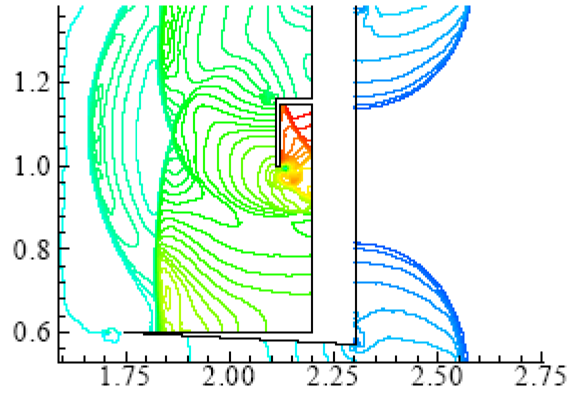

This page intentionally blank

CHAPTER 3 - BLAST LOADS ON STRUCTURES

When a blast wave propagates into a building surface that blocks the propagation and redirects the blast wave, the pressure, density, and temperature near the surface are increased to values greater than those for the incident, or incoming blast wave by the reflection process. This causes the reflected blast load applied on any surface that faces, or partially faces, the explosive source, and therefore reflects the blast wave, to be greater than the side-on blast load at the same point. The reflected blast load has maximum values based on the fully reflected blast pressure and impulse described in Chapter 2 if the surface faces directly towards the explosive charge.

Figure 3-1 illustrates blast loads applied to different surfaces of a building. Each surface can experience a different blast pressure based on its orientation relative to the direction of shock wave propagation. A reflected blast pressure load is shown on the side of the building facing the explosive source. The blast wave reflects off the building face back towards the source. The shock wave also envelops the whole building. The blast load on all sides of the building parallel to the direction of shock wave propagation, such as the flat roof in Figure 3-1 and sidewalls of a building, is equal to the side-on blast load. The blast load on the back or leeward surface of a building can conservatively be assumed equal to the side-on blast load. However, it can be affected significantly by vortices in the shock wave at the corners of the surface and is often less than the side-on blast load.

Figure 3-1 Blast Loads on Building Surfaces

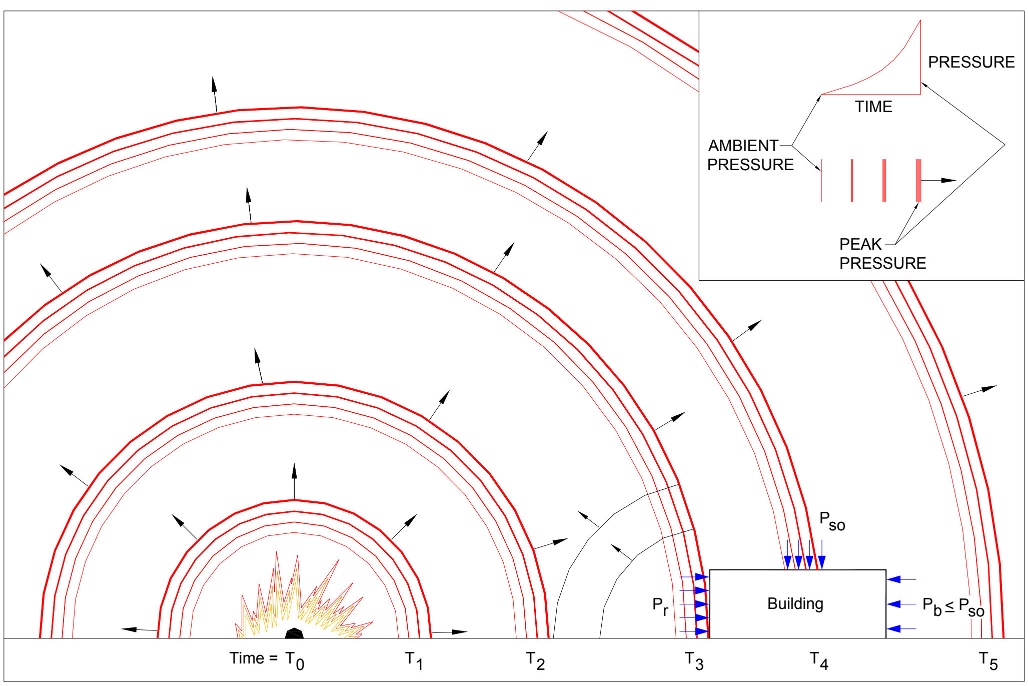

3-1 REFLECTED BLAST LOADS

The magnitude of the reflected blast load on a surface depends on the angle between the surface and the direction of the shock wave propagation, which is referred to as the angle of incidence. The peak reflected pressure and reflected impulse for the positive phase of the blast load can be predicted based on the side-on blast load at the reflecting surface and the angle of incidence using Figure 3-2 and Figure 3-3. Figure 3-2 shows values for the reflection factor, which is the ratio of the peak positive phase reflected pressure to the peak side-on pressure predicted with Figure 2-4 and Figure 2-9. Therefore, the peak reflected pressure is equal to the reflection factor multiplied by the peak side-on pressure. The reflected impulse is equal to the scaled reflected impulse in Figure 3-3 multiplied by the cube root of the charge mass. The angle of incidence is shown in Figure 3-4 for the case of a plane wave propagating into the wall of a building, where all points on the wall have the same angle of incidence. This is typically the case when the standoff is large compared to the building dimensions. If a building surface is directly normal to the direction of blast wave propagation, which corresponds a zero angle of incidence (α = 0 in Figure 3-2 and Figure 3-3), a fully reflected blast load is applied to the surface as described in Chapter 2. The peak pressure and impulse from a fully reflected blast load can be predicted directly from Figure 2-4 or Figure 2-9, or from the side-on peak pressure from these two figures and Figure 3-2 and Figure 3-3 using α = 0.

Figure 3-2 Reflected Pressure Coefficient Versus Angle of Incidence

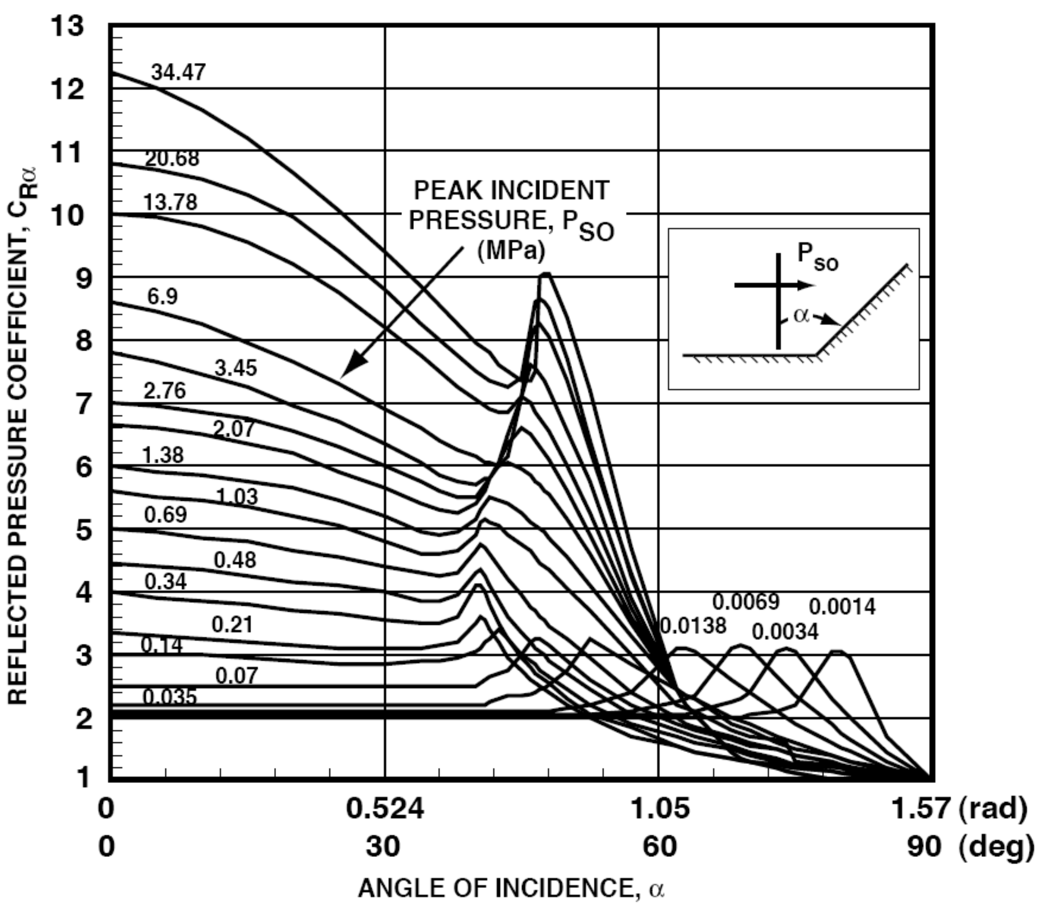

Methodology Manual TOC

Figure 3-3 Scaled Reflected Impulse Versus Angle of Incidence

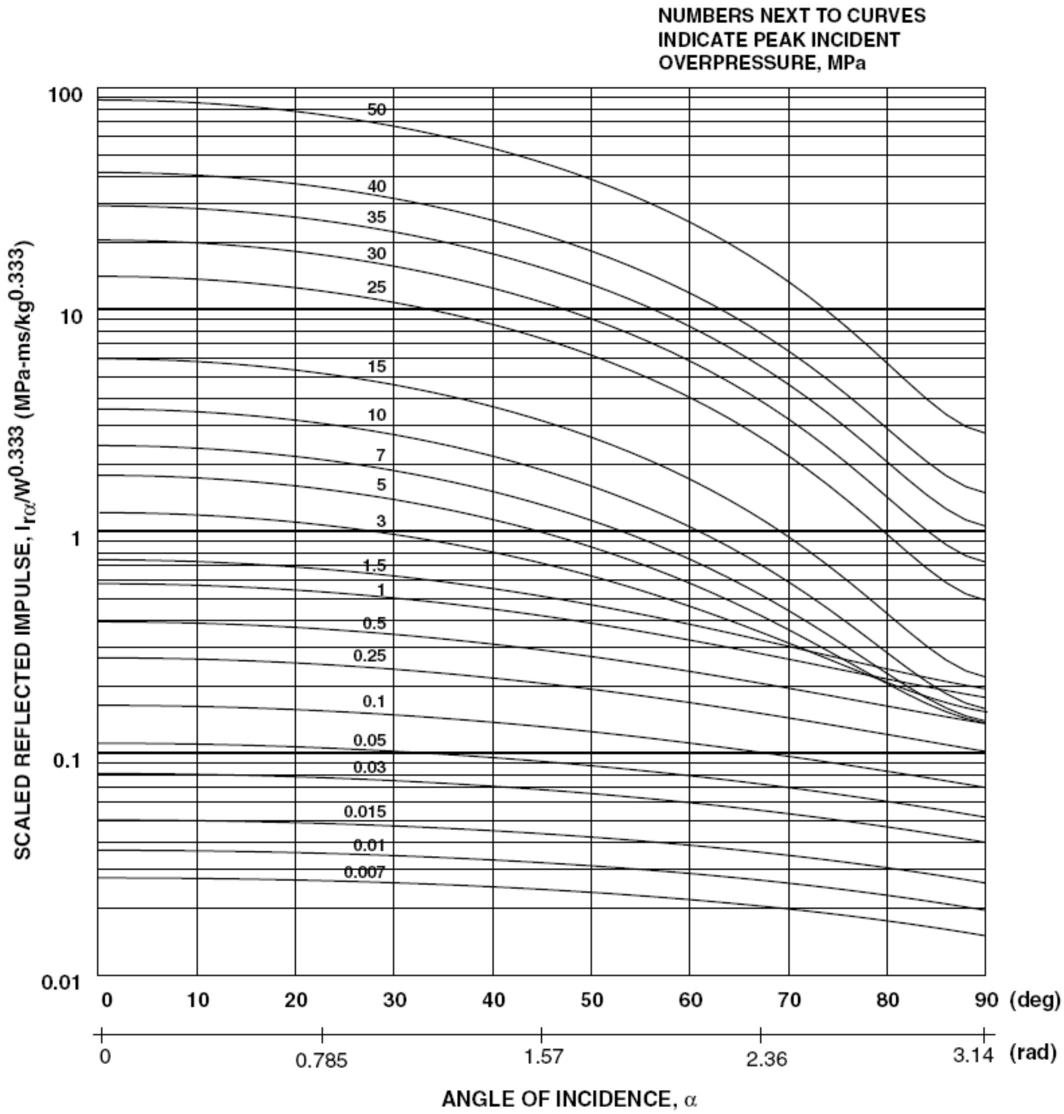

Figure 3-4 Plan View Showing Angle of Incidence of Shock Front Relative to Building Wall

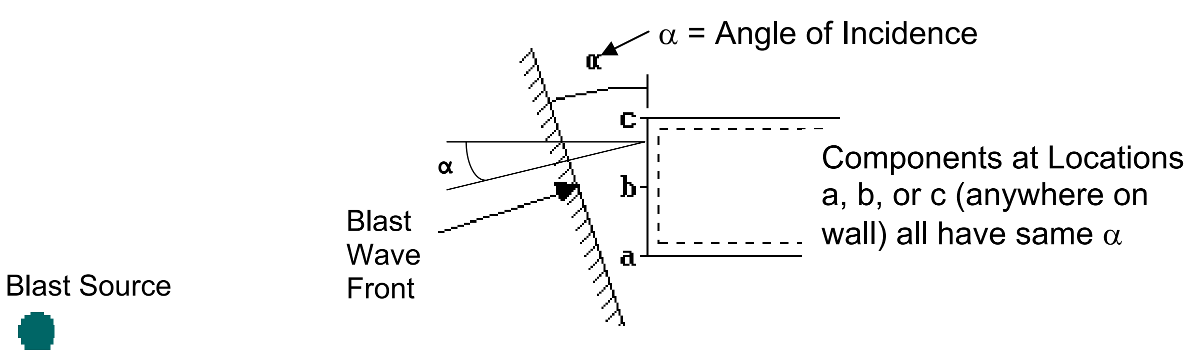

Methodology Manual TOC

Figure 3-5 shows how different points on a building surface subject to a close-in explosion have differing angles of incidence, α, as well as differing standoff distances, R. The blast load at each point has a peak pressure equal to the reflection factor from Figure 3-2 multiplied by P_{so}, as determined from Chapter 2 based on the TNT charge weight and standoff distance (assuming a free-air burst in this case), and an impulse equal to the scaled reflected impulse from Figure 3-3 multiplied by the cube root of the charge weight. The value of P_{so} from Chapter 2 is needed for both Figure 3-2 and Figure 3-3. SBEDS calculates the blast load at a given point on the building component based on the user inputs of charge weight, range, component height and width and angle of incidence.

Figure 3-5 Shock Wave Loads on Building Surface

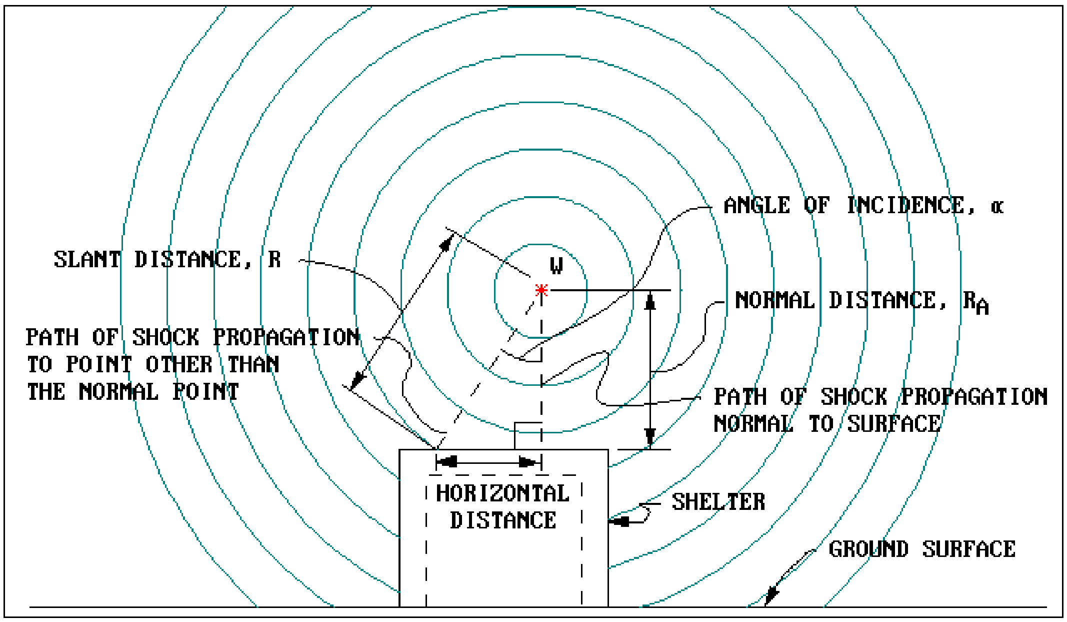

There is a “hump” in the reflection factors in Figure 3-2 at angles between 45 and 70 degrees, depending on the peak side-on pressure, where the reflection factor increases with the angle of incidence instead of decreasing as it generally does. Based on analysis and testing, this is due to a very short duration pressure spike that occurs at the very front of the pressure pulse for these cases (Ketchum et al, 1998). Figure 3-6 shows calculated pressure spikes with durations on the order of microseconds at the front of the pressure pulse that cause the hump in the reflection factors in Figure 3-2. These pressure spikes, which were not noted for angles of incidences and pressures outside the hump region, were confirmed with shock tube testing. Numerous analyses of structural components showed that this type of pressure spike with very short durations does not significantly affect response of typical components in hardened or conventional buildings (Ketchum et al, 1998). This is expected because the spike applies a very small amount of impulse with a duration much less than the natural period of almost any structural component. Based on this work, the curves defining reflection factors in Figure 3-2 can be smoothed so that there is monotonic decay in the reflection factor with increased angle of incidence, as shown in Figure 3-7 from ASCE (1997). However, it is current practice to conservatively include the effect of the hump in Figure 3-2 for blast loads used in most analysis and design of structural components subject to blast loads.

Figure 3-6 Numerical Calculations Showing Pressure Spike at Angle of Large Angle of Incidence

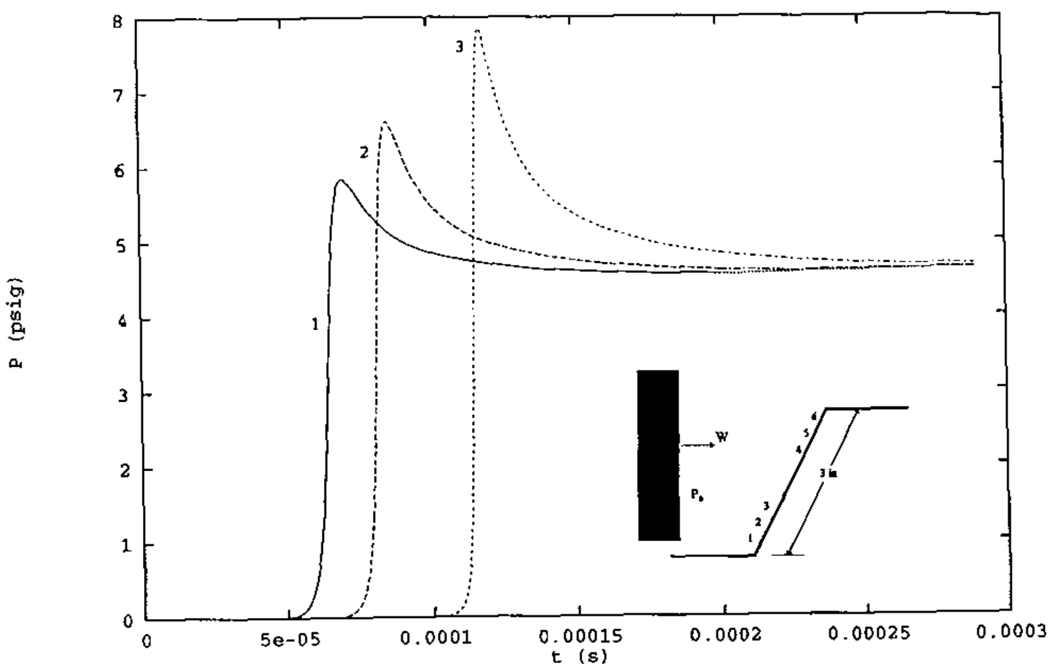

Figure 3-7 Reflected Pressure Coefficient Versus Angle of Incidence Without Hump (from ASCE)

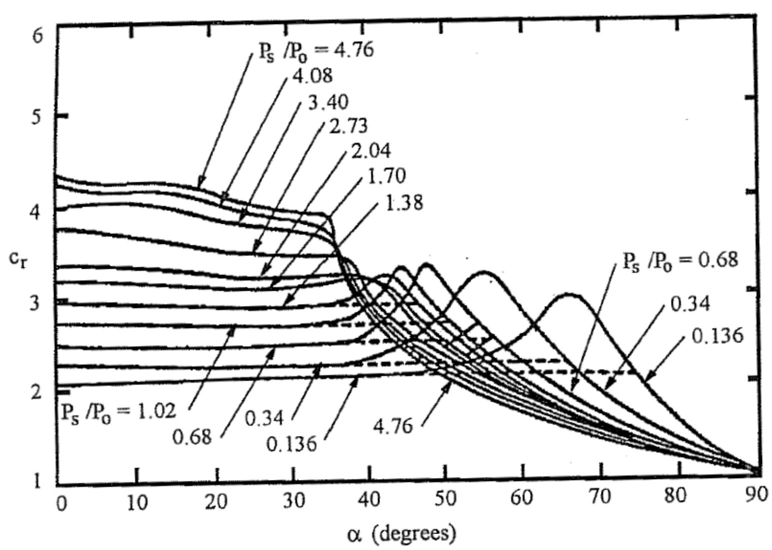

3-2 CLEARING OF REFLECTED BLAST LOADS

A dynamic discontinuity exists at the edges of reflecting surfaces immediately after the shock wave impacts the surface, where there is a higher reflected pressure on the surface and a lower, free-field pressure a very short distance away from the corner. There is no physical means to maintain this pressure imbalance. As a result, a “clearing” wave propagates towards the center of a reflecting surface from all the free edges that reduces the reflected pressure to a pressure based on the side-on pressure and dynamic pressure. The time required for the clearing wave to propagate from the nearest edge of a surface to the point of interest on the surface is the clearing time, t_c. If t_c is less than the duration of the positive phase of the reflected blast load, the blast load will have a lower, non-reflected blast pressure from time t_c until the end of the positive phase duration. The dynamic pressure can be predicted from the side-on pressure, P_{so}, using Figure 2-13.

Figure 3-8 shows a blast load affected by clearing if t_c is less than the equivalent triangular load duration of the reflected blast load, t_{rf} in Equation 3-1. In this case clearing occurs prior to the end of the reflected blast load and the pressure after t_c is defined by the side-on blast pressure, P_{so}, and the dynamic pressure, q_0, multiplied by a drag coefficient, C_D. The dynamic pressure is shown as q_s in Figure 2-13. The drag coefficient is equal to 1.0 for points on flat building surfaces that reflect the shock wave. For other cases, such as blast loads on a cylindrical surface, it can be based on available testing that preferably is done at particle velocities (see Figure 2-13) representative of those caused by the shock wave. DOE-TIC 11268 (1992) has limited information on drag coefficients for components with different shapes. The combined side-on and dynamic pressure acts on the component between times t_c and t_{of} from Equation 3-2. If the clearing time is greater than t_{rf}, there is no effect from clearing. Figure 3-8 also shows a simplified representation of the negative blast load.

Figure 3-8 Reflected Blast Load Affected by Clearing

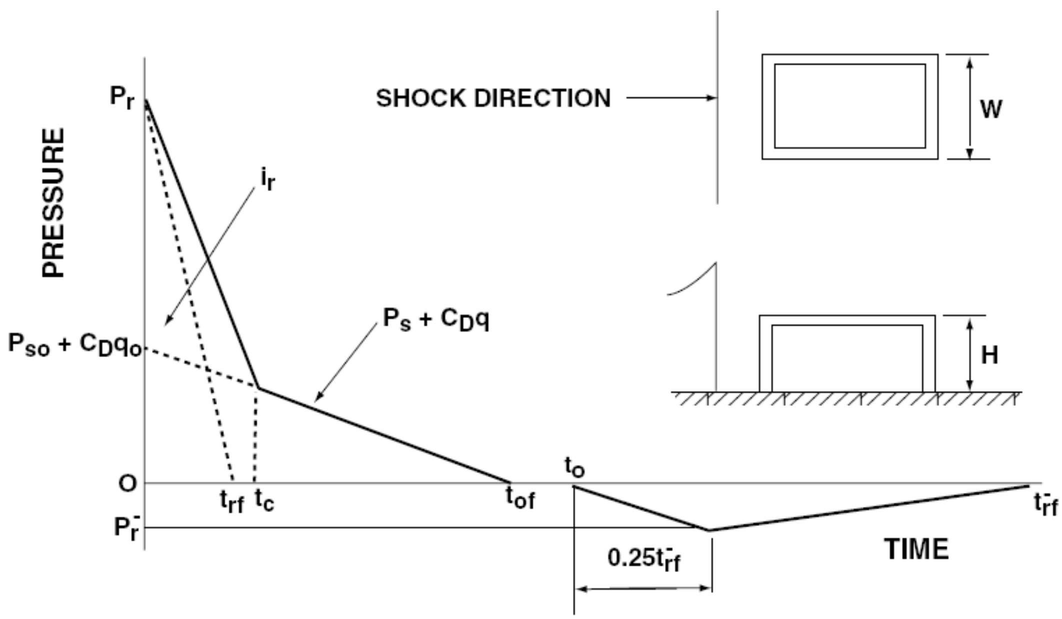

Equation 3-1

$$t_{rf} = 2i_r / P_r$$

where:

t_{rf} = triangular loading duration
i_r = reflected impulse
P_r = peak reflected pressure

Equation 3-2

$$t_{of} = 2i_s / P_{so}$$

where:

t_{of} = positive phase duration
i_s = overpressure impulse
P_{so} = peak side-on overpressure

The clearing time, tc, can be determined using one of two equations depending on the type of blast load that is calculated. The average clearing time needed to clear the reflected pressure on an entire surface from free edges at the sides and roof is given by Equation 3-3. The clearing time for a point on the wall is more closely defined by Equation 3-4. Equation 3-3 is typically used when the calculated blast load represents the average blast load over an entire structural component. This is the most typical case for practical problems and the assumption in the SBEDS workbook.

Equation 3-3

$$t_c = \frac{4HW}{(W + 2H)C_r}$$

where:

t_c = average reflected pressure clearing time on a building surface (ms)
H =structure height – see Figure 3-10 (m)
W =structure width – see Figure 3-10 (m)
C_r = sound velocity (see Figure 3-9) (m/ms)

Equation 3-4

$$t_{cp} = \frac{3S_p}{U}$$

where:

t_{cp} = average reflected pressure clearing time at a point (ms)
S_p = shortest distance from the point of interest to a free edge (m)
U = shock front velocity (m/ms) (see Figure 2-9)

Figure 3-9 Sound Velocity in Reflected Overpressure Region

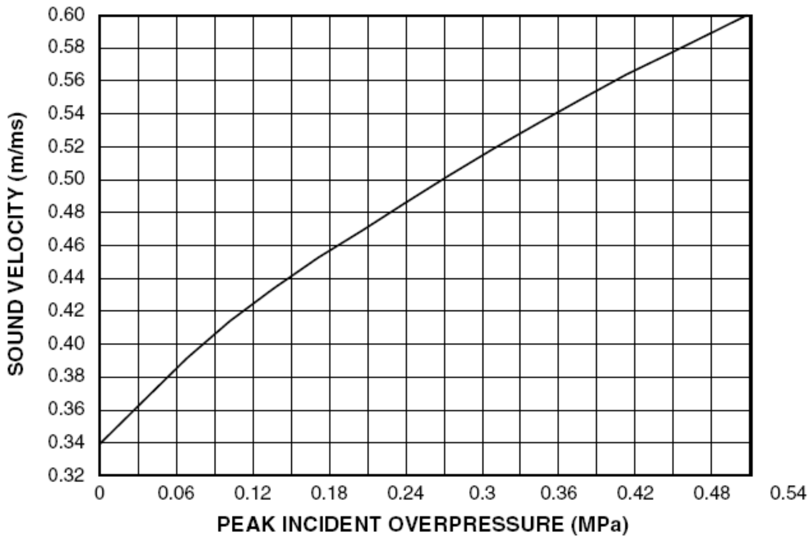

Figure 3-10 Dimensions of Reflecting Surface

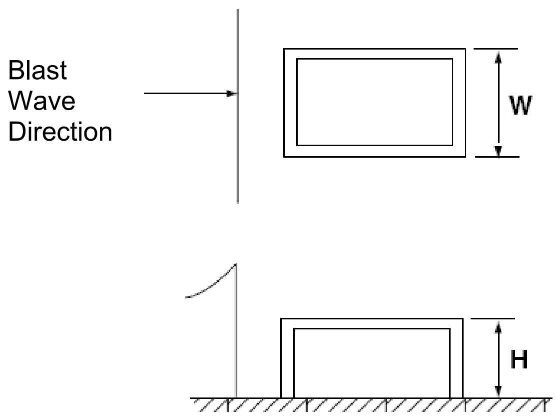

3-3 CONSIDERATION OF NEGATIVE PHASE BLAST LOAD

Methods for calculating both positive and negative phase blast loads are presented in this manual. However, the negative phase blast load is not understood as well as the positive phase load due to much less available data. In many tests, only positive phase blast load has been measured. Traditionally, analysis of component response to blast loads has only considered positive phase loading.

In almost all cases, excluding the negative phase blast load has either a conservative effect on calculated maximum component response (i.e., increases response) or has little effect. The negative phase blast load has maximum effect on the component response when the whole negative phase duration occurs prior to maximum component response. Conversely, it has no effect when the duration of the positive phase blast load exceeds the component maximum response time. The latter case is most often true when the blast load duration is longer than one or two times the natural period of the component, while the former case is most often true with the blast load duration is shorter than approximately one-third of the component natural period. In most practical cases where non-confined high explosive loading is applied to building components (i.e., the explosion is outside the building), the blast load duration is less than the natural period of the component so that inclusion of negative phase blast load does affect the calculated maximum component response, reducing it in the large majority of cases. In a limited number of cases, the negative phase of the blast load can be in phase with rebound of the structural component from positive phase blast load and a resonance effect occurs, where the maximum component response occurs in rebound or during the second inbound response phase.

An important simplification in SBEDS is that it uses the fully reflected negative phase blast load from Figure 2-11 for all incidence angles less than, or equal to 45 degrees, and the side-on negative phase blast load for all incidence angles greater than 45 degrees. This approach is exact compared to the available prediction method only when the input angle of incidence is zero degrees (fully reflected) or 90 degrees (side-on) and becomes less accurate as the angle of incidence approaches 45 degrees. It tends to over predict the negative phase blast load for angles of incidence between 0 and 45 degrees and under predict the negative phase blast load for angles of incidence between 45 and 90 degrees. Also, there never any clearing calculated for the negative phase blast load in SBEDS, which may over predict the negative phase impulse when for components on one or two story buildings. These simplified approaches are used because so little is known about the negative phase blast load, including the effect of angle of incidence and clearing. Generally speaking, the maximum component response to blast load can be under predicted if the negative phase blast load is over predicted. Therefore, the user may want to use positive phase blast load only, or at least analyze this case also, if the angle of incidence is between 30 and 45 degrees.

A recent comprehensive study of measured and calculated component response to blast loads indicates that inclusion of negative phase blast load using the methods in this manual causes more accurate calculation of component response than consideration of only positive phase blast load (Oswald, 2005). However, the lack of a well-validated method for predicting the negative phase blast load is a legitimate reason for using the traditional approach of ignoring negative phase blast load when calculating component response. An approach used by some engineers with experience in blast effects is to include the negative phase blast load when analyzing blast damage to existing building components and to ignore the negative phase blast load when designing new blast resistant components. This approach recognizes that some conservatism is usually desired for building design, whereas the most realistic estimate of blast damage is usually desired for existing components.

3-4 STRUCTURAL COMPONENTS WITH NON-UNIFORM BLAST LOADS

Figure 3-5 shows a case where the explosion is relatively close to the surface of interest (i.e., the roof), causing a significant variation in the standoff distance, R, and angle of incidence, α, at each point on roof components. Therefore, there is a significant variation in the blast load applied to different points on the roof components and some averaging of the blast load may be required for blast response analyses. If a dynamic finite element analysis is used to determine component response, than blast loads can be calculated at points representing the nodes in the finite element analysis and the differing magnitude and arrival times at each point can be considered if they are significant. This is the most straight-forward case for determining representative loads when there is significant blast load variation over the component of interest. However, component response is usually calculated with simplified methods based on a spatially uniform "equivalent" blast load over the whole component at each time step. Ideally, the equivalent uniform load will cause the same dynamic response as the actual non-uniform load.

An equivalent uniform blast load can be determined using a number of different methods. The simplest approach is to calculate the blast load at midspan on the component and use this as an equivalent uniform load over the whole component. This approach is usually used if there is not too much variation (i.e., less than approximately 25%) in the blast load over the middle two-thirds of the component span length, which typically occurs if the scaled standoff to midspan is greater than approximately 1.2 to 2.0 m/kg$^{1/3}$ (3.0 to 5.0 ft/lb$^{1/3}$). Dynamic response is most affected by loading near the midspan region and least affected by loading applied near the supports, similarly to static loading, except for localized shearing and breaching effects that can occur at very small scaled standoff in the range of 0.4 to 0.8 m/kg$^{1/3}$ (1.0 to 2.0 ft/lb$^{1/3}$).

When the blast load variation on a reflecting surface is such that the midspan blast load cannot be used as an average over the whole span, the variation in impulse over the component span can be defined in terms of step function with small regions of constant impulse or with a curve-fit mathematical function. Dynamic response is almost always much more sensitive to the impulse of the blast load than any other parameter for the relatively close-in standoff cases causing blast loads that vary significantly over the span on a reflecting surface. The calculated distribution of the blast load impulse over the component span can be normalized relative to the peak impulse to have the form $i_{max}\mathrm{I}(x,y)$, where $\mathrm{I}(x,y)$ is the impulse at each point along the area of interest divided by the peak impulse, i_{max}. The equivalent uniform impulse i_e can then be calculated from Equation 3-5, where $\phi(x,y)$ is the component deflected shape function based on an assumed modal response shape as explained in Section 4-1.1.1.

Equation 3-5

$$i_e = \frac{i_{\max}\int_0^L\int_0^H \mathrm{I}(x,y)\varphi(x,y)dxdy}{\int_0^L\int_0^H \varphi(x,y)dxdy} \qquad where \qquad \mathrm{I}(x,y) = \frac{i(x,y)}{i_{\max}}$$

where:

- i_e = equivalent impulse of uniformly distributed load
- L = length of loaded area
- H = width of loaded area
- $\phi(x,y)$ = deflected shape function of blast-loaded component
- $i(x,y)$ = Non-uniform impulse applied to loaded area
- i_{max} = maximum impulse over loaded area
- $\mathrm{I}(x,y)$ = normalized impulse shape function over loaded area

If significant plastic response is expected, $\phi(x,y)$ can usually be based on the shape of the component after it has yielded under uniform static pressure (i.e., the yield line pattern). Otherwise, an elastic deflected shape can be used. For one-way components, such as beams, all parameters are only a function of one direction.

The peak pressure of the equivalent uniform blast load, which will not affect the calculated response very much, can be based on the peak pressure at midspan. The equivalent uniform blast load therefore has this equivalent uniform peak pressure and an impulse from Equation 3-5 with the simplified shape of a right triangle. This method is discussed in Chapter 9 of UFC 3-340-01, along with several other methods for determining an equivalent uniform blast load. UFC 3-340-01 recommends using a 1.25 safety factor if a highly non-uniform blast load is simplified as an equivalent uniform impulse in a blast analysis.

The ConWep computer program distributed by the U.S government calculates the average impulse over a given loaded area from a reflected free-air or surface burst explosion with Equation 3-5 taking into account clearing and the different angles of incidence of the blast load at each point on the surface (ConWep, Version 2.1.0.3). This capability is included in the “Slab Loading” option in the program. It calculates the average peak pressure over the loaded area in a similar manner. ConWep also calculates all the properties of the blast wave from free-field and surface blast explosions using the applicable figures in Chapter 2.

Simplified methods are also available for determining the equivalent uniform blast load on components along non-reflecting surfaces with non-uniform blast load. This occurs if the arrival time of the shock wave varies significantly along components that span in the direction of the shock wave propagation, such as roof component or sidewall component on a building that is parallel to the direction of shock wave propagation. In this case, the loading on the surface is non-uniform at the points along the component span at any given time, as illustrated in Figure 3-11, since the load at any time along the span depends on how far the shock wave has traveled along the component length. However, there is no variation in the incidence angle, which is always 90 degrees.

An equivalent uniform blast load can be calculated for this case, as shown in Figure 3-11, in terms of the blast wave parameters at Point b, the back-end of the component. It is assumed in Figure 3-11 that the component spans the full dimension of the building, but points “f” and “b” can be the front and back, respectively, of a shorter component that spans parallel to the direction of shock wave propagation. The distance L will be the projection of the span length along the direction of shock wave propagation if the component spans at an angle relative to the direction of shock wave propagation, but the procedure will otherwise be the unaffected.

Figure 3-11 Equivalent Uniform Roof and Side Wall Loading

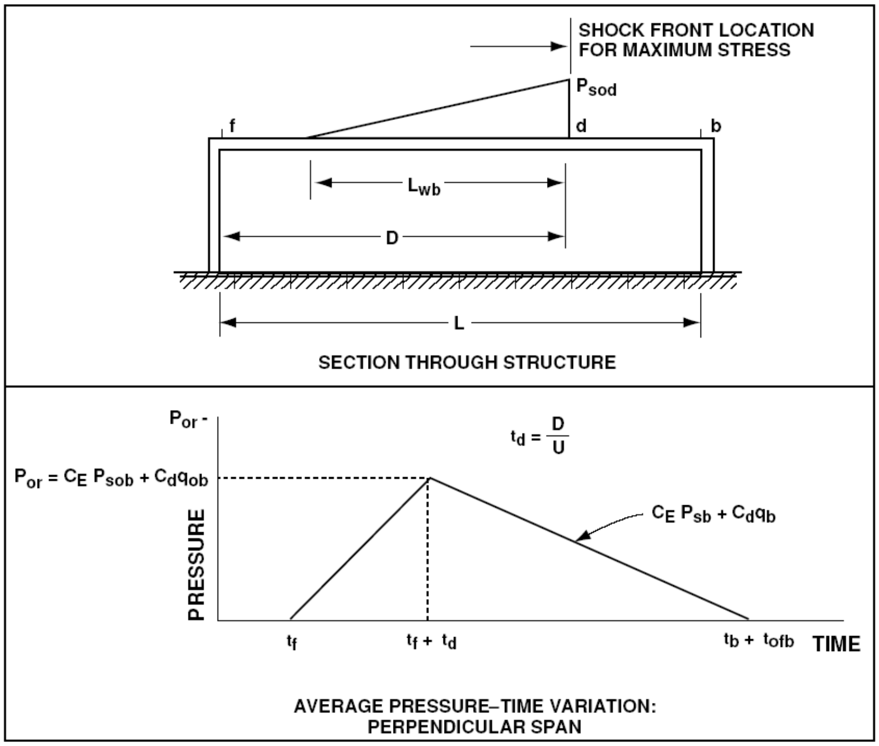

Equation 3-6

$$P_{or} = C_E P_{sob} + C_d q_{ob}$$

where:

P_{or} = peak pressure of equivalent uniform blast load
P_{sob} = peak incident pressure at Point b from Figure 2-10
C_E = equivalent load factor = f (L_{wb}/L) (see Figure 3-12)
L_{wb} = wavelength of shock wave at Point b from Figure 2-10
L = length of component span parallel to direction of shock wave propagation
q_{ob} = peak dynamic pressure at Point b calculated using Figure 2-13
C_d = side-on element dynamic drag coefficient (see Table 3-1)
t_f = shock wave arrival time at point f, equal to R_f/U
t_b = shock wave arrival time at point b, equal to R_b/U
R_i = standoff distance from explosive source to point i (representing either point f or b)
t_d = time of shock wave propagation to peak stress point on span = D/U
D = distance to point on component with peak stress (see Figure 3-12)
U = shock wave velocity based on standoff to point of interest (see Figure 2-9)
t_{ofb} = duration of the positive phase blast load at point b using Equation 3-2

Figure 3-12 Equivalent Load Factor and Blast Wave Location Ratio

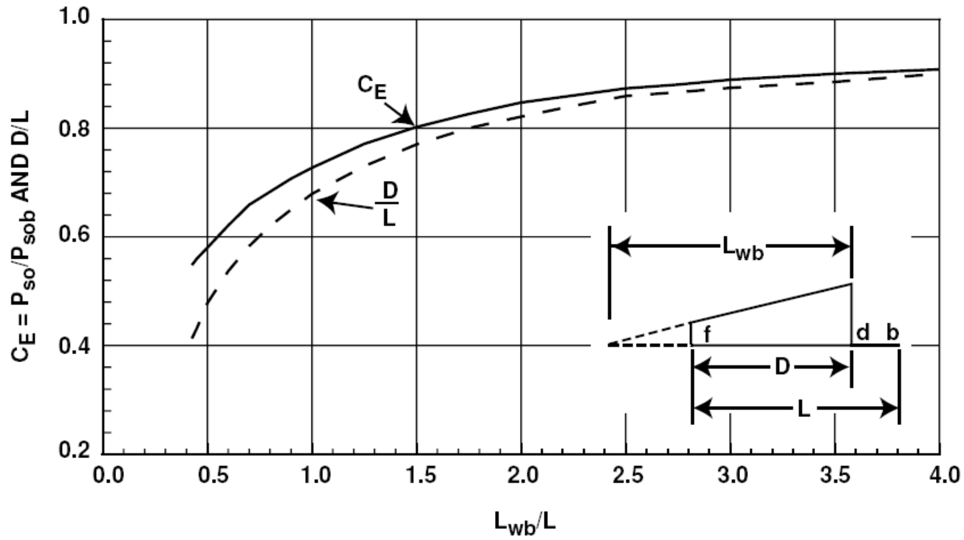

The peak pressure of the equivalent uniform blast load, P_{or}, in Figure 3-11 is calculated using Equation 3-6. The equivalent load factor, C_E, and the ratio of the point of maximum stress, d, to span length L (D/L), are given as functions of the wavelength-span ratio, L_{wb}/L in Figure 3-12 (see definitions of L_{wb} and L in Equation 3-6). The equivalent uniform blast load on the component is assumed to increase linearly from zero at the time, t_f, when the blast wave reaches the beginning of the component (Point f) to the peak pressure, P_{or}, at time, $t_f + t_d$, when the blast wave reaches Point d. The equivalent uniform pressure then decays linearly to zero at time, $t_b + t_{ofb}$, where t_{ofb} is the equivalent triangular pulse duration of the positive phase side-on blast load calculated as shown in Equation 3-2 at Point b. C_d for components spanning parallel to the direction of shock wave propagation is a function of the peak dynamic pressure as provided in Table 3-1. A similar method can be used to determine the equivalent uniform blast load along a component on the sidewall of a building that spans parallel to the direction of blast wave propagation.

Table 3-1 Side-on Element Dynamic Drag Coefficients

Peak Dynamic Pressure q_o	Drag Coefficient C_d
0 to 170 kPa	-0.40
170 to 350 kPa	-0.30
350 kPa to 1 MPa	-0.20

It is usually a simplified, conservative value for the equivalent uniform blast load on a component spanning parallel to the direction of shock wave propagation is the side-on blast load at midspan on the component, since it will have an immediate rise time to a peak pressure that is greater than or equal to P_{or} in Figure 3-11. The blast loads at any specific points on the roof or sidewalls of buildings can be based on the side-on peak pressure and impulse from Figure 2-9 with a modified standoff distance, R_m. R_m is the "line of site" standoff distance, equal to the slant distance from the explosive source to the nearest edge of the building side facing the explosive source to the point of interest plus the distance from this edge to the point of interest. Blast loads calculated with this approach have compared well to measured blast loads on the sides and roof of five story building in repeated explosive tests (Coltharp and Mosher, 1999).

As the shock front passes over the rear of the structure, the pressure front expands over the roof and around the sidewalls, and loads the rear or back wall. The applied pressures from these waves are reinforced by reflections of the shock wave up off the ground. However, vortices in the shock wave that form at the free edges of the back wall may reduce the strength of the shock waves that propagate onto the back wall. Limited experimental information is available on the blast load on the rear wall. Conservatively, the equivalent uniform blast load for the back wall can be assumed equal to the side-on blast load at Point b in Figure 3-13. The equivalent uniform blast load may also be determined as shown in Figure 3-13. The peak value of the pressure, P_{or}, is the sum of the contributions of the peak side-on pressure and drag pressures shown in Equation 3-7, where Point e occurs at a distance of Hs from the rear edge of the roof slab. The distance Hs is the lesser of the back wall height or one-half the building width (see H and W in Figure 3-10).

Figure 3-13 Back Wall Blast Loading

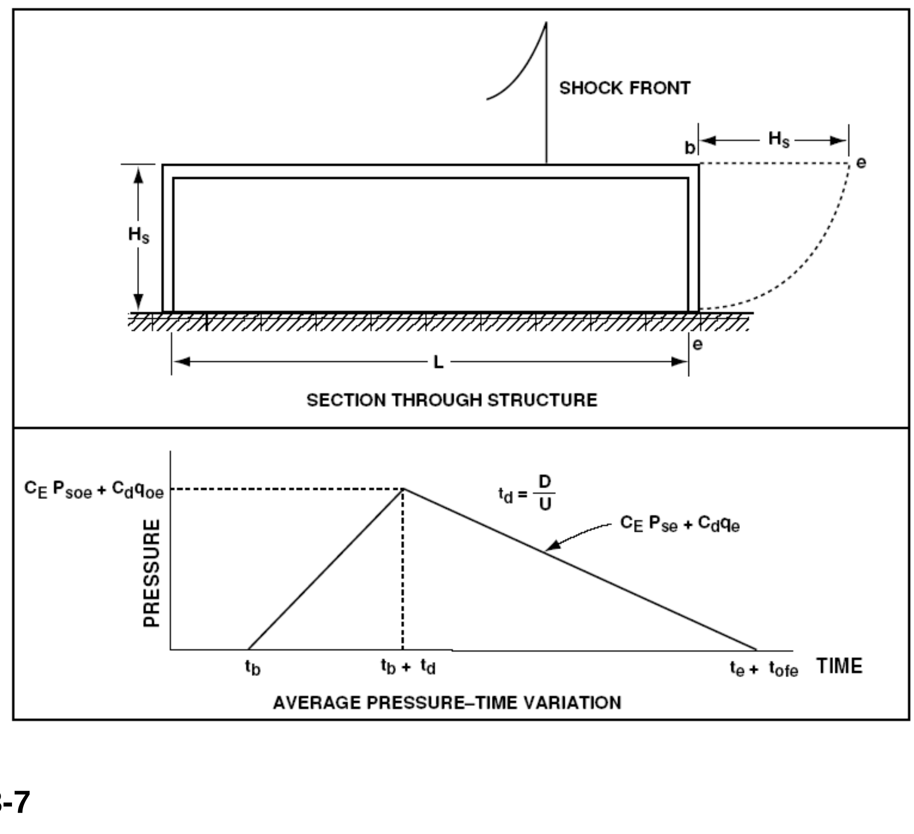

Equation 3-7

$$P_{or} = C_E P_e + C_d q_{oe}$$

where:

P_{or} = peak pressure
P_e = peak incident pressure at Point e

C_E = equivalent load factor = f (L_{wb}/H_s) (see Figure 3-12 with L=H_s)
L_{wb} = wavelength of shock wave at Point b from Figure 2-9
H_s = height of back wall
q_{oe} = peak dynamic pressure at Point e calculated using Figure 2-13
C_d = dynamic drag coefficient = f (q_{oe}) (see Table 3-1)
t_d = time of shock wave propagation to peak stress point on span = D/U
D = distance to point on component with peak stress (see Figure 3-12 with L=H_s) see Equation 3-6 for definitions of analogous parameters

3-5 BLAST LOADS ON PRIMARY FRAMING COMPONENTS

Primary framing components (i.e., girders and columns) are loaded along their span by dynamic reaction loads from secondary framing members (i.e., beams, girts, or purlins) that frame into the primary component. The dynamic reaction pressure history is calculated as described in Section 4-3.1. The loads on primary members can be based on these dynamic reaction loads or on the blast pressure history applied over the tributary area of the supported secondary framing components. In the latter case, the secondary components are assumed to transfer the blast load into the primary component as an infinitely rigid system, which is obviously a simplification. Figure 3-14 shows a comparison of a blast load that can be directly applied to a primary component over its supported area and the calculated dynamic reaction pressure history from a secondary component supported by the primary component. The dynamic reaction pressure history in Figure 3-14 must be doubled to be comparable to the blast load, due to the manner in which it is typically calculated as explained later in this section.

Figure 3-14 Comparison of Blast Load and Dynamic Reaction for Secondary Component

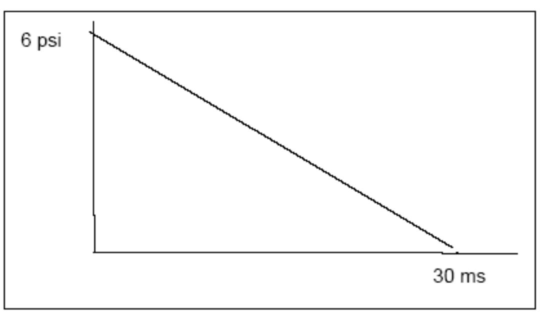

Blast Load on Secondary Component

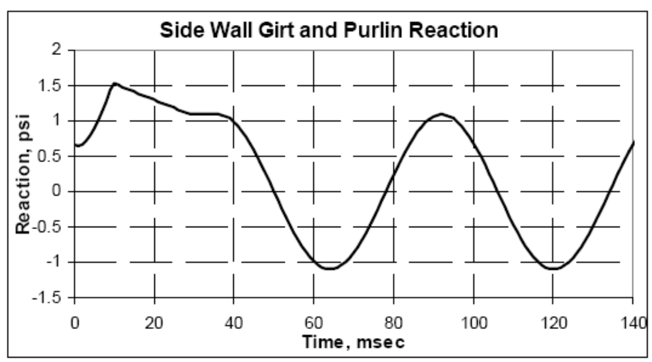

Dynamic Reaction from Secondary Component on One Side of Framing Component

Figure 3-14 shows that the peak pressure in the doubled dynamic reaction pressure (3 psi) is significantly less than the peak applied blast pressure (6 psi), since the dynamic reaction pressure is affected by the relative low flexural strength of the component. However, the impulse of the first positive pulse of the doubled dynamic reaction pressure is slightly larger than the impulse of the blast load. The dynamic reaction pressure on a primary component typically “smears out” the applied blast pressure, so that it has a lower peak pressure than the applied blast pressure, a longer duration, and approximately the same impulse. This is not always true, but it is very typical for secondary components subject to blast loads large enough to cause permanent deformation. Also, the dynamic pressure history includes multiple positive and negative pressure oscillations based on the dynamic response of the supported secondary component. Comparisons to blast tests show that dynamic response calculations are not typically as accurate for the second, third, etc. oscillations of the response of blast-loaded components as for initial response and therefore the calculated dynamic reaction history is much less reliable after initial response. In particular, observed damping of the response is usually not calculated very well.

Usually it is simpler and more conservative to calculate the response of primary components to the blast pressure, rather than to the dynamic reaction from the supported components. The blast pressure typically applies approximately the same positive phase impulse with a higher peak pressure. The dynamic reaction, however, can be considered more accurate and, if it has a lower peak pressure than the blast pressure history, it can significantly reduce the calculated response of the primary component in some cases. This is particularly true when the peak dynamic reaction pressure is significantly less than the ultimate resistance, or load capacity of the primary component. Either approach is consistent with established procedures for analysis and design of blast resistant components. If negative phase dynamic reaction pressure is included in the dynamic reaction load applied to a primary component, as it often is, then it is recommended that only one negative phase pulse should be used. This is due to lower expected accuracy in successive calculated positive and negative phase pulses of the dynamic reaction pressure. In some cases, a false resonance effect can be calculated in the primary component response if many oscillations in a calculated dynamic pressure history are included in the applied load.

As noted above, the dynamic reaction pressure must typically be multiplied by a factor of two to compare to the blast load over the tributary area of a supporting component. This is true because of a characteristic in the way the dynamic reaction pressure histories are traditionally calculated in blast design. As shown in Equation 4-24, the dynamic reaction pressure applied by a secondary component must be multiplied by the full loaded area to get the reaction force, whereas the tributary area of the secondary component that loads a primary component is only one-half of the full secondary component area. This inconsistency requires that SBEDS multiplies the calculated reaction pressure histories of a component ($V_R(t)$ in Equation 4-24) by a factor of 2 when it writes reaction pressure histories to save files that can be read as an applied load file for a primary component. This is because the dynamic reaction history that is read in will only be applied over the tributary area of the primary component. See Equation 3-8 and Figure 3-15 for additional explanation. An exception is the nontypical case where the secondary component cantilevers off the primary component. In this case, SBEDS does not multiply the saved reaction pressure history by a factor of 2.

$$V(t) = V_R(t) L_G = 2V_R(t) B$$

Equation 3-8

where:

P = total blast load on girder from dynamic reaction loads
V(t) = dynamic reaction load along primary component (girder)
$V_R(t)$ = dynamic reaction pressure from component spanning L_c (see Equation 4-24)

B = width of tributary area of component supported by girder
L_G = girder span
See Figure 3-15 for more information on parameters

Note: SBEDS saves $2V_R(t)$ as the dynamic reaction pressure that can be read in as a applied blast load pressure on tributary area of supporting component (i.e., girder) unless input component is cantilever and then it saves $V_R(t)$

Figure 3-15 Dynamic Reactions Over Tributary Area of Supporting Component

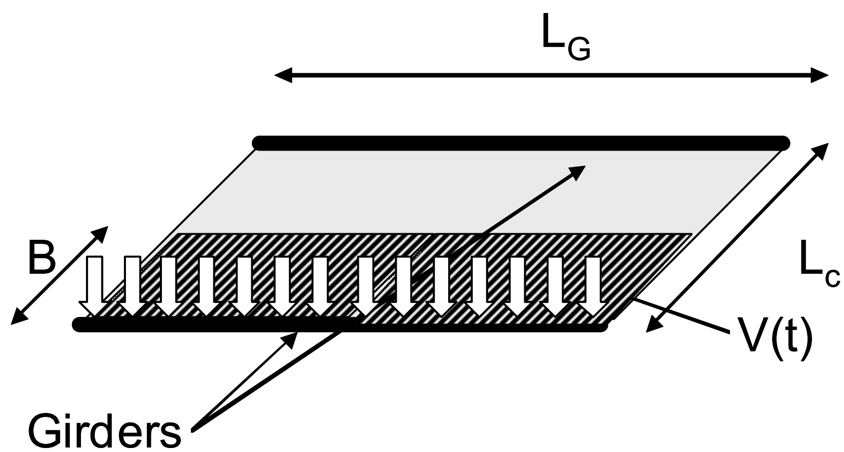

3-5.1 LOADED AREA FACTOR, A_F, FOR COMPONENTS WITH CONCENTRATED LOADS

The SBEDS workbook analyzes components with concentrated blast loading at midspan or at one-third points along the span. The concentrated blast loads at these points are based on an input blast pressure history applied over the tributary area that the secondary framing components loads the primary component. The input blast pressure history can be the applied blast pressure history or to the dynamic reaction history input as a pressure, as shown in Figure 3-14, increased by a factor of two as applicable.

Roof and wall framing plans typically include some secondary components that transfer blast load directly into columns, rather than into the primary framing component of interest. This is illustrated in Figure 3-16. In this case, the blast load or representative dynamic reaction pressure does not represent load along the entire span. This effect is accounted for in SBEDS with a "Loaded Area Factor", A_F, input by the user. As shown in Figure 3-16, A_F is the ratio of the actual blast tributary area of secondary components that frame into primary component of interest divided by the maximum tributary area, which equals the primary component span multiplied by the primary component spacing. In Figure 3-16, only one beam frames into the primary component to cause a concentrated midspan load condition and this beam only transfers blast load into the girder from one-half the default tributary area of the girder. The columns are indicated by small triangles. *If the blast load is uniformly applied along the entire length of the primary component, A_F =1.* This is also applicable for cases where multiple closely spaced secondary components frame into the primary component of interest. If more than three secondary components are supported by a primary component, a simplified conservative approach is to assume A_F=1.

Figure 3-16 Example of Roof Girder with Loaded Area Factor (A_F) Equal to 0.5

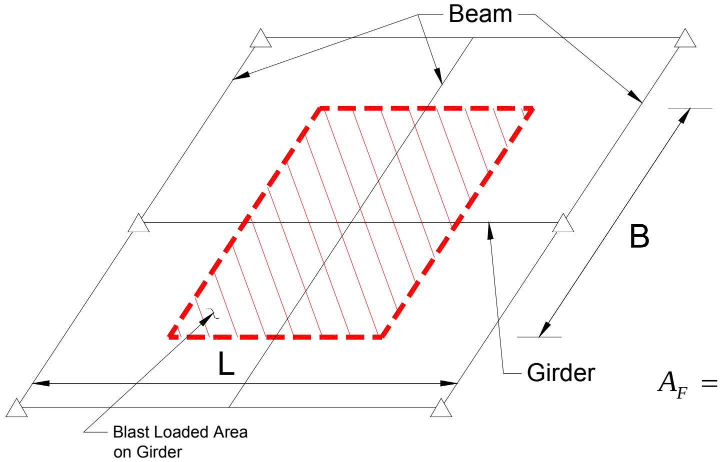

$$A_F = \frac{blast\_loaded\_area}{BL}$$

.

*Note that beams only transfer blast load from 50% of the area B*L into girder in this example where the beams have a pinned connection to girders. The blast load from the rest of this area is transferred by beams directly into columns supporting girder*

All resistance and stiffness values in the equivalent SDOF system for a beam component in SBEDS are divided by the loaded area factor. However, the loaded area factor is not applied to the mass. It does apply to the component self weight mass and the supported weight is input per unit loaded area. The mass factor and load factors could both be increased when A_F<1, but this would have partially offsetting effects on the load-mass factor as described in the first sections of the next chapter so that it is conservative to ignore it and it is considered acceptable to ignore it compared to other approximations in the overall SDOF analysis approach.

CHAPTER 4 - SINGLE-DEGREE-OF-FREEDOM (SDOF) ANALYSIS OF STRUCTURAL COMPONENT RESPONSE TO BLAST LOAD

In many cases, structural components subject to blast load can be modeled as an equivalent SDOF mass-spring system with a non-linear spring. This is illustrated in Figure 4-1. The mass and dynamic load of the equivalent system are based on the component mass and blast load, respectively, and the spring stiffness and yield load are based on the component flexural stiffness and lateral load capacity. The properties of the equivalent SDOF system are also based on load and mass transformation factors, which are calculated to cause conservation of energy between the equivalent SDOF system and the component assuming a deformed component shape and that the deflection of the equivalent SDOF system equals the maximum deflection of the component at each time. The definition of the equivalent SDOF system parameters, the solution of the equation of motion for this system, and the calculation of corresponding response parameters for the structural component are discussed in general in this chapter. Specific details of equivalent SDOF systems that are component-type dependent are discussed in the following chapters.

Figure 4-1 Equivalent Spring-Mass SDOF System

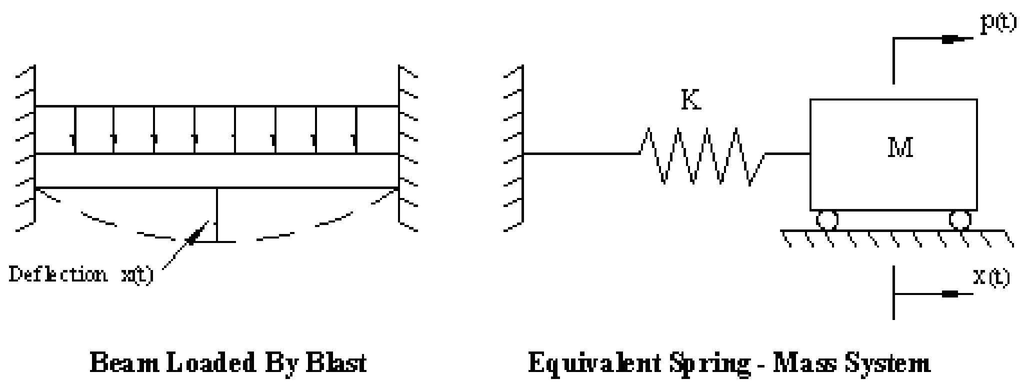

4-1 DYNAMIC RESPONSE OF ELASTIC AND ELASTIC-PLASTIC SDOF SYSTEMS

The maximum deflection of the equivalent SDOF mass-spring system is determined by solving the equation of motion in Equation 4-1. The resistance term in Equation 4-1 represents the resisting force that develops in the component due internal stresses as it deflects. For example, the resistance in a spring-mass system is equal to the spring force. The “effective” mass, damping, resistance, and force terms in Equation 4-1 cause the equivalent SDOF system to represent a given blast-loaded component responding in a given assumed mode shape such that the SDOF system has the same work, strain, and kinetic energies at each response time as the structural component.

Equation 4-1

$$M_e u''(t) + C_e u'(t) + R_e(u(t)) = F_e(t)$$

where:

M_e = effective mass of equivalent SDOF system
$u''(t)$ = acceleration of the mass
$u'(t)$ = velocity of the mass
C_e = effective viscous damping constant of equivalent SDOF system
$R_e(u)$= effective resistance of equivalent SDOF system
$u(t)$ = displacement of the mass
$F_e(t)$ = effective load history on the equivalent SDOF system
t = time

4-1.1 TRANSFORMATION FACTORS

By the principle of energy conservation, the work done by the external force, the energy stored in the member as kinetic energy, and the strain energy of a dynamically loaded component must be in equilibrium as shown in Equation 4-2 at each time. An equivalent SDOF system is defined as a system that has the same energy in terms of work energy, strain energy, and kinetic energy, as the blast-loaded component responding in a given, assumed mode shape. This is accomplished by relating the applicable parameters of the blast-loaded component and the corresponding effective parameters of the equivalent SDOF system with transformation factors, as shown in

Equation 4-3. The transformation factors are calculated to cause the equivalent SDOF system to have the same work, kinetic, and strain energies as the component, as explained in the next sections. The transformation factors are also calculated assuming the deflection of the equivalent SDOF system equals the maximum deflection of the blast-loaded component at all times.

Equation 4-2

$$WE = SE + KE$$

where:

WE = work done
KE = kinetic energy
SE = strain energy

The equivalent mass, stiffness, and load of the SDOF system in Equation 4-1 are obtained by multiplying the mass, stiffness, and load of the blast-loaded component by transformation factors as shown in

Equation 4-3. As stated in

Equation 4-3, K_R and K_d are assumed equal to K_L, as discussed in Section 4-1.1.1. This implies that Equation 4-1 can be written as Equation 4-4. This can be simplified further and written as Equation 4-5.

Equation 4-3

$$M_e = K_m M_c$$
$$F_e(t) = K_L F_c(t)$$
$$R_e(u(t)) = K_R R_c(u(t))$$
$$C_e = K_d C_c$$

where:

M_c = mass of blast-loaded component
$F_c(t)$ = load history on blast-loaded component
$R_c(u(t))$= resistance of blast-loaded component
C_c = viscous damping constant of blast-loaded component
K_m = mass transformation factor
K_L = load transformation factor
K_R = resistance transformation factor, however K_R=K_L
K_d = viscous damping transformation factor, however, K_d=K_L

Equation 4-4

$$K_m M_c u''(t) + K_L C_c u'(t) + K_L R_c(u(t)) = K_L F_c(t)$$

Equation 4-5 is the basic equation of motion for an equivalent SDOF system. It is solved to determine the response of the equivalent SDOF system, which is directly related to the response of the blast-loaded component since it has a deflection equal to the maximum deflection of the blast-loaded component. Therefore, assuming that all the terms for the blast-loaded component in

Equation 4-3 can be defined as described in this manual, all the terms in Equation 4-5 can be defined if the transformation factors KL and Km are known. For some simplified load vs. time relationships, a closed-form solution of Equation 4-5 is possible. However, a time-stepping solution using approximate numerical methods is generally required and numerous available computer programs have been developed for this purpose.

Equation 4-5

$$K_{Lm} M_c u''(t) + C_c u'(t) + R_c u(t) = F_c(t)$$

where:

K_{Lm} = load-mass factor, equal to K_m/K_L

4-1.1.1 **LOAD FACTOR**

The load factor, K_L, is derived by setting the external work energy done on the equivalent SDOF system by the equivalent load $F_e(t)$ equal to the external work energy done by the total load F_c(,t) acting on the blast-loaded component, as shown in Equation 4-6. It is assumed that the component has a constant deflected shape ϕ(x) (i.e.

single mode shape) and constant spatial blast load distribution shape p(x) at all time when K_L applies. This allows the deflections and load along the component span to be written in terms two uncoupled terms that are functions of time and span, respectively. The dimensionless shape functions ϕ(x) and p(x) are usually normalized to have a peak value of 1.0. The assumption of a constant deflected shape is analogous to assuming response in a single, dominant mode shape. For the typical case of a uniformly distributed blast load, p(x)=1.0 and P_{max}(t) equals the uniform load magnitude at each time t in Equation 4-6. For a concentrated blast load, p(x) only has non-zero values at the loaded points. A spatially non-uniform blast load will have a more complex p(x) function, but p(x) is still assumed constant with time when K_L applies. Finally, it is also assumed in Equation 4-6 that the SDOF system deflection and the maximum component deflection are equal. This assumption is crucial for applying the SDOF system analysis results to the blast-loaded component.   A similar procedure to that shown in Equation 4-6 is used to calculate K_L of a two-way spanning component, except the shape functions ϕ(x) and p(x) are functions of x and y and all integrals are double integrals over the span lengths in each direction.

Equation 4-6

$$WE(t)_{component} = \int_0^L P(x,t)U(x,t)dx \quad let \quad U(x,t) = U_{\max}(t)\varphi(x) \quad and \quad P(x,t) = p(x)P_{\max}(t)$$

$$Thus: WE(t)_{component} = P_{\max}(t)U_{\max}(t)\int_0^L p(x)\varphi(x)dx \quad where \quad \varphi(x) = \frac{U(x,t)}{U_{\max}(t)} \quad p(x) = \frac{P(x,t)}{P_{\max}(t)}$$

$$WE(t)_{SDOF} = F_e(t)u(t)$$

$$Set \quad WE(t)_{component} = WE(t)_{SDOF}$$

$$F_e(t)u(t) = P_{\max}(t)U_{\max}(t)\int_0^L p(x)\varphi(x)dx \quad and \quad Let \quad u(t) = U_{\max}(t)$$

$$F_e(t) = P_{\max}(t)\int_0^L p(x)\varphi(x)dx = K_L F_c(t) \quad where \quad K_L = \frac{\int_0^L p(x)\phi(x)dx}{\int_0^L p(x)dx} \qquad F_c(t) = P_{\max}(t)\int_0^L p(x)dx$$

where:

WE(t) =	work energy on SDOF spring and blast loaded component at each time
U(x,t) =	displacement of blast-loaded component
P(x,t) =	dynamic load on blast-loaded component
U_{max}(t) =	maximum displacement of blast-loaded component at constant x location
P_{max} (t) =	maximum dynamic load on blast-loaded component at constant x location
F_e(t) =	dynamic load applied to SDOF system at each time
F_c(t) =	total dynamic load on blast-loaded component at each time
u(t) =	deflection of SDOF system at each time
L =	length of blast-loaded component
ϕ(x) =	deflected shape function of blast-loaded component
p(x) =	load shape function of blast-loaded component

K_L= load factor

Figure 4-2 shows an example of assumed deflected shape functions, $\phi(x)$, for a one-way component (i.e., a beam) with a uniformly distributed load and simple supports during elastic response and during plastic response, which occurs after the component has yielded at all maximum moment regions and becomes a mechanism. Both response realms are typically modeled during an analysis of a blast-loaded component with the equivalent SDOF system. The deflected shape of the component changes during plastic response because the maximum moment region(s) become hinges. Therefore, K_L has different values for elastic response, when u(t) in Equation 4-5 is less than the deflection at which the component becomes a mechanism (i.e., the yield deflection), and for plastic response, when u(t) is greater than this deflection.

Figure 4-2 Deflected Shape Functions for Simply Supported Beam

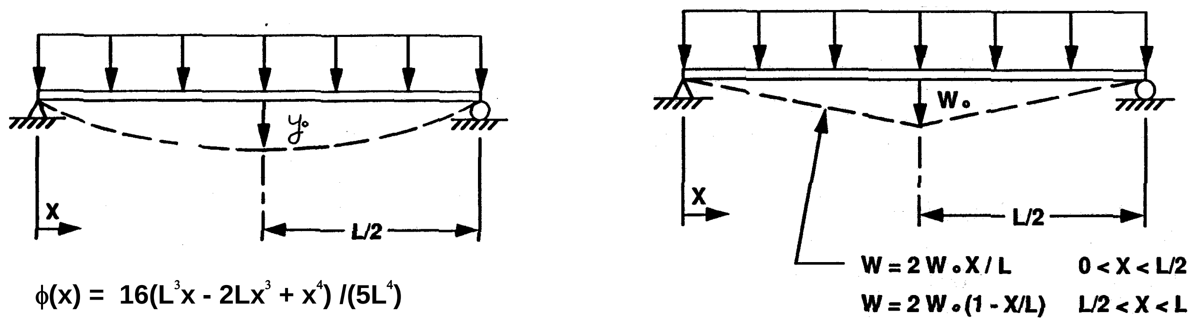

$\phi(x) = 16(L^3x - 2Lx^3 + x^4)/(5L^4)$

prior to yield at maximum moment region *after yield in maximum moment region*

K_L can also be calculated for an intermediate "elastoplastic" region of an indeterminate component where yielding has occurred at only some of the maximum moment regions. The deflected shape of a component in the elastic region is usually assumed equal to the component deflection from a static load with the same spatial distribution as the blast load. Similarly, the deflected shape of a component in the elastoplastic region is assumed equal to the deflection of the component with appropriate hinges inserted at yielded moment regions from a static load with the same spatial distribution as the blast load. These shape functions can be determined from deflection functions in many available handbooks and manuals (Roark, 2000), AISC (2001). Appendix A of TM 5-1300 has a detailed example where K_L is calculated.

The resistance factor, K_R, can be derived by setting the internal strain energy due to stress and strain in the spring of the equivalent SDOF system equal to the internal strain energy due to the stresses and strains in the blast-loaded component. The strain energy of both the blast-loaded component and equivalent SDOF system can also be defined in terms of an internal work energy equal to a resisting force multiplied by the maximum deflection at each time, where the resisting force has the same spatial distribution as the applied load. The component is also assumed to have the same deflected shape used to define the load factor, K_L. Therefore, all the shape functions in

Equation 4-6 are also applicable to the internal work energy of the blast-loaded component. Equation 4-6 also shows the equivalency of strain energies, or internal work, for the equivalent SDOF system and blast loaded component except that all the load terms are replaced with similar internal resisting force terms and the final equation is $R_e = K_L R_c$, where K_L is defined as shown in Equation 4-6. Therefore the transformation factors K_R and K_L are equal. The concept of the internal resisting force is discussed in Section 4-1.2.

Also, as stated in

Equation 4-3, the transformation factor for damping, K_d, is assumed equal to K_L. This is not necessarily mathematically correct. It is a matter of convenience so that only a single K_{Lm} factor is needed in Equation 4-5, which is justified by the fact that the damping term only contributes a small amount of energy to the response of the equivalent SDOF system during the response of typical blast-loaded components. Damping is discussed further in Section 4-1.3.

4-1.1.2 **MASS FACTOR**

The mass factor, K_m, is derived by setting the kinetic energy done by the equivalent mass M_e of the SDOF system equal to the kinetic energy done by the total mass M_c of the blast-loaded component, as shown in Equation 4-7. The dot signifies differentiation with respect to time. It is assumed that the component has the same deflected shape $\phi(x)$ at all time during which K_m applies, and that the SDOF system and the component maximum deflections and velocities are equal at all time. For a uniformly distributed load, m(x) in Equation 4-7 is equal to 1.0. For a concentrated mass(s), m(x) only has non-zero value(s) at the mass point(s).This latter case occurs when a secondary component transfers mass into a primary component at the point where it is supported by the primary component (i.e., mass from a beam that is supported by a girder) and the self-mass of the primary component is negligible. Often in this case a small portion of the supported beam mass, on the order of 20%, is lumped in with the distributed mass of the girder and treated as a uniformly distributed girder mass. This accounts for the fact that all the beam mass may not deflect equally with the girder at each time, as discussed more in Section 4-7. A similar procedure to that shown in Equation 4-7 is used to calculate K_m of a two-way spanning component, except the deflected shape function, $\phi(x)$, and the special mass distribution, m(x), are functions of x and y and all integrals are double integrals over the span lengths in each direction.

4-1.1.3 **LOAD-MASS FACTORS**

The load-mass factor is the ratio of the mass factor to the load factor, as shown in Equation 4-5. The load factor, mass factor, and load-mass factors have been calculated for a wide range of typical load and mass distributions and boundary conditions for one-way and two-way components. Table 4-1, Table 4-2, and Figure 4-3 show load and mass factors, and load-mass factors for one-way and two-way spanning components. The load-mass factors for elastic response of two-way spanning components in Table 4-2 are based on an approximate average deflected shape representative of the deflected shapes occurring as the component undergoes yielding at multiple maximum moment locations before it becomes a mechanism. Figure 4-3 for two-way spanning component response after yielding at all maximum moment regions (i.e., plastic response) is based on deflected shapes determined from yield line theory. The values of y/H and x/L must be determined from the component yield line pattern, as described in Section 4-1.2.1.

Equation 4-7

$$KE(t)_{component} = \frac{1}{2}\int_0^L m(x)\dot{U}^2(x,t)dx \quad let \quad U(x,t) = U_{\max}(t)\varphi(x) \quad and \quad thus \quad \dot{U}(x,t) = \dot{U}_{\max}(t)\varphi(x)$$

$$KE(t)_{component} = \frac{1}{2}\int_0^L m(x)\dot{U}_{\max}{}^2(t)\varphi^2(x)dx \quad where \quad \varphi(x) = \frac{U(x,t)}{U_{\max}(t)} = \frac{\dot{U}(x,t)}{\dot{U}_{\max}(t)}$$

$$KE(t)_{SDOF} = \frac{1}{2}M_e KE(t)_{SDOF}{}^2(t)$$

$$Set \quad KE(t)_{component} = KE(t)_{SDOF}$$

$$\frac{1}{2}M_e\dot{u}^2(t) = \frac{1}{2}\int_0^L m(x)\dot{U}_{\max}{}^2(t)\varphi^2(x)dx \quad Let \quad u(t) = U_{\max}(t) \quad and \quad thus \quad \dot{u}(t) = \dot{U}_{\max}(t)$$

$$M_e = \int_0^L m(x)\dot{U}_{\max}{}^2(t)\varphi^2(x)dx = K_m M_c \quad where \quad K_m = \frac{\int_0^L m(x)\phi^2(x)dx}{\int_0^L m(x)dx} \ and \quad M_c = \int_0^L m(x)dx$$

where:

- KE(t) = kinetic energy on SDOF spring and blast loaded component at each time
- U(x,t)* = displacement of blast-loaded component
- m(x) = mass per unit length of blast-loaded component
- U_{max}(t)* = maximum displacement of blast-loaded component at constant x location
- M_e = equivalent mass of SDOF system
- M_c = total mass of blast-loaded component
- u(t)* = deflection of SDOF system at each time
- L = length of blast-loaded component
- ϕ(x) = deflected shape function of blast-loaded component
- K_m= mass factor

* A dot over displacement indicates velocity

4-1.2 RESISTANCE-DEFLECTION RELATIONSHIPS

For a static load, the acceleration and velocity in Equation 4-5 are zero and the resisting force, or resistance, $R_c(u)$, is equal to the applied force, F_c. Thus, for each given maximum deflection of the component, u, there is resisting force equal to the applied force, which can be plotted as the resistance-deflection relationship. In static cases, this resisting force is always equal to the applied load and we do not typically differentiate between them. In dynamic loading, this is not true because of non-zero inertial and damping forces. The resistance of the SDOF system is the spring force and the resistance of the blast-loaded component is the resisting force generated by the internal resisting moments that occur for a given maximum component deflection.

The resisting force always has the same spatial distribution along the component span as the applied load (e.g., uniformly distributed). It is a function of the maximum component deflection, as mentioned previously in this paragraph, and the plot of component resistance (or resisting force) vs. maximum deflection is called the resistance-deflection relationship. This relationship allows the resisting force, R_c, in Equation 4-5 to be defined at each time based on the deflection of the equivalent SDOF system. Note that the deflection of the equivalent SDOF system equals the maximum deflection of the blast-loaded component at each time step. The slope at each point of the resistance-deflection relationship of a component represents the component stiffness. The stiffness is the ratio of a delta static load increase to the corresponding delta deflection of the component.

Table 4-1 Load and Mass Factors for One-Way Components

Edge Conditions and Loading Diagrams	Range of Behavior	Load Factor K_L	Mass Factor K_M	Load-Mass Factor K_{LM}
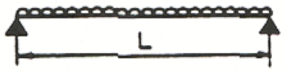	Elastic Plastic	0.64 0.50	0.50 0.33	0.78 0.66
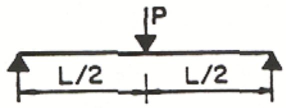	Elastic Plastic	1.0 1.0	0.49 0.33	0.49 0.33
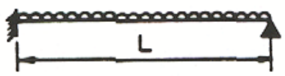	Elastic Elasto-Plastic Plastic	0.58 0.64 0.50	0.45 0.50 0.33	0.78 0.78 0.66
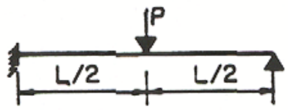	Elastic Elasto-Plastic Plastic	1.0 1.0 1.0	0.43 0.49 0.33	0.43 0.49 0.33
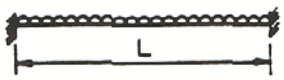	Elastic Elasto Plastic Plastic	0.53 0.64 0.50	0.41 0.50 0.33	0.77 0.78 0.66
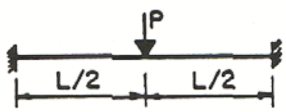	Elastic Plastic	1.0 1.0	0.37 0.33	0.37 0.33
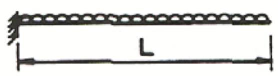	Elastic Plastic	0.40 0.50	0.26 0.33	0.65 0.66
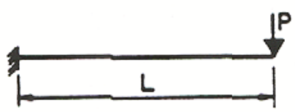	Elastic Plastic	1.0 1.0	0.24 0.33	0.24 0.33
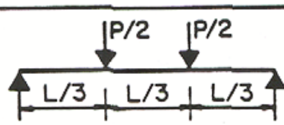	Elastic Plastic	0.87 1.0	0.52 0.56	0.60 0.56

Table 4-2 Load-Mass Factors for Elastic Response of Two-Way Spanning Components

Support Conditions		Value of L/H	Elastic and Elasto-Plastic Ranges (Support Conditions): All Supports Fixed	One Support Simple Other Supports Fixed	Two Supports Simple Other Supports Fixed	Three Supports Simple Other Supports Fixed	All Supports Simple
Two adjacent edges supported and two edges free	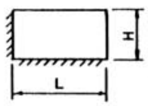	ALL	0.65	0.66	—	—	0.66
Three edges supported and one edge free	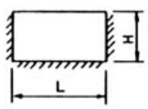	L/H<0.5	0.77	0.77	0.79	—	0.79
		.5≤L/H≤2	$0.65-0.16(\frac{L}{2H}-1)$	$0.66-0.144(\frac{L}{2H}-1)$	$0.65-0.186(\frac{L}{2H}-1)$	—	$0.66-0.175(\frac{L}{H}-1)$
		L/H ≥ 2	0.65	0.66	0.65	—	0.66
Four edges supported	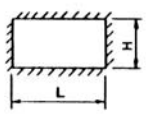	L/H=1	0.61	0.61	0.62	0.63	0.63
		1≤L/H≤2	$0.61+0.16(\frac{L}{H}-1)$	$0.61+0.16(\frac{L}{H}-1)$	$0.62+0.16(\frac{L}{H}-1)$	$0.63+0.16(\frac{L}{H}-1)$	$0.63+0.16(\frac{L}{H}-1)$
		L/H ≥ 2	0.77	0.77	0.78	0.79	0.79

Figure 4-3 Load-Mass Factors for Plastic Response of Two-Way Spanning Components

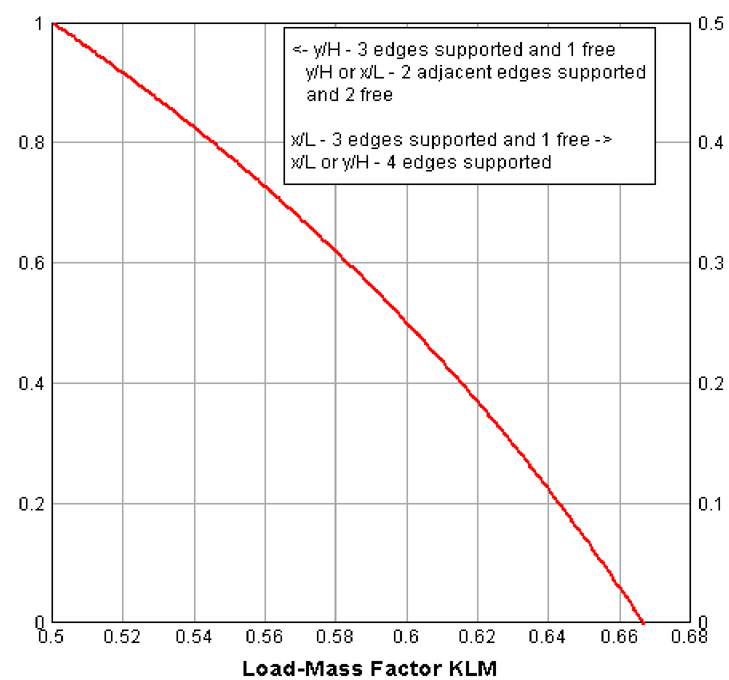

The resistance-deflection relationships of most blast-loaded components are based on ductile flexural response. Components that exhibit tension and compression membrane response and arching due to axial load have more complex resistance-deflection relationships that can also be incorporated into the equation of motion for an equivalent SDOF system. All of these resistance-deflection relationships are discussed in a general sense in this chapter. They are also affected by component-specific factors that are discussed as applicable in Chapter 5 through Chapter 8.

4-1.2.1 RESISTANCE-DEFLECTION RELATIONSHIP FOR DUCTILE FLEXURAL RESPONSE

The first column in Figure 4-4 shows ductile flexural response of a beam subject to uniformly distributed blast load and the corresponding resistance-deflection relationship. The beam resistance-deflection relationship in Figure 4-4 is based on uniform applied load that initially causes elastic flexural response until the beam yields simultaneously at both supports. Next, the beam responds in an "elastoplastic" mode as it resists increased load with less stiffness up to an "ultimate resistance" when yield occurs at midspan and the beam becomes a mechanism. Finally, the beam responds in a ductile "plastic" mode as it maintains the ultimate resistance without any assumed strain-hardening out to a failure deflection where material failure strains occur in the maximum moment regions. Similar resistance-deflection relationships can be developed for different load shapes (e.g., concentrated load at midspan) applied to the component by the blast. In all cases, the resistance-deflection relationship is based on a load with the same spatial distribution along the span as the applied blast load.

In the case shown in Figure 4-4 the beam has indeterminate boundary conditions and therefore has two stiffness regions as described in the previous paragraph. However, the corresponding resistance-deflection relationship for the equivalent SDOF spring is simplified to have a single "equivalent" elastic region, which has the same area under its resistance-deflection curve as the elastic and elastoplastic regions of the beam's resistance-deflection curve.

Figure **4-5** shows typical resistance-deflection relationships for structural components with determinate and indeterminate boundary conditions and the equivalent elastic region (with stiffness kE) of the simplified resistance-deflection relationship for the case of an indeterminate boundary condition. The parameters xE and kE in

Figure **4-5** are calculated as shown in

Equation **4-8** for a component that is one degree indeterminate so that areas under the actual and simplified resistance-deflection relationships are equal at the deflection xp in

Figure **4-5**. Similar formulas can be developed for more complicated resistance-deflection relationships with yielding at multiple maximum moment regions that have more than two non-zero slopes. SBEDS uses the formula in

Equation **4-8** to determine the equivalent elastic stiffness for two-way spanning components.

Figure 4-4 Fixed-End Beam in Ductile, Flexural Response

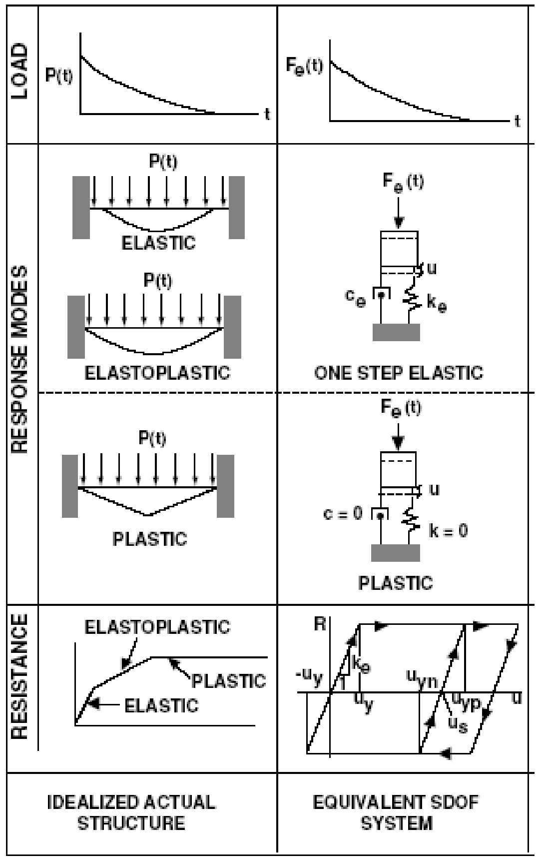

Figure 4-5 Resistance-Deflection Curve For Flexural Response

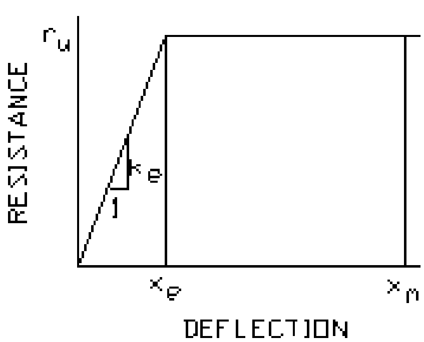

Determinate Boundary Conditions

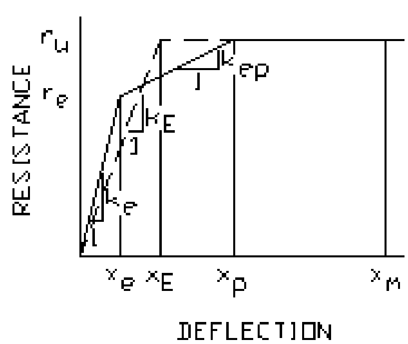

Indeterminate Boundary Conditions

Equation 4-8

$$x_E = x_e + x_p\left(1 - \frac{r_e}{r_u}\right)$$

$$k_E = \frac{r_u}{x_E}$$

The resistance-deflection relationship for a one-way component with ductile flexural response, such as the fixed-end beam in Figure 4-4, can be determined by elastic analysis as shown below.

1. Determine the dynamic moment capacity of the component at each maximum moment location, taking into account any dynamic yield strength enhancement factors and any axial load effects as discussed in Chapters 5 through 8. In Figure 4-4, the fixed-end beam has maximum moment locations at both supports and at midspan.

2. Determine the location along the beam with the highest ratio of applied moment to dynamic moment capacity for a load with the same spatial distribution as the blast load. In Figure 4-4, where the blast load is uniformly distributed, this point is at both supports if the beam has a constant moment capacity along its length. Then, solve for the load causing an applied moment at this location equal to the dynamic moment capacity. This load is the initial elastic resistance, r_e, as shown in

Equation 4-9. If the component was determinate, it would be the ultimate resistance, r_u. The maximum deflection caused by this load is the initial yield deflection, x_e, in

3. Figure 4-5. The ratio of the r_e to x_e is the initial stiffness, k_e.

Equation 4-9

$$M_{\max}^{-} = \frac{wL^2}{12}$$

$$Let \quad M_{du}^{-} = M_{\max}^{-} \quad and \quad solve \quad for \quad w = R_e$$

$$r_e = \frac{12M_{du}^{-}}{L^2} \quad and \quad x_e = \frac{384 r_e L^4}{EI}$$

where:

M_{max}^{-}= moment at fixed supports from uniform load
w = uniform load per unit length on beam
L = span length
M_{du}^{-} = dynamic moment capacity of beam at supports
r_e = elastic resistance (uniform load per unit length causing yielding at supports). This can be converted to a pressure by dividing by the beam spacing.
x_e = initial yield deflection of beam
E = Young's modulus for beam

I = moment of inertia for beam

4. If the component is indeterminate, place a hinge at the location(s) of the initial yield with an applied resisting moment equal to the dynamic moment capacity. Repeat step 2 for the modified component with the hinge and applied resisting moment. If the component becomes a mechanism after repeating step 2, this load and corresponding maximum deflection are the ultimate resistance r_u, and yield deflection x_p, respectively. This is shown in Equation 4-10. Yield line theory can also be used. The stiffness after first yield is the elastoplastic stiffness, k_{ep}, equal to $(r_u-r_e)/(x_p-x_e)$.

5. If the component is not a mechanism after step 3, repeat step 2 by adding additional hinge(s) where yielding occurred during step 2 and applied resisting moments equal to the dynamic moment capacity until it is a mechanism. In this case, the resistance-deflection relationship will have more than two non-zero slopes. The final load causing the component to become a mechanism is the ultimate resistance. The ultimate resistance can also be determined using yield line theory as described in this section.

6. At deflections greater than the deflection at which the component becomes a mechanism, x_p, the resistance is assumed to remain constant at the ultimate resistance out to a failure deflection. The failure deflection, which can be quite large for a very ductile component, is contingent on component material properties, lateral bracing, detailing, and other considerations, depending on the component type. The deflections causing failure and other damage levels are discussed in Section 4-5.

7. It should be verified that a load on the component equal to the ultimate resistance does not cause component failure in any response mode other than flexural response. Therefore, the loads with the same spatial distribution as the blast load causing shear failure, buckling failure, connection failure, and failure in any other applicable response mode of the component should be greater than the ultimate resistance. For blast resistant design, the component should be sized, if possible, so that the ultimate resistance from flexural response of the component is less than the loads causing failure in other response modes.

8. If the ultimate load capacity from any other response mode is less than the ultimate resistance determined from flexural response as described in step 1-3, then the ultimate resistance is set equal to the lower ultimate load capacity from the controlling response mode. The resistance-deflection relationship based on flexure is usually applicable up the new, lower ultimate resistance. The resistance is then assumed to be constant at the ultimate resistance for greater deflections up to a limited failure deflection. However, the failure deflection for a response mode other than flexure may only be slightly greater than the deflection causing the ultimate resistance.

Equation 4-10

$$M_{\max}{}^{+} = \frac{wL^2}{8} - M_{du}{}^{-}$$

$$Let \quad M_{\max}{}^{+} = M_{du}{}^{+} \quad and \quad solve \quad for \quad w = r_u$$

$$r_u = \frac{8\left(M_{du}{}^{+} + M_{du}{}^{-}\right)}{L^2} \quad and \quad x_p = x_e + \frac{384\left(r_u - r_e\right)L^4}{5EI}$$

where:

$M_{max}{}^{+}$= maximum moment in beam at midspan
$M_u{}^{+}$ = dynamic moment capacity of beam at midspan
$M_u{}^{-}$ = dynamic moment capacity of beam at supports
r_u = ultimate resistance (uniform load per unit length causing yielding at midspan). This can be converted to a pressure by dividing by the beam spacing.
x_e = initial yield deflection of beam
x_p = final yield deflection of beam

This approach can be used to determine resistance-deflection relationships similar to those in Table 4-3 from Chapter 3 in TM 5-1300 and Appendix D.10.2 in UFC 3-340-01 for one-way components. Table 4-3 shows formulas for resistance and stiffness values that are used in SBEDS to define the flexural resistance-deflection relationships for one-way components with typical load and boundary conditions. The shear stiffness in Table 4-3 is not used in SBEDS.

The approach used in SBEDS to calculate the terms that define the resistance-deflection relationship of two-way components is more complicated. First, available design procedures for defining these terms will be discussed, and then the approach in SBEDS, which is based on these procedures, will be discussed.

Table 4-4 shows formulas for the ultimate resistances of two-way components based on yield line theory, where interior yield lines were extended straight into the corners and the moment capacities near the corners were conservatively limited to two-thirds of the dynamic moment capacity. This accounts for the fact that rotation in the corner is limited along the yield lines so that the full resisting moment capacity is not developed. The yield line dimensions (i.e., x and y) are determined based on the boundary conditions and moment capacities at yield locations as shown in Figure 4-6 through

Figure 4-8. Simple supports are accounted for with a zero negative moment capacity. See other notes at the bottom of

Table 4-4.

Chapter 3 in TM 5-1300 and Appendix D.10.2 in UFC 3-340-01 have examples showing the usage of these charts. Equivalent support shears, which equal the support reaction forces, are discussed in Section 4-3. Chapter 3 in TM 5-1300 and Appendix D.10.2 in UFC 3-340-01 have identical procedures that can be used to define the elastic and elastoplastic stiffnesses and resistances of the full resistance-deflection relationship for a variety of two-way slab components in a step-by-step method with simple equations and look-up values from graphs. The resulting resistance-deflection relationship may involve up to five stiffnesses.

Table 4-3 Flexural Resistances, Stiffnesses, and Support Shears for One-Way Members

Support Conditions and Loading Diagrams	Elastic Resistance	Ultimate Flexural Resistance	Stiffness: Bending[1,2]	Stiffness: Shear[3]	Equivalent Support Shears
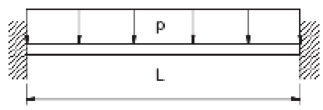	$r_e = \frac{12M_n}{L^2}$	$r_u = \frac{8\left(M_n + M_p\right)}{L^2}$	$k_e = \frac{384EI}{L^4}$ $k_{ep} = \frac{384EI}{5L^4}$ $k_E = \frac{307EI}{L^4}$	$k_e = k_{ep}$ $= \frac{hE}{0.35L^2}$	$V = \frac{r_u L}{2}$
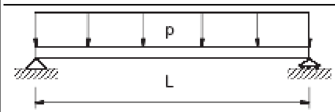	$r_e = r_u$	$r_u = \frac{8M_p}{L^2}$	$k_e = k_E = \frac{384EI}{5L^4}$	$k_e = \frac{hE}{0.35L^2}$	$V = \frac{r_u L}{2}$
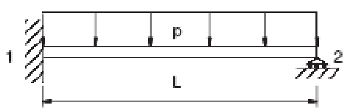	$r_e = \frac{8M_n}{L^2}$	$r_u = \frac{4\left(M_n + 2M_p\right)}{L^2}$	$k_e = \frac{185EI}{L^4}$ $k_{ep} = \frac{384EI}{5L^4}$ $k_E = \frac{160EI}{L^4}$	$k_e = k_{ep}$ $= \frac{hE}{0.35L^2}$	$V_1 = \frac{5r_u L}{8}$ $V_2 = \frac{3r_u L}{8}$
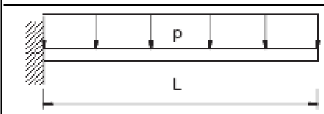	$r_e = r_u$	$r_u = \frac{2M_n}{L^2}$	$k_e = k_E = \frac{8EI}{L^4}$	$k_e = \frac{hE}{1.4L^2}$	$V = r_u L$
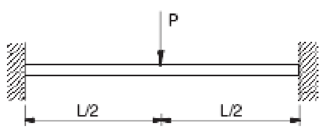	$r_e = \frac{8M_n}{L}$	$r_u = \frac{4\left(M_n + M_p\right)}{L}$	$k_e = \frac{192EI}{L^3}$ $k_{ep} = \frac{48EI}{L^3}$ $k_E = \frac{192EI}{L^3}$	$k_e = k_{ep}$ $= \frac{hE}{0.7L}$	$V = \frac{R_u}{2}$
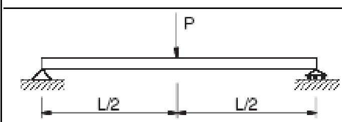	$r_e = r_u$	$r_u = \frac{4M_p}{L}$	$k_e = k_E = \frac{48EI}{L^3}$	$k_e = \frac{hE}{0.7L}$	$V = \frac{R_u}{2}$
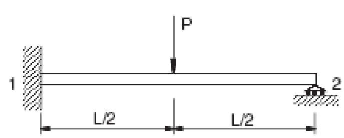	$r_e = \frac{16M_n}{3L}$	$r_u = \frac{2\left(M_n + 2M_p\right)}{L}$	$k_e = \frac{107EI}{L^3}$ $k_{ep} = \frac{48EI}{L^3}$ $k_E = \frac{106EI}{L^3}$	$k_e = k_{ep}$ $= \frac{hE}{0.7L}$	$V_1 = \frac{11r_u}{16}$ $V_2 = \frac{5r_u}{16}$
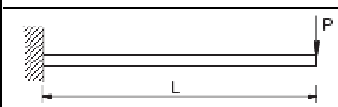	$r_e = r_u$	$r_u = \frac{M_n}{L}$	$k_e = k_E = \frac{3EI}{L^3}$	$k_e = \frac{hE}{2.8L}$	$V = r_u$

[1]Elastoplastic stiffnesses, k_{ep}, based on first yield occurring at fixed supports
[2]Equivalent stiffnesses, k_E, based on $M_n = M_p$.
[3]For concrete members where shear deformation is significant (L/h<5) it can be accounted for by combining bending stiffness (k_b) and shear stiffness (k_s) in the manner $k = 1/(1/k_b + 1/k_s)$.

Definitions and units:

- L = member span length (mm)
- M_n = ultimate negative (support) moment capacity per unit width (N-mm/mm)
- M_p = ultimate positive (interior) moment capacity per unit width (N-mm/mm)
- E = modulus of elasticity (MPa)
- I = moment of inertia per unit width (mm^4/mm) (I_a for slabs, see 10.3.6)
- P = point load (N)
- r_e = elastic unit resistance (MPa or N/mm)
- r_u = ultimate unit resistance (MPa or N/mm)
- k_e = elastic unit stiffness (MPa/mm or N/mm/mm)
- k_{ep} = elastoplastic unit stiffness (MPa/mm or N/mm/mm)
- k_E = equivalent elastic unit stiffness (MPa/mm or N/mm/mm)
- V = equivalent static support shears (N/mm)
- h = concrete member thickness (mm)
- p = uniform load (N/mm)

Table 4-4 Ultimate Flexural Resistances and Support Shears for Uniformly-Loaded Two- Way Members with Uniform Moment Capacities

Support Conditions and Yield Line Locations[3]	Ultimate Unit Resistance[4]	Equivalent Support Shears[5]	
		X-Span Support	Y-Span Support
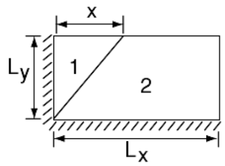	$r_1 = \dfrac{5\left(M_{nx} + M_{px}\right)}{x^2}$ $r_2 = \dfrac{6L_x M_{ny} + x\left(5M_{py} - M_{ny}\right)}{L_y^2\left(3L_x - 2x\right)}$	$V_x = \dfrac{3r_u x}{5}$	$V_y = \dfrac{3r_u L_y\left(2 - \frac{x}{L_x}\right)}{\left(6 - \frac{x}{L_x}\right)}$
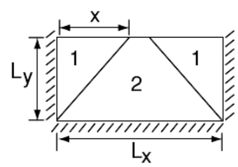	$r_1 = \dfrac{5\left(M_{nx} + M_{px}\right)}{x^2}$ $r_2 = \dfrac{2M_{ny}\left(3L_x - x\right) + 10x\,M_{py}}{L_y^2\left(3L_x - 4x\right)}$	$V_x = \dfrac{3r_u x}{5}$	$V_y = \dfrac{3r_u L_y\left(1 - \frac{x}{L_x}\right)}{\left(3 - \frac{x}{L_x}\right)}$
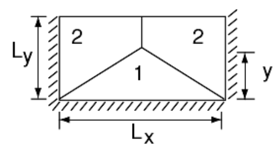	$r_1 = \dfrac{5\left(M_{ny} + M_{py}\right)}{y^2}$ $r_2 = \dfrac{4\left(M_{nx} + M_{px}\right)\left(6L_y - y\right)}{L_x^2\left(3L_y - 2y\right)}$	$V_x = \dfrac{3r_u L_x\left(2 - \frac{y}{L_y}\right)}{2\left(6 - \frac{y}{L_y}\right)}$	$V_y = \dfrac{3r_u y}{5}$
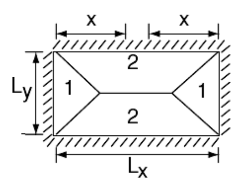	${}_1 = \dfrac{5\left(M_{nx} + M_{px}\right)}{x^2}$ $r_2 = \dfrac{8\left(M_{ny} + M_{py}\right)\left(3L_x - x\right)}{L_y\left(3L_x - 4x\right)}$	$V_x = \dfrac{3r_u x}{5}$	$V_y = \dfrac{3r_u L_y\left(1 - \frac{x}{L_x}\right)}{2\left(3 - \frac{x}{L_x}\right)}$

[1]Definitions and units:

- L_x and L_y = x- and y-span lengths (mm)
- M_{nx} and M_{ny} = ultimate negative (support) moment capacity per unit width in x- and y-span directions (N-mm/mm)
- M_{px} and M_{py} = ultimate positive (interior) moment capacity per unit width in x- and y-span directions (N-mm/mm)
- r_u = ultimate unit resistance (MPa)
- V_x and V_y = equivalent static support shears in x- and y-span directions (N/mm)
- x and y = yield line locating dimensions (mm)

[2]Numeric subscripts on variables refer to member sector numbers.

[3]Simply supported edges may be accounted for by setting the appropriate support capacity (M_n) equal to zero.

[4]Ultimate resistance, r_u, is obtained by solving $r_1 = r_2$ for x or y, then back substituting for $r_u = r_1 = r_2$.

[5]Equivalent support shears are calculated using r_u for a Type I section.

Figure 4-6 Location of Symmetrical Yield Lines for Two-Way Component with Four Edges Supported

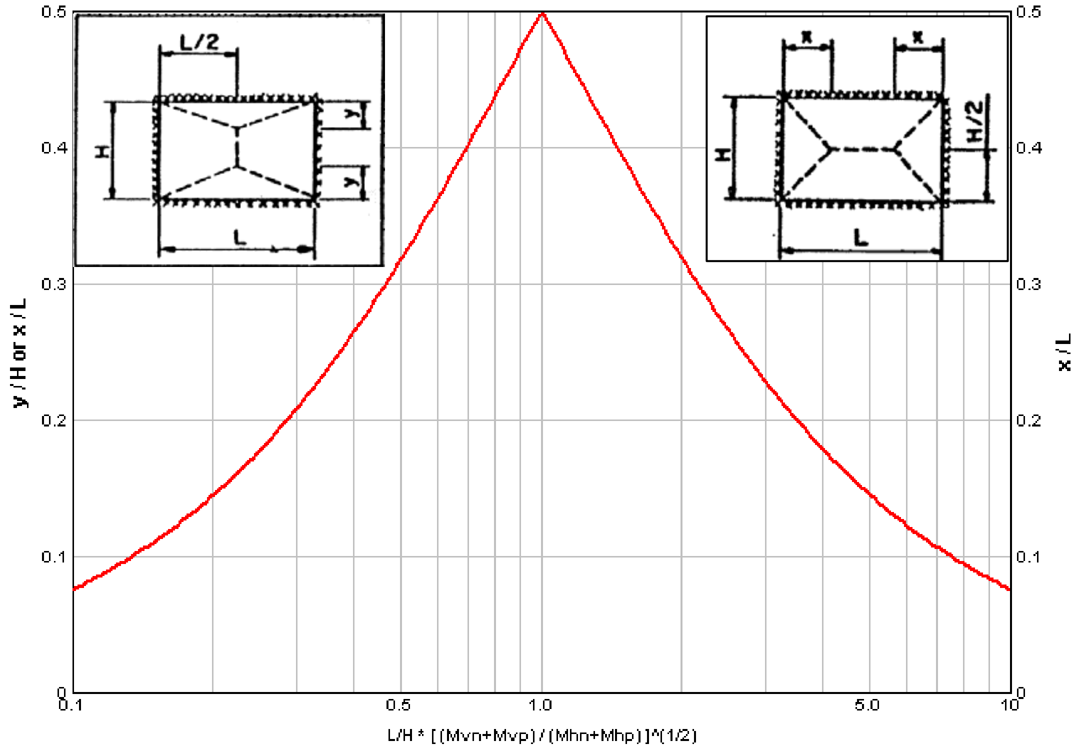

Figure 4-7 Location of Symmetrical Yield Lines for Two-Way Component with Three Edges Supported

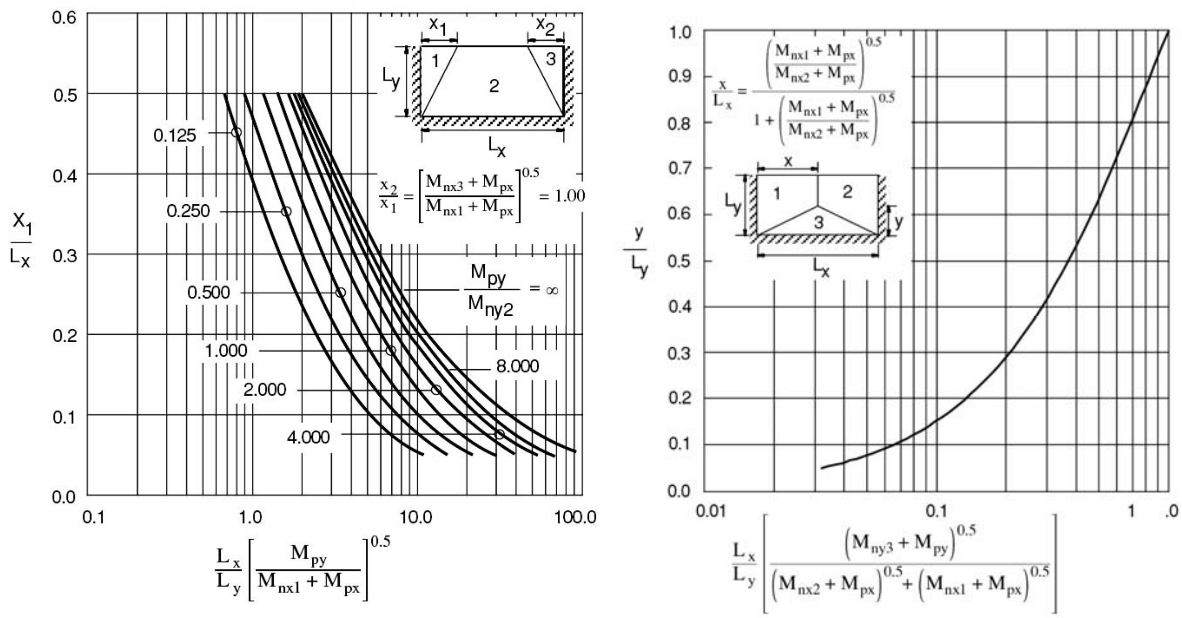

Figure 4-8 Location of Yield Lines for Two-Way Component with Two Adjacent Edges Supported

Methodology Manual TOC

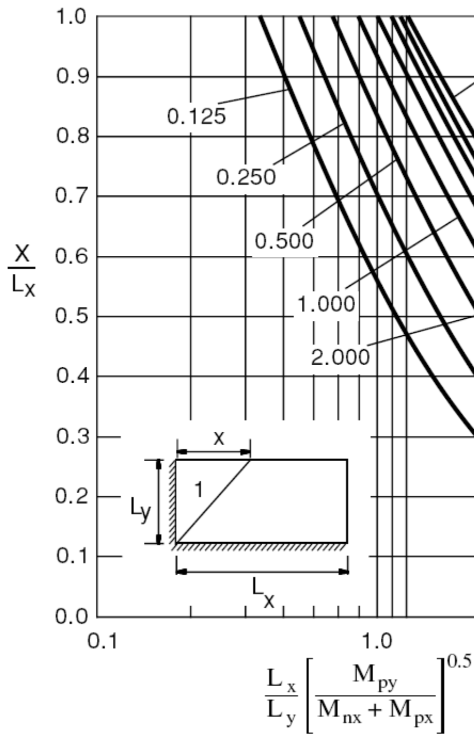

A simplified approach for determining the resistance-deflection relationships for two-way components is presented in Chapter 10 of UFC 3-340-01. This resistance-deflection relationship consists of two non-zero stiffness ranges for components with fixed boundary conditions, representing the initial elastic stiffness and resistance and an average elastoplastic stiffness up to the ultimate resistance. A single elastic stiffness is used for components with simple supports. Table 4-5 shows recommended stiffness and resistance values for this approach. The nomenclature for moment capacities in Table 4-5 is such that moments at positive yield lines cause compressive stresses at the loaded face of the member while moments at negative yield lines cause tensile stresses at the loaded face. Terms in Table 4-5 are defined in the notes that follow the table

The ultimate resistances for two-way components in Table 4-5 are determined with yield line theory of slabs using 0.785-rad (45-deg) yield line locations from all corners as shown in the table and adding a 10 percent reduction to correct for corner effects for cases with fixed supports (Morison, 2005). Although the resulting equations are not exact, the error in ultimate resistance is less than 5 percent for plates with uniform moment capacities in both directions. The previously described yield line method from Chapter 3 in TM 5-1300 and Appendix D.10.2 in UFC 3-340-01 is generally more accurate because it does not assume equal moment capacities in both directions. However, Table 4-5 is a simpler procedure and its usage is often justified by the overall approximate nature of the SDOF analysis procedure, as discussed in Section 4-8.

Table 4-5 Approximate Flexural Resistances, Stiffnesses, and Support Shears for Two-Way Members

Methodology Manual TOC

Member Support Conditions and Yield Line Locations	L_y/L_x	Resistances[1,2] r_e	Resistances[1,2] r_u	Stiffness[1,3] k_e ($\times EI/L_xL_y^3$)	Stiffness[1,3] k_{ep} ($\times EI/L_xL_y^3$)	Equivalent Support Shears[1] V_x ($\times r_uL_x$)	Equivalent Support Shears[1] V_y ($\times r_uL_y$)
① 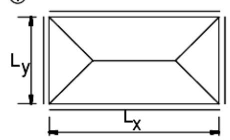	1.0	–	$(12.0/L_xLy)(M_{px}+1.00M_{py})$	252	–	0.30	0.30
	0.9	–	$(12.0/L_xLy)(M_{px}+1.02M_{py})$	230	–	0.27	0.32
	0.8	–	$(12.0/L_xLy)(M_{px}+1.07M_{py})$	212	–	0.24	0.35
	0.7	–	$(12.0/L_xLy)(M_{px}+1.17M_{py})$	201	–	0.21	0.37
	0.6	–	$(12.0/L_xLy)(M_{px}+1.29M_{py})$	197	–	0.18	0.39
	0.5	–	$(12.0/L_xLy)(M_{px}+1.50M_{py})$	201	–	0.15	0.41
② 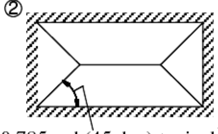	1.0	$29.2M_{ny}/L_xLy$	$(10.8/L_xLy)[M_{nx}+M_{px}+1.00(M_{ny}+Mpy)]$	810	252	0.30	0.30
	0.9	$27.4M_{ny}/L_xLy$	$(10.8/L_xLy)[M_{nx}+M_{px}+1.02(M_{ny}+Mpy)]$	740	230	0.27	0.32
	0.8	$26.4M_{ny}/L_xLy$	$(10.8/L_xLy)[M_{nx}+M_{px}+1.07(M_{ny}+Mpy)]$	700	212	0.24	0.35
	0.7	$26.2M_{ny}/L_xLy$	$(10.8/L_xLy)[M_{nx}+M_{px}+1.17(M_{ny}+Mpy)]$	690	201	0.21	0.37
	0.6	$27.3M_{ny}/L_xLy$	$(10.8/L_xLy)[M_{nx}+M_{px}+1.29(M_{ny}+Mpy)]$	730	197	0.18	0.39
0.785 rad (45 deg) typical[1]	0.5	$30.2M_{ny}/L_xLy$	$(10.8/L_xLy)[M_{nx}+M_{px}+1.50(M_{ny}+Mpy)]$	810	201	0.15	0.41
③ 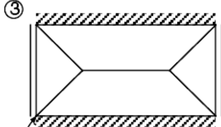	1.0	$20.4M_{ny}/L_xLy$	$(10.8/L_xLy)[M_{px}+1.00(M_{ny}+M_{py})]$	530	252	0.30	0.30
	0.9	$19.5M_{ny}/L_xLy$	$(10.8/L_xLy)[M_{px}+1.02(M_{ny}+M_{py})]$	540	230	0.27	0.32
	0.8	$19.5M_{ny}/L_xLy$	$(10.8/L_xLy)[M_{px}+1.07(M_{ny}+M_{py})]$	560	212	0.24	0.35
	0.7	$20.2M_{ny}/L_xLy$	$(10.8/L_xLy)[M_{px}+1.17(M_{ny}+M_{py})]$	600	201	0.21	0.37
	0.6	$21.2M_{ny}/L_xLy$	$(10.8/L_xLy)[M_{px}+1.29(M_{ny}+M_{py})]$	670	197	0.18	0.39
Fixed Edge, typical	0.5	$22.2M_{ny}/L_xLy$	$(10.8/L_xLy)[M_{px}+1.50(M_{ny}+M_{py})]$	790	201	0.15	0.41
④ 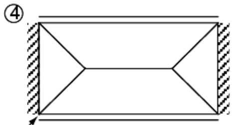	1.0	$20.4M_{nx}/L_xLy$	$(10.8/L_xLy)(M_{nx}+M_{px}+1.00M_{py})$	530	252	0.30	0.30
	0.9	$(10.2/L_xLy)(M_{nx}+1.20M_{py})$	$(10.8/L_xLy)(M_{nx}+M_{px}+1.02M_{py})$	440	230	0.27	0.32
	0.8	$(10.2/L_xLy)(M_{nx}+1.26M_{py})$	$(10.8/L_xLy)(M_{nx}+M_{px}+1.07M_{py})$	360	212	0.24	0.35
	0.7	$(9.3/L_xLy)(M_{nx}+1.49M_{py})$	$(10.8/L_xLy)(M_{nx}+M_{px}+1.17M_{py})$	300	201	0.21	0.37
	0.6	$(8.5/L_xLy)(M_{nx}+1.82M_{py})$	$(10.8/L_xLy)(M_{nx}+M_{px}+1.29M_{py})$	260	197	0.18	0.39
Simple Edge, typical	0.5	$(7.4/L_xLy)(M_{nx}+2.43M_{py})$	$(10.8/L_xLy)(M_{nx}+M_{px}+1.50M_{py})$	240	201	0.15	0.41
⑤ 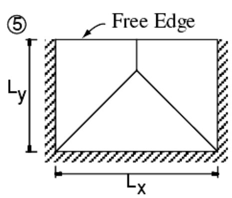	2.0	$27.1M_{nx}/L_xLy$	$(5.4/L_xLy)[M_{ny}+M_{py}+2.80(M_{nx}+M_{px})]$	3410	564	0.46	0.15
	1.8	$24.8M_{nx}/L_xLy$	$(5.4/L_xLy)[M_{ny}+M_{py}+2.54(M_{nx}+M_{px})]$	2090	409	0.45	0.17
	1.6	$22.3M_{nx}/L_xLy$	$(5.4/L_xLy)[M_{ny}+M_{py}+2.27(M_{nx}+M_{px})]$	1320	288	0.45	0.19
	1.4	$19.9M_{nx}/L_xLy$	$(5.4/L_xLy)[M_{ny}+M_{py}+2.01(M_{nx}+M_{px})]$	838	196	0.44	0.21
	1.2	$17.5M_{nx}/L_xLy$	$(5.4/L_xLy)[M_{ny}+M_{py}+1.75(M_{nx}+M_{px})]$	521	128	0.43	0.25
	1.0	$15.1M_{nx}/L_xLy$	$(5.4/L_xLy)[M_{ny}+M_{py}+1.50(M_{nx}+M_{px})]$	310	79	0.41	0.30
	0.9	$14.3M_{nx}/L_xLy$	$(5.4/L_xLy)[M_{ny}+M_{py}+1.38(M_{nx}+M_{px})]$	233	61	0.40	0.33
	0.8	$13.5M_{nx}/L_xLy$	$(5.4/L_xLy)[M_{ny}+M_{py}+1.26(M_{nx}+M_{px})]$	171	46	0.38	0.38
	0.7	$13.1M_{nx}/L_xLy$	$(5.4/L_xLy)[M_{ny}+M_{py}+1.15(M_{nx}+M_{px})]$	121	34	0.36	0.43
	0.6	$13.4M_{nx}/L_xLy$	$(5.4/L_xLy)[M_{ny}+M_{py}+1.05(M_{nx}+M_{px})]$	82	25	0.34	0.50
	0.5	$14.6M_{nx}/L_xLy$	$(5.4/L_xLy)[M_{ny}+M_{py}+1.00(M_{nx}+M_{px})]$	52	18	0.30	0.60

Methodology Manual TOC

Notes:
[1]Equations for r^u,V^x, and V_y in this table are based on approximate (0.785 rad [45 deg]) positive yield line positions. Equations for r_e, k_e, and k_{ep} in this table are based on elastic uniform plate theory, except that for fixed edge cases r_e has been determined when most of the support length has yielded. Values of k_{ep} are given for the condition of all supports fully yielded, effectively omitting one intermediate elastoplastic step for Cases 2 and 5.
[2]Ultimate resistance, r_u, values for members with fixed supports (Cases 2 through 5) have been reduced 10 percent to account for a more detailed yield line configuration (fan pattern) near corners.
[3]Stiffness coefficients listed are for a Poisson's ratio of 0.15 (concrete). For a Poisson's ratio of 0.30 (steel), stiffness values are approximately 7 percent greater.
[4]Definitions and Units.
L_x and L_y = x and y-span lengths (mm or inch)
M_{nx} and M_{ny} = Ultimate negative (support) moment capacity per unit width in x- and y-span directions (N-mm/mm or b-in/in)
M_{px} and M_{py} = Ultimate positive (interior) moment capacity per unit width in x- and y-span directions (N-mm/mm or b-in/in)
E =Modulus of elasticity (MPa or psi)
I =Moment of inertia per unit width (mm^4/mm of in^4/in) (Ia for slabs, see 10.3.6)
r =Elastic unit resistance (MPa or psi)
r_u = Ultimate unit resistance (MPa or psi)
k_e = Elastic unit stiffness (MPa/mm or psi/in)
k_{ep} = Elastoplastic unit stiffness (MPa/mm or psi/in)
V_x and V_y = Equivalent static support shears in x- and y-span directions (N/mm or lb/in)

Further information on available procedures for determining the resistance-deflection relationship of two-way spanning components is available in other references. A detailed description of yield line theory using both the virtual work and equilibrium methods is provided by Park and Gamble (2000). Chapter 3 in TM 5-1300 has a very useful discussion based on the equilibrium method that is concise and oriented towards SDOF design applications. Appendix D.10.2 in UFC 3-340-01 also has formulas based on yield line theory, which are similar to those in

Table 4-4, for determining the ultimate resistance of slabs with openings, including windows and doors. Elastic and elastoplastic resistances and stiffnesses slabs with openings are typically assumed equal to those without openings. A static finite element approach with material non-linearity can also be used to develop the full resistance-deflection relationship for two-way components responding in flexure. This approach can be particularly useful for cases with unusual geometry and loading conditions.

SBEDS determines the resistances of two-way components based on

Table 4-4 with an 8% increase factor and curve-fits to Figure 4-6 through

Figure 4-8. The ultimate resistance in

Table 4-4 is based on the assumption that only two-thirds of the moment capacity acts at corners, as discussed previously. The 8% increase factor is included because studies by Morison (2005) show that this approach overcorrects for straight extension of yield lines into corners by 6% to 10% compared to advanced analyses with yield lines that transition to multiple fan-shaped and triangular shaped yield lines in the corners.

The initial stiffness of the resistance-deflection relationship in SBEDS for two-way components is equal to the elastic stiffness of the component using Figure 3-23 through

Figure 3-38 in Chapter 3 of TM 5-1300, which are also shown in Appendix D.10.2 in UFC 3-340-01. Figure 4-9 shows one of these figures to determine the stiffness of a two-way component with three edges simply supported and one edge free. A curve-fit for the parameter γ_1 in these figures is used in SBEDS to get the stifffnesses of two-way spanning components. If the component only has simple supports, the resistance-deflection relationship only has one stiffness equal to the elastic stiffness. If the component has fixed supports, the resistance-deflection relationship also has an elastoplastic stiffness equal to the elastic stiffness for the same component with simple supports (i.e., assuming yield at all negative supports). The elastic resistance is equal to the elastic resistance for the component from Table 4-5. The elastic resistance from Table 4-5 is much easier to use than similar values determined with the TM 5-1300 methodology. An exception to this is the boundary condition with two adjacent fixed edges and two adjacent free edges, which is not included in Table 4-5. In this case, the initial elastic resistance is assumed equal to 60% of the ultimate resistance.

Figure 4-9 Stiffness Coefficients for Uniformly-Loaded Two-Way Component with Three Edges Simply-Supported and One Edge Free

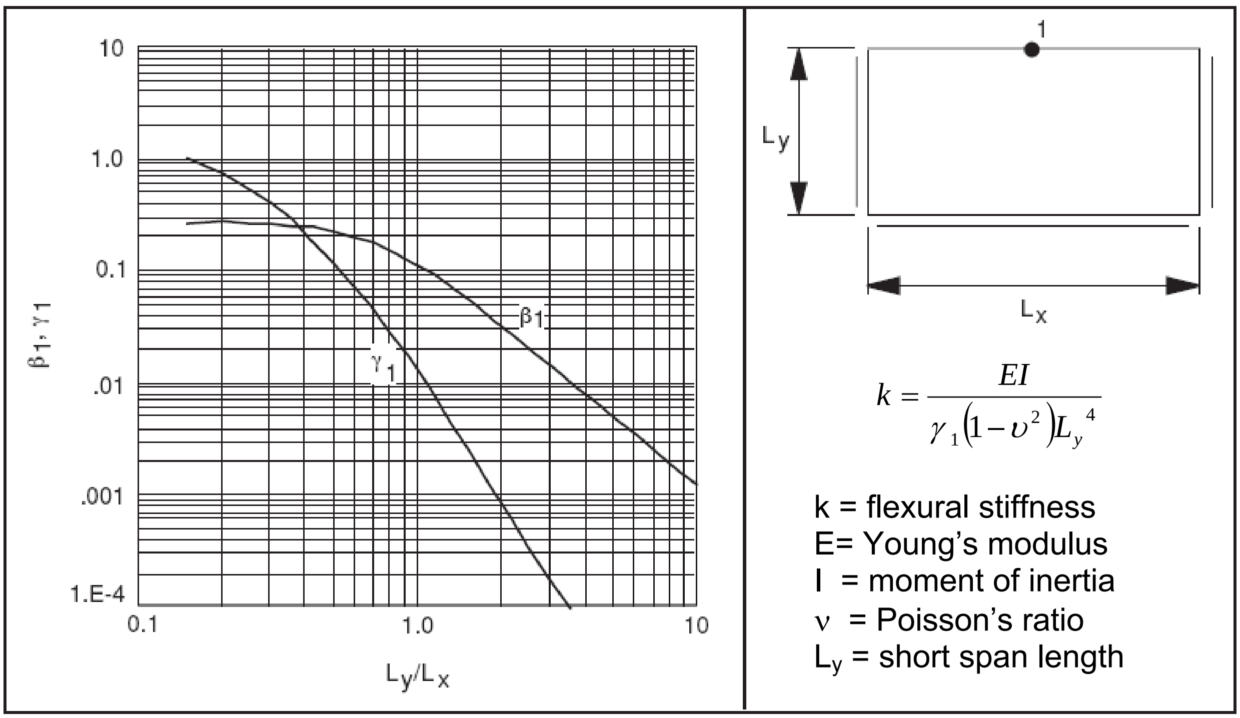

As discussed in Section 4-1.2.4, the strain energy for ductile flexural response, and therefore the maximum response, is usually dependent primarily on plastic response. Therefore, the ultimate resistance usually has a much larger affect on the maximum dynamic response than the elastic and elastoplastic resistances and stiffnesses and a simplified approach for determining these parameters is justified.

4-1.2.2 RESISTANCE-DEFLECTION RELATIONSHIPS FOR OTHER STRUCTURAL RESPONSE MODES

Compression membrane, tension membrane, shear, and arching from axial load are other response modes that can significantly affect the component resistance-deflection relationships, depending on the component type and boundary conditions. These response modes can act together with flexural response, as discussed in the following paragraphs.

4-1.2.2.1 **TENSION MEMBRANE RESPONSE**

Tension membrane response occurs at relatively large lateral displacements when the boundary conditions prevent inward, in-plane movement of the supports so that catenary action occurs. The component develops tension forces that form a resisting couple with in-plane restraining forces at the supports, which acts to resist applied out-of-plane lateral load as shown in Figure 4-10. Theoretically, tension membrane response begins as soon as the component deflects if the component has very rigid supports against in-plane movement. However, this level of support rigidity almost never occurs in buildings and tension membrane response is almost always assumed to occur after flexural response. Therefore, flexural response occurs initially as the component deflects, followed by tension membrane response that acts with flexural response at deflections after flexural yielding. If the maximum tension force in the component is not limited by the connection strength, all the stress in the maximum moment region transitions to tension stress at very large lateral deflections and the response is predominately only tension membrane.

Figure 4-11 shows the measured resistance-deflection relationship for a cold formed steel beam with boundary conditions fully restrained against in-plane movement. In a series of many such tests, it was only possible to bound the measured the resistance-deflection relationships as indicated in Figure 4-11 (Salim et al, 2003). In an actual building, there is typically more flexibility in the supports and local yielding around the connections than for these tests. There is no well validated approach for including tension membrane response in a resistance-deflection relationship due to a number of variables affecting tension membrane that are difficult to fully understand and control, even under test conditions.

Figure 4-10 Illustration of Tension Membrane Response

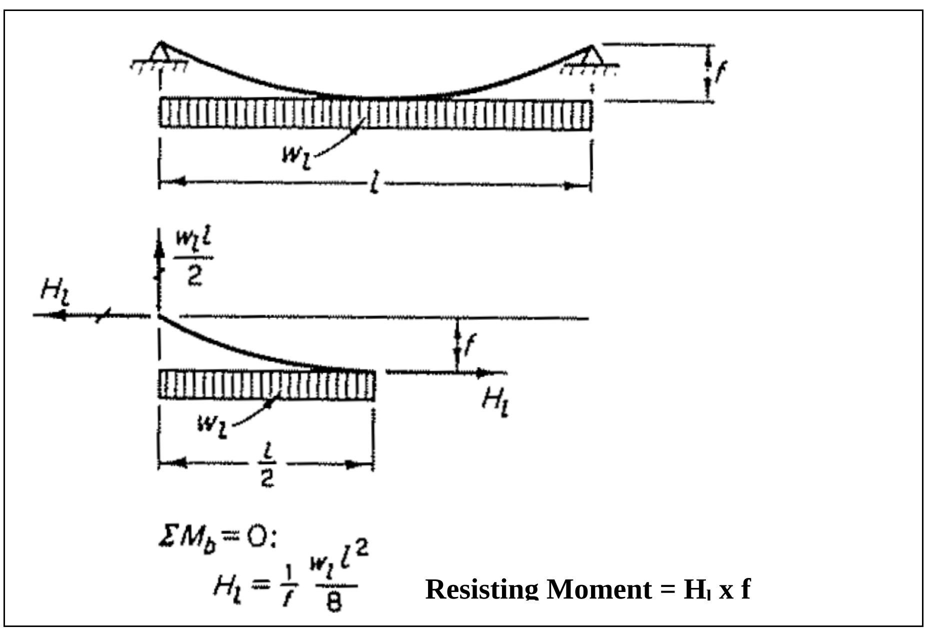

Figure 4-12 shows how tension membrane response is simplistically included in the resistance-deflection relationships for steel components in SBEDS. It is intended to be used primarily with light, cold-formed steel components, as discussed more in Section 6-6. A constant tension membrane stiffness based on the maximum tension that can develop in the component is assumed to add to the flexural response at deflection greater than x_{TM}, which is calculated as shown in Equation 4-11. The maximum tension of lightweight steel components is usually limited by the shear capacity of the connections rather than the cross sectional tension capacity of the component. x_{TM} in Equation 4-11 is the sum of the deflection at which the component becomes a mechanism in flexure plus the theoretical deflection required to develop the maximum tension in the component in pure, elastic catenary action with no support or connection flexibility.

Figure 4-11 Resistance-Deflection Relationship for Steel Stud with Restrained Boundaries (from Salim et al, 2003)

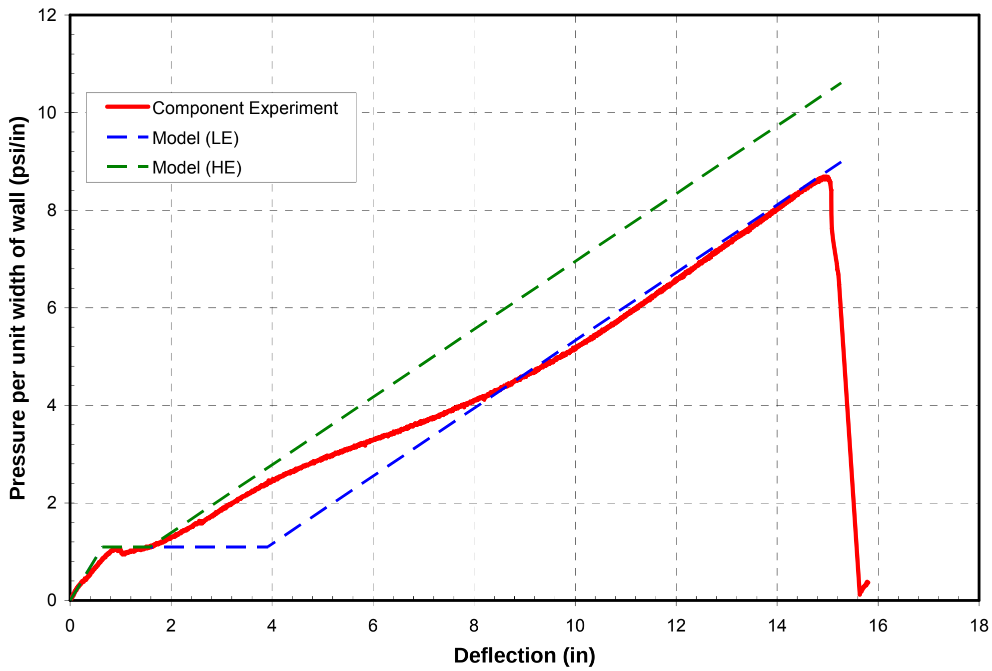

The approximate approach in Figure 4-12 is an attempt to account for support and connection flexibility in structures with typical lightweight steel components, such as panels and cold-formed beams, and be generally consistent with static and blast test data for components with combined flexure and tension membrane response. The support and connection flexibility are assumed to delay significant tension buildup in the component until after it fully yields, and then the supports are assumed to act rigidly against further in-plane movement. The maximum deflections based on SDOF calculations with the resistance-deflection relationship in Figure 4-12 compared reasonably well to test data on cold-formed steel girts from one-half scale shock tube tests, as indicated in Figure 4-13 (Oswald et al, 1998).

A typical resistance-deflection relationship for reinforced concrete or masonry with in-plane restraint at the boundaries is shown in Figure 4-14, where tension

membrane response is modeled with a linear increase in resistance above the ultimate flexural resistance as shown in the figure. This figure also shows compression membrane response, which is discussed in the next section. Static tests on reinforced concrete slabs show that x_{TM} can be based on the intersection of the tension membrane slope, K_{Tm}, and the ultimate flexural resistance, r_u, as shown in Figure 4-14. This typically results in a larger value for x_{TM} than using Equation 4-11, which is considered more applicable for light steel components. Unfortunately, only semi-empirical methods that are component-type dependent are available including tension membrane response in resistance-deflection relationships, such as those in Figure 4-12 and Figure 4-14. There is a slight reduction in r_u to r_{uII} in Figure 4-14, to account for a Type II cross section in reinforced concrete components as discussed in Chapter 5-2.1. Formulas for K_{Tm} for one-way and two-way reinforced concrete and masonry components are shown in Equation 4-12 and

Equation 4-13, respectively.

Figure 4-12 Resistance Deflection Curve for Steel Components with Tension Membrane

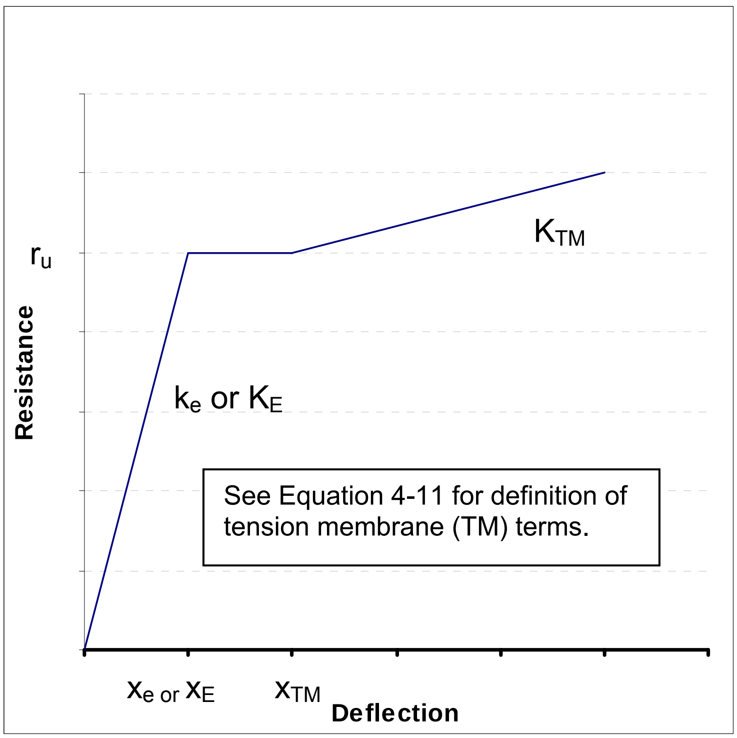

Equation 4-11

Methodology Manual TOC

$$x_{TM} = x_E + \sqrt{\frac{4TL^2}{\pi^2 EA}} \quad \text{where} \quad T = \text{Minimum}\left[\left(f_{dy}A\right), V_c\right]$$

$$K_{TM\_1} = \frac{8T}{bL^2}$$

$$K_{TM\_2} = \frac{T\pi^3}{4bL_y{}^2 \sum\limits_{n=1,3,5,7}\left[\frac{1}{n^3}(-1)^{(n-1)/2} A\right]} \quad \textit{where} \quad A = 1 - \frac{1}{\cosh \frac{n\pi L_x}{2L_y}} \quad \textit{and} \quad L_x \geq L_y$$

where:
- x_{TM}= assumed deflection at beginning of linear tension membrane response adding to flexural response for one and two-way response
- K_{TM_i}= linear tension membrane slope for one-way (i=1) or two-way (i=2) response
- x_E = equivalent elastic yield deflection
- f_{dy} = dynamic yield strength
- A = component cross sectional area within loaded width b
- V_c = support force available for resisting component tension (Based on lesser of connection capacity or in-plane flexural capacity of supporting framing member)
- L = span length (least span length for two-way components)
- E = Young's modulus for steel
- b = supported width loaded by blast (typically a unit width for panels or plates)

Figure 4-13 Comparison of Measured Maximum Deflections of Lightweight Steel Beams to Predicted Values with SBEDS Method

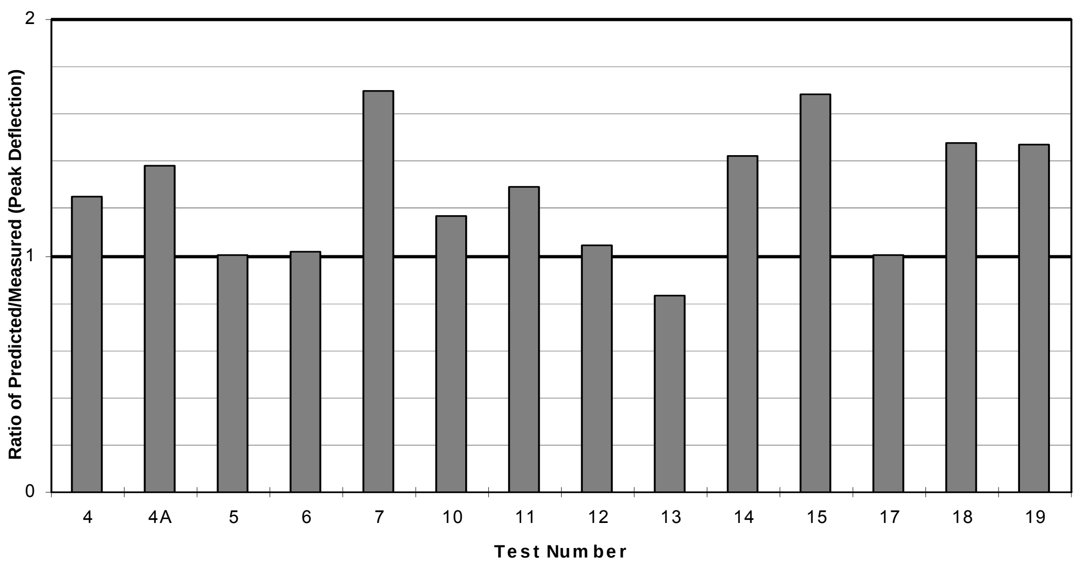

Tension and/or compression membrane response can be assumed for a component only if the component boundary conditions meet the restraint requirements in

Figure 4-15. As shown in

Figure 4-15, a two-way component with an aspect ratio between 0.5 and 2 can be assumed to develop a compression ring, as shown in Figure 4-16, so that tension membrane resistance occurs even if the supports provide no in-plane restraint. As the central portion of the slab reaches large deflections, compression struts that form along the component edges parallel to the span direction keep the edges of the component from deflecting inward near midspan. This occurs in both directions. Reinforced concrete components must also have continuous steel through the span that is unspliced or has splices that can develop the full tension strength at large deflections.

4-1.2.2.2 **COMPRESSION MEMBRANE RESPONSE**

Compressive membrane response can also occur after flexural response in a component if it has rigid supports on both sides of the span length that do not allow rotation of the component cross section into the supports. Components with non-rigid supports that are fixed against rotation in flexure (i.e., fixed supports) allow rotation at the support after yielding of the reinforcing steel. Figure 4-17 shows the forces that develop during compression membrane response. Compressive bearing stresses develop at the boundaries between the rigid support, which prevents the component from rotating into the support, and the unloaded face of the component. Similar compressive stresses develop between the compression block areas near the loaded face of the component at the yield region near midspan. The component can only rotate, and therefore deflect, as increasing amounts of crushing occur at these two locations.

Figure 4-14. Resistance-Deflection Curve for Reinforced Concrete and Masonry Components with Compression and Tension Membrane

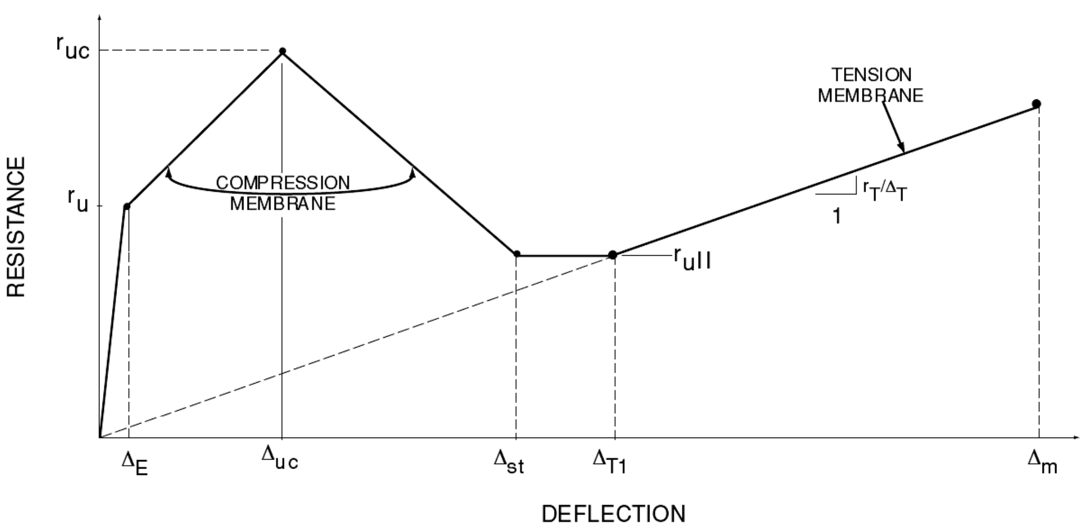

r_{uc} = COMPRESSIVE MEMBRANE ULTIMATE RESISTANCE TO UNIFORM LOAD (PARAGRAPH 10.4.2)

Δ_{uc} = CENTRAL DEFLECTION OCCURING AT r_{uc} (PARAGRAPH 10.4.2)

r_{uII} = FLEXURAL RESISTANCE USING TYPE II ULTIMATE MOMENT CAPACITY (PARAGRAPHS 10.3.3.2 AND 10.9.1)

r_T/Δ_T = TENSILE MEMBRANE RESISTANCE/CENTRAL DEFLECTION (PARAGRAPH 10.4.3)

Δ_m = MAXIMUM CENTRAL DEFLECTION, CORRESPONDING TO DESIGN RESPONSE LIMIT (PARAGRAPH 10.10)

Δ_{st} = CENTRAL DEFLECTION AT SNAP-THROUGH (PARAGRAPH 10.4.2)

Δ_{T1} = CENTRAL DEFLECTION WHERE TENSILE MEMBRANE SLOPE THROUGH ORIGIN REACHES r_{uII} (BUT $\Delta_{T1} \geq \Delta_{st}$)

r_u = ULTIMATE FLEXURAL RESISTANCE TO UNIFORM LOAD (PARAGRAPH 10.9.1)

Δ_E = EQUIVALENT ELASTIC DEFLECTION IN FLEXURE (PARAGRAPH 10.9.1)

Equation 4-12

$$\frac{r_T}{\Delta_T} = K_{Tm} = \frac{8T_t}{L^2} \qquad where \quad T_t = 0.5 f_u A_{tot}$$

where: K_{Tm} = tension membrane stiffness
T_t = ultimate tensile force per unit width assuming 50% of total reinforcement along span effectively resists tension at large displacement and is fully strain hardened
A_{tot} = total reinforcement per unit width continuous over span from both faces (based on lesser of input negative and positive moment area steel at each face in SBEDS)
L = clear span dimension
f_u = ultimate strength of reinforcing steel

Equation 4-13

$$\frac{r_T}{\Delta_T} = K_{Tm} = \frac{T_{ty}\pi^3}{4L_y^2 \sum_{n=1,3,5...}^{\infty}\left[\frac{1}{n^3}(-1)^{\frac{n-1}{2}}(A)\right]}$$

$$A = 1 - \frac{1}{\cosh\left[\frac{n\pi L_x}{2L_y}\sqrt{\frac{T_{ty}}{T_{tx}}}\right]}$$

$$T_{ty} = 0.5 f_u A_{y\_tot} \quad T_{tx} = 0.5 f_u A_{x\_tot}$$

where: $r_T / \Delta_T = K_{Tm}$ = tension membrane stiffness
r_T = tensile membrane resistance to uniform load
Δ_T = midspan deflection
T_{ti} = ultimate tensile force per unit width in the i direction (i=x or y), assuming 50% of total reinforcement along span effectively resists tension at large displacement and is fully strain hardened
A_{i_tot} = total reinforcement per unit width continuous over span in "i" direction from both faces (based on lesser of input negative and positive moment area steel at each face in SBEDS)
L_y = lesser of the clear span dimensions
f_u = ultimate strength of reinforcing steel

The compressive forces associated with the crushing at the loaded face near midspan and at the unloaded faces at the supports, as shown in Figure 4-17 where the material crushing strength is represented as f'_m, form a resisting couple. This couple, or resisting moment, resists lateral load in addition to any ductile flexural resisting moments. The compression membrane forces are based on the material crushing strength acting over an area that increases as the component deflects. The moment arm between the compression forces at midspan and at the supports is a maximum value at small deflections and decreases to zero at a deflection near the component thickness.

Figure 4-14 shows the assumed resistance deflection response for compression membrane response in a component with ductile flexural response. The resistance increases linearly above the flexural resistance due to compression membrane response to a peak resistance, and then reduces to the flexural resistance at a deflection that is a little less than the component thickness when the resisting moment caused by compression membrane response becomes equal to zero. Therefore, compression membrane response adds a large triangular area above the resistance-deflection relationship of a component with ductile flexural response. The resistance-deflection relationship of a component with brittle flexural response is similar except that all resistance after peak flexural response is due to compression membrane response alone. Therefore, the total resistance reduces to zero at a deflection that is a little less than the component thickness.

Figure 4-15. Boundary Conditions for Tension and Compression Membrane Response

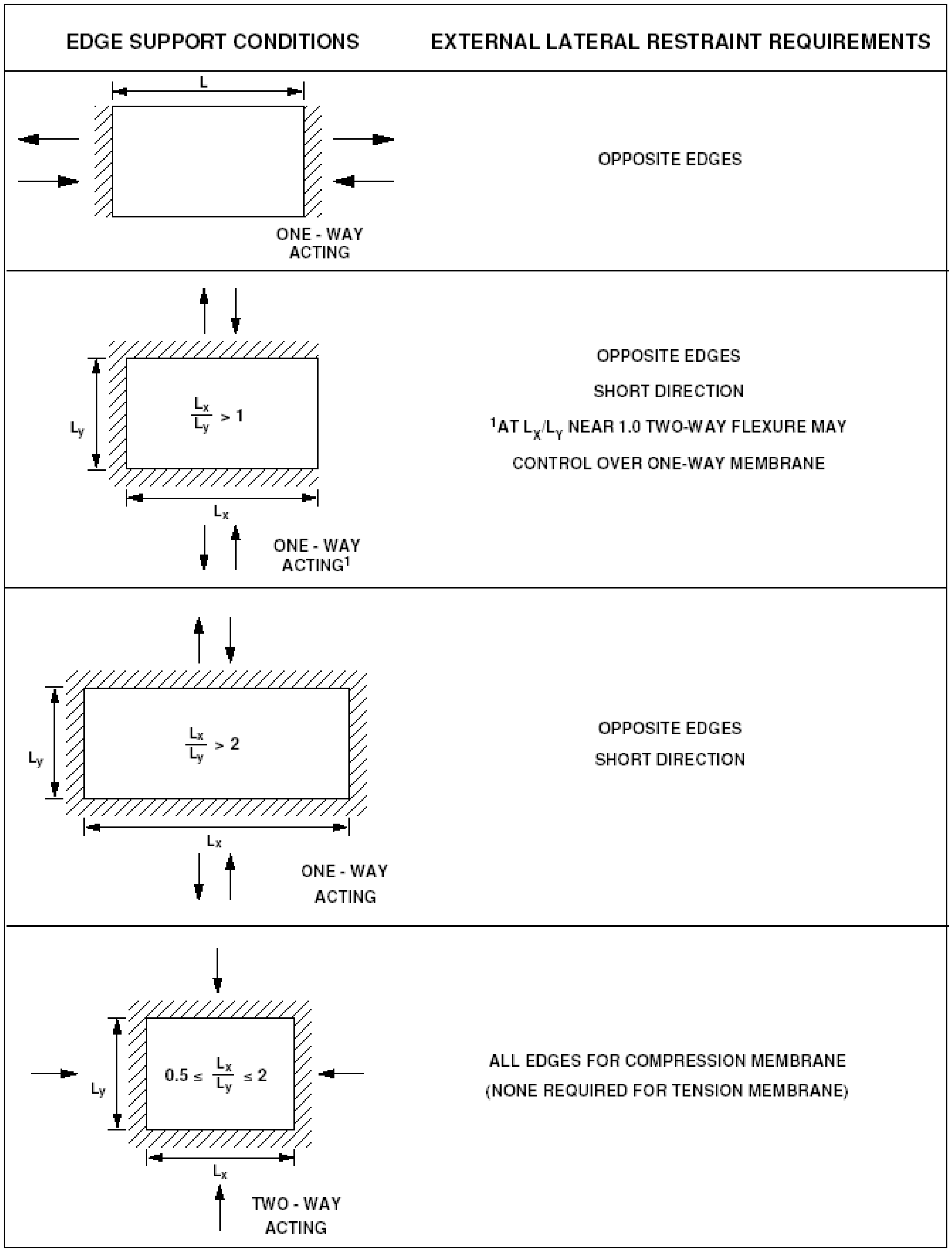

Figure 4-16 Compression Ring Effect Providing In-Plane Restraint for Tension Membrane in Two-Way Component (from Park and Gamble, 2000)

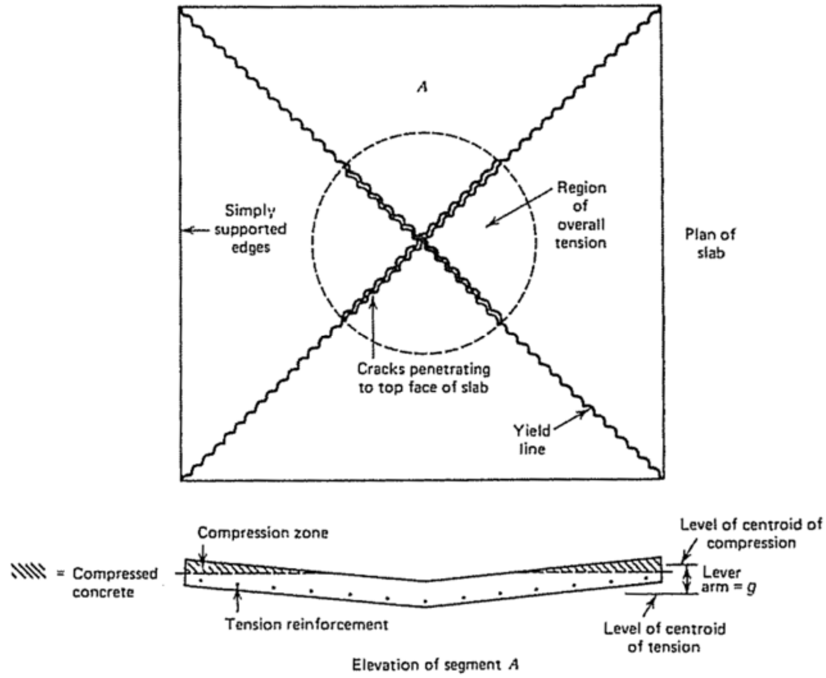

Figure 4-17 Forces Developing During Compression Membrane Response

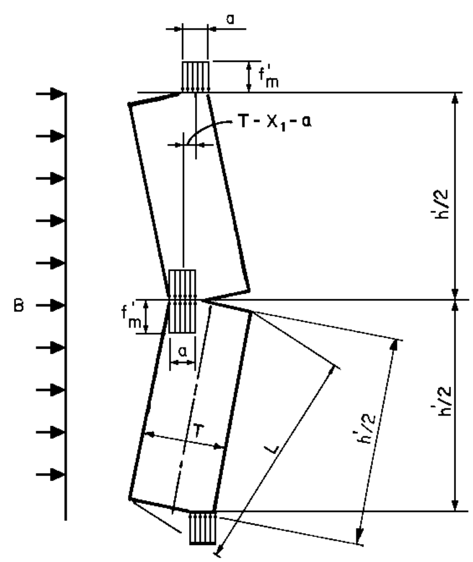

Resisting moment = $f'_m\, a(T - x_1 - a)$, *where* x_1 *= midspan deflection*
f'_m *represents material crushing strength*

Significant compression membrane resistance typically develops in relatively thick components, such as reinforced concrete and masonry, rather than thin components, such as steel plate and panels. Compression membrane is very sensitive to support flexibility (i.e., much more so than tension membrane) and to any small gap between the component and framing, such as an expansion gap between an in-fill wall and the surrounding frame. Therefore, it only develops in thick components with a relatively tight fit between the component and massive, stiff, supports, and components where adjacent spans rotate against each other at their common support. Examples include an infill concrete or masonry wall within a reinforced concrete frame, the interior spans of a reinforced concrete slab that is continuous over its supports, and a monolithic reinforced concrete box structure with heavy corner reinforcing steel such as that required in TM 5-1300. Compression membrane response is only included in the list of available resistance-deflection relationships for concrete and masonry components in SBEDS, as shown in Table 4-6.

Table 4-6 Consideration of Compression Membrane Between Rigid Supports for SBEDS Component Types

Component Type	Compression Membrane Plus Flexure	Comments
One-Way or Two-Way Reinforced Concrete Slab	Yes	
Reinforced Concrete Beam or Beam-Column	Yes	
One-Way or Two-Way Reinforced Masonry	Yes	Effect of any ungrouted voids in CMU is not included in compression membrane analysis. *Analyze as unreinforced with compression membrane if reinforcing spaced at 600 mm (24 in) or more* since this implies less than 50% solid and a relatively low flexural strength compared to compression membrane strength.
One-Way or Two-Way Unreinforced Masonry	Compression membrane is considered without flexure (Low flexural resistance is ignored)	Gap between wall and support can be input. Effect of any ungrouted voids is included in compression membrane analysis.
Prestressed Concrete Beam or Panel	No compression membrane	

The peak resistance from compression membrane response and ductile flexural yielding at midspan and at the supports, r_{uc}, for concrete and masonry components with a solid cross section and a one-way span is calculated as shown in Equation 4-14. Equation 4-15 shows the similar equation for two-way components. Equation 4-16 defines the deflections Δ_{uc} and Δ_{st} in Figure 4-14 causing peak compression membrane resistance and zero compression membrane resistance, respectively, for one-way and two-way components. All three equations are from Chapter 10 of UFC 3-340-01. They are derived in Park and Gamble (2000), which discusses static reinforced concrete slab tests that are the basis for the equations. They are used in SBEDS to calculate the contribution of compression membrane to the resistance-deflection relationships of reinforced concrete, reinforced masonry, and unreinforced masonry except for concrete masonry units (CMU) that have large internal void areas.

The internal void space reduces the compression membrane resistance of a component. Compression membrane response is calculated non-conservatively for reinforced CMU in SBEDS, ignoring the effects of any voids, because these voids typically do not significantly decrease the peak compression membrane resistance. CMU walls reinforced at 400 mm (16 inches) on center have approximately 25% to 30% void space located near the center of the cross section, where solid material would have the smallest resisting moment arm in compression membrane response. Therefore, it is typically acceptable to analyze this case in SBEDS assuming solid material. More conservatively, or if the wall reinforcement spacing is greater than 400 mm (16 inches), a reinforced CMU wall with compression membrane should be analyzed as an unreinforced masonry wall because the compression membrane resistance of unreinforced CMU does include the effects of voids. An accurate assessment of the more dominant compression membrane response is more important than including the lesser effect of flexural response from wall reinforcement spaced at more than 400 mm.

Equation 4-14

$$r_{uc} = \frac{8}{L^2}\left(M'_{uc} + M_{uc} - N_{uc}\Delta_{uc}\right)$$

$$r_{uc} = \frac{8\left(0.85 f'_{dc}\, \beta_1 h\right)}{L^2}\left\{\begin{array}{l}\frac{h}{2}\left(1-\frac{\beta_1}{2}\right)+\frac{\Delta_{uc}}{4}\left(\beta_1-3\right)+\frac{\beta L^2}{4\Delta_{uc}}\left(\beta_1-1\right)\left(\varepsilon+\frac{2t}{L}\right)+\frac{\Delta_{uc}^2}{8h}\left(2-\frac{\beta_1}{2}\right)+\frac{\beta L^2}{4h}\left(1-\frac{\beta_1}{2}\right)\varepsilon' \\ -\frac{\beta_1\beta^2 L^4}{16h\Delta_{uc}^2}\varepsilon'^2\end{array}\right\}$$

$$-\frac{8}{L^2}\left\{\frac{1}{3.4 f_{dc}}\left(T' - T - C'_s + C_s\right)^2 + \left(C'_s + C_s\right)\left(\frac{h}{2} - d' - \frac{\Delta_{uc}}{2}\right) + \left(T' + T\right)\left(d - \frac{h}{2} + \frac{\Delta_{uc}}{2}\right)\right\}$$

$$where \quad \varepsilon' = \varepsilon + \frac{2t}{L} = \left(\frac{1}{hE_c} + \frac{2}{LS}\right)\frac{\left[.85 f_{dc}\beta_1\left(\frac{h}{2} - \frac{\Delta_{uc}}{4} - \frac{T' - T - C'_s + C_s}{1.7 f_{dc}\beta_1}\right) + C_s - T\right]}{1 + 0.2125\frac{f'_{dc}\,\beta_1\beta L^2}{\Delta_{uc}}\left(\frac{1}{hE_c} + \frac{2}{LS}\right)}$$

It is assumed in SBEDS that the effects of small, uniformly distributed voids in European insulated block are accounted for in the compressive prism strength, f'_m, where f'_m is determined based on the compressive failure force divided by the gross area. Therefore, these blocks can be treated as solid material with an input compressive prism strength that accounts for the effects of voids.

Equation 4-17 and

Equation 4-18 show modified versions of Equation 4-14 and Equation 4-15 for unreinforced masonry with large voids centered at midthickness, such as CMU. These equations account for the reduced compression force in compression membrane response caused by voids concentrated at the center of the cross section. They assume a cross section typical of CMU block, where there is solid exterior shell and interior rectangular voids centered at midthickness at a regular spacing. These two equations also account for a gap between the top of the wall and the rigid supporting component, which is common construction practice to allow expansion at the top of in-fill masonry walls. The values of Δ_{uc} and Δ_{st} in Equation 4-17 are modifications of Equation 4-16 that include the effect of a gap. For two-way unreinforced CMU, see notes at end of

Equation 4-18.

Equation 4-15

$$
r_{uc} = \frac{24\left(0.85 f'_{dc}\,\beta_1 h^2\right)}{L_y^2\left(3\frac{L_x}{L_y}-1\right)}
\left\{\begin{array}{l}
\frac{L_x}{L_y}\left(\frac{1}{2}-\frac{3\Delta_{uc}}{4h}+\frac{\Delta_{uc}^2}{4h^2}-\beta_1\left(\frac{1}{4}-\frac{\Delta_{uc}}{4h}+\frac{\Delta_{uc}}{16h^2}\right)\right)+\left(\frac{1}{2}-\frac{\Delta_{uc}^2}{12h^2}-\beta_1\left(\frac{1}{4}-\frac{\Delta_{uc}^2}{48h^2}\right)\right) \\
+\frac{\varepsilon'_x}{16}\left(\frac{L_y}{h}\right)^2\frac{L_x}{L_y}\left(\beta_1\left(\frac{2h}{\Delta_{uc}}-\frac{1}{2}\right)+1-\frac{h}{\Delta_{uc}}\right) \\
+\frac{\varepsilon'_y}{16}\left(\frac{L_y}{h}\right)^2\left(2\frac{L_x}{L_y}\left(\frac{\beta_1 h}{\Delta_{uc}}-\frac{\beta_1}{2}+1-\frac{2h}{\Delta_{uc}}\right)+\left(.5\beta_1-1\right)\right) \\
-\frac{\beta_1 h^2}{64\Delta_{uc}^2}\frac{L_x}{L_y}\left(\frac{L_y}{h}\right)^4\left(\left(\varepsilon'_x\right)^2\frac{L_x}{L_y}+\left(\varepsilon'_y\right)^2\right)
\end{array}\right\}
$$

$$
+\quad \frac{24}{L_y^2\left(3\frac{L_x}{L_y}-1\right)}
\left\{\begin{array}{l}
-\frac{1}{3.4 f_{dc}}\left(\left(T'_x-T_x-C'_{sx}+C_{sx}\right)^2+\frac{L_x}{L_y}\left(T'_y-T_y-C'_{sy}+C_{sy}\right)^2\right) \\
+\left(C'_{sx}+C_{sx}\right)\left(\frac{h}{2}-\frac{\Delta_{uc}}{2}-d_x\right)+\left(T'_x+T_x\right)\left(d_x-\frac{h}{2}+\frac{\Delta_{uc}}{4}\right) \\
+\left(C'_{sy}+C_{sy}\right)\left[\frac{L_x}{L_y}\left(\frac{h}{2}-\frac{\Delta_{uc}}{2}-d_y\right)+\frac{\Delta_{uc}}{4}\right]+\left(T'_y+T_y\right)\left[\frac{L_x}{L_y}\left(d_y-\frac{h}{2}+\frac{\Delta_{uc}}{2}\right)-\frac{\Delta_{uc}}{4}\right]
\end{array}\right\}
$$

$$
\textit{where}\quad \varepsilon'_x=\varepsilon_x+\frac{2t_x}{L_x}\quad \textit{and}\quad \varepsilon'_y=\varepsilon_y+\frac{2t_y}{L_y}
$$

Note: subscript x or y refers to x or y span direction

where:

r_{uc} = peak resistance from compression membrane and ductile flexural response
Δ_{uc} = midspan deflection at which ruc is reached
M_{uc}= ultimate flexural moment capacity at midspan
M'_{uc}= ultimate flexural moment capacity at supports
N = axial force from compression membrane forces
L = clear span length of the member
h = overall thickness of the member
β_1 = ratio of the concrete compression block depth to the distance from the compression face to the neutral axis = 0.85 for f'_c =30 MPa and decreases by 0.008 for each 1 MPa that f'_c exceeds 30 MPa; $B_1 \geq 0.65$
β = ratio of the distance from the support to the interior yield line, to the member length L
C_s, C'_s = compression force per unit width in the reinforcing steel at interior yield lines and supports, respectively, assuming yielding of steel
T, T'= tension force per unit width in the reinforcing steel at the interior yield lines and at the supports, respectively, assuming yielding of steel
d = distance from the compression face to the centroid of the tension

Methodology Manual TOC

reinforcement; assumed to be the same at interior yield lines and supports

d'= distance from compression face to the centroid of the compression reinforcement; assumed to be the same at interior yield lines and supports

f'_{dc} = dynamic ultimate compressive strength of the concrete

E_c = concrete modulus of elasticity

S =lateral stiffness of the supports (assumed equal to 0.2 E_c in SBEDS)

ε= member axial strain

ε'= combined member strain and support strain (definition for ε' in Equation 4-14 applies in each direction in Equation 4-15)

t = lateral displacement of each support corresponding to ruc

Equation 4-16

$$\Delta_{uc} = 0.033\mathrm{L} \le 0.5\mathrm{h}$$
$$\Delta_{st} = 0.08\mathrm{L} \le 0.8\mathrm{h}$$

where:

Δ_{uc} = midspan deflection at ultimate compression membrane capacity

Δ_{st} = midspan deflection for snap-through of compression membrane response

L = clear span length (minimum span of two-way components)

h = overall thickness of the component

Note: Equation 4-16 recommended primarily for 2 < L/h < 30, but used for all cases in SBEDS

Equation 4-17

$$r_{uc} = \frac{8}{L^2}\left[2C_1\left(\frac{h}{2}-\frac{t_s}{2}\right)+2C_2\left(\frac{h}{2}-t_s-\frac{(0.85c-t_s)}{2}\right)-(C_1+C_2)\Delta_{uc}\right]$$

$$c = \frac{h}{2}-\frac{\Delta_m}{2}-\beta L^2\left(\varepsilon'+\frac{\delta_g}{L}\right) \quad where \quad \varepsilon' = \varepsilon+\frac{2t}{L}$$

$$C_1 = 0.85 f'_m t_s$$

$$C_2 = 0.85 f'_m k(0.85c-t_s)$$

$$\Delta_{uc} = MIN\left(\frac{\mathrm{L}}{30},\frac{\mathrm{h}}{2}\right)+\Delta_g$$

$$\Delta_g = h-\sqrt{\left(\frac{L}{2}\right)^2+h^2-\left(\frac{L+\delta_g}{2}\right)^2}$$

$$\Delta_{st} = \left[MIN(0.08\mathrm{L},0.8\mathrm{h})+\Delta_g\right] \le h$$

Equation 4-18

$$r_{uc} = \frac{24}{L_y\left(3L_x - L_y\right)}\left[m'_x + m_x + m'_y + + m_y + \left(m_y + m'_y\right)\frac{L_x - L_y}{L_y} - \frac{\Delta_{uc}}{2}\left(n_x - n_y + 2n_y\frac{L_x}{L_y}\right)\right]$$

$$m_x = m'_x = C_{1x}\left(\frac{h}{2} - \frac{t_s}{2}\right) + C_{2x}\left(\frac{h}{2} - t_s - \frac{\left(0.85c_x - t_s\right)}{2}\right)$$

$$m_y = m'_y = C_{1y}\left(\frac{h}{2} - \frac{t_s}{2}\right) + C_{2y}\left(\frac{h}{2} - t_s - \frac{\left(0.85c_y - t_s\right)}{2}\right)$$

$$C_{1x} = C_{2x} = 0.85 f'_m t_s$$

$$C_{2x} = 0.85 f'_m k_x (.85c_x - t_s)$$

$$C_{2y} = 0.85 f'_m k_y (.85c_y - t_s)$$

$$c_x = \frac{h}{2} - \frac{\Delta_{uc}}{2} - \beta L_x^{\,2}\left(\varepsilon' + \frac{\delta_g}{L_x}\right) \quad where \quad \varepsilon' = \varepsilon + \frac{2t}{L_x}$$

$$c_y = \frac{h}{2} - \frac{\Delta_{uc}}{2} - \beta L_y^{\,2}\left(\varepsilon' + \frac{\delta_g}{L_y}\right) \quad where \quad \varepsilon' = \varepsilon + \frac{2t}{L_y}$$

$$n_x = C_{1x} + C_{2x}$$

$$n_y = C_{1y} + C_{2y}$$

Note: subscript x or y refers to x or y span direction

where:

r_{uc} = maximum resistance from compression membrane response
Δ_{uc} = midspan deflection at maximum resistance
c = compression block depth
h = overall wall thickness
ε' = compression strain due to arching forces and support movement strain (see Equation 4-14 for calculation of ε' with no steel forces and $f'_{dc}=f'_m$)
t = outward movement of each support caused by arching forces (Note: support stiffness assumed equal to $0.2E_m$ per UFC 3-340-01)
δ_g = gap between edge of wall and rigid supports
f'_m = prism compressive strength for masonry (on net cross section area)
t_s = masonry shell thickness
k = solid ratio of masonry through webs
L = span length
C_1 = compression force per unit width in shell
C_2 = compression force per unit width in webs
Δ_g = deflection when corner of wall engages rigid support ($\Delta_g = 0$ if $\delta_g = 0$)
Δ_{st} = arching snap through deflection causing zero arching resistance

β = distance from support to yield location divided by span length = 0.5
m_i = resisting positive moment from arching per unit width in the i direction
m'_i = resisting moment at supports from arching per unit width in the i direction
n_i = compression force from arching per unit width in the i direction

Notes: 1) $\beta(x,y)<=0.5$ for two-way component depending on yield line pattern, however, conservatively β = 0.5 in SBEDS
3) δ_g conservatively assumed equal in both directions for two-way spans

Flexural response of unreinforced masonry components is brittle, rather than ductile. Therefore, the flexural resistance reduces to zero at a very small deflection when the peak tension flexural stress equals the tensile strength at the maximum moment regions. Also, the peak flexural resistance for unreinforced masonry typically is typically small compared to the peak compression membrane resistance of these components. For these reasons, the resistance-deflection relationship for unreinforced masonry in SBEDS does not include any contribution from flexure. It increases linearly from zero to r_{uc} at a deflection equal to Δ_{uc} and then decays linearly to zero at a deflection Δ_{st}, where both deflections are defined in Equation 4-17.

4-1.2.2.3 **AXIAL LOAD ARCHING RESPONSE**

As shown in Figure 4-18, applied axial load can act in a similar manner as compression membrane forces. The component initially responds in flexure. When significant rotation occurs at midspan and at the supports after flexural yielding, the axial load is resisted primarily at the unloaded face near the supports and primarily at the loaded face near midspan. The resulting couple resists applied load with a resistance equal to r_3 in

Equation 4-19 as long as the deflection is less than the component thickness. The peak magnitude of the resisting couple, and thus r_3, is a function of the applied axial load, including component self-weight above midspan, and component thickness.
The typical applied axial loads in buildings are much less than the compressive forces associated with material crushing in compression membrane response. Therefore, axial load arching should be ignored for components with rigid supports that cause compression membrane response.

Figure 4-18 Response of Brittle Component Under Combined Lateral and Axial Load

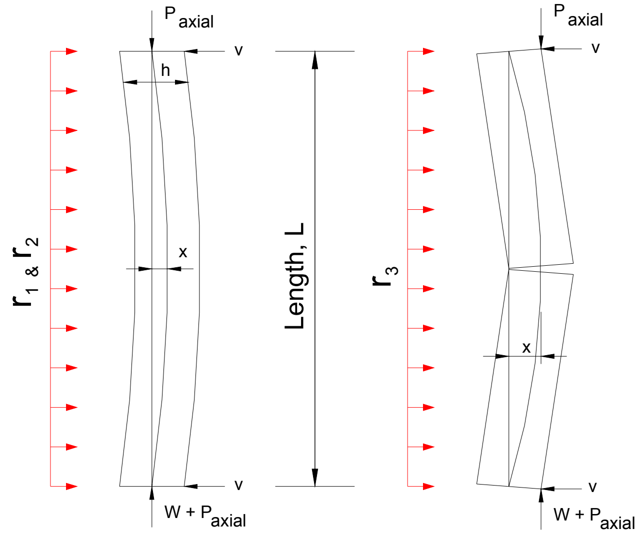

Response prior to ultimate flexural resistance, r_2 Response after r_2 where x= arching moment arm

Equation 4-19

$$r_3 = \frac{8}{L^2}\left(h - x_2\right)\left(P + \frac{WL}{2}\right)$$

where:

r_3 = maximum resistance from axial load effects
x_3 = flexural deflection at r_2+ (r_3 – r_2) /K_{ep}
K_{ep} = elastic-plastic stiffness for indeterminate components, otherwise equal to elastic stiffness
h = overall wall thickness
P = input axial load per unit width along wall, P_{axial}
W = areal self-weight and supported weight of wall
L = span length equal to wall height

Resistance from axial load arching, as illustrated in Figure 4-18, is only significant for thick components with a low post-yield flexural capacity such as unreinforced masonry. Unreinforced masonry, which is the only component type where axial load arching response can be considered in SBEDS, responds brittlely in flexure, essentially loosing all flexural resistance after flexural yielding in the maximum moment regions. Axial load arching is more significant for load bearing walls, but even the self-weight above midspan of an unreinforced masonry wall may cause enough resistance and strain energy through arching action to be significant compared to the resistance and strain energy from brittle flexural response.

Figure 4-19 shows the resistance-deflection relationship for unreinforced masonry with brittle flexural response and axial load arching that is assumed in SBEDS. At deflections less than x_2, before flexural yielding has occurred at all maximum moment regions and the component becomes a mechanism, all resistance is due to flexural response. At deflections between x_3 and the component thickness, h, all resistance is due to axial load arching. The

resistance-deflection relationship transitions between these two response modes between x_2 and x_3 at an assumed slope equal to the elastic stiffness. Figure 4-19 is not drawn to scale, the deflections x_1 through x_3 are very small compared to h for a typical component. For two-way spans, axial load arching is assumed to act only in the short span direction in SBEDS, since unreinforced masonry walls are typically wider than they are tall and axial load almost always acts vertically. However, this is unconservative if the vertical wall span is significantly larger than the horizontal wall span. The input axial load can be reduced in this unusual case based on

Equation 4-19 to cause the correct value of r_3 assuming that SBEDS will use L for the shorter horizontal span instead of the vertical span.

4-1.2.2.4 **SHEAR RESPONSE MODE**

The shear response mode occurs when the component flexural load capacity (i.e., ultimate flexural resistance) is greater than the ultimate load resisted by the component shear strength. In this case, flexural response occurs only up to the load causing shear failure, referred to as the ultimate shear resistance. The resistance-deflection relationship for flexural response, as described in Section 4-1.2.1, is applicable up to the ultimate shear resistance. The resistance can be assumed equal to the ultimate shear resistance for greater deflections, implying ductile response, up to a limited failure deflection that may be only slightly greater than the deflection causing the ultimate shear resistance. The ultimate shear resistance is equal to the shear force capacity of the component cross section per unit loaded width along the supports divided by the shear span, as shown in Equation 4-20. The ultimate resistance from compression membrane, tension membrane, and axial load arching response are not limited by the component shear strength, since the shear strength is required to resist only the diagonal tension stresses and direct shear stresses caused by flexural response.

Figure 4-19 Resistance-Deflection Relationships for Unreinforced Masonry with Brittle Flexural Response and Axial Load

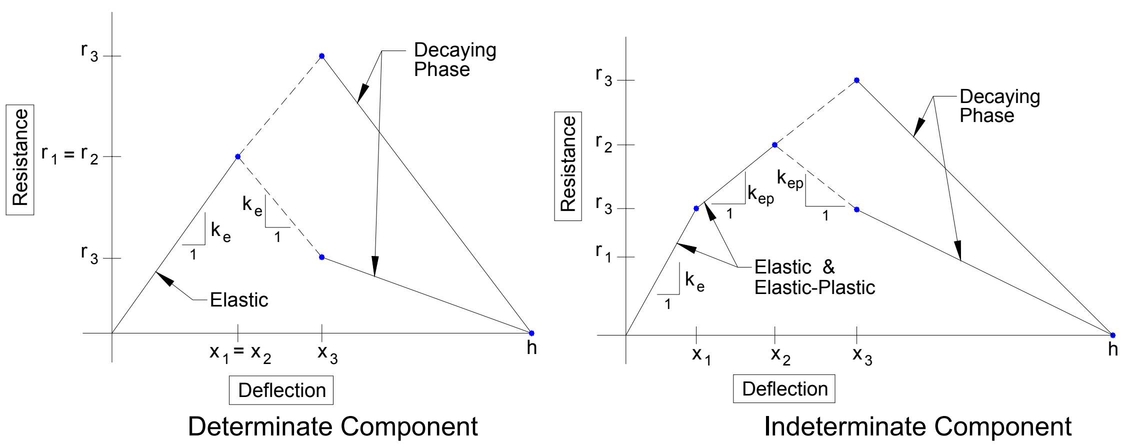

Equation 4-20

$$R_v = \frac{vA_v}{C_v L - kd}$$

where:

Methodology Manual TOC

R_v = ultimate shear resistance
v = dynamic diagonal shear capacity of component as discussed in Chapter 5 through 8
= lower of dynamic diagonal shear or direct shear strength of reinforced concrete or masonry components
A_v = component shear area per unit loaded width along supports
= total cross sectional shear area of beam components divided by beam spacing (see discussion on shear forces in Chapter 5-8 for more information on shear area)
k = 1 for components where critical shear area is a distance "d" from support (see Section 4-3.2), otherwise k=0
d = depth of reinforcing steel from component face with compression stress for reinforced concrete and masonry components
= component thickness of unreinforced masonry
= not applicable for other component types since k=0
L = component span (span in short direction of two-way span)
C_v = shear span coefficient from Table 4-3 and

Table 4-4
= $V/(r_uL)$ from Table 4-3 for one-way components
= $V_x/(r_ux)$, $V_y/(r_uy)$, $V_x/(r_uL_x)$, or $V_y/(r_uL_y)$ from

Table 4-4 as applicable
based on yield line pattern and larger value of V_x or V_y for given two-way component

If the ultimate shear resistance of the component is less than its ultimate flexural resistance, all *flexural* resistances in the resistance-deflection relationship that are greater than the ultimate shear resistance (i.e., this may or may not involve the initial elastic flexural resistance) are set equal to the ultimate shear resistance if they are larger. Parts of the resistance-deflection relationship based on compression membrane, tension membrane, or axial load arching response are unaffected. Also, all flexural stiffness values corresponding to resistances less the ultimate shear resistance are unaffected. Therefore, the ultimate shear resistance is used only to limit the maximum flexural response in the component at the ultimate shear resistance. This assumes that component response after the resistance equals the ultimate shear resistance (i.e., shear yielding) involves ductile yielding in a similar manner as flexural yielding. Shear yielding is not well understood, so the shape of the resistance-deflection curve after the component deflects past the ultimate shear resistance is not known. However, as discussed in Section 0, the allowable deflections in a component after shear yielding are usually very limited.

For example, if a simply supported beam has an ultimate dynamic shear capacity of 40,000 lbs near each support, and shear span of 100 inches, and a loaded width of 100 inches, the ultimate shear resistance is 4 psi. If the ultimate flexural resistance is 5 psi, then the ultimate shear resistance of 4 psi is used as the ultimate resistance for the component's resistance-deflection relationship because it is lower than the ultimate flexural resistance. All stiffness values in the resistance-deflection relationship are unchanged and any initial elastic yield resistance is unchanged if it is less than 4 psi. The component is assumed to yield ductilely at 4 psi, where the resistance remains constant at this value with increasing deflection. The plastic yield deflection is the deflection in the resistance-deflection relationship where the resistance is equal to 4 psi.

SBEDS will automatically prompt the user to set a “shear flag” if the calculated ultimate shear resistance is lower than the ultimate flexural resistance. After setting the shear flag to 1 or 2, corresponding to a k value of 0 or 1, respectively in Equation 4-20, SBEDS will automatically adjust the resistance-deflection relationship as stated above and the user can click the SDOF button to recalculate the SDOF equation of motion based on the modified resistance-deflection relationship where all flexural response is capped by the ultimate shear resistance. Also, the user may decide to ignore the shear flag if the blast load causes limited response and the shear loads are less than the shear capacity of the component. However, this should only be considered when the threat is well known and is unlikely to ever be exceeded.

4-1.2.3 GENERAL DESCRIPTION OF RESISTANCE-DEFLECTION RELATIONSHIPS IN SBEDS

The many different possible resistance-deflection relationships described in this chapter point out the need for a general methodology for solving the SDOF equation of motion (Equation 4-5) that can consider a wide range of resistance-deflection relationships. The SDOF solver in SBEDS considers a very general resistance-deflection relationship that can fit all of the resistance-deflection relationships described in this section, as well as many others. In general, SBEDS can solve the SDOF equation of motion (i.e., Equation 4-5) for any point-wise linear resistance-deflection relationship with up to five stiffness regions. This is significant because other available programs for solving the SDOF equation of motion assume a more simplified form of resistance-deflection relationship that is only applicable for one or two response modes.Figure 4-20 shows the types of general resistance-deflection relationships that can be considered by SBEDS. Table 4-7 shows a definition of terms inFigure 4-20. The stiffness, resistance, and deflection terms in Figure 4-20 are determined on a case-by-case basis for each component based on the component material and geometry properties and boundary conditions, as explained in this manual. Table 4-8 shows rules used to transition between stiffness regions inFigure 4-20. These rules were set up to cover situations for the component types and response types in SBEDS, including special rules for rebound when components have softening (i.e., negative stiffness) in the input inbound resistance-deflection curve.

Softening, which is shown in Figure 4-20b, occurs for components with compression membrane response and axial load arching. For components with compression membrane response, SBEDS automatically arranges the rebound resistance-deflection curve to prohibit compression membrane during rebound until the deflection is negative, since this response mode depends on the location of the midspan deflection relative to the supports. Similarly, it automatically arranges the resistance-deflection curve for subsequent inbound response to prohibit compression membrane until the deflection is positive. It is arguable if previously crushed material can still provide the same stiffness and strength during subsequent response cycles, but SBEDS simplistically assumes no degradation of compressive strength or stiffness due to multiple response cycles.

For components with axial load arching (only unreinforced masonry), SBEDS automatically arranges the rebound resistance-deflection curve to prohibit flexural response during rebound if the ultimate flexural resistance has occurred during initial inbound response, implying that the component has cracked in a brittle fashion through the thickness. Otherwise, this case is identical to the case with compression membrane from rigid supports. Therefore, this case is identical to the case with compression membrane from rigid supports except that the maximum negative flexural resistance is zero. If the ultimate flexural resistance does not occur during inbound response, then no axial load arching occurs and the resistance-deflection relationship is symmetric for inbound and rebound response. More information on this case is provided in Section 7-8. These rules used in SBEDS to automatically modify the resistance-deflection relationship during rebound as summarized in Table 4-8. The user can specify these rules for a General SDOF component with the input Rebound Flag value in Table 4-9.

Figure 4-20 General Resistance-Deflection Diagrams in SBEDS

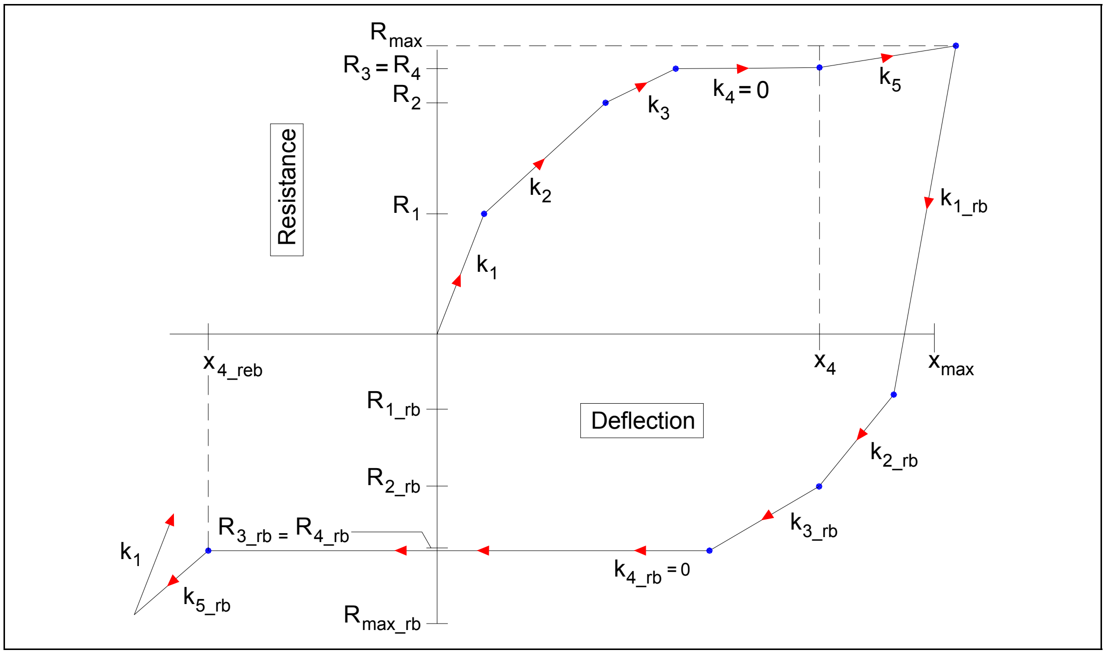

a) General Resistance-Deflection Relationship without Softening

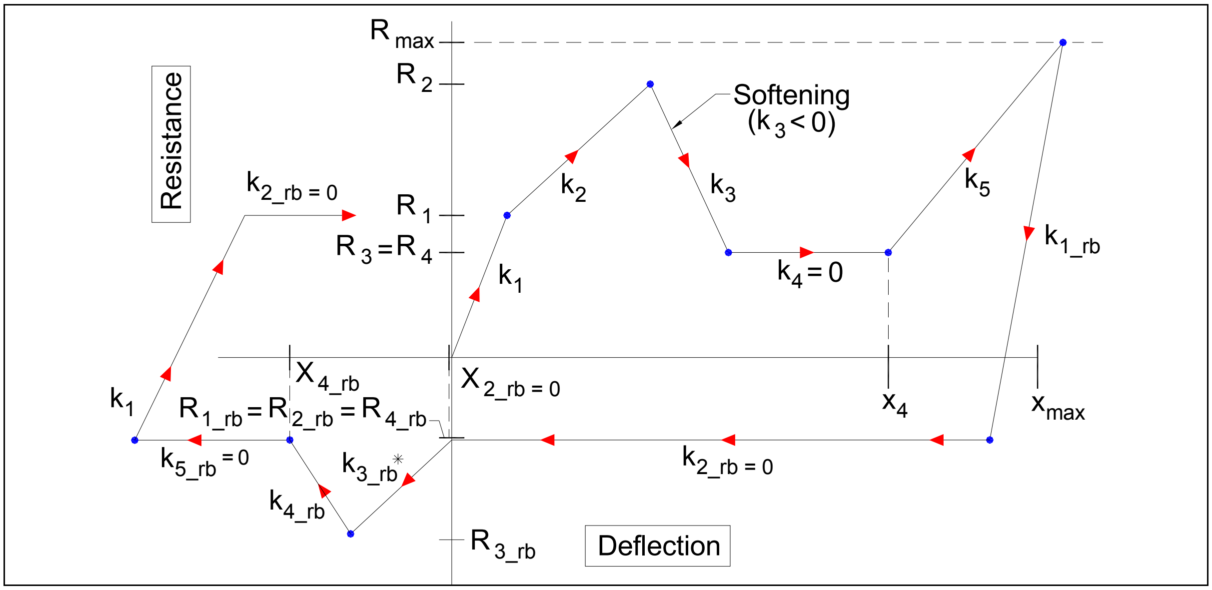

b) General Resistance-Deflection Relationship with Softening

Note: **k_i** are input stiffness for stiffness regions i = 1 to 5
k_{i_rb} are input stiffness for stiffness regions i = 1 to 5
R_i are input inbound resistances for stiffness regions i = 1 to 5: $r_i \geq 0$
R_{i_rb} are input rebound resistances for stiffness regions i = 1 to 5: $r_{i\_rb} \leq 0$
x_i are input inbound maximum deflections for stiffness regions i = 1 to 5: $x_i \geq 0$
x_{i_rb} are input rebound maximum deflections for stiffness regions i = 1 to 5: $x_i \leq 0$
x_i is only used if $k_i = 0$ and $k_{i+1} \neq 0$ and x_{i_rb} is only used if $k_{i\_rb} = 0$ and $k_{i+1\_rb} \neq 0$ (see Table 4-8)

Table 4-7 Definition of Terms for Stiffness Region Criteria Tables

Term	Definition
R_i where i=1..4	Inbound yield resistance for i^{th} stiffness region ($R_i \geq 0$)
R_{i_rb} where i=1..4	Rebound yield resistance for i^{th} stiffness region ($R_{i\_rb} \leq 0$)
R_{max}	Maximum resistance from previous cycle
k_i	Stiffness value for i^{th} stiffness region in inbound response
k_{i_rb}	Stiffness value for i^{th} stiffness region in rebound.
x_i and x_{i_reb}	Yield displacements for i^{th} stiffness region in inbound and rebound. SBEDS uses these values as a basis for changing stiffness region when the current stiffness equals zero. Otherwise, SBEDS compares the resistance at the current time step to the yield resistance for the current stiffness region to change stiffness regions,. see Table 4-8 for more information.

Table 4-8 Criteria for Determining To Stay in Current Stiffness Region During Dynamic Response

Case	Criteria for Staying in i^{th} Region [1,2]
Response in i^{th} region if region has no softening in resistance-deflection relationship (i.e., no negative stiffnesses)	SBEDS stays in current i^{th} stiffness region for $k_i > 0$ when $R<R_i$ during inbound and $R>R_{i\_rb}$ during rebound and for $k_i < 0$ when $R>R_i$ during inbound and $R<R_{i\_rb}$ during rebound. See next two rows for cases with $k_i = 0$ and $k_{i\_rb} = 0$.
Response in i^{th} inbound region when k_i = 0 and no softening	SBEDS stays in current i^{th} stiffness region for $x<x_i$ if $k_{i+1} \neq 0$, otherwise $k_i = 0$ until rebound response.
Response in i^{th} rebound region when k_{i_rb} = 0 and no softening	SBEDS stays in current i^{th} stiffness region for $x>x_{i\_rb}$ if $k_{i+1\_rb} \neq 0$, otherwise $k_{i\_rb} = 0$ until next inbound response.
Response in i^{th} region for components with softening from compression membrane response between rigid supports	Same as all three cases above for first inbound and rebound response except SBEDS creates rebound resistance-deflection relationships where no rebound compression membrane occurs until x< 0, using a zero stiffness as required (see Figure 4-20b), and R_i=-R_{i_reb} during subsequent inbound (i.e., rebound resistances and stiffnesses used for inbound response after first inbound cycle) – *see discussion in paragraphs below*.
Response in i^{th} region for components with softening from brittle flexural response and axial load arching (only unreinforced masonry components)	Same as first three cases above if no cracking (i.e., no softening) has occurred during inbound response. Otherwise, same as softening case above except maximum resistance during rebound = 0 until x< 0 (i.e., no negative flexural resistance assumed during rebound, negative axial load arching resistance occurs for x<0) *see discussion in paragraphs below*.
Note 1: If velocity changes sign, stiffness is changed to input k_1 value for opposite response direction Note 2: When criteria for staying in region is not met, stiffness is changed to the input stiffness value for next highest region. When i=5, the stiffness is only changed by rebound (i.e., velocity sign change).	

Finally, when any inbound stiffness K_1 through K_5 exceeds K_{1_rb}, calculations are stopped at the maximum deflection in SBEDS and no rebound response is calculated because the area under the resistance-deflection curve could become negative during rebound. This is only of practical concern for unusual cases, such as where the tension membrane stiffness (K_{Tm}) of a component is unusually large and exceeds the flexural stiffness (K_E) in Figure 4-12. Usually K_{1_rb} is assumed equal to K_1 in SBEDS and K_1 is larger than any other inbound stiffness.

Table 4-9 Rebound Flag Information

Rebound Flag	Rules Used by SBEDS for Rebound Response Based on Rebound Flag
1	Rebound stiffnesses and resistances input into the General SDOF input sheet are always used for rebound response. This the default value on the SDOF input sheet.
0	Rules for stiffness applicable for components with compression membrane response are used in SBEDS. These rules cause the negative value of the input rebound resistance values and the input rebound stiffness values to be used as the inbound resistance and stiffness inbound values after the first inbound cycle. The rebound stiffness and resistance should be input by the user to prevent compression membrane stiffness from occurring until the deflection is less than zero during rebound as shown in Figure 4-20b.
-1	Rules for stiffness applicable for unreinforced masonry components with brittle flexural response and arching from axial load are used in SBEDS. These rules for based on loss of all flexural stiffness and resistance after cracking (i.e., after first negative stiffness value in calculated response). User should input rebound assuming cracking occurs first inbound response with initial rebound yielding at zero resistance and no negative phase axial load arching until x<0, similar to Figure 4-20b with $R_{1\ rb}= R_{2\ rb}= R_{4\ rb}=0$.

4-1.2.4 **STRAIN ENERGY**

An important concept of dynamic response related to the resistance-deflection relationship is strain energy. For SDOF-based analyses, this can be defined as the area under the resistance-deflection relationship up to the maximum component deflection caused by the blast load, x_m, as shown in Figure 4-21. The resistance-deflection relationship in Figure 4-21 includes ductile flexural response and tension membrane response, but the concept is the same for a resistance-deflection relationship based on any response mode including only flexural response. As stated in Equation 4-2, the work energy from the applied blast load must be absorbed by strain energy and kinetic energy of the blast-loaded component. Therefore, a component resists blast load based on its strain energy. This is a fundamental difference from static loading cases, where a component resists load based only on its strength, which can be stated in terms of resistance. The ability of a component to absorb strain energy at large, post-yield deflections during dynamic response without failing is generally referred to as ductile response.

As shown in Figure 4-21, the strain energy is a function of both the component ultimate resistance and maximum deflection. It is generally much better to absorb strain energy with a large maximum deflection than a large ultimate resistance. The component shear and connection forces increase directly with the resistance, so that a large ultimate resistance causes larger component shear and connection forces that are transferred into the building lateral or gravity resisting system - all of which must be accounted for in design. On the other hand, large component displacements are only a problem in rare cases where the component may impact nearby personnel or sensitive equipment. Therefore, it is better, when possible, to absorb sufficient strain energy to resist the blast load by increasing component ductility or using a ductile component, so that it can undergo large deflection without failing, rather than increased component strength and ultimate resistance.

Also, Figure 4-21 demonstrates how the strain energy is most dependent on plastic, or post-yield, flexural response occurring between deflections x_y and x_m, as opposed to elastic response before the component becomes a mechanism (i.e., for deflections when $x<x_y$). The strain energy absorbed during elastic flexural response is usually a low

percentage of the total strain energy, except for components with very low ductility. Consequently, the accuracy of the calculated elastic and elastoplastic stiffnesses is less important than the accuracy of the ultimate flexural resistance, r_{uf}. Components typically exhibit low ductility when the ultimate resistance is controlled by brittle response modes such as shear, buckling, rebar slip, etc. Usually components can be designed to avoid these conditions.

Figure 4-21 Strain Energy for Component with Ductile Flexural and Tension Membrane Response

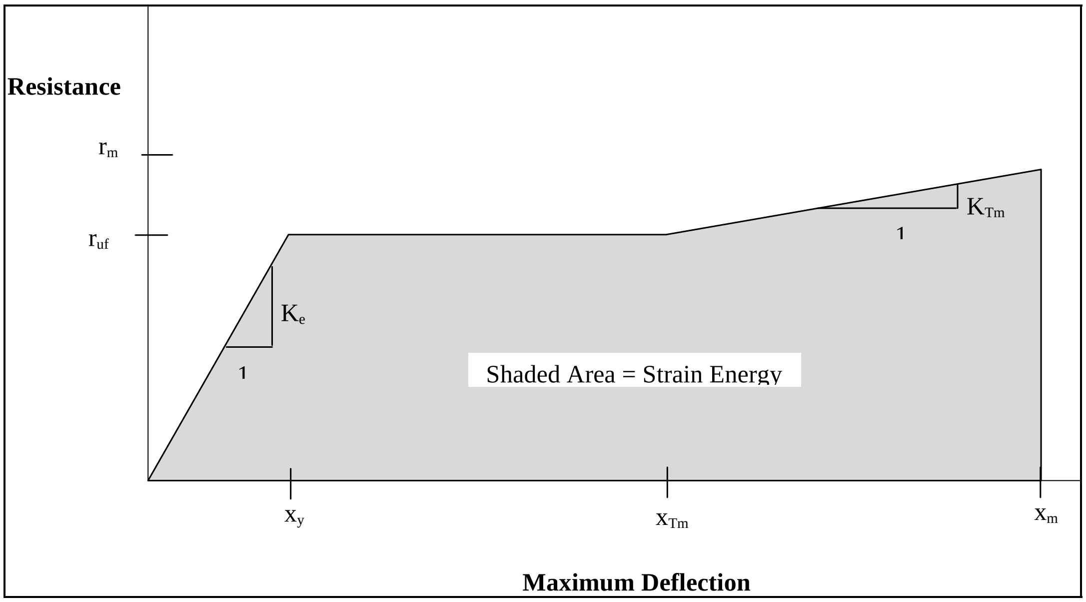

4-1.2.5 **REBOUND**

Rebound response occurs after the component reaches maximum deflection and begins moving back in the direction of the applied blast load. Peak rebound stresses and connection forces are directly related to the maximum rebound resistance. Figure 4-22 from TM 5-1300 shows ratios of maximum rebound resistance to the inbound ultimate resistance of a SDOF spring-mass system, where all contours are upper bounds for the contour values shown in the figure. This diagram is provided mainly to help provide an understanding of rebound response since SBEDS will directly calculate the rebound response of input components as part of its solution of the equation of motion of the equivalent SDOF system representing the component.

All cases lying above and to the left of the -1.0 contour have a rebound resistance equal to the inbound ultimate resistance. T_n in the figure is the natural period of the SDOF system (see Equation 4-22). If x_m/x_e is less than 1.0 (i.e. elastic response), the rebound resistance can be assumed equal to the peak inbound resistance. Long duration blast load durations, relative to the component natural period, and low inbound maximum deflections, x_m, relative to the component yield deflection, x_e, both tend to decrease the rebound resistance. An equivalent static design load for rebound equal to one-half the inbound ultimate resistance is often used as a rule of thumb for blast design. Figure 4-22 shows that this assumption is applicable when T/T_n >1.5 to 2 and x_m/x_e < 5 (i.e., low plasticity during inbound response) and when T/T_n>3 to 4 for larger x_m/x_e values. Typically, a component will have some reserve capacity and ductility that will help prevent failure if the rebound resistance from Figure 4-22 is a little larger than the ultimate rebound resistance calculated for the component.

Figure 4-22 Ratio of Maximum Rebound Resistance to Inbound Ultimate Resistance for SDOF System

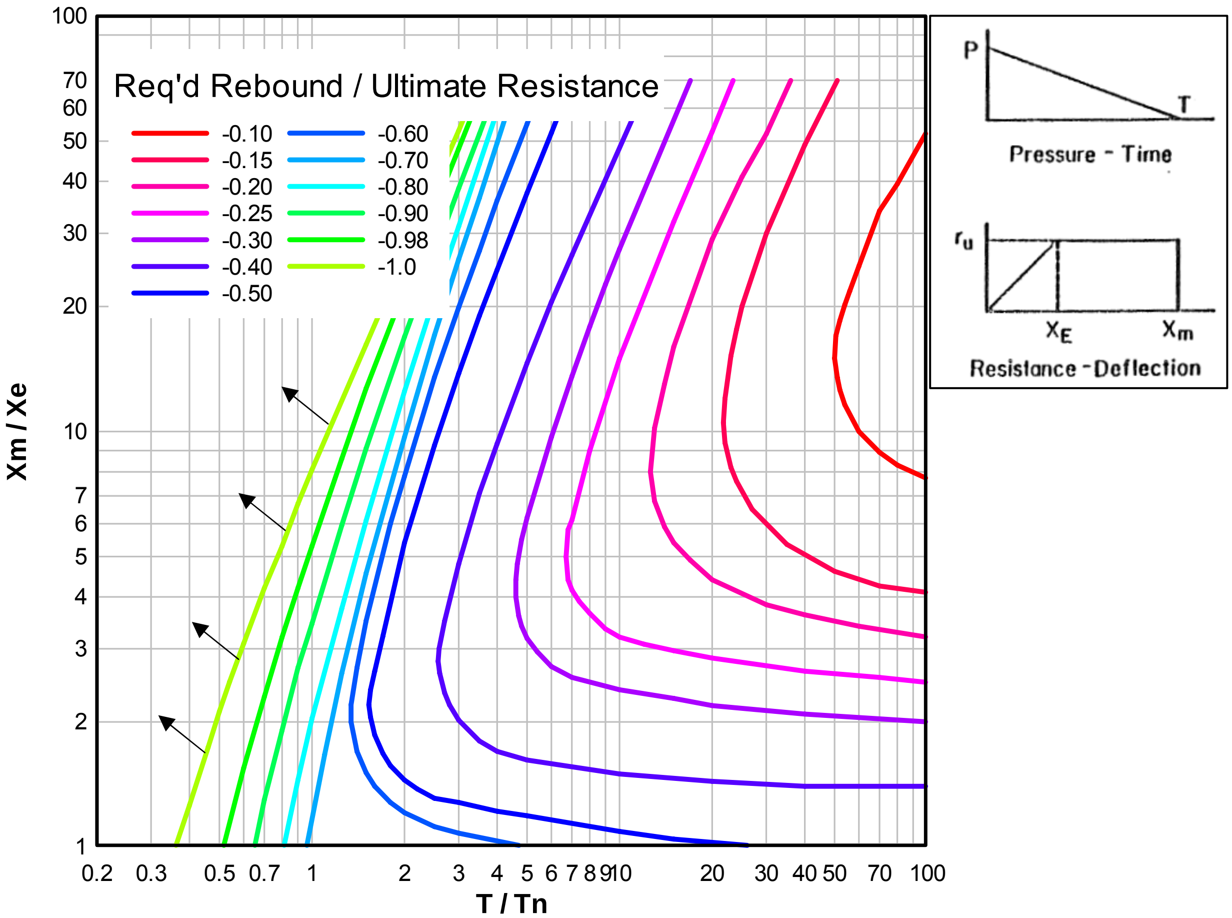

Usually, maximum response of blast-loaded components occurs during the first inbound response cycle. However, this is not always the case. Components with nonsymmetrical section properties or nonsymmetrical bracing can be much weaker during rebound than during inbound response because the cross section or bracing is designed to be effective against inbound response stresses rather than the reversed stresses that occur during rebound (i.e., reversal of locations within cross section where tension and compression stresses occur). Also, any damage to the component during inbound response can reduce its properties during rebound, although such damage is usually very difficult to quantify. Finally, in some relatively unusual cases the negative phase blast load can coincide with rebound response, causing the rebound response to be larger than inbound response.

In spite of its possible importance, component response to blast loads during rebound is not well understood. This is due in large part to a scarcity of observed rebound phase damage to components in blast tests and accidental or terrorist explosions. A blast load must be small enough not to cause significant damage during inbound motion, but large enough to cause observable damage during rebound. Also, components may have redundant response modes, such as limited tension membrane capacity, that are large enough to compensate for lower flexural resistance during rebound for the brief period before a second inbound response occurs.

The SDOF analyses in SBEDS account for nonsymmetrical conditions that reduce the ultimate flexural resistance in rebound based on user input properties for some component types, as discussed in Chapter 5 through 8. These inputs are only provided for cases where a parameter of the resistance-deflection relationship can be different during rebound response based on typical construction practice. However, the resistance-deflection relationships for most component types are assumed to be symmetric for inbound and rebound response in SBEDS, No degradation of component properties from inbound response. The only exception for this is unreinforced masonry with brittle flexural response and axial load arching, as explained in Section 4-1.2.3.

4-1.3 **DAMPING**

Damping is a resisting force that develops during dynamic component response due to energy dissipation that is not included in the strain energy, work energy, or kinetic energy. It is only well understood for simple systems, such as mass oscillation in a viscous fluid (i.e., viscous damping) or along a frictional surface (i.e., Coulomb damping). In practice, damping is a catch-all category that approximately accounts for all energy dissipated during dynamic response that is not accounted for with other terms in the equation of motion. In blast-loaded components, it is used to account for numerous complex factors that cause energy losses, such as slip and frictional action at joints and supports, material cracking, and concrete reinforcement bond slip.

Damping can be measured in a given dynamic system based on the decay in maximum response during successive response cycles of unforced elastic oscillation (i.e., free vibration). However, there are not any available methods to predict damping force coefficients for typical blast-loaded components other than approximate viscous damping coefficients recommended for structural response to earthquake motion. The damping values recommended for earthquake response are intended for cyclic response of larger component systems, such as reinforced concrete and steel frames in sway response, that is mainly elastic response. There is no available discussion on the validity of these methods for large plastic component response, which is usually the case for blast-loaded structures. Thus, there is very little available guidance on damping that is directly applicable for blast-loaded components.

In spite of this, a viscous damping term is generally included in the equivalent SDOF system for a blast-loaded component, as shown in Equation 4-5, so that some damping can be accounted for if desired. The damping force is equal to a damping constant multiplied by the velocity of the SDOF system at each time step. The damping constant is usually defined in terms of a damping ratio, ζ, which is multiplied by the critical damping constant for the system, C_{cr}, to calculate the damping constant as shown in Equation 4-21. C_{cr} is a property of the SDOF system, which is usually based on the initial elastic stiffness and load-mass factor of the system. In SBEDS, the user inputs a damping ratio, ζ, as a percentage, which is multiplied by C_{cr} within SBEDS to get the damping constant C_c used in the equation of motion in Equation 4-5 for the equivalent SDOF system representing the input component.

Equation 4-21

$$C_{cr} = 2\sqrt{kMK_{Lm}}$$

$$C_c = \frac{\zeta}{100} C_{cr}$$

where:

C_{cr} = critical damping constant
C_c = damping constant used in equation of motion (See Equation 4-5)
ζ = input damping ratio (as a percentage)
k = elastic stiffness of component
M = mass of component
K_{Lm} = load-mass factor

Different approaches have been recommended for including damping in SDOF analyses of component response to blast load. TM 5-1300 states that damping is rarely used for the reasons below. However, it also goes on to recommend that if damping is used, it can be based on damping ratios of 5% for steel structures and 1% for reinforced concrete structures.

- Damping has very little effect on the first peak of response, which is usually the only cycle of response that is of interest.
- The strain energy dissipated through plastic deformation is much greater than the energy dissipated by normal structural damping.
- Ignoring damping is a conservative approach.

UFC 3-340-01 recommends that damping values commonly used for earthquake analysis and design in Table 4-10 can be used for elastic and elastoplastic component response only. Therefore, the damping term is set to zero for all plastic response. This is recommended because the damping forces for structure response to earthquake loading were developed primarily for elastic component response, which involves deformation over the whole volume of the component. After ultimate resistance, deformation consists primarily of localized hinging at maximum moment regions, which occurs over a much smaller volume, so that no significant additional damping occurs. Also, damping is not specifically defined for plastic response in available blast design and analysis references, including TM 855-1, TM 5-1300, or in a number of structural dynamics textbooks that were reviewed.

Damping is calculated in SBEDS as recommended in UFC 3-340-01, where Equation 4-21 is used to define the damping constant for time steps during the solution of the equation of motion for inbound or rebound response when the resistance is less than the ultimate flexural resistance. Otherwise, the damping constant is set to zero. In the case of General SDOF input, Equation 4-21 is used to define the damping constant for time steps when the resistance is less than the first input yield resistances for inbound and rebound response and damping is otherwise set to zero. Damping values in Table 4-10 may be used, although damping ratios greater than 5% have rarely been used for blast design and analysis. An input damping ratio of 2% is recommended for unreinforced masonry components with brittle flexural response and axial load arching.

This response consists is elastic flexural response followed by axial load arching, which inherently causes some frictional response. The use of a 2% damping ratio causes the calculated maximum deflection and damage to match data much better in limited comparisons than the more conservative case of zero damping after brittle flexural response (Oswald, 2005).

Table 4-10 Damping Ratio Information For Primarily Elastic Dynamic Response

Structure	Structural Damping Ratio
Welded Steel, Fixed-End, No Attachments	0.0001 to 0.001
Welded Steel, Fixed-End, Attachments	0.01 to 0.03
Welded Steel, Simple Support, Support Friction	0.01 to 0.03
Bolted Steel	0.04 to 0.07
Reinforced Concrete, Lightly Cracked	0.02 to 0.05
Reinforced Concrete, Heavily Cracked	0.05 to 0.15

4-1.4 INITIAL DISPLACEMENT AND VELOCITY

The initial velocity and displacement are initial conditions for the SDOF equation of motion in Equation 4-5. The time-stepping solution to this equation in SBEDS is based on user input for these two values. The initial displacement and velocity are assumed in SBEDS to cause only elastic response for the input component, with a stiffness equal to the initial stiffness of the resistance-deflection relationship. Therefore, the total initial displacement should not cause any significant yielding. Similarly, a displacement equal to the time step multiplied by the initial velocity should not cause any significant yielding.

4-1.4.1 INITIAL VELOCITY

Blast-loaded components very seldom have an initial velocity. However, this input is useful for cases where the duration of the initial segment of an input blast load is very short compared the maximum response time of the component. In order for the numerical solution in SBEDS to function properly, the time step should be a fraction of the shortest duration of the segments of the blast load history, as described in Section 4-2.1. However, SBEDS uses a fixed number of 2900 time steps and this may not be sufficient to calculate maximum response if the time step is very small. If this is a problem and the shortest segment of a blast load history is the initial segment (a common case), the initial segment of the input blast load may be expressed as an equivalent initial velocity as discussed below and the blast load can in be input beginning of the second segment of the blast load at time zero.

The impulse i’ from the initial segment of the blast load history can be input into the SBEDS as an equivalent initial velocity, v_o, based on Equation 4-22 if the duration of this segment, t_d’, is less than one-third of the natural period of the equivalent SDOF system. The user should calculate and input v_0 based on Equation 4-22 and input the remainder of the blast load not including the impulse i’, as discussed in the previous paragraph, since it is accounted for with v_0. This will cause SBEDS to recommend a larger input time step based on a longer segment of the blast load history, so that response can be calculated over a longer response time.

Equation 4-22

$$v_0 = \frac{i'}{mK_{LM1}} \quad where \quad t_d' < \frac{1}{3}T_n \quad and \quad t_d' = \frac{2i'}{P'}, \; T_n = 2\pi\sqrt{\frac{K_{LM1}m}{k_1}}$$

where:

i' = impulse from segment of blast load with duration t_d'
v_o = equivalent initial velocity representing i'
K_{LM1} = load mass factor for initial elastic response
k_1 = stiffness for initial elastic response
T_n = natural period of component
m = mass of component

The effect of fragments on the global response of a component can also be included in SBEDS by inputting the impulse applied by the fragments as an initial velocity using Equation 4-22. The fragment impulse, equal to the summed momentum of all fragments impacting the component area divided by the component area, is equal to i' Equation 4-22. It can be assumed for this case that t_d', representing the duration of the load pulse from fragment impact, is less than one-third of the natural period of the component. The effect of fragment localized penetration and breaching should be investigated separately using applicable methods in TM 5-1300 or UFC 3-340-01.

4-1.4.2 INITIAL DISPLACEMENT

Initial displacement is not a direct input into SBEDS except in the case of General SDOF Program input. In all other cases, SBEDS automatically determines the initial displacement from gravity effects relative to the user defined direction of initial blast load as described below.

- If the component is perpendicular to the ground surface, such as a wall, no initial displacement is considered in SBEDS because there is no component initial deflection from gravity in the direction of applied blast load.

- If the component is parallel to the ground surface and deflects under gravity in the same direction as the applied blast load, such as a roof component loaded by exterior blast load, the initial displacement is calculated as the sum of the component self-weight and supported weight divided by the initial component stiffness. SDOF calculations start at time zero with this initial displacement and a resistance equal to the self-weight and supported weight. This condition causes no initial movement. Both the initial displacement and resistance have positive sign in this case.

- If the component is parallel to the ground surface and deflects under gravity in the opposite direction as the applied blast load, such as a roof component under internal blast load, an identical approach is used except the initial displacement and resistance have negative sign.

The SBEDS user must define one of these three cases in a dropdown box on the Input Sheet for the component orientation relative to the applied blast load. Initial displacement not caused by static conditions (e.g., when a spring is pulled and then suddenly released) can only be input as an initial deflection in the General SDOF input in SBEDS. This displacement adds to any displacement from gravity effects. It is rarely applicable in practical blast design problems..

4-2 METHODS FOR SOLVING SDOF EQUATION OF MOTION

Equation 4-5 must be solved in order to determine the maximum response of the equivalent SDOF system representing the input blast-loaded component as discussed in Section 4-1.1. The equation may be solved in a closed form manner for simple dynamic loading functions, as described in many structural dynamics textbooks. For most blast loads, however, a time-stepping numerical solution must be used. Any of a wide range of available numerical solution methods may be used (Tedesco et al, 1999). All these methods are approximate, but they are accurate enough for almost all practical applications if the time step is small enough.

The SDOF equation of motion can be written in a non-dimensional format for given blast loading time history shapes and solved numerically to determine non-dimensional solutions (UFC 3-340-01). The parameters defining the non-dimensional equation of motion can be plotted against the non-dimensional solution to obtain a generalized SDOF response graph, such as shown in

Figure 4-23. The graph in

Figure 4-23 allows a user to determine the maximum deflection, u_{max}, of an equivalent SDOF system based on the peak load, F_1, and duration, t_d, of a blast load history with a right triangular shape, and the ultimate resistance (R_m), yield deflection (u_y), and natural period (T_n) of the SDOF system.

Figure 4-23 only considers a single load-mass factor within T_n and no elastoplastic response.

The natural period is calculated as shown in Equation 4-22 based on an equivalent elastic stiffness for an indeterminate component (see Section 4-1.2.1) and a representative load-mass factor for the whole response, which may be an average between load-mass factors for elastic and plastic response.

Figure 4-23 also shows the time to maximum displacement, t_m. Graphical solutions such as

Figure 4-23 are very useful when the blast load history has a given simplified shape and the simplifying assumptions noted above for the equivalent SDOF system are acceptable. Similar graphs for some other simplified blast-load history shapes are available in Appendix D of UFC 3-340-01 and Chapter 3 of TM 5-1300.

Figure 4-23 Undamped Response Charts for SDOF Response to Right Triangular Blast Load History

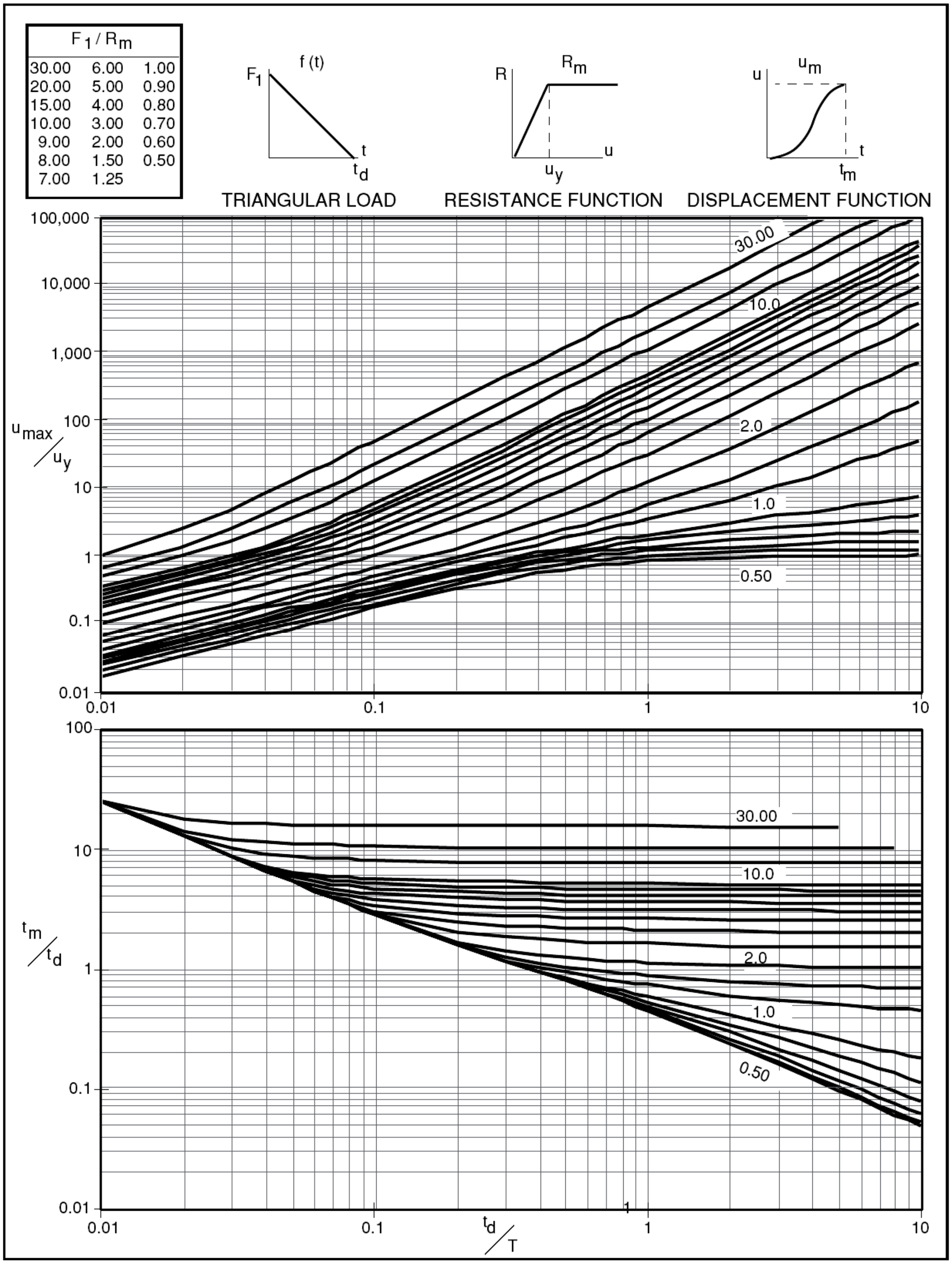

SBEDS uses a numerical method to solve the equation of motion for the equivalent SDOF system representing the input component at each time step. The Newmark-Beta method is most commonly used in available computer programs that solve the SDOF equation of motion in this manner. The constant velocity method is probably the simplest numerical method recommended for solving the equation of motion for blast design and analysis problems (Biggs, 1964). The choice of a numerical solution method is a tradeoff between the complexity of terms used to determine the approximate acceleration, velocity, and displacement at each time step and the number of time steps required to achieve a given level of accuracy. For example, Biggs found that approximately 1.5 times more time steps were necessary to achieve the same accuracy with the constant velocity method compared to the more complex linear acceleration method for a given SDOF system. Numerical solution methods are also unconditionally stable (i.e., they will always tend to converge to the correct solution as the time step is reduced) or conditionally stable (i.e., will converge when the time step is less than a limit value). However, any time step that is small enough to cause the numerical solution to meet accuracy requirements will almost always ensure stability.

The SBEDS workbook uses the constant velocity method, as described by Biggs (1964), to perform the time-stepping solution of the equation of motion. It was noted in trial analyses with several numerical solution methods that were initially considered that "overshoot" of the resistance at a time step where a yield occurred in the resistance-deflection relationship was the primary cause of error. In a computer program, this problem can be corrected by backtracking in time and subdividing the time step based on an interpolation so that the stiffness prior to yield is used only for that portion of the time step prior to yield and the new stiffness is used for the remainder of the time step. In a spreadsheet such as SBEDS, however, backtracking is very difficult. Therefore, SBEDS recommends a very small time step to the user that practically eliminates the overshoot. Since a small time step is required for this reason, the simple constant velocity method is used in SBEDS as the numerical solution method. Based on comparisons to computer programs using the Newmark-Beta method, very accurate solutions (i.e., typically within 2%) are obtained using the small recommended time step in SBEDS.

4-2.1 TIME STEP

The accuracy of any time-stepping numerical solution method is dependent on a small enough time step. A time step is sufficiently small for any given case if the solution calculated with a smaller time step (e.g., smaller by a factor of 2 or 3) changes by less than a desired accuracy level. From a practical viewpoint, there are many parameters in the equivalent SDOF system and blast load for a given blast-loaded component that may have uncertainties in the range of +/- 20%. Therefore, any solution to the SDOF equation of motion that is numerically accurate within 2% to 5% would normally be considered acceptable.

The bulleted list below shows upper bound limits on the recommended time step in SBEDS used to determine SDOF response for an input blast-loaded component. As shown in the list, a smaller time step is recommended for cases where blast loads histories are calculated from charge weight-standoff input, which have an exponential decay (see Figure 2-1) where the load changes more than proportionally with time near the peak pressure. The last bulleted requirement helps ensure that a small time step will be used even when the natural period and time segments associated with the blast load history are large. This is necessary in SBEDS to help minimize overshoot of the resistance during time steps where yielding occurs. SBEDS displays a recommended time step based on the smallest time step determined from the bulleted list below, but not less than 0.01 millisecond.

- 10% of the natural period
- 10% of the smallest time increment in a manually input, point-wise linear blast load
- 3% of the equivalent triangular positive phase duration or 1.5% of the equivalent triangular negative phase duration of an input charge weight-standoff blast load
- 3% of the smallest calculated time between local maxima and minima points of an input blast load file
- eight natural periods divided by 2900 time steps

A large number of time steps are hardcoded into SBEDS (i.e., 2900), but SBEDS will not calculate response all the way out to the peak deflection if the time step is too small compared to the component response time. In this case, which is rarely occurs, SBEDS displays a warning message. If no peak deflection is calculated, but the maximum deflection is very large, this may indicate that the component is failed and no further analysis is required. If the recommended time step is controlled by a short duration for the initial segment of the blast load history, the impulse in this segment can be replaced by an equivalent initial velocity as described in Section 4-1.4.1. Then the time step can be increased. Otherwise, the user can usually increase the time step to approximately 1.5 times the recommended time step without causing an unacceptable decrease in the accuracy of the calculated solution.

4-3 SHEAR FORCES AND END REACTION FORCES

The end reaction force, equal to the maximum shear force, acting at the supports of a blast-loaded component can be determined from the calculated SDOF response in terms of; 1) a equivalent static reaction force, or 2) a dynamic reaction force. In both cases, the calculated force is only due to flexural response. The equivalent static reaction force is the reaction force from the maximum calculated resistance in a component applied as a load. This force is used to check the shear capacity of components and to design the component connections using a static design approach. The dynamic reaction force, on the other hand, is a reaction force history based on a dynamic force equilibrium equation for the blast-loaded component. It is a function of both the component resistance and the applied load at each time step.

The dynamic reaction forces from a supported component, such as a beam, can be used as the applied load on a supporting component, such as a girder. Although it is more complicated, this approach is generally more accurate than applying the blast load directly to the supporting component because it accounts for the significant change that can occur in the load as it is transmitted through the supported component. This is particularly true if the supported component has a low ultimate resistance compared to the peak blast load. Dynamic reaction forces are not usually used to determine the maximum shear stress in a component or to design connections since the design strengths used for these cases are based on dynamic strength increase factors for overall component response rather than dramatic fluctuations that can occur in the first milliseconds of dynamic reaction force histories.
In-plane reactions are not considered in either the equivalent static, or dynamic reaction forces when tension or compression membrane response occurs. Out-of-plane

reactions from tension or compression membrane response can be considered since these response modes increase the resistance, and therefore the calculated reaction forces. However, only the reactions due to flexural response are typically considered in blast design because tension and compression membrane response is based on available capacity at the supports (i.e., compression membrane is only considered if the supports are rigid and therefore resist the maximum connection forces associated with crushing of masonry/concrete, tension membrane response is calculated based on input connection force capacity). Also, diagonal shear stresses are only compared to the reaction force caused by flexural response since they are caused by flexure.

4-3.1 DYNAMIC REACTION FORCES

Figure 4-24 from Biggs (1964) shows the free body diagram for a beam subject to uniformly distributed blast load. The free body diagram is based on one-half of the beam since the shear force is zero at midspan. The resultant of the inertial force in the free body is calculated to act through a line at (61/192)L from the support, based on the assumed shape function for beam deflection. Since this shape is constant with time for assumed SDOF response, the shape function of the beam velocities and accelerations along the span is equal to the shape function for deflection. All the other parameters are known as a function of time, where the resisting moment is related to the component resistance (i.e., in the same manner as M_p is related to r_u in Table 4-3). Therefore, the dynamic reaction force history can be solved for as shown in

Equation 4-23. The reaction force V(t) is solved for by taking the sum of moments around the resultant of the inertial force, so that it is not necessary to know the magnitude of this force.

Figure 4-24 Free Body Diagram Used to Determine Dynamic Reaction Force for Uniformly Loaded Beam (From Biggs)

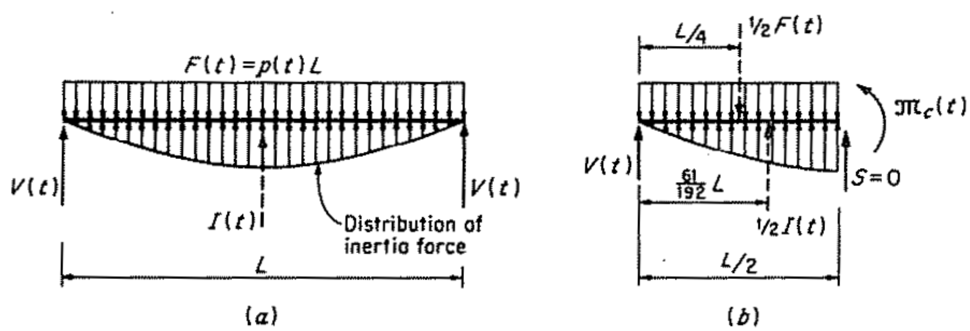

The assumption that the acceleration distribution along the span equals the deflected shape is correct only if the shape function does not vary with time. However, this is an approximate approach because dynamic finite element calculations show that very early in time the deflected shape of blast-loaded components subject to blast loads is flatter than the static deflected shape, with almost all deflection occurring very close to the supports. At later times, when significant deflections occur, the shape changes to more closely approximate the first mode, or static flexural response shape that is typically assumed in SDOF analyses. Therefore, the dynamic reaction is typically least accurate during very early time response.

Equation 4-23

$$V(t)\frac{61}{192}L - M_c(t) - 0.5F(t)\left(\frac{61}{192}L - 0.25L\right) = 0$$

$$M_c(t) = \frac{R(t)L}{8}$$

$$V(t) = 0.39R(t) + 0.11F(t)$$

where:

V(t) = dynamic reaction force
R(t) = resisting force
M_c = midspan resisting moment
F(t) = applied blast load
L = span length

Similar free body diagrams and equations can be developed for one-way components with other boundary conditions and load distributions, and for two-way components with uniform blast load. The dynamic reaction can be solved in the form shown in Equation 4-24 for each of these cases. Since different shape factors are assumed for elastic and plastic response, the factors C_R and C_F in Equation 4-24 are a function of the response realm, as well as the boundary conditions and blast load distribution. Static deflection shape functions are assumed for elastic response and linear deflection shape functions based on the yield line pattern are assumed for plastic response. See the discussion in Section 3-5 for use of $V_R(t)$ as a load on a primary component in SBEDS.

Equation 4-24

$$V_R(t) = C_R R(t) + C_F F(t)$$

where:

$V_R(t)$ = dynamic reaction force of component[1,2]
R(t) = resistance of equivalent SDOF system[1]
F(t) = blast load on equivalent SDOF system[1]
C_R = coefficient applied to resistance
C_F = coefficient of applied to blast load
t = time

Note 1: These parameters have same units as applied blast load in SBEDS
Note 2: $V_R(t)$ must be multiplied by the full blast loaded area of the component to get the reaction force

SBEDS calculates V(t) for each support for each SDOF analysis based on Equation 4-24 using C_R and C_F values for elastic response at all time steps when the resistance is between the inbound and rebound ultimate flexural resistances and C_R and C_F values for plastic response at all other time steps. C_R and C_F for many different one-way and two-way cases with differing boundary conditions and loading distributions are published in Chapter 11 of UFC 3-340-01. Also, C_R and C_F values are provided at, or along each support for components with nonsymmetrical support conditions. Morison (2005) also provides C_R and C_F values derived from dynamic force equilibrium equations using MathCad calculations for one-way spans and static finite element analyses for two-way spans. Unlike the C_R and C_F values in UFC 3-340-01, Morison's values are based on documented calculation procedures and present day computational methods. There are many cases of “small” disagreement between the two sets of C_R and C_F, values, which are within 20%, and a limited number of cases where the disagreement is more significant. SBEDS predominantly uses C_R and C_F, values in UFC 3-340-01 because it is based primarily on DoD procedures. However, Morison’s values are used in some cases where there was significant disagreement between the two sets of values.

Table 4-11 shows the C_R and C_F coefficients from Equation 4-24 used in SBEDS for one-way spanning components. The elastic values are also used for elastoplastic response. These values are taken from UFC 3-340-01, except shaded coefficient values are taken from Morison (2005) because they differed from UFC values by more than 20%. Table 4-12 through Table 4-15 show equations for the dynamic reactions of two-way components with uniformly applied blast load from UFC 3-340-01. The C_R and C_F values for two-way components in SBEDS are based on curve-fits to the values in the equations in these tables. The curve-fits values are within 0.02 of the coefficients in the tables for the large majority of cases, with a maximum difference of 0.04. The C_R and C_F values in Table 4-12 through Table 4-15 are based on yield line patterns for two-way components with equal moment capacities in each direction. The elastoplastic values in the tables are not used in SBEDS since it does not consider dynamic reaction in this response region.

Table 4-11 Dynamic Reaction Force Coefficients for One-Way Components

Boundary & Loading Conditions	Elastic		Plastic	
	C_R	C_F	C_R	C_F
Cantilever, Conc. Load at End	1.74	-0.74	1.50	-0.50
Fixed-Fixed, Conc. Load at Midspan	0.71	-0.21	0.75	-0.25
Fixed-Simple, Conc. Load at Midspan (simple end)	0.50	-0.18	$0.75-\left[2(1+2\frac{M_S}{M_M}\right]^{-1}$	-0.25
Fixed-Simple, Conc. Load at Midspan (fixed end)	0.97	-0.28	$0.75+\left[2(1+2\frac{M_S}{M_M}\right]^{-1}$	-0.25
Simple-Simple, Conc. Load at Midspan	0.78	-0.28	0.75	-0.25
Cantilever, Uniformly Loaded	0.69	0.31	0.75	0.25
Fixed-Fixed, Uniformly Loaded	0.36	0.14	0.38	0.12
Fixed-Simple, Uniformly Loaded (simple end)	0.29	0.08	$0.38-\left[4\left(1+2\frac{M_M}{M_S}\right)\right]^{-1}$	0.12
Fixed-Simple, Uniformly Loaded (fixed end)	0.43	0.19	$0.38+\left[4\left(1+2\frac{M_M}{M_S}\right)\right]^{-1}$	0.12
Simple-Simple, Uniformly Loaded	0.39	0.11	0.38	0.12
Note 1: Shaded values are from Morison (2005). All other values are from UFC 3-340-01 Note 2: M_S is the moment capacity at support, M_M is the moment capacity at midspan.				

There are some very significant differences between the C_R and C_F coefficients in Table 4-12 through Table 4-15 and similar coefficients from Morison in the elastic response range, and lesser differences in the plastic realm. Morison’s values are not used in

SBEDS for two-way response because there are few cases of significant difference in the plastic response realm where most response to blast loads typically occurs. Also, there are more inherent assumptions in the calculation of the dynamic reaction forces of two-way components for an equivalent SDOF system that cause both procedures to be very approximate. In particular, Morison's finite element analyses show that the dynamic reaction forces of two-way components vary significantly along the supports, which is not addressed at all in the SBEDS approach. Based on Morison's calculations, the equations in Table 4-12 through Table 4-15 from the UFC can be considered to represent approximate average dynamic reaction force values. Significantly higher localized dynamic reaction forces occur along the supports. V_A is the dynamic reaction along the short side of the two-way spanning component in Table 4-12 through Table 4-15, and V_B is the dynamic reaction along the long side.

Table 4-12 Dynamic Reaction Coefficients for Two-Way Slabs with Four Sides Fixed and Two Sides Fixed

Strain Range	L_y/L_x	Four Sides Fixed	
		V_A	V_B
Elastic	1.0	0.10P + 0.15R	0.10P + 0.15R
	0.9	0.09P + 0.14R	0.10P + 0.17R
	0.8	0.08P + 0.12R	0.11P + 0.19R
	0.7	0.07P + 0.11R	0.11P + 0.21R
	0.6	0.06P + 0.09R	0.12P + 0.23R
	0.5	0.05P + 0.08R	0.12P + 0.25R
Elastoplastic	1.0	0.07P + 0.18R	0.07P + 0.18R
	0.9	0.06P + 0.16R	0.08P + 0.20R
	0.8	0.06P + 0.14R	0.08P + 0.22R
	0.7	0.05P + 0.13R	0.08P + 0.24R
	0.6	0.04P + 0.11R	0.08P + 0.26R
	0.5	0.04P + 0.09R	0.09P + 0.28R
Plastic	1.0	$0.09P + 0.16R_m$	$0.09P + 0.16R_m$
	0.9	$0.08P + 0.15R_m$	$0.09P + 0.18R_m$
	0.8	$0.07P + 0.13R_m$	$0.10P + 0.20R_m$
	0.7	$0.06P + 0.12R_m$	$0.10P + 0.22R_m$
	0.6	$0.05P + 0.10R_m$	$0.10P + 0.25R_m$
	0.5	$0.04P + 0.08R_m$	$0.11P + 0.27R_m$

Strain Range	L_y/L_x	Two Adjacent Sides Fixed	
		V_A	V_B
Elastic	1.0	0.22P + 0.28R	0.22P + 0.29R
	0.9	0.21P + 0.25R	0.23P + 0.30R
	0.8	0.20P + 0.23R	0.24P + 0.32R
	0.7	0.19P + 0.21R	0.25P + 0.36R
	0.6	0.17P + 0.18R	0.26P + 0.40R
	0.5	0.15P + 0.15R	0.26P + 0.45R
Elastoplastic	1.0	0.22P + 0.28R	0.22P + 0.29R
	0.9	0.21P + 0.25R	0.23P + 0.30R
	0.8	0.20P + 0.23R	0.24P + 0.32R
	0.7	0.19P + 0.21R	0.25P + 0.36R
	0.6	0.17P + 0.18R	0.26P + 0.40R
	0.5	0.15P + 0.15R	0.26P + 0.45R
Plastic	1.0	$0.17P + 0.33R_m$	$0.17P + 0.33R_m$
	0.9	$0.16P + 0.32R_m$	$0.17P + 0.35R_m$
	0.8	$0.15P + 0.30R_m$	0.18P + 0.37Rm
	0.7	0.14P + 0.28Rm	$0.19P + 0.39R_m$
	0.6	$0.13P + 0.26R_m$	$0.19P + 0.42R_m$
	0.5	$0.12P + 0.24R_m$	$0.20P + 0.45R_m$

Table 4-13 Dynamic Reaction Coefficients for Two-Way Slabs with Four Sides Simply Supported

Strain Range	L_y/L_x	Four Sides Simply Supported	
		V_A	V_B
Elastic	1.0	0.07P + 0.18R	0.07P + 0.18R
	0.9	0.06P + 0.16R	0.08P + 0.20R
	0.8	0.06P + 0.14R	0.08P + 0.22R
	0.7	0.05P + 0.13R	0.08P + 0.24R
	0.6	0.04P + 0.11R	0.09P + 0.26R
	0.5	0.04P + 0.09R	0.09P + 0.28R
Plastic	1.0	$0.09P + 0.16R_m$	$0.09P + 0.16R_m$
	0.9	$0.08P + 0.15R_m$	$0.09P + 0.18R_m$
	0.8	$0.07P + 0.13R_m$	$0.10P + 0.20R_m$
	0.7	$0.06P + 0.12R_m$	$0.10P + 0.22R_m$
	0.6	$0.05P + 0.10R_m$	$0.10P + 0.25R_m$
	0.5	$0.04P + 0.08R_m$	$0.11P + 0.27R_m$

Table 4-14 Dynamic Reaction Coefficients for Two-Way Slabs with Opposite Edges Fixed and Simply Supported

Strain Range	L_y/L_x	Simply-Supported Short Edges, Fixed Long Edges		Simply-Supported Long Edges, Fixed Short Edges	
		V_A	V_B	V_A	V_B
Elastic	1.0	0.07P + 0.18R	0.09P + 0.16R	0.09P + 0.16R	0.07P + 0.18R
	0.9	0.06P + 0.16R	0.10P + 0.18R	0.08P + 0.14R	0.08P + 0.20R
	0.8	0.06P + 0.14R	0.11P + 0.19R	0.08P + 0.12R	0.08P + 0.22R
	0.7	0.05P + 0.13R	0.11P + 0.21R	0.07P + 0.11R	0.08P + 0.24R
	0.6	0.04P + 0.11R	0.12P + 0.23R	0.06P + 0.09R	0.09P + 0.26R
	0.5	0.04P + 0.09R	0.12P + 0.25R	0.05P + 0.08R	0.09P + 0.28R
Elastoplastic	1.0	0.07P + 0.18R	0.07P + 0.18R	0.07P + 0.18R	0.07P + 0.18R
	0.9	0.06P + 0.16R	0.08P + 0.20R	0.06P + 0.16R	0.08P + 0.20R
	0.8	0.06P + 0.14R	0.08P + 0.22R	0.06P + 0.14R	0.08P + 0.22R
	0.7	0.05P + 0.13R	0.08P + 0.24R	0.05P + 0.13R	0.08P+ 0.24R
	0.6	0.04P + 0.11R	0.09P + 0.26R	0.04P + 0.11R	0.09P+ 0.26R
	0.5	0.04P + 0.09R	0.09P + 0.26R	0.04P + 0.09R	0.09P+ 0.28R
Plastic	1.0	$0.09P + 0.16R_m$	$0.09P + 0.16R_m$	$0.09P + 0.16R_m$	$0.09P + 0.16R_m$
	0.9	$0.08P + 0.15R_m$	$0.09P + 0.18R_m$	$0.08P + 0.15R_m$	$0.09P + 0.18R_m$
	0.8	$0.07P + 0.13R_m$	$0.10P + 0.20R_m$	$0.07P + 0.13R_m$	$0.10P + 0.20R_m$
	0.7	$0.06P + 0.12R_m$	$0.10P + 0.22R_m$	$0.06P + 0.12R_m$	$0.10P + 0.22R_m$
	0.6	$0.05P + 0.10R_m$	$0.10P + 0.25R_m$	$0.05P + 0.10R_m$	$0.10P + 0.25R_m$
	0.5	$0.04P + 0.08R_m$	$0.11P + 0.27R_m$	$0.04P + 0.08R_m$	$0.11P + 0.27R_m$

Table 4-15 Dynamic Reaction Coefficients for Two-Way Slabs with Three Edges Fixed

Strain Range	L_y/L_x	Three Sides Fixed V_A	Three Sides Fixed V_B
Elastic	2.0	0.14P + 0.33R	0.07P + 0.04R
	1.8	0.14P + 0.32R	0.08P + 0.04R
	1.6	0.14P + 0.31R	0.09P + 0.04R
	1.4	0.13P + 0.30R	0.10P + 0.06R
	1.2	0.13P + 0.29R	0.12P + 0.08R
	1.0	0.13P + 0.27R	0.13P + 0.10R
	0.9	0.12P + 0.25R	0.14P + 0.11R
	0.8	0.12P + 0.23R	0.16P + 0.13R
	0.7	0.12P + 0.21R	0.17P + 0.15R
	0.6	0.11P + 0.18R	0.19P + 0.19R
	0.5	0.11P + 0.15R	0.21P + 0.24R
Elastoplastic	2.0	0.14P + 0.33R	0.07P + 0.04R
	1.8	0.14P + 0.32R	0.08P + 0.04R
	1.6	0.14P + 0.31R	0.09P + 0.04R
	1.4	0.13P + 0.30R	0.10P + 0.06R
	1.2	0.13P + 0.29R	0.12P + 0.08R
	1.0	0.13P + 0.27R	0.13P + 0.10R
	0.9	0.12P + 0.25R	0.14P + 0.11R
	0.8	0.12P + 0.21R	0.17P + 0.15R
	0.7	0.12P + 0.21R	0.17P + 0.15R
	0.6	0.11P + 0.18R	0.19P + 0.19R
	0.5	0.11P + 0.15R	0.21P + 0.24R
Plastic	2.0	$0.11P + 0.29R_m$	$0.07P + 0.13R_m$
	1.8	$0.11P + 0.28R_m$	$0.07P + 0.14R_m$
	1.6	$0.11P + 0.27R_m$	$0.08P + 0.16R_m$
	1.4	$0.11P + 0.26R_m$	0.09P + 0.17R
	1.2	$0.10P + 0.25R_m$	$0.10P + 0.20R_m$
	1.0	$0.10P + 0.21R_m$	$0.12P + 0.24R_m$
	0.9	$0.10P + 0.21R_m$	$0.12P + 0.24R_m$
	0.8	$0.10P + 0.21R_m$	$0.13P + 0.26R_m$
	0.7	$0.09P + 0.20R_m$	$0.14P + 0.28R_m$
	0.6	$0.09P + 0.18R_m$	$0.15P + 0.30R_m$
	0.5	$0.09P + 0.17R_m$	$0.17P + 0.33R_m$

4-3.2 EQUIVALENT STATIC REACTION FORCE

The equivalent static reaction forces are the reaction forces from a static load equal to the component's maximum calculated resistance during dynamic flexural response, r_{max}, where the static load has the same spatial distribution (i.e., uniformly distributed or concentrated) as the blast load. Equivalent static reaction forces are compared to the component shear capacity to determine if shear failure occurs, and may be used to design connections. Therefore, they are also referred to as equivalent support shears or equivalent static shear loads. Connections are typically designed to have an ultimate capacity that will statically resist the equivalent static reaction force. SBEDS calculates the equivalent static reaction forces (i.e., equivalent support shears) of one-way spanning components using formulas in Table 4-3 from TM 5-1300 and UFC 3-340-01. It calculates similar values for two-way spanning components using the formulas from TM 5-1300 in

Table 4-4, which are based on yield line theory. The equivalent support shears in Table 4-3 and

Table 4-4 are calculated at the supports of the components.

The equivalent static reaction forces in SBEDS are never based on a static load greater than the ultimate flexural resistance, r_u. This is true even when tension or compression membrane causes the overall resistance to exceed r_u, because the equivalent static reaction force is typically not used to calculate shear or connection forces for these response modes. SBEDS always calculates the maximum equivalent static reaction loads based on r_u, even when the calculated maximum component resistance is less than r_u, because this ensures that the connections will not be the weak point in the component design. Connections typically have significantly less ductility than the connected components and therefore the ultimate strength of the component should not be controlled by the connections. The user can redefine the maximum equivalent static shear forces calculated by SBEDS based on the ratio of r_{max}/r_u for cases where the component does not yield at all maximum moment regions if they are confident that the calculated blast load will not be exceeded and the maximum equivalent static shear force calculated by SBEDS causes the connection force or maximum shear stress to be too large.

For reinforced concrete and masonry components, SBEDS also calculates the equivalent static reaction force at a distance “d” from the support using modifications of the formulas in Table 4-3 and

Table 4-4 as shown in the bulleted list below. The shear at a distance “d” from the support (where d is the distance from the loaded face of the component to the reinforcing steel nearest the opposite face) is the critical shear section for reinforced concrete and masonry components loaded on the opposite face from the support, as discussed in Section 5-3 and 7-5. More accurate, less conservative, formulas for determining the equivalent support shears at a distance d from the supports of two-way spanning reinforced concrete and masonry components from Chapter 4 of TM 5-1300 are shown in Table 4-16. However, these formulas are significantly more complicated and are not programmed into SBEDS. To apply these formulas use the following procedure:

- Use (L-2d) in place of L in formulas for Equivalent Support Shears in Table 4-3 for cases with two supports and uniform load
- Use (L-d) in place of L in formulas for Equivalent Support Shears in Table 4-3 for cases with one support and uniform load
- No change in formulas for Equivalent Support Shears in Table 4-3 for cases with concentrated loads

Use (x-d) in place of x and (y-d) in place of y in formulas for Equivalent Support Shears in

- Table 4-4

Table 4-16 Ultimate Shear Stress at Distance d from Face of Support for Two-Way Elements

Edge conditions	Yield line location	Limits	Ultimate horizontal shear stress	Limits	Ultimate vertical shear stress
Two adjacent edges fixed and two edges free	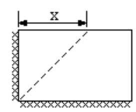	0 ≤ de/x ≤ ½	$\frac{3r_u(1-d_e/x)^2}{d_e/x(5-4d_e/x)}$	0 ≤ de/H ≤ ½	$\frac{3r_u(1-d_e/H)(2-x/L-d_ex/HL)}{d_e/H(6-x/L-4d_ex/HL)}$
		½ ≤ de/x ≤ 1	$\frac{r_u(1-d_e/x)}{2(d_e/x)}$	½ ≤ de/H ≤ 1	$\frac{r_u(1-d_e/H)(2-x/L-d_ex/HL)}{2d_e/h(1-d_ex/HL)}$
	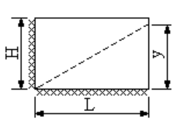	0 ≤ de/L ≤ ½	$\frac{3r_u(1-d_e/L)(2-y/H-d_ey/LH)}{d_e/L(6-y/H-4d_ey/LH)}$	0 ≤ de/y ≤ ½	$\frac{3r_u(1-d_e/y)^2}{d_e/y(5-4d_e/y)}$
		½ ≤ de/L ≤ 1	$\frac{r_u(1-d_e/L)(2-y/H-d_ey/LH)}{2d_e/L(1-d_ey/LH)}$	½ ≤ de/y ≤ 1	$\frac{r_u(1-d_e/y)}{2d_e/y}$
Three edges fixed and one edge free	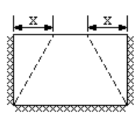	0 ≤ de/x ≤ ½	$\frac{3r_u(1-d_e/x)^2}{d_e/x(5-4d_e/x)}$	0 ≤ de/H ≤ ½	$\frac{3r_u(1-d_e/H)(1-x/L-d_ex/HL)}{d_e/H(3-x/L-4d_ex/HL)}$
		½ ≤ de/x ≤ 1	$\frac{r_u(1-d_e/x)}{2(d_e/x)}$	½ ≤ de/H ≤ 1	$\frac{r_u(1-d_e/H)(1-x/L-d_ex/HL)}{d_e/H(1-2d_ex/HL)}$
	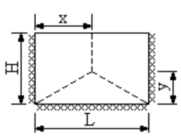	0 ≤ de/L ≤ ¼	$\frac{3r_u(1-2d_e/L)(2-y/H-2d_ey/LH)}{2d_e/L(6-y/H-8d_ey/LH)}$	0 ≤ de/y ≤ ½	$\frac{3r_u(1-d_e/y)^2}{d_e/y(5-4d_e/y)}$
		¼ ≤ de/L ≤ ½	$\frac{r_u(1-2d_e/L)(2-y/H-2d_ey/LH)}{4d_e/L(1-2d_ey/LH)}$	½ ≤ de/y ≤ 1	$\frac{r_u(1-d_e/y)}{2d_e/y}$
Four edges fixed	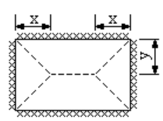	0 ≤ de/x ≤ ½	$\frac{3r_u(1-d_e/x)^2}{d_e/x(5-4d_e/x)}$	0 ≤ de/H ≤ ¼	$\frac{3r_u(1/2-d_e/H)(1-x/L-2d_ex/HL)}{d_e/H(3-x/L-8d_ex/HL)}$
		½ ≤ de/x ≤ 1	$\frac{r_u(1-d_e/x)}{2d_e/x}$	¼ ≤ de/H ≤ ½	$\frac{r_u(1/2-d_e/H)(1-x/L-2d_ex/HL)}{d_e/H(1-4d_ex/HL)}$
	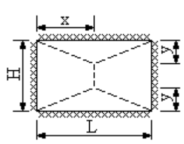	0 ≤ de/L ≤ ¼	$\frac{3r_u(1/2-d_e/L)(1-y/H-2d_ey/LH)}{d_e/L(3-y/H-8d_ey/LH)}$	0 ≤ de/y ≤ ½	$\frac{3r_u(1-d_e/y)^2}{d_e/y(5-4d_e/y)}$
		¼ ≤ de/L ≤ ½	$\frac{r_u(1/2-d_e/L)(1-y/H-2d_ey/LH)}{d_e/L(1-4d_ey/LH)}$	½ ≤ de/y ≤ 1	$\frac{r_u(1-d_e/y)}{2d_e/y}$

4-4 COMBINED AXIAL AND LATERAL LOADS

An inherent limitation of SDOF analyses, such as SBEDS, is that they only consider one degree-of-freedom and therefore cannot directly consider dynamic interaction between multiple components responding to blast load. Interactive effects must be accounted for approximately in an indirect manner by modifying the properties of the equivalent SDOF systems of the affected components. Interaction occurs in components that are subject to blast load and axial tension or compression force from the dynamic reaction applied by a supported component. This occurs in an internal explosion as shown in Figure 4-25, where the dynamic reaction force, vu, from the horizontal component causes axial tension in the supporting vertical component, which is also subject to blast load. All the wall and roof slab components of a cubical structure with an internal explosion are simultaneously subject to direct blast loading and axial tension loads from the dynamic reaction forces of connected components. Another example is a load-bearing wall, where both the wall and the supported roof beams are simultaneously subject to blast load. The dynamic reaction force from the roof beam causes axial compression load in the load-bearing wall as it is subject to direct lateral blast load.

Figure 4-25 Connection Between Components Subject to Internal Blast Loads

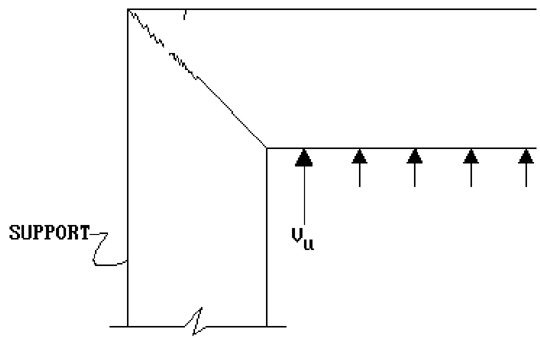

In an SDOF analysis, the ultimate flexural resistance for components with combined axial and lateral load is calculated based on a reduced ultimate dynamic moment capacity that accounts for simultaneous stress from the applied dynamic axial load. The reduced moment capacity is based on an applicable static interaction formula for combined flexure and axial tension or compression load, where the axial load is equal to the equivalent static reaction force from the supported component. The interaction diagrams used in SBEDS are discussed for reinforced concrete and steel components in Section 5-4 and Section 6-4, respectively. This procedure is conservative because it treats the peak dynamic axial load, which actually has a short duration, as a static load. A more accurate determination of the response of components with combined lateral and axial load from blast can be obtained by using a multi-degree of freedom (MDOF) model (e.g., finite element), which can directly account for the simultaneous interaction of all affected elements.

4-4.1 P-DELTA EFFECTS

Additionally, a secondary P-delta bending moment acts on a component with simultaneous lateral deflection from blast load and axial compression load, which is equal to the axial load, P, multiplied by the component deflection, delta. During elastic response, the sum of the moment caused by lateral blast load and the P-delta moment can be determined using the moment magnifier method. Another accepted method to account for P-delta effects is the equivalent lateral load method (Timoshenko and Gere, 1961). The equivalent lateral load acts in addition to the applied lateral load and causes the same moment distribution as the axial load acting with the component deflections.

This approach is more applicable for a SDOF analysis, since it is in terms of an additional load that can act during both elastic and plastic response. However, very little study has been devoted to P-delta effects during dynamic, plastic response. P-delta effects can be included in a time-stepping SDOF analysis with an additional equivalent lateral load (w_{equiv}) applied at each time step that causes an applied midspan moment, assuming no fixity at the supports, equal to the axial load multiplied by the current SDOF deflection, which represents the maximum component deflection. The P-delta effect only causes applied moment in the midspan area, where there is component deflection, and not at the supports. Also, the equivalent lateral load must have the same spatial distribution as the blast load so that it can be directly added to the blast load. It is calculated as shown in Equation 4-25. No special modifications are needed for wall type components with openings that receive dynamic axial load, unless there are compression elements around the openings (i.e., posts) that directly support part of the axial load and thereby reduce the effective width of the wall receiving dynamic axial load. In this case, see the discussion in Appendix A of the SBEDS User's Guide.

Equation 4-25

$$w_{equiv} = W_F\left(P + P_{DYN}(t)\frac{B_a}{B_L}\right)\Delta(t)$$

$$W_F = \frac{K}{L^2}C$$

$$Note: W_F = 0 \quad when \quad \frac{\mathrm{L}}{\sqrt{\frac{\mathrm{I_{avg}}}{\mathrm{A}}}} < 22 \quad for \quad concrete \quad and \quad masonry \quad components$$

where:

$w_{equiv}(t)$ = equivalent lateral load with same spatial distribution as blast load causing P-delta moments in component (psi or KPa) (added to applied blast load)

W_F = equivalent P-delta load factor (in^{-2} or mm^{-2})

K = 8 for uniformly loaded component supported top and bottom over axially loaded span (including all 3 side supported component
= 4 for component supported top and bottom with concentrated midspan load
= 2 for uniform load component supported at bottom of axially loaded span

C = load factor in direction perpendicular to axially loaded span accounting for component deflection distribution over axially loaded width
C = 0.64 for all two-way spans (this is conservative in some cases)
C = 1.0 for all one-way spans

L = span length (in or mm) (in direction of axial load for two-way spanning components)

P = total applicable static axial load applied over blast-loaded width of analyzed component divided by the blast loaded width. Do not include static or dynamic load from roof components if $P_{DYN}(t)$ is also input. Alternatively, static and dynamic effects from roof components can be conservatively included per PDC-TR 06-08 hot-linked to SBEDS with COE Response Limits button. (lb/in or N/m)
(*Note*: P is input as an axial force for beam-column type components and divided by the blast loaded width of the analyzed component in SBEDS calculations.)

$P_{DYN}(t)$ = dynamic axial load per unit width from supported component (lb/in or N/m) (usually the dynamic reaction force from a supported component along its support, which includes dead weight effects)

$\Delta(t)$ = displacement of SDOF system at each time step (in or mm)
I_{avg} = average of gross and cracked moment of inertia
A = cross sectional area
B_a = loaded width of analyzed component subject to dynamic axial load (*Note*: B_a is only an input for beam-column type components. B_a is assumed equal to B_w for wall-type components in SBEDS. See Appendix A of User's Guide if $B_a \neq B_L$ for wall-type components with dynamic axial load.) (ft or mm)
B_L = blast loaded width of analyzed component (ft or mm)

This is an approximate approach for components with fixed boundary conditions because it only causes the same moment as the P-delta effect at midspan rather than along the whole component span. It is also approximate for two-way spanning components, where the maximum deflection does not occur over the full loaded width. This is accounted for in Equation 4-25 with an approximate load factor, C. The P-delta moment acts only in the direction of the applied axial load in two-way spanning components, which is specified by the user. This is almost always the direction of gravity. As indicated in Equation 4-25, no P-delta effects are analyzed in SBEDS for reinforced concrete and masonry components subject to axial load if the slenderness ratio for the component with simple supports is less than 22, conservatively simplifying similar criteria in ACI 318-02.

The equivalent lateral load method is incorporated into SBEDS using Equation 4-25 for the component types shown in Table 4-17. These component types are the most likely to have significant axial loads. The user can always use the General SDOF component type to include P-delta effects in the SDOF analysis for any component, where the user calculates and inputs W_F from Equation 4-25.The equivalent lateral load method was tested against the moment magnifier method in the elastic load range in SBEDS by applying uniform lateral load equal to 50% of the load causing first yield with a very long rise time compared to the component natural period (i.e., essentially statically) and axial load equal to 50% of the component axial load capacity to a W12x40 beam-column, where the weak axis had continuous lateral support. The maximum deflection was calculated in SBEDS with and without axial load and the deflection magnification was compared to the moment magnifier.

Table 4-17 SBEDS Component Types with P-Delta Effects

Component Types
One-Way Steel Beam or Beam-Column
Metal Stud Wall
One-Way Reinforced Concrete Beam or Beam-Column
One-Way Wood Beam or Beam-Column
One-Way or Two-Way Reinforced Concrete Slab
One-Way or Two-Way Reinforced Masonry
General SDOF Program

Table 4-18 shows a comparison of results for a uniform load distribution, where the moment magnifier method included C_m values as shown in the notes. SBEDS matched the moment magnifier method well for all boundary conditions, particularly for simple supports. The SBEDS calculations were repeated with a concentrated lateral load at midspan and the calculated ratios of SBEDS magnification to the theoretical moment magnifier were generally within 5% of those shown Table 4-18. This comparison showed that the method in SBEDS is generally more approximate for point loads, but not by a large amount. All moment magnifiers in both series of SBEDS calculations were less than 1.8.

Table 4-18 Calculated Deflections from SBEDS for W12x40 Beam-Column Compared to Theoretical Values (Moment Magnifier)

Boundary Condition	Span (ft)	SBEDS Deflection Magnification	Moment Magnifier (C_m Based on B.C.*)	SBEDS/Theoretical
Fixed-Fixed	50	1.25	1.11	1.13
	40	1.16	1.02	1.14
	30	1.09	0.94	1.16
Fixed-Simple	50	1.46	1.45	1.01
	40	1.33	1.28	1.04
	30	1.19	1.13	1.05
Simple-Simple	50	1.81	1.78	1.02
	30	1.45	1.43	1.01
	15	1.11	1.11	1.00

*C_m=0.85 for fixed support, C_m=1.0 for simple support, C_m estimated as 0.93 for fixed simple support
Note: Static uniform lateral load in SBEDS was 50% of load causing first yield and axial load was 50% of axial load capacity in all cases above for W12x40 where weak axis had continuous lateral support.

Comparisons were also made between the theoretical buckling load and the limit axial load in SBEDS, where increasing values of axial load were input until a very small lateral “blast” load with a very long rise time (i.e., a very small, essentially static lateral load) caused lateral instability. These comparison ratios between buckling loads based on theory and SBEDS analyses were 5% to 10% higher than the ratios in Table 4-18. This is probably because the comparison in Table 4-18 involved axial loads considerably less than the limit buckling load. Therefore, the SBEDS method may be more conservative at higher axial loads. Theoretical buckling loads for two-way slabs (Timoshenko and Gere, 1961) were compared to the limit axial load determined in SBEDS as described previously in this paragraph. This comparison showed wide results depending on the boundary conditions and aspect ratio, where SBEDS was conservative in all cases by factors ranging from 1.16 to 3.0. This is due, at least in part, to the simplified assumption that C in Equation 4-25 is equal to 0.64 for all two-way components. This assumption can be improved with more study.

While these limited elastic response comparisons indicate that SBEDS is conservative, it would be beneficial to perform additional comparisons of P-delta effects from dynamic finite element analyses considering non-linear material and geometry effects to comparable SBEDS calculations for both elastic and plastic response. This comparison would possibly lead to an improved methodology in SBEDS to account for P-delta effects, especially for two-way spanning components. It would also provide information on the accuracy of the SBEDS approach during plastic response for one-way and two-way components.

4-5 MAXIMUM RESPONSE PARAMETERS

The calculated maximum dynamic deflection of the equivalent SDOF system is used to calculate two maximum response parameters in SBEDS, the maximum support rotation and the ductility ratio. These two parameters are defined in Figure 4-26 and Equation 4-26, respectively. The portion of the span used to determine the support rotation for one-way components in SBEDS is always one-half the span length, except for cantilevers when it is the full span length. This is true for fixed-simple beams even though the maximum deflection point for elastic response is not at midspan. For this case, the maximum deflection is within approximately 15% of midspan and moves closer to midspan during elastoplastic response. Since it is relatively complicated to determine the exact location, the maximum deflection point is assumed at midspan when determining the support rotation. The support rotation of two-way components in SBEDS is based on the shortest distance from the supports to the yield line area with maximum deflection, as determined from the calculated yield line pattern.

Figure 4-26 Support Rotation Angle

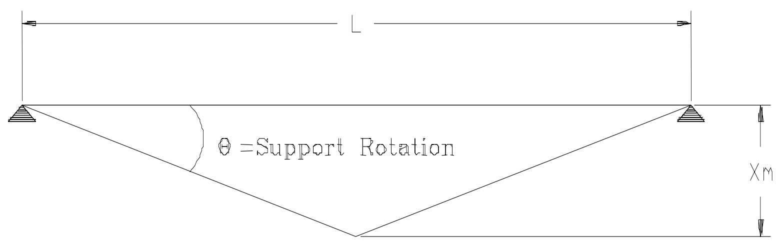

$$\textit{where} \quad \theta = \tan^{-1}\left(\frac{2x_m}{L}\right)$$

Equation 4-26

$$\mu = \frac{x_m}{x_e}$$

where: μ = ductility ratio
x_m = maximum component deflection
x_e = deflection causing yield of determinate component or yield of equivalent elastic slope of indeterminate component (see

Figure 4-5)

SBEDS also compares the calculated maximum support rotation and the ductility ratio to maximum support rotation and ductility criteria for a user defined building level of protection (LOP) from the DoD and a user defined component framing type (i.e., secondary or primary component). The calculated response is acceptable only if both the calculated maximum support rotation and ductility ratio are less than corresponding maximum criteria values. The component framing type and building LOP are discussed more in the next section. For some component types, only the calculated support rotation or ductility ratio is compared to maximum support rotation or ductility criteria from the DoD because only one of the two parameters correlates well to blast damage. For non-DoD analyses, the user can directly input a limit support rotation and/or ductility ratio. As stated in Equation 4-26, the ductility ratio for indeterminate components is calculated in SBEDS based on the equivalent yield deflection, x_E in

Figure 4-5. This is an average ductility ratio, which is less the ductility ratio at the initial yield areas and greater than the ductility ratio at the final yield location.

4-5.1 COMPONENT DAMAGE LEVELS AND BUILDING LEVELS OF PROTECTION

Acceptable maximum component damage/performance levels for DoD Antiterrorism/Force Protection (AT/FP) are defined by the U.S. Army Corps of Engineers (COE) for building Levels of Protection (LOP) and for each of three structural component framing categories (i.e., secondary, primary, non-structural component). Secondary and non-structural components have the same maximum component damage/performance levels and can be considered together. Table 4-19 shows the five building component damage/performance levels in the DoD criteria, ranging from blowout to superficial damage, and how these damage levels are associated with building LOP and component framing categories. The DoD criteria also define maximum acceptable ductility ratios and/or support rotations for each component damage/performance level in Table 4-19. PDC-TR 06-08 Revision 1 “Single Degree of Freedom Structural Response Limits for Antiterrorism Design” has more information on DoD component damage levels and building damage levels. This document is hot-linked to SBEDS on the Input sheet (i.e., with a button labeled COE Response Criteria).

Separate maximum allowable support rotations and/or ductility ratios are defined in SBEDS for up to eight sub-categories for each component type (i.e., metal stud walls, reinforced concrete slab, etc.). The sub-categories depend on specific factors for each component type such as reinforcing steel ratio, tension membrane response, etc. The user selects the most appropriate sub-category for the input component from a drop-down list in SBEDS. They also select a primary or secondary component, as applicable for the input component based on definitions in the notes of Table 4-19, and the required building LOP. The required LOP for the building with the input component must be determined separately using an approved security engineering approach. SBEDS displays the maximum allowable support rotations and/or ductility ratios based on this selections and criteria in PDC-TR 06-08 Revision 1.

The maximum acceptable ductility ratios and/or support rotations defining each damage/performance level for all available component types and sub-categories are maintained by the Protective Design Center (PDC) at the Omaha District, U.S. Army Corps of Engineers, in the Response_limits.xls workbook. These maximum acceptable response criteria are applicable for flexural, compression, and/or tension membrane response, as noted in the sub-category definitions for each set of criteria. They are not applicable for shear controlled response.

Table 4-19 Levels of Protection – New and Existing Buildings

Level of Protection	Building Component Damage			*Descriptions of Potential Structural Damage as well as Door and Window Hazards and Potential Injury*		
	Primary Structural Component [2]	Secondary Structural Component [3]	Non-structural Component [4]	*Potential Structural Damage and Performance*	*Potential Door and Glazing Hazards* [10]	*Potential Injury*
Below AT standards [1]	B3 to B4 Hazardous [6]	Greater than B4 Blowout [5]	Greater than B4 Blowout [5]	***Severe Damage*** *Progressive collapse likely. Space in and around damaged area is unusable.*	*Doors and windows will fail catastrophically and result in lethal hazards. (High hazard rating)*	*Majority of personnel in collapse region suffer fatalities. Potential fatalities in areas outside of collapsed area likely.*
Very Low	B2 to B3 Heavy [7]	B3 to B4 Hazardous [6]	B3 to B4 Hazardous [6]	***Heavy Damage*** *Onset of structural collapse: Progressive collapse is unlikely. Space in and around damaged area is unusable.*	*Glazing will fracture, come out of the frame, and is likely to be propelled into the building, with the potential to cause serious injuries. (Low hazard rating). Doors may be propelled into rooms, presenting serious hazards.*	*Majority of personnel in damaged area suffer serious injuries with a potential for fatalities. Personnel in areas outside damaged area will experience minor to moderate injuries.*
Low	B1 to B2 Moderate [8]	B2 to B3 Heavy [7]	B2 to B3 Heavy [7]	***Unrepairable Damage*** *Progressive collapse will not occur. Space in and around damaged area is unusable.*	*Glazing will fracture, potentially come out of the frame, but at a reduced velocity, does not present a significant injury hazard. (Very low hazard rating) Doors may fail, but they will rebound out of their frames, presenting minimal hazards.*	*Majority of personnel in damaged area suffer minor to moderate injuries with the potential for a few serious injuries, but fatalities are unlikely. Personnel in areas outside damaged areas will potentially experience minor to moderate injuries.*
Medium	Less than B1 Superficial [9]	B1 to B2 Moderate [8]	B1 to B2 Moderate [8]	***Repairable Damage*** *Space in and around damaged area can be used and is fully functional after cleanup and repairs.*	*Glazing will fracture, remain in the frame and results in a minimal hazard consisting of glass dust and slivers. (Minimal hazard rating) Doors will stay in frames, but will not be reusable.*	*Personnel in damaged area potentially suffer minor to moderate injuries, but fatalities are unlikely. Personnel in areas outside damaged areas will potentially experience superficial injuries.*
High	Less than B1 Superficial [9]	Less than B1 Superficial [9]	Less than B1 Superficial [9]	***Superficial Damage*** *No permanent deformations. The facility is immediately operable.*	*Glazing will not break. (No hazard rating) Doors will be reusable.*	*Only superficial injuries are likely.*

Notes:
1. This is not a level of protection, and should never be a design goal. It only defines a realm of more severe structural response, and may provide useful information in some cases.
2. Primary structural component can be identified as a member whose loss would affect a number of other components supported by that member and whose loss could potentially affect the overall structural stability of the building in the area of loss. Examples include: columns, girders, and other primary framing components directly or in-directly supporting other structural or non-structural members, and any load-bearing structural components such as walls are included.
3. Secondary structural component is a Non-load bearing infill wall components and any other structural component supported by a primary framing component.
4. Non-structural component can be identified as a member whose loss would have little effect on the overall structural stability of the building in the area of loss. Examples include interior non-load bearing walls, overhead lights, heaters, and other mechanical or architectural items attached to building structural components.
5. **Blowout**: The component is overwhelmed by the blast load causing debris with significant velocities.
6. **Hazardous failure**: The component has failed, and debris velocities range from insignificant to very significant.
7. **Heavy damage**: The component has not failed, but it has significant permanent deflections causing it to be un-repairable. The component is not expected to withstand the same blast load again without failing.
8. **Moderate damage**: The component has some permanent deflection. It is generally repairable, if necessary, although replacement may be more economical and aesthetic. The component is expected to withstand the same blast load again without failing but the end state may be a lower level of protection.
9. **Superficial damage**: No visible permanent damage. The component is expected to withstand the same blast load and maintain the level of protection.
10. Glass hazard levels are from ASTM F 1642.

SBEDS displays the maximum allowable support rotations based on this file located in the same directory as the SBEDS.xls file for the user input building LOP, component framing type (i.e., primary or secondary/non-structural), and component sub-category. For a building not subject to DoD AT/FP design criteria, the user can refer to other blast design and analysis references to determine a limit support rotation and ductility ratio for given damage levels or blast design for given component types, including ASCE (1997), TM 5-1300, and UFC 3-340-01. The documents are used primarily for design against explosions in petrochemical facilities, explosive safety design, and design of military hardened structures, respectively.

4-5.2 SHEAR CONTROLLED RESPONSE

SBEDS allows SDOF analysis of shear controlled response, as discussed in Section 4-1.2.2.4.However, the response criteria displayed in SBEDS are not applicable for shear controlled response since PDC-TR 06-08 does not currently address shear controlled response. Therefore, the user must determine applicable criteria from other published blast design documents, or rely on engineering judgment. Table 4-20 and Table 4-21 show response criteria from the American Society of Civil Engineers (ASCE, 1997) for reinforced masonry and concrete components controlled by their shear strength. Flexural response is assumed to occur until the shear force in the maximum shear region exceeds the shear strength, when shear yielding occurs, which is consistent with the analysis approach in SBEDS. The ductility ratios in Table 4-20 are based on shear yielding, where the yield deflection is equal to the ultimate resistance assuming shear controlled response (i.e., ultimate shear resistance) divided by the equivalent elastic flexural stiffness (k_E or k_e), as discussed in Section 4-1.2.1. If the ultimate shear resistance is less than the initial elastic flexural resistance, then the ductility ratios are based on the ultimate shear resistance divided by the initial elastic flexural stiffness. The values in Table 4-20 can be used as a guide for other component types that do not have available published response criteria for shear-controlled response.

Table 4-20 Response Limits for Reinforced Concrete (R/C) and Reinforced Masonry (R/M) Components Controlled by Shear Response from ASCE

Component	Low Response		Medium Response		High Response	
	μ_a	θ_a	μ_a	θ_a	μ_a	θ_a
R/C and R/M Shear Walls & Diaphragms	3		3		3	
R/C and R/M Components (shear control, without shear reinforcement)	1.3		1.3		1.3	
R/C and R/M Components (shear control, with shear	1.6		1.6		1.6	
Note: μ_a is the maximum allowable ductility ratio for each damage level. See Table 4-21 for definitions of damage levels. The allowable support rotation (θ_a) is not used as response criteria for these cases.						

Table 4-21 ASCE Component Damage Level Descriptions

Damage Level	Description
High	Component has not failed, but it has significant permanent deflections causing it to be unrepairable
Medium	Component has some permanent deflection. It is generally repairable, if necessary, although replacement may be more economical and aesthetic
Low	Component has none to slight visible permanent damage

4-6 STRAIN-RATE TO FIRST YIELD

Most structural materials exhibit a higher yield strength when they are subject to a high strain-rate, such as the strain-rates that typically occur during structural component response to blast load. The higher dynamic yield strength, which is accounted for by multiplying the static yield strength by a dynamic increase factor (DIF), is used to calculate the component's ultimate moment capacity and shear strength. SBEDS analyzes component response to blast loads based on an input DIF. Approximate, default DIF values are typically used to determine component SDOF response to blast loads, as described in Chapter 5 through Chapter 8.

Alternatively, the average strain-rate to yield of a blast-loaded component can be calculated with Equation 4-27 and used in an applicable DIF vs. strain rate relationships to determine a DIF that is applicable to the given component and blast load. An initial SDOF analysis based on a default or assumed DIF must be performed to determine the time for the component to reach its yield deflection, t_E, in Equation 4-27. The average strain-rate is then determined as shown in Equation 4-27 and used in the applicable DIF vs. strain rate relationships to determine a more accurate DIF that is used in a second SDOF analysis. Specific relationships for the DIF vs. strain rate are material dependent, and are described in Chapter 5 through Chapter 8.

Equation 4-27

$$\varepsilon'_y = \frac{\varepsilon_y}{t_E}$$

$$\varepsilon_y = \frac{DIF(f_y)}{E}$$

where:

ε'_y = average strain rate for component material
ε_y = dynamic yield strain of component material
DIF = dynamic increase factor, which is a function of ε'_y
f_y = estimated actual static yield strength
E = Young’s modulus
t_E = time required for component deflection to equal yield deflection based on calculated component response to applied blast load

Therefore, an iterative process is necessary to determine an accurate value for the DIF. The strain-rate is recalculated based on t_E from the second SDOF analysis and used in

Methodology Manual TOC

the applicable DIF vs. strain-rate relationship to recalculate the DIF. If this recalculated DIF is not equal to the DIF used in the second SDOF analysis within a tolerance of approximately 5% to 10%, the whole process is repeated during a third SDOF analysis using the recalculated DIF. Fortunately, the DIF is a relatively weak function of strain-rate and usually either the default DIF value is acceptable, or only one iteration is required to define an acceptable DIF. The equivalent static reaction force used to check for shear failure and connection design increases with the component moment capacity, and therefore with the DIF, so an unacceptably low DIF value is not conservative for these parts of a blast design. If a component has more than one material, such as reinforced concrete, separate strain rates and DIF values are determined for each material based on their different dynamic yield strains and the same value of t_E, which is dependent on the overall component response.

SBEDS simplifies the process of determining or checking the DIF by calculating the strain-rate for each component material, if there is more than one, for most component types. The user can keep the default DIF recommended by SBEDS, or calculate a more accurate DIF based on the output strain-rate and the applicable DIF vs. strain-rate relationship. If the component is indeterminate, the time to yield, t_E, in Equation 4-27 based on the equivalent yield deflection, x_E,(see

Figure 4-5) in SBEDS. No DIF is calculated for open-web steel joists, since a default DIF for this component is embedded in the methodology used to calculate the ultimate flexural resistance. The user must input the strain to yield for the General SDOF component.

4-7 CONNECTIONS

Typically, equivalent static reaction loads are used for design or analysis of connections of blast-loaded members (see Section 4-3.2). In this approach, the ultimate flexural resistance of the component is applied as an equivalent static load to determine the maximum end reaction loads on the connections. The ultimate dynamic capacity of the connection should be equal to, or greater than the equivalent static reaction load. The ultimate dynamic connection capacity can be based on Load and Resistance Factor Design (LRFD), using the applicable dynamic yield strength of the connection material in place of the static yield strength. The applicable strength reduction factor (i.e., the φ factor) from LRFD design should typically be included in the dynamic connection strength. The DIF for structural bolts and welds, which typically have a high yield strength greater than approximately 620 MPa (90,000 psi), is only on the order of 1.05.

The connection strength of components that are bolted or screwed to supports, such as cold-formed steel, is often controlled by failure of the connected material around the bolt or screw. Therefore, the overall connection strength calculations should also consider the strength of the connected material in the same manner as static LRFD connection design, where the dynamic yield strength of the connected material is used in place of the static yield strength. Also, LRFD design methods are not available for some connections, such as drilled anchors and screws, where manufacturers provide allowable connection capacity information. In these cases, the dynamic connection strength can be assumed equal to 1.7 times the allowable connection strength.

Most of the observed failures of components subject to blast loads have occurred at connections. When components are overloaded by blast loads, they often transition from flexural response to tension membrane, or catenary, response even if this response was not assumed for their design. The large reaction forces from tension membrane response overload the connections and cause failure. Therefore, the most cost-effective manner to increase the blast capacity of components is usually to design extra strength into the connections, which can usually be done at a relatively low incremental cost.

4-8 LIMITATIONS OF SDOF ANALYSIS

The assumption of a dominant mode shape during elastic, elastoplastic, and plastic response allows the response of a blast-loaded component to be calculated with an equivalent SDOF system. This is usually considered a good assumption when the component is subject to relatively uniform blast load, or a concentrated load near midspan, and has relatively rigid supports. It also tends to be a better assumption when most deflection occurs during plastic response, when response is dominated more by the fundamental response mode, rather than during early time elastic response, which is more likely to be affected by higher mode shapes. In most cases, the blast load is uniformly distributed and the component response is dominated by plastic response. Thus, SDOF response is widely used for analysis of blast-loaded components because usually the assumption of a single dominant response mode shape is acceptable. However, there are numerous limitations of the SDOF analysis method for determining component response to blast load as described in this section.

<u>Limitations Due to Structural Response Mode Assumptions</u> The equivalent SDOF system for blast-loaded components is based on response mode(s) defined by the user in the input resistance-deflection relationship. Multiple response modes, including flexure, compression and tension membrane, and axial load arching can be modeled in an approximate manner by appropriately including them in the input resistance-deflection relationship. However, the accuracy of the SDOF analysis is dependent on the user's knowledge of when and how to include the applicable response modes. This limitation is more of a problem as complicating issues, such as insufficient lateral support, local buckling, and combined structural response modes, affect the response of the blast-loaded component. However, even dynamic finite element analyses can have problems modeling some of these complexities unless a very detailed model is used. More complex response modes that may control the overall component blast damage, such as breach, fragment penetration, rebar pullout, etc. often cannot be modeled directly except in the most complex finite element analyses and are typically investigated separately with empirical approaches. It is up to the user to recognize the cases where these additional complexities must be considered.

<u>Limitations Due to Component Interaction Assumptions</u> Blast-loaded components are decoupled from the surrounding building in a SDOF analysis, since each component is analyzed as an independent SDOF system with rigid boundaries. This approach does not directly account for component interactions, such as the interaction between a supported component, which is directly loaded by blast, and the supporting component, which is loaded by the dynamic reaction forces from the supported component. A portion of mass from the supported component contributes to the inertial force of the

supporting component and the deflection of the supporting component affects the response of the supported component. The effects from this interaction are usually greatest when the natural periods of the two components are within a factor of two. Fortunately, it is usually conservative to ignore interaction effects on the supported components and to account for them simplistically for the supporting component by using a load equal to the dynamic reaction force from the supported component and including approximately 20% of the supported component mass. It is also conservative to apply the blast load directly to the supporting component.

Combined axial and lateral load from component interaction is also modeled in an equivalent SDOF system in an approximate, conservative manner, as described in Section 4-4. Components that intersect at right angles and support each other can have dynamic reaction forces that cause axial load in the supporting component, which is also directly loaded by blast. Secondary P-delta moments can also occur in components subject to simultaneous axial compression load and lateral blast load due to the combination of axial load and lateral deflection. This can be modeled approximately in a SDOF analysis as described in Section 4-4.1. Global structural response that involves more than one blast-loaded component, such as frame sway response, can also be analyzed in an approximate manner as an equivalent SDOF system if a mode shape is assumed. The response of components that make up the frame responding between their supports to direct blast load and their response as part as frame sway must be combined in a conservative manner. Therefore, many types of component interaction can be modeled in an approximate, conservative manner in SDOF analysis if the dynamic interactions are recognized and understood by the user.

A more accurate, explicit determination of the interaction between blast-loaded components can be obtained by using a multi-degree of freedom (MDOF) model (e.g., dynamic finite element method), where all interacting components are input into the structural model. The fact that dynamic nonlinear finite element codes have become much more accessible and user-friendly in the last several years makes this more possible. However, it still takes considerable time to build up sufficient experience and knowledge of these codes to use them for multi-component blast analyses. It is often useful to perform a SDOF analysis that approximately accounts for interactions between blast-loaded components to compare to finite element calculations.

<u>Limitations Due to Blast Load Assumptions</u> Finally, it can be very difficult to model component response to blast loads with complex spatial load distributions using a SDOF analysis. Blast loads that vary significantly over the area of a structural component, such as close-in explosions and confined explosions with several nearby reflecting surfaces, must be converted into an “equivalent” blast load that is spatially uniform over the whole area of the component at each time step because the load factor in SDOF analyses almost always assumes spatially uniform loading. The process of calculating equivalent uniform loads usually involves simplifying assumptions regarding the deflected shape of the component. Additionally, blast loads with very non-uniform spatial distributions can excite higher mode shapes that are not accounted for in the SDOF analysis. Blast loads with significant spatially non-uniformity can be modeled directly with dynamic finite element analyses.

In summary, equivalent SDOF systems can be used to model most blast-loaded components if complexities associated with the limitations of the SDOF approach are accounted for in a conservative manner. Alternative approaches include the use of equivalent multi-degree-of-freedom spring-mass system analyses and dynamic finite element analyses. Many commercially available finite element programs have upgraded dynamic analysis capabilities to include modeling geometric and material non-linearity with user-friendly input schemes. Engineering judgment and experience is usually necessary, however, to interpret the results in a meaningful manner for a particular problem and verify that all the relevant blast load and response issues for the given problem are included in the analysis. Also, analyses with these more complex analysis tools are more time consuming. Often a SDOF based analysis can provide an engineer with an understanding of the most relevant response issues involved in a complex problem, which may help to set up a finite element analysis, and can provide an upper bound on the dynamic response. A finite element analysis, on the other hand, can provide more precise results that do not involve nearly as many user assumptions regarding the component response.

CHAPTER 5 - REINFORCED CONCRETE COMPONENTS

5-1 DYNAMIC MATERIAL PROPERTIES

Both concrete and reinforcing steel typically exhibit greater strength under rapid strain-rates that occur during reinforced concrete component response to blast loads. Also, the actual static strengths of concrete and reinforcing steel are almost always larger than the minimum specified values used for design. Both the higher static and dynamic strengths are accounted for in the design and analysis of blast-loaded reinforced concrete components. However, the modulus of elasticity and strain at rupture and failure remain nearly constant with strain-rate for concrete and steel. Therefore, the static modulus of elasticity and strains at rupture/failure are usually assumed representative for response to blast load.

5-1.1 CONCRETE DYNAMIC STRENGTH

Concrete strength sensitivity to strain-rate and the increase in actual concrete static strengths compared to minimum specified strengths are accounted for in blast design and analysis by using the dynamic compressive strength, f'_{dc}, in place of the minimum specified static compressive strength, f'_c. The concrete dynamic compressive strength is equal to the minimum specified static strength multiplied by static and dynamic strength increase factors, as shown in Equation 5-1 from UFC 3-340-01. The static strength increase factor, K_e, is based on a review of test data for in-situ 28 day concrete compressive strength, which indicate that actual material strengths exceed specified minimums by ten percent or more in approximately ninety percent of the tests. K_e may be assumed equal to 1.1, or adjusted according based on project-specific materials testing. In addition, the static compressive strength of moist-cured concrete will increase with age beyond the 28 day compressive strength normally specified. Recommended age increase factors, K_a, for the most commonly used Portland Cement, Type I, and are 1.10 at 6 months and 1.15 at 1 year or more. K_a for concrete with high early-strength Type III cement may be taken as half that for Type I (UFC 3-340-01).

Equation 5-1

$$f'_{dc} = f'_c \, K_e K_a \left(DIF\right)$$

where:

- f'_{dc} = concrete dynamic compression stress
- f'_c = concrete minimum specified compression stress
- K_a = concrete aging factor (conservatively 1.1)
- K_e = static strength increase factor (1.1 for most cases)
  - Note: K_e also referred to as an average strength factor (ASF)
- DIF = dynamic increase factor (conservatively 1.19)

Figure 5-1 from UFC 3-340-01 shows the empirical relationship between strain-rate and the dynamic increase factor (DIF) in Equation 5-1 for the ultimate unconfined concrete compressive strength. The strain-rate in Figure 5-1 should be based on a concrete strain to yield of 0.002 and the time to yield of the concrete component caused by the blast load of interest as described in Section 4-6.

Figure 5-1 Strain-Rate vs. Concrete Compression Strength

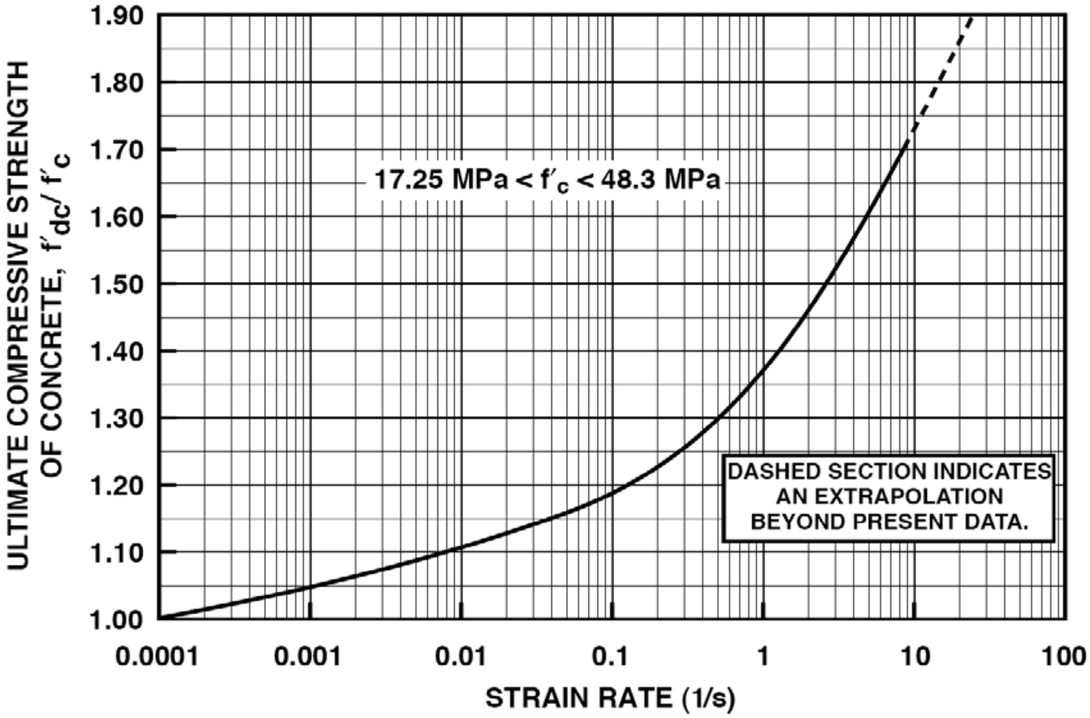

According to guidance in TM 5-1300, the strain-rates in reinforced concrete components responding to far-range blast loads (i.e., scaled standoff > 1.2 kg/m$^{1/3}$) are usually at least 0.10 sec^{-1}. For close-in response, the strain-rates are at least 0.30 sec^{-1}. Based on Figure 5-1, these correspond to minimum DIF for each load range of 1.19 and 1.25, respectively. TM 5-1300 recommends lower DIF values for each load range of 1.12 and 1.16, respectively, for columns responding to axial compression loads because they receive a filtered reaction loads from roof components that has a longer time to peak applied pressure. Therefore, except for axially loaded columns, a DIF of 1.19 can conservatively be assumed for the DIF in Equation 5-1. The overall calculated blast response is not very sensitive to the concrete compressive strength and therefore use of the default DIF from TM 5-1300 is normally recommended.

Figure 5-2 from UFC 3-340-01 shows the effect of strain-rate on the concrete splitting tensile strength. This shows very little increase in tensile strength at the recommended default strain-rates of 0.1 to 0.3 sec^{-1}. However, the tensile strength DIF increases rapidly with strain-rate at higher strain-rates. The tensile strength DIF in Figure 5-2 can be used to calculate concrete dynamic shear according to UFC 3-340-01. TM 5-1300 more conservatively recommends that the no DIF be used to calculate the concrete dynamic shear strength.

Figure 5-2 Strain-Rate vs. Concrete Splitting Tensile Strength

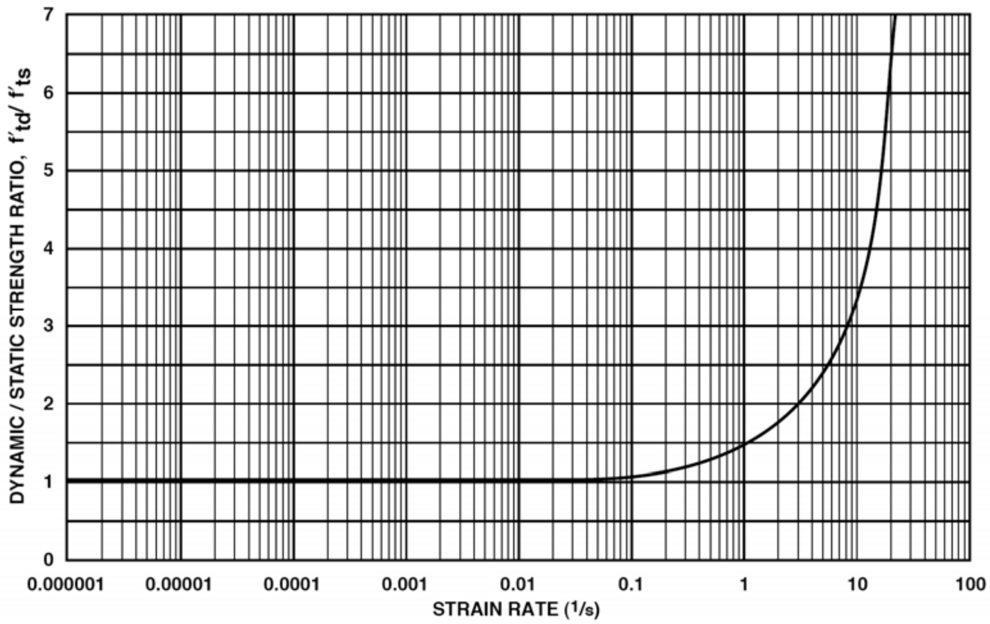

5-1.2 REINFORCING STEEL DYNAMIC STRENGTH

Reinforcing steel also exhibits greater strength under rapid strain rates. Also, the actual static strength is almost always at least 10% greater than the minimum specified strength based on many available static tests. The higher dynamic and static yield strength of reinforcing steel are accounted for in the design and analysis of blast-loaded reinforced concrete components by using the dynamic steel yield stress in Equation 5-2.

Equation 5-2

$$f_{dy} = f_y K_e (DIF)$$

where:

f_{dy} = reinforcing steel dynamic yield stress
f_{du} = reinforcing steel dynamic ultimate stress
f_y = minimum specified reinforcing steel static yield stress
f_u = minimum specified reinforcing steel static ultimate stress
K_e = static strength increase factor
Note: K_e also referred to as an average strength factor (ASF)
DIF = dynamic increase factor for f_y (see Figure 5-3)

Figure 5-3 shows the empirical relationship between strain-rate and the DIF for yield stress (f_y) and ultimate stress of steel (f_u) conforming to ASTM A615 Grades 40 and 60. Default DIF from Figure 5-3 based on strain-rates of 0.1 sec^{-1} and 0.3 sec^{-1} for far-range and close-in blast loading discussed in Section 5-1 can be used in Equation 5-2. These default DIF values are 1.22 and 1.3 for far-range and close-in blast loading, respectively, for Grade 60 reinforcing steel. Based on a slightly different relationship between strain-rate and DIF, TM 5-1300 recommends a default DIF value of 1.17 for far-range loading that is also used often for blast design. Larger default DIF values based on these two strain-rates can be determined from Figure 5-3 for Grade 40 reinforcing steel.

Almost all reinforcing steel placed in the United States after approximately 1970 is Grade 60. Prior to this, Grade 40 was used extensively. Welded wire fabric (WWF) is used extensively in reinforced concrete slabs. Dynamic yield strength information for conventional reinforcing steel used in SBEDS is summarized in Table 5-1. WWF has a low DIF value per TM 5-1300. Table 5-2 has cross sectional area information for WWF in English units from ACI 318-95.

Prestressed concrete is typically reinforced with conventional reinforcing steel and high strength prestressing cables that are Grade 250 (1723 MPa or 250,000 psi) or Grade 270 (1860 MPa or 270,000 psi). K_e and DIF values equal to 1.0 are typically assumed for these steels. Table 5-3 contains cross sectional area information for steel prestressing strands from ACI 318-95. Most concrete is prestressed with seven-wire strand.

Figure 5-3 Strain-Rate vs. Reinforcing Steel Yield and Ultimate Strength

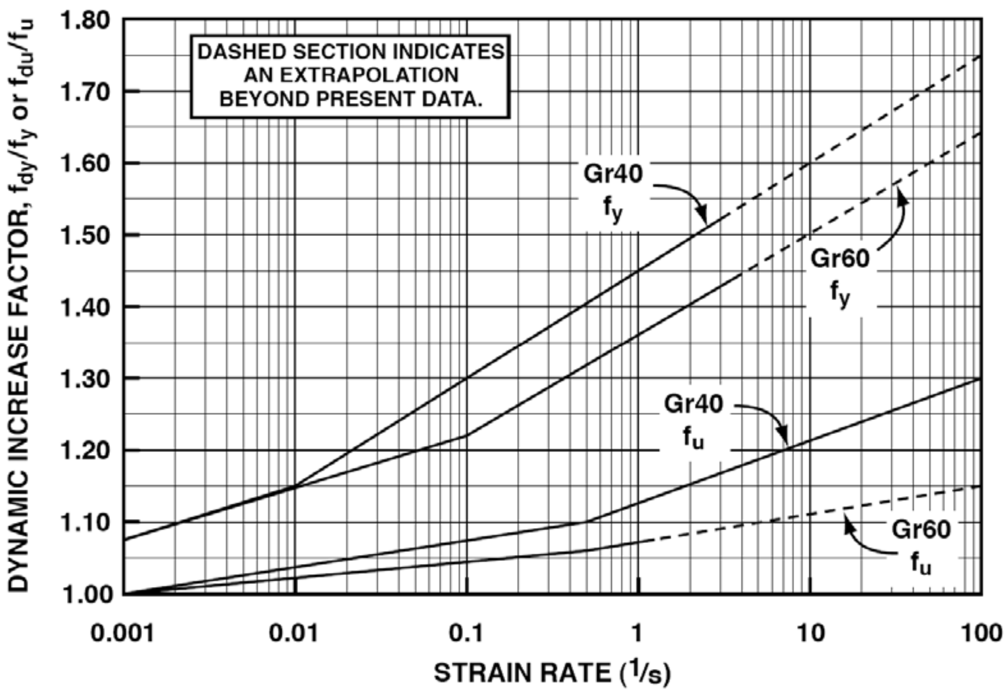

Table 5-1 Dynamic Yield Strength Information for Conventional Reinforcing Steels

Type of Steel	Yield Strength	Ultimate Strength	K_e	DIF
ASTM A615, A616, A706 (Grade 60)	415 (60000 psi)	620 (90000 psi)	1.1	1.17
ASTM A615 (Grade 40)	275 (40000 psi)	517 (75000 psi)	1.1	1.17
ASTM A82, A496 (Welded Wire Fabric)	482 (70000 psi)	550 (80000 psi)	1.0	1.1

5-2 FLEXURAL RESPONSE OF REINFORCED CONCRETE COMPONENTS

Most blast-loaded concrete components respond to blast load primarily in a flexural response mode, as discussed in Section 4-1.2.1. This requires determining the ultimate dynamic moment capacity of the component. Also the shear capacity must be determined since it may also control the ultimate resistance.

Table 5-2 Cross Sectional Area Information for Welded Wire Fabric (WWF)

ASTM STANDARD WIRE REINFORCEMENT

W & D size		Nominal	Nominal	Nominal	Area, in.^{2}/ft of width for various spacings						
					Center-to-center spacing, in.						
Plain	Deformed	diameter, in.	area, in.^{2}	weight, lb/ft	2	3	4	6	8	10	12
W31	D31	0.628	0.310	1.054	1.86	1.24	0.93	0.62	0.465	0.372	0.31
W30	D30	0.618	0.300	1.020	1.80	1.20	0.90	0.60	0.45	0.366	0.30
W28	D28	0.597	0.280	0.952	1.68	1.12	0.84	0.56	0.42	0.336	0.28
W26	D26	0.575	0.260	0.934	1.56	1.04	0.78	0.52	0.39	0.312	0.26
W24	D24	0.553	0.240	0.816	1.44	0.96	0.72	0.48	0.36	0.288	0.24
W22	D22	0.529	0.220	0.748	1.32	0.88	0.66	0.44	0.33	0.264	0.22
W20	D20	0.504	0.200	0.680	1.20	0.80	0.60	0.40	0.30	0.24	0.20
W18	D18	0.478	0.180	0.612	1.08	0.72	0.54	0.36	0.27	0.216	0.18
W16	D16	0.451	0.160	0.544	0.96	0.64	0.48	0.32	0.24	0.192	0.16
W14	D14	0.422	0.140	0.476	0.84	0.56	0.42	0.28	0.21	0.168	0.14
W12	D12	0.390	0.120	0.408	0.72	0.48	0.36	0.24	0.18	0.144	0.12
W11	D11	0.374	0.110	0.374	0.66	0.44	0.33	0.22	0.165	0.132	0.11
W10.5		0.366	0.105	0.357	0.63	0.42	0.315	0.21	0.157	0.126	0.105
W10	D10	0.356	0.100	0.340	0.60	0.40	0.30	0.20	0.15	0.12	0.10
W9.5		0.348	0.095	0.323	0.57	0.38	0.285	0.19	0.142	0.114	0.095
W9	D9	0.338	0.090	0.306	0.54	0.36	0.27	0.18	0.135	0.108	0.09
W8.5		0.329	0.085	0.289	0.51	0.34	0.255	0.17	0.127	0.102	0.085
W8	D8	0.319	0.080	0.272	0.48	0.32	0.24	0.16	0.12	0.096	0.08
W7.5		0.309	0.075	0.255	0.45	0.30	0.225	0.15	0.112	0.09	0.075
W7	D7	0.298	0.070	0.238	0.42	0.28	0.21	0.14	0.105	0.084	0.07
W6.5		0.288	0.065	0.221	0.39	0.26	0.195	0.13	0.097	0.078	0.065
W6	D6	0.276	0.060	0.204	0.36	0.24	0.18	0.12	0.09	0.072	0.06
W5.5		0.264	0.055	0.187	0.33	0.22	0.165	0.11	0.082	0.066	0.055
W5	D5	0.252	0.050	0.170	0.30	0.20	0.15	0.10	0.075	0.06	0.05
W4.5		0.240	0.045	0.153	0.27	0.18	0.135	0.09	0.067	0.054	0.045
W4	D4	0.225	0.040	0.136	0.24	0.16	0.12	0.08	0.06	0.048	0.04
W3.5		0.211	0.035	0.119	0.21	0.14	0.105	0.07	0.052	0.042	0.035
W3		0.195	0.030	0.102	0.18	0.12	0.09	0.06	0.045	0.036	0.03
W2.9		0.192	0.029	0.098	0.174	0.116	0.087	0.058	0.043	0.035	0.029
W2.5		0.178	0.025	0.085	0.15	0.10	0.075	0.05	0.037	0.03	0.025
W2		0.159	0.020	0.068	0.12	0.08	0.06	0.04	0.03	0.024	0.02
W1.4		0.135	0.014	0.049	0.084	0.056	0.042	0.028	0.021	0.017	0.014

5-2.1 ULTIMATE DYNAMIC MOMENT CAPACITY OF REINFORCED CONCRETE BEAMS AND SLABS

The ultimate dynamic moment capacity of a rectangular reinforced concrete member for the typical case of a Type I cross section (see Figure 5-4) and only tension reinforcement (singly reinforced) is given by Equation 5-3. This equation is also used in SBEDS for a double reinforced member prior to crushing of the concrete at the compression face, since it is conservative for this case and does not cause very much error. Figure 5-4 shows Type I and Type II cross sections. When the support rotation (see Section 4-5) exceeds 2 degrees, the compression face concrete can become crushed such that all compressive forces must be carried by the compression face reinforcement. At this stage the cross section becomes a Type II cross section. The reduced ultimate dynamic moment capacity of Type II cross sections is calculated as shown in Equation 5-4 based on a resisting moment arm d_c between the compression and tension face steel and a resisting force equal to the yield force of the lesser of the steel areas at each face.

Table 5-3 Cross Sectional Area Information for Steel Prestressing Strands

Type*	Nominal diameter, in.	Nominal area, in.^{2}	Nominal weight, lb/ft
Seven-wire strand (Grade 250)	1/4 (0.250)	0.036	0.122
	5/16 (0.313)	0.058	0.197
	3/8 (0.375)	0.080	0.272
	7/16 (0.438)	0.108	0.367
	1/2 (0.500)	0.144	0.490
	(0.600)	0.216	0.737
Seven-wire strand (Grade 270)	3/8 (0.375)	0.085	0.290
	7/16 (0.438)	0.115	0.390
	1/2 (0.500)	0.153	0.520
	(0.600)	0.217	0.740
Prestressing wire	0.192	0.029	0.098
	0.196	0.030	0.100
	0.250	0.049	0.170
	0.276	0.060	0.200
Prestressing bars (plain)	3/4	0.44	1.50
	7/8	0.60	2.04
	1	0.78	2.67
	1-1/8	0.99	3.38
	1-1/4	1.23	4.17
	1-3/8	1.48	5.05
Prestressing bars (deformed)	5/8	0.28	0.98
	3/4	0.42	1.49
	1	0.85	3.01
	1-1/4	1.25	4.39
	1-3/8	1.58	5.56

* Availability of some tendon sizes should be investigated in advance.

Equation 5-3

$$M_{du} = \frac{A_s f_{dy}}{b}\left(d - \frac{A_s f_{dy}}{1.7 b f'_{dc}}\right)$$

where:

M_{du} = dynamic ultimate moment capacity per unit width
A_s = area of tension reinforcement in width, b
f_{dy} = dynamic design stress
d = effective depth of Type I cross section (distance from the extreme compression fiber to the centroid of the tension reinforcement – see Figure 5-4)
b = width of rectangular section
f'_{dc} = concrete dynamic compressive strength

Figure 5-4 Type I and II Cross Sections

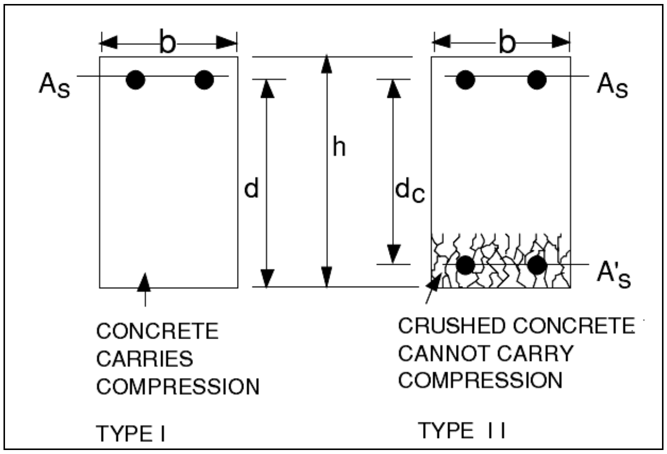

Equation 5-4

$$M_{du\_II} = \frac{A_s' f_{dy}}{b}\left(h - d_{ct} - d_{cb}\right)$$

where:

M_{du_II} = dynamic ultimate moment capacity per unit width for Type II cross section
A_s' = lesser of the top or bottom face reinforcing steel areas in width, b
f_{dy} = dynamic design stress
h = cross section thickness
d_{cb} = cover depth to bottom face reinforcing steel
d_{ct} = cover depth to top face reinforcing steel

Type II cross sections must be used for blast design of DoD buildings according to UFC 3-340-01 and TM 5-1300 for response with a support rotation greater than 2 degrees. The assumption that a Type II cross section develops at 2 degrees of support rotation is based primarily on static tests and is intended to be a design conservative approach for hardened blast resistant structures with relatively high reinforcing ratios. It implies immediate failure of singly reinforced concrete components at 2 degrees of support rotation. This does not occur in blast tests on singly reinforced concrete slabs and reinforced masonry walls, especially for lower reinforcing ratios used in typical conventional design (Oswald, 2005).

The ultimate dynamic moment capacity for reinforced concrete slabs and beams in SBEDS can be based on Equation 5-3 without any consideration of a Type II cross section, even at support rotations greater than 2 degrees. This is considered the most realistic approach for blast analysis of conventionally constructed concrete components. Alternatively, SBEDS has a user option so that it will to transition to a Type II cross section at support rotations greater than 2 degrees. In this case, the ultimate resistance in the resistance-deflection relationship transitions in SBEDS from a resistance based on the Type I moment capacity to a resistance based on the Type II moment capacity

Methodology Manual TOC

over a deflection range from 2.0 to 2.2 degrees of support rotation. There is no theoretical basis for this 10% transition range. It is simply used because it is realistic to assume some transition range and a gradual transition is preferable for computer programming purposes. The resistance-deflection relationship for a component with compression membrane response transitions directly to an ultimate flexural resistance based on a Type II moment capacity at deflections greater than those causing compression membrane response.

5-2.2 DYNAMIC MOMENT CAPACITY OF PRESTRESSED CONCRETE BEAMS AND SLABS

The ultimate dynamic moment capacity M_{du} of a rectangular prestressed cross section (or of a flanged section where the thickness of the compression flange is greater than or equal to the depth of the equivalent rectangular stress block, a) is calculated as shown in Equation 5-5. The most accurate way to determine the average stress in the prestressed reinforcement at ultimate load, f_{ps}, is a trial-and-error stress-strain compatibility analysis. This may be tedious and difficult, especially if the specific stress-strain curve of the steel being used is unavailable. In lieu of such a detailed analysis, Equation 5-6 can be used to obtain an appropriate value of f_{ps} for prestressed components with bonded prestressing tendons.

Equation 5-5

$$M_u = A_{ps} f_{ps}\left(d_p - \frac{a}{2}\right) + A_s f_{dy}\left(d - \frac{a}{2}\right)$$

$$a = \frac{\left(A_{ps} f_{ps} + A_s f_{dy}\right)}{.85 f'_{dc}\, b}$$

where:

- M_u = ultimate moment capacity
- A_{ps} = total area of prestress reinforcement
- f_{ps} = average stress in the prestressed reinforcement at ultimate load
- d_p = distance from extreme compression fiber to the centroid of the prestressed reinforcement
- a = depth of equivalent rectangular stress block
- A_s = total area of non-prestressed tension reinforcement (within spacing b for slabs)
- f_{dy} = dynamic design strength of non-prestressed reinforcement
- d = distance from extreme compression fiber to the centroid of the non-prestressed tension reinforcement
- f'_{dc} = dynamic compressive strength of concrete
- b = width of the beam for a rectangular section, width of the compression flange for a flanged section, prestressing strand spacing for slab

According to ACI 318-02, if any non-prestressed compression reinforcement is taken into account when calculating f_{ps} in Equation 5-6, then d' must not be greater than $0.15d_p$ and Equation 5-7 must be satisfied. SBEDS conservatively does not include any effects from non-prestressed compression reinforcement in Equation 5-6 if Equation 5-7 is not satisfied.

Equation 5-6

$$f_{ps} = f_{pu}\left\{1-\frac{\gamma_p}{\beta_1}\left[p_p\frac{f_{pu}}{f'_{dc}}+\frac{df_{dy}}{d_p f'_{dc}}(p-p')\right]\right\}$$

$$where \quad p=\frac{\mathrm{A_s}}{\mathrm{bd}} \quad p'=\frac{\mathrm{A'_s}}{\mathrm{bd}} \quad p_p=\frac{\mathrm{A_{ps}}}{\mathrm{bd_p}}$$

where:

f_{ps} = effective prestressing tendon strength at maximum moment capacity
f_{pu} = specified ultimate tensile strength of prestressing tendon
γ_p = factor for type of prestressing tendon
= 0.40 for $f_{py}/f_{pu} \geq 0.80$
= 0.28 for $f_{py}/f_{pu} \geq 0.90$
$ß_1$ = 0.85 for f'_{dc} up to 4000 psi and is reduced 0.05 for each 1000 psi in excess of 4000 psi
ρ_p = Prestressed reinforcement ratio
ρ = reinforcing ratio of non-prestressed tension reinforcement
ρ' = reinforcing ratio of non-prestressed compression reinforcement
A'_s = total area of non-prestressed compression reinforcement within width b
d' = distance from extreme tension fiber to the centroid of the non-prestressed compression reinforcement

See Equation 5-5 for additional parameter definitions

Equation 5-7

$$\mathrm{p_p}\frac{\mathrm{f_{pu}}}{\mathrm{f'_{dc}}}+\frac{\mathrm{df_{dy}}}{\mathrm{d_p f'_{dc}}}(\mathrm{p}-\mathrm{p'}) \geq 0.17$$

In lieu of a detailed analysis based on strain compatibility, f_{ps} for prestressed components with unbonded prestressing tendons can be determined with Equation 5-8.

Equation 5-8

$$For \quad \frac{L}{d} \leq 35 \qquad f_{ps} = f_{se} + 10{,}000 + \frac{f'_{dc}}{100\rho_p} \leq f_{py} \qquad where \quad f_{ps} \leq f_{se} + 60{,}000$$

$$For \quad \frac{L}{d} > 35 \qquad f_{ps} = f_{se} + 10{,}000 + \frac{f'_{dc}}{300\rho_p} \leq f_{py} \qquad where \quad f_{ps} \leq f_{se} + 30{,}000$$

where:

f_{se} = effective stress in prestressed reinforcement after allowances for all prestress losses (assumed equal to 60% of f_{pu} in SBEDS)
L = span length

Note: See Equation 5-5 and Equation 5-6 for additional parameter definitions

Equation 5-9 must be satisfied to insure against sudden compression failure of rectangular beams and slabs and of flanged beams where the thickness of the compression flange is greater than or equal to the depth of the equivalent rectangular stress block.

Equation 5-9

$$\frac{p_p f_{ps}}{f'_{dc}} + \frac{d f_{dy}}{d_p f'_{dc}}\left(p - p'\right) \le 0.36\beta_1$$

Equation 5-5 through Equation 5-8 are used in SBEDS to determine the ultimate dynamic moment capacity of prestressed beams and slabs. Equation 5-9 is used in SBEDS to check that the ultimate moment capacity is controlled by yielding of the prestressing steel rather than crushing of concrete. It is always assumed in SBEDS that the thickness of the compression flange is greater than or equal to the depth of the equivalent rectangular stress block, as is almost always the case in conventional design. This assumption is checked and the ratio of compression block thickness to flange thickness is printed out near the bottom of the left side of the input form for flanged beam input. Ideally this ratio should not be greater than 1.0 for Equation 5-5 to be applicable. However, as long as this ratio is no more than 1.2, the assumptions in SBEDS do not typically cause significant error in the ultimate moment dynamic capacity.

5-2.3 MOMENT OF INERTIA AND MODULUS OF ELASTICITY

The moment of inertia and modulus of elasticity are used to calculate the stiffness of reinforced concrete components, as discussed in 4-1.2.1. The moment of inertia of a reinforced concrete component changes during response to blast load from the uncracked moment of inertia, assuming no cracking from previous loading, to a fully cracked moment of inertia. This transition is not well understood, especially for high strain-rates. Fortunately, the overall response of reinforced concrete components is usually dominated by plastic response, when the stiffness equals zero and response is therefore independent of the moment of inertia. TM 5-1300 and UFC 3-340-01 recommend that the dynamic response of reinforced concrete members be calculated using the average moment of inertia in Equation 5-10, which is a simple, approximate approach.

Equation 5-10

$$I_a = \frac{\left(I_g + I_c\right)}{2}$$

where:
- I_a = average moment of inertia per unit width of reinforced concrete cross section
- I_g = moment of inertia per unit width of uncracked gross concrete section (neglect reinforcement)
- I_c = moment of inertia per unit width of cracked reinforced concrete section

The moment of inertia of the cracked concrete section, I_c, is based on the concrete compression area and the transformed steel areas computed about the centroid of the transformed section. The cracked moment of inertia per unit width of a slab or a beam with a rectangular cross section is given by Equation 5-11.

Equation 5-11

$$I_c = Fd^3$$

where:

> I_c = moment of inertia per unit width of cracked reinforced concrete section
> F = coefficient for cracked moment of inertia
> d =distance from the extreme compression fiber to the centroid of the tension reinforcement (use average value for multiple maximum moment regions)

The coefficient, F, is can be calculated with Figure 5-5 for singly reinforced concrete cross sections, with reinforcement on one face only, and for doubly reinforced cross sections with equal reinforcement in both faces. The coefficient depends on the modular ratio as given by Equation 5-12.

Figure 5-5 Coefficient for Moment of Inertia of Cracked Sections

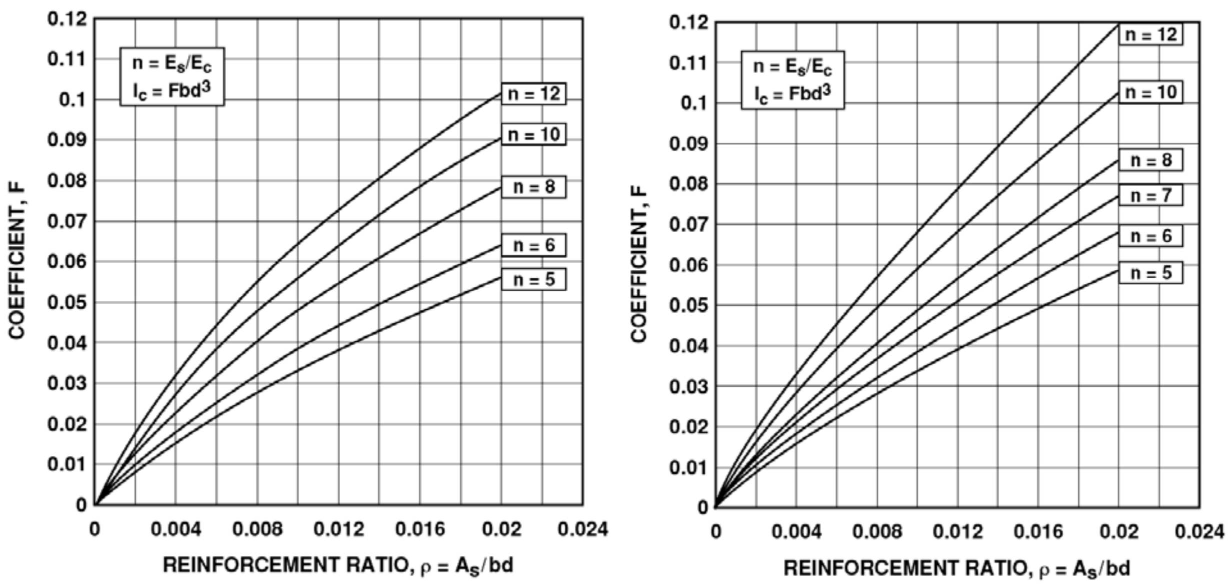

Singly Reinforced Components *Symmetrically Reinforced Components*

Equation 5-12

$$n = \frac{E_s}{E_c}$$

where:

> n = modular ratio
> E_s = modulus of elasticity of the reinforcement
> E_c = modulus of elasticity of the concrete (see Equation 5-14)

For prestressed elements the moment of inertia of the cracked section may be approximated by Equation 5-13, where n is given in Equation 5-12. This cracked moment of inertia is used in Equation 5-10 with the gross moment of inertia to determine the average moment of inertia. The average moment of inertia is used to

Methodology Manual TOC

calculate the spring stiffness for the equivalent SDOF system representing the component. See Equation 5-5 and Equation 5-6 for definitions of the terms in Equation 5-13.

Equation 5-13

$$I_c = nA_{ps}d_p{}^2\left[1-\left(p_p\right)^{1/2}\right]$$

Equation 5-10 is used in SBEDS to determine the moment of inertia of conventionally reinforced concrete components. I_c for conventionally reinforced concrete components is always based on F in Figure 5-5 for singly reinforced cross sections. This approach is conservatively used for all cross sections, regardless of the amount of compression reinforcement. I_c for prestressed reinforced concrete components is calculated with Equation 5-13. In both cases the gross moment of inertia is based only on the concrete cross section, not including the transformed steel area. This is simple, conservative approach that typically underestimates the actual gross moment of inertia by a small amount. The gross moment of inertia of a prestressed I-beam is calculated based only on the assumption the section is a T-beam with a compression flange because SBEDS does not consider an I-beam.

The modulus of elasticity for concrete in dynamic response to blast loads is assumed identical to that for static loads. The formula for the concrete modulus of elasticity in SBEDS is shown in Equation 5-14.

Equation 5-14

$$E_c = 0.043\mathrm{w}^{1.5}\sqrt{\mathrm{f'c}} \qquad Metric$$

$$E_c = 33\mathrm{w}^{1.5}\sqrt{\mathrm{f'c}} \qquad English$$

where:

E_c = concrete modulus of elasticity, MPa (psi)
w = concrete unit weight, kg/m^3 (lb/ft^3)
f'_c = concrete compression strength, MPa (psi)

5-3 SHEAR RESPONSE OF REINFORCED CONCRETE COMPONENTS

In SBEDS, direct and diagonal shear from flexural response only are considered. Other response modes are not assumed to cause these types of shear forces. The equivalent static reaction forces are calculated at the supports and a distance “d” from the supports, as discussed in Section 4-3.2, and compared to the concrete dynamic diagonal shear capacity in SBEDS. The user must determine which of these two locations is critical for the component of interest. The location of the critical shear section depends on the type of loading and whether the loaded component induces compression or tension at its supports. When the supports are put in compression, the critical section is at a distance, d, from the support face provided that no concentrated load occurs between the critical section and the support. This usually occurs when the component is subject to external blast load. When the supports are put in tension or when a concentrated load occurs near the supports, the critical section is at the face of the support. This usually occurs when the component is subject to internal blast load. These two cases are shown in Figure 5-6a and Figure 5-6b, respectively.

The depth, d, used for shear calculations in SBEDS, which equals the thickness minus the cover distance to the tensile reinforcing steel, is illustrated in Figure 5-4 for a Type I cross section. It is based on the concrete cover depth to the top layer of reinforcing steel at the supports of one-way spans, except for a simply support span where it is based on the concrete cover depth to bottom steel at midspan. For two way spans, the above approach is used except the depths in both span directions are averaged. If the two-way span is fixed on two opposite sides and simply supported on two opposite sides, then the depth is based on the cover distance to the top steel only in the direction of the fixed span. This is summarized in Table 5-4. The intent is to use the depth at the maximum moment region nearest the highest shear area.

Figure 5-6 Locations of Critical Sections for Diagonal Tension Shear

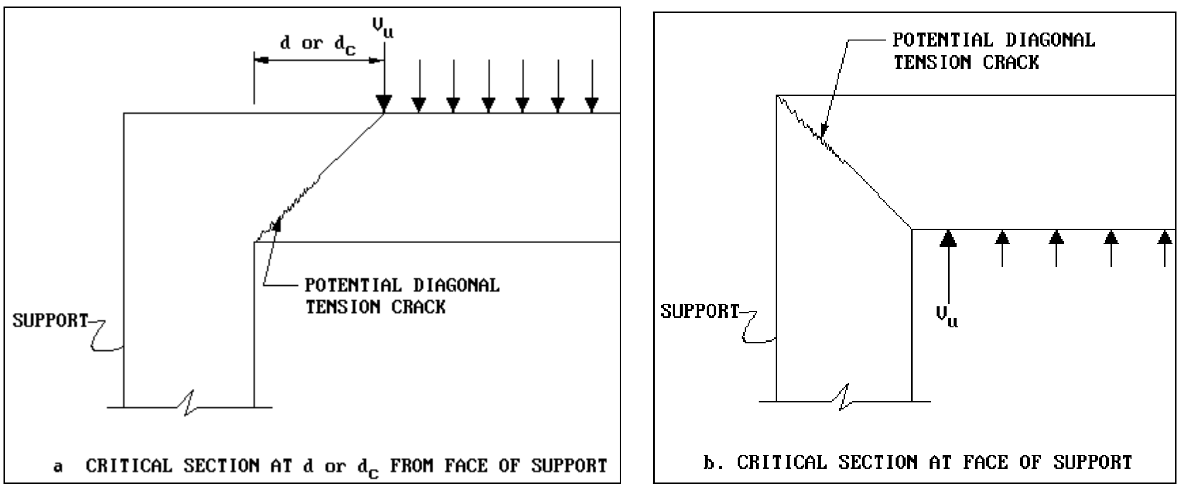

Table 5-4. Depth to Reinforcing Steel Used by SBEDS for Shear Strength Calculations

Boundary Condition	Depth (d) Used for Shear Strength Calculations
One-way, Cantilever	d at support
One-way, Fixed-Fixed	d at supports
One-way, Fixed-Simple	d at fixed support*
One-way, Simple-Simple	d at midspan
Two-Way, All Edges Simply Supported	Average d at midspan in both directions
Two-Way, All Edges Fixed	Average d at supports in both directions
Two-Way, Opposite Edges Fixed and Simply Supported	d at fixed supports *
*Highest shear load is at fixed support	

If the diagonal shear capacity, as discussed in the next sections of this chapter, is less than the equivalent static reaction force at the critical location, SBEDS calculates the required area of shear reinforcing steel so that the sum of the concrete and steel shear strengths is equal to the equivalent reaction force. If this amount of reinforcing steel is not provided (which may occur in an existing component), the component is subject to shear yielding when resistance equals the ultimate shear resistance, as discussed in

Section 4-1.2.2.4, which is less than the ultimate flexural resistance used in the SDOF analysis of the component. The can account for shear yielding using the “shear flag” in SBEDS as discussed in Section 4-1.2.2.4.

SBEDS also calculates the direct shear capacity of reinforced concrete components and compares it to the equivalent static reaction at the support. The user should refer to Chapter 4 of TM 5-1300 (1990) for calculating the required area of diagonal reinforcing bars that can be used at the supports if the equivalent static reaction force exceeds the direct shear capacity of the concrete. SBEDS does not calculate this steel area, which is rarely needed for components subject to external explosions.

The equivalent static reaction force in SBEDS is always based on the ultimate flexural capacity, which may be greater than the maximum calculated resistance for a given blast load. In this case, the direct and diagonal shear capacity checks in SBEDS, which are based on the ultimate flexural capacity, are conservative. However, it always good design practice to provide shear capacities that are at least equal to the equivalent static reaction force based on the ultimate flexural capacity of a blast-loaded component to prevent less ductile, shear controlled response if the blast load exceeds the design blast load.

5-3.1 DYNAMIC DIAGONAL SHEAR CAPACITY OF CONCRETE

The concrete dynamic shear strength for a concrete component subject to shear and flexure is calculated with Equation 5-15 in UFC 3-340-01, for cases with and without significant axial load. It is generally conservative to ignore compressive axial load effects on the concrete shear strength. Additional tension reinforcing steel may be used at midthickness in blast resistant reinforced concrete members to resist the maximum axial tension forces in the component without yielding. Available blast design documents, such as TM 5-1300 and UFC 3-340-01, do not address this case. TM 5-1300 does state that the concrete shear strength can be calculated ignoring any tension when laced steel reinforcement is used. Lacing reinforcement provides continuous shear reinforcement and concrete confinement against very close-in blast loading that could otherwise cause concrete breaching.

A conservative approach is to calculate the concrete shear strength assuming that some concrete tension strain occurs as the tension steel strains, which could affect the shear strength. However, dynamic tension force in blast-loaded components is usually from the dynamic reaction force of an intersecting component and this force occurs only over a very short time period until the intersecting component goes into rebound from the blast load. Also, the tension steel is designed not to yield. Therefore, the user may consider calculating the shear resistance neglecting the axial tension for cases where a less conservative design is desired and tension steel is provided.

Equation 5-15

$$v_c = \frac{DIF}{6}\left(K_e K_a f'_c\right)^{0.5} \quad \textit{for} \quad \textit{shear} \quad \textit{and} \quad \textit{flexure}$$

$$v_c = \frac{DIF}{6}\left(1+\frac{N_u}{14A_g}\right)\left(K_e K_a f'_c\right)^{0.5} \quad \textit{for} \quad \textit{shear, flexure} \quad \textit{and} \quad \textit{axial load}$$

Methodology Manual TOC

where:

v_c = shear stress capacity provided by the concrete
DIF = dynamic increase factor for concrete in splitting tension (see Figure 5-2)
K_e = static strength increase factor (see Equation 5-1)
Note: K_e also referred to as an average strength factor (ASF)
K_a = concrete age increase factor (see Equation 5-1)
f'_c = concrete static compressive strength
N_u = axial load normal to the cross section (tension negative)
A_g = gross area of the cross section

The concrete tensile DIF inEquation 5-15 is a function of strain-rate, and therefore must be defined based on the default strain-rates or the iteration process described for the concrete compression DIF in Section 5-1.1. The concrete tensile DIF is very sensitive to strain-rate at higher strain-rates, as shown in Figure 5-2, and it may be worth the effort to perform the iterative process for some cases. TM 5-1300, which is an older and more conservatively based blast design document, recommends a DIF of 1.0 and no increase in the static strength when calculating concrete shear strength. Therefore, the dynamic concrete shear strength equals the static shear strength. This is a much more conservative approach than Equation 5-15, which can result in 10% to 30% less calculated concrete strength, or more for very high strain-rates.

The concrete dynamic shear capacity is calculated in SBEDS using a simplified, intermediate approach for the concrete dynamic shear strength, as shown in Equation 5-16. The shear strength includes the effect of the compressive DIF, rather than the tensile DIF, under the square root sign through the f'_{dc} term. The compressive DIF can be assumed equal to a default value of 1.19 for most cases, as discussed in Section 5-1.1. No effects of axial load on shear strength are calculated in SBEDS. The user must consider these effects separately if they are important. The shear capacity, V_c, in Equation 5-16 is compared to the equivalent static reaction forces at the critical sections along the span in SBEDS in the form of a force per unit width for slabs and a total force for beams. A reaction force can be converted to a reaction force per unit width by dividing by the loaded width (e.g., beam spacing).

Equation 5-16

$$V_c = v_c d \quad for \quad slabs, \qquad V_c = v_c bd \quad for \quad beams$$

$$v_c = \frac{\sqrt{f'_{dc}}}{6}$$

where:

V_c = concrete dynamic diagonal shear force capacity (per unit supported width for slabs)
v_c = diagonal shear stress capacity provided by the concrete (MPa)
f'_{dc}= dynamic concrete compressive strength from Equation 5-1
b = beam width
d = effective depth for Type I cross section in Figure 5-4 at supports or midspan based on boundary conditions (see Table 5-4)

5-3.2 DYNAMIC DIAGONAL SHEAR STRENGTH OF PRESTRESSED CONCRETE

Under conventional service loads, prestressed elements remain almost entirely in compression, and hence are permitted a higher concrete shear stress than non-prestressed elements. However at ultimate loads the effect of prestress is lost and therefore concrete shear capacity should be calculated in the same manner as normally reinforced concrete. Therefore, the shear strength of prestressed concrete is calculated in SBEDS using Equation 5-16.

In TM 5-1300, it is recommended that the loss of the effect of prestress also means that depth, d, is the actual distance to the prestressing tendon and is not limited to 0.8h as it is in the ACI 318 code. The distance d is greatly reduced at supports of a prestressed component with draped tendons. However, draped tendons also make it difficult to properly anchor shear reinforcement at the supports. Thus it is recommended that only straight tendons be used for blast design. The depth in Equation 5-16 is conservatively based on the greater of the depth to any conventional reinforcing steel or the depth to the prestressing steel.

5-3.3 REQUIRED STEEL SHEAR REINFORCEMENT FOR DIAGONAL SHEAR

Steel shear reinforcement can be used to increase the total shear capacity of concrete and prestressed concrete so the combined shear strength from concrete and shear reninforcing steel is equal to the equivalent static reaction force at the critical section. The required reinforcing steel shear capacity is calculated in SBEDS as shown in Equation 5-17. The required area of shear reinforcing steel per unit length of shear reinforcement spacing is calculated in SBEDS as shown in Equation 5-18 for the typical case of reinforcement perpendicular to the span direction, as shown in Figure 5-7. Single leg stirrups in slabs and interior stirrups in beams must enclose the flexural bars with a 135^0 bend at the tension face as a minimum. In addition to the configuration shown in Figure 5-7, these stirrups can have a 90^0 degree hook on the end that is anchored into the compression face. This greatly simplifies placement of the stirrups during construction. The perimeter tie stirrups in beams must be closed with 135^0 bends as shown in Figure 5-7. Both legs of perimeter tie stirrups are included in shear area provided by the stirrup. Interior stirrups shown in Figure 5-7 for beams are not typically necessary. For very high required shear areas in beams, perimeter tie stirrups can also be doubled up at a given spacing.

Equation 5-17

$$V_s = V_{\max} - V_c$$

where:

- V_s = required shear force capacity provided by shear reinforcement
- V_{max} = equivalent static reaction forces at critical span locations
- V_c = concrete dynamic shear force capacity from Equation 5-16

Equation 5-18

$$\frac{A_v}{s} = \frac{V_s}{f_{dy} d} \quad for \quad beams$$

$$\frac{A_v}{bs} = \frac{V_s}{f_{dy} d} \quad for \quad slabs$$

where:

V_s = reinforcing steel shear force capacity from Equation 5-17 in units of force/width along support for slabs and total force for beams
A_v = area of required shear reinforcement within reinforcement spacing, s, for beams and within reinforcement spacings, s and b, for slabs
b = spacing of slab shear reinforcing in direction along support
s = spacing of shear reinforcing along span direction (maximum of d/2)
d = effective depth of flexural reinforcing steel for Type I cross section in Figure 5-4
f_{dy} = shear reinforcement dynamic yield stress from Equation 5-2

Figure 5-7 Shear Steel Reinforcement for Blast-Loaded Components

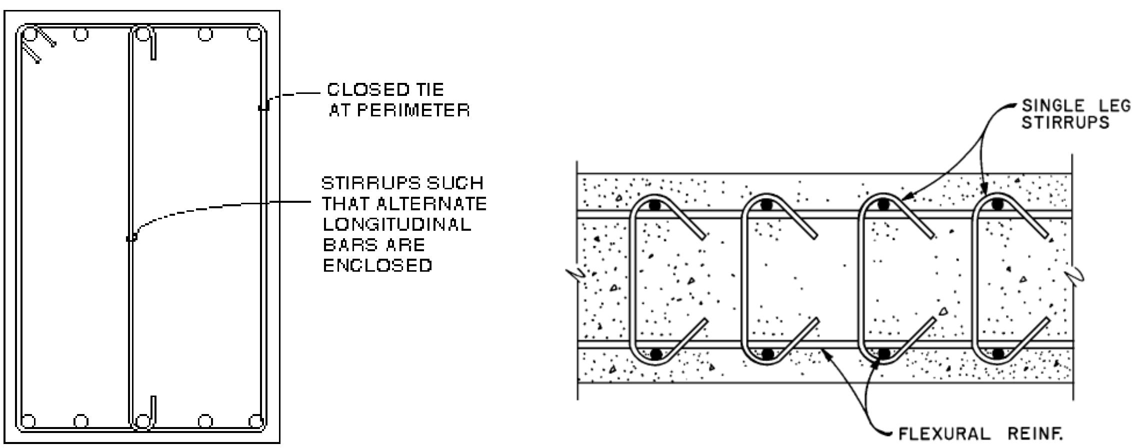

<u>*Beam shear reinforcement*</u> *(interior stirrup optional)* <u>*Slab shear reinforcement*</u>

(Note: Interior stirrup and slab shear reinforcement only require 135^0 bend on tension side and 90^0 bend on compression side as a minimum)

The maximum spacing along the span direction, s, for shear reinforcement to be considered effective is d/2, which guarantees that at least one stirrup crosses a hypothetical shear crack at a 45^0 angle anywhere along the span. In many cases column tie stirrups spaced only to prevent buckling of longitudinal steel are not effective as shear reinforcement because of this requirement. Also, the shear reinforcement in slabs is always placed at a spacing, b, along the supports equal to the flexural reinforcing steel spacing. In most cases, this means that any shear reinforcement in two-way slabs will only be effective if the flexural reinforcement spacing is limited to d/2. This may require using more flexural bars with a smaller area in a blast design than would otherwise be used.

5-3.4 DIRECT SHEAR

Direct shear failure of concrete is characterized by the rapid propagation of a crack through the depth of the component perpendicular to the span direction. The crack usually occurs at the peak dynamic shear location, which is at the face of a support, very early in the component response before significant flexural motion occurs. Therefore, a Type I cross section is assumed for direct shear stress. The direct shear capacity at the support face of a monolithic concrete joint is calculated as shown in Equation 5-19 from UFC 3-340-01. This is a slightly unconservative (by about 15%) for cleaned and roughened joints. The concrete direct shear capacity for the unusual case of an unroughened joint is conservatively assumed equal to zero. SBEDS always uses Equation 5-19 to calculate the direct shear capacity, since the roughness of the joint is not an input. If necessary, the user must modify the value calculated by SBEDS.

Equation 5-19

$$V_d = v_{dc} d \quad \textit{for} \quad \textit{slabs}, \qquad V_d = v_{dc} bd \quad \textit{for} \quad \textit{beams}$$
$$v_{dc} = 0.16 f'_{dc}$$

where:

V_d = concrete dynamic direct shear force capacity (per unit supported width for slabs)
v_{dc} = direct shear stress capacity provided by the concrete
f'_{dc} = dynamic concrete compressive strength from Equation 5-1
b = beam width
d = effective depth for Type I cross section in Figure 5-4

If $V_d > V_{max}$ (i.e., the equivalent static shear force), shear friction reinforcement is required such that the combined direct shear capacity of concrete and shear reinforcement at least equals V_{max}. The direct shear capacity of concrete with shear friction reinforcement, V_{du}, is given by Equation 5-20 from UFC 3-340-01, where the contribution of the concrete depends on the type of joint between the component and the support, as indicated in Table 5-5. The shear friction reinforcement area is in the span direction perpendicular to the plane of the face of the support (i.e., the same as the flexural reinforcement). All reinforcement crossing the crack plane, except that which is required to resist net tension in the component, is allowed to serve as shear friction reinforcement. This includes flexural bars. Usually the flexural steel and concrete provide sufficient direct shear resistance. In the cases where they do not, diagonal bars may also be used as shown in Figure 5-8. Only the area of these bars acting perpendicular to the direct shear crack, equal to ($A_s \sin\alpha$), is included as A_{vf} in Equation 5-20. Equation 5-20 is not calculated in SBEDS. The user must perform this check in the unusual case when SBEDS output indicates that V_d from Equation 5-19 is less than V_{max}.

Equation 5-20

$$V_{du} = v_{du} d \quad \textit{for} \quad \textit{slabs}, \qquad V_{du} = v_{du} bd \quad \textit{for} \quad \textit{beams}$$
$$v_{du} = K_1 f'_{dc} + \frac{K_2}{d}\left(N_c + A_{vf} f_{dy}\right) \le K_3 f'_{dc}$$

where: V_{du} = concrete dynamic direct shear force capacity (per unit supported width for slabs) including effects of reinforcing steel

Methodology Manual TOC

v_{du} = ultimate direct shear stress capacity
N_c = applied axial compression force per unit width
A_{vf} = area of the shear friction reinforcement per unit width
d =distance from the extreme compression fiber to the centroid of the tension reinforcement
f'_{dc} = concrete dynamic ultimate compressive stress
f_{dy} = reinforcement dynamic yield stress
K_i = see Table 5-5

Table 5-5 Values for Constants in Equation 5-20

Case	K_1	K_3	K_3
Monolithic concrete at joint	0.14	1.2	0.6
Cleaned and Roughened Joints (to 5 mm)	0.12	1.1	0.6
Cleaned Joints	0.0	1.0	0.4

Figure 5-8 Diagonal Bars Resisting Direct Shear

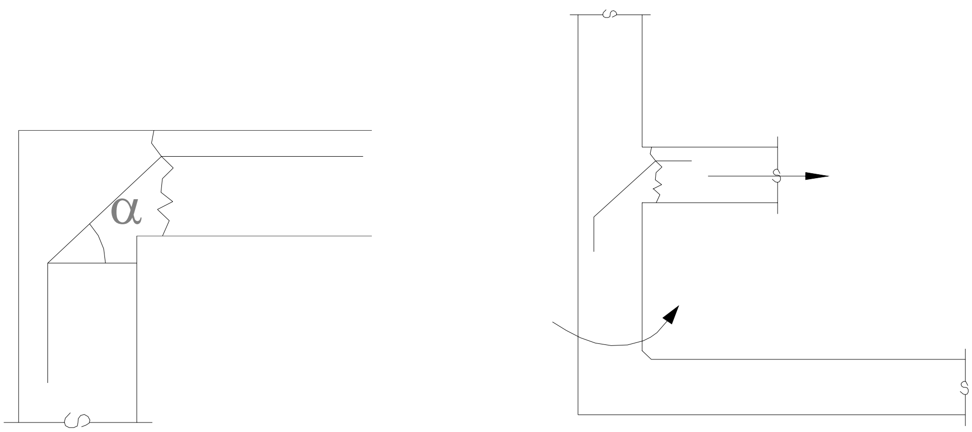

Diagonal bars at corner *Diagonal bars at intermediate slab*

5-4 COMBINED AXIAL AND LATERAL LOAD

A general discussion of components subject to combined axial and lateral load from blast is provided in Section 4-4. These components can be conservatively modeled with an equivalent SDOF system if the dynamic moment capacity used to determine the ultimate flexural resistance is calculated accounting for the stress from the peak dynamic axial load. This can be accomplished using an appropriate static interaction formula, as described for reinforced concrete components in this section. Additionally, any P-delta effects from combined compressive axial load and lateral blast load should be considered separately with an equivalent lateral P-delta load, as described in Section 4-4.1.

5-4.1 REINFORCED CONCRETE COMPONENTS WITH COMBINED AXIAL TENSION AND LATERAL LOADS

Axial tension forces are usually resisted by tensile steel area that is separate from flexural reinforcing steel area in blast resistant design. This area of longitudinal reinforcing steel is given by Equation 5-21. It must be developed within the supports on each end of the component span so that the steel area is effective over the whole clear span. The maximum equivalent reaction force from the intersecting component causing tension in the component of interest is conservatively resisted without any yielding of the tension steel in Equation 5-21.

Equation 5-21

$$A_t = \frac{N_t}{f_{dy}}$$

where:

A_t = area of axial tension reinforcement per unit width
N_t = axial tension force per unit width, taken as the maximum equivalent support reaction force of the intersecting member
f_{ds} = dynamic design stress for the member carrying axial tension, based on its flexural response

For blast resistant design, A_t can be incorporated by adding it to the quantity of flexural bars equally in each face or by placing separate longitudinal bars at the middepth of the component. It is more conservative to place separate tension steel at middepth since this will ensure that tensile steel does not contribute to the dynamic moment capacity of the component and cause higher than expected equivalent static reactions. If the area of flexural steel is fixed, as in an existing component, A_t from Equation 5-21 can be subtracted from the flexural steel that is continuous across the component and the ultimate dynamic moment capacity can be determined based on the remaining steel area. A_t can be subtracted from the continuous flexural steel at each face of doubly reinforced components in proportion to the steel areas at each face.

SBEDS does not directly consider the case where applied axial tension forces act with lateral blast loads. The user can subtract the area A_t from the flexural steel of an existing component to determine a reduced flexural steel input into SBEDS or separately calculate A_t for a designed component. The shear strength in SBEDS is calculated without accounting for any tension forces.

5-4.2 REINFORCED CONCRETE BEAM-COLUMNS WITH COMBINED COMPRESSION AND LATERAL LOAD

Reinforced concrete beam-columns, such as perimeter columns that support beams, are laterally loaded by blast and resist axial compression load. This situation should be avoided whenever possible by using a wall system that spans floor-to-floor, and therefore directly transfer lateral load into the floor and roof diaphragms. The ultimate flexural resistance of a reinforced concrete beam-column can be calculated based on the interaction diagram between axial load and moment capacity in a short column shown in Figure 5-9, which is very similar to the interaction diagram used for static design. M_o in Figure 5-9 is the dynamic moment capacity without axial load calculated using Equation 5-3. Only the input static compressive axial load is used in SBEDS to determine the moment capacity. The axial load almost always increases the moment capacity and it is therefore conservative to ignore the dynamic axial load, which is variable with time.

As shown in Figure 5-9, the available moment capacity with axial load increases initially at lower axial loads up to P_b, the balanced axial load, and then decreases as the axial

Methodology Manual TOC

load approaches the ultimate axial load capacity, P_{do}. Even though more moment capacity is available at axial load up to P_b, the axial load causes a reduction in the maximum support rotation causing failure. Therefore, axial load may reduce the available strain energy to failure, and therefore the maximum blast load that can be resisted compared to the same component without axial load.

Figure 5-9. Reinforced Concrete Beam-Column Axial Load Moment Capacity Interaction Diagram

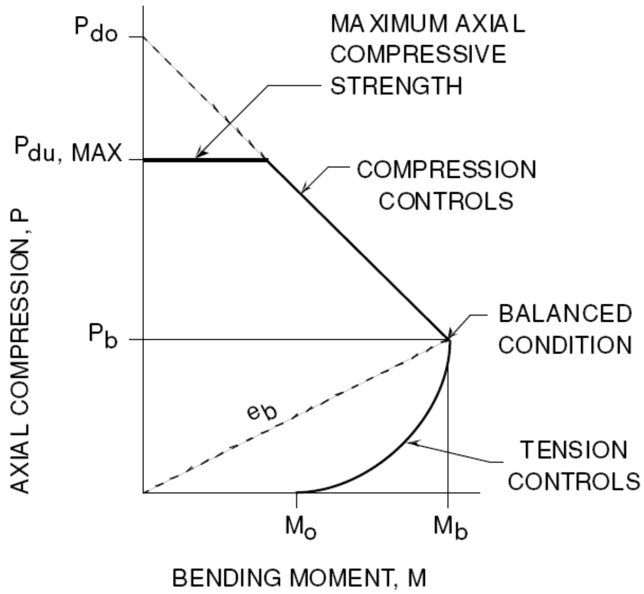

SBEDS calculates the ultimate moment capacity of a reinforced concrete beam-column based on Figure 5-9, as defined by equations in Chapter 10 of UFC 3-340-01, except that a straight line is conservatively assumed between M_0 and the balanced condition (P_b,M_b). P_{du} is calculated assuming there is symmetrical column steel at both faces, which is very common for reinforced concrete columns, equal to the average of the input inbound negative and positive steel areas. Reduced allowable support rotations are shown in SBEDS for reinforced concrete components with significant axial load.

Although the shear strength is enhanced by axial compressive load, as discussed in Section 5-3.1, SBEDS does not consider this even when there is user input compressive loads. This enhancement can be included separately from SBEDS if the phasing of the dynamic axial force relative to the component lateral response causing shear is considered. It is conservative to ignore the effects of compressive axial load on concrete shear strength.

5-5 DEEP BEAMS

Traditional principles of stress analysis used to develop the equations for ultimate dynamic moment capacity and shear capacity in Section 5-2.1 and Section 5-3.1 are not suitable for reinforced concrete components with low span to thickness or depth ratios, which are referred to as deep beams. Deep beams respond more like a tied arch than a component in flexure. Therefore, the development of the tension steel within the support is critical because the peak tension stress acts throughout most of the span. Also, plane sections do not remain plane during response to lateral load, so that a nonlinear strain distribution develops through the cross section. A laterally unrestrained beam or slab can be considered deep when its effective span-to-thickness ratio, L_e/h, is less than 2 for simple supports, or less than 2.5 for continuous support conditions. The effective span length, L_e, is taken as the smaller of the center-to-center distance between supports, or 1.15 times the clear span. In the case of two-way slabs, L_e is the short span direction. A laterally restrained concrete member is considered a deep beam when its clear span-to-thickness ratio, L/h, is less than five.

The lateral load capacity of deep beams is usually controlled by the shear capacity of the member. The shear capacity can be designed to exceed the flexural capacity, but this will not necessarily improve the ductility of a deep beam significantly because crushing of the concrete after yielding of the reinforcement in flexure occurs at much lower support rotations in deep beams than for components with conventional span-to-height ratios. This is due to enhanced compression strains from arching action. The moment capacity and shear capacity of deep beams can be calculated as shown in Chapter 10 of UFC 3-340-01. SBEDS does not consider deep beams, which are not commonly used in conventional construction.

5-6 TENSION AND COMPRESSION MEMBRANE RESPONSE

Tension and compression membrane response can occur in reinforced concrete components with in-plane restraint from supports, as described in Section 4-1.2.2.1 and Section 4-1.2.2.2. These two response modes cause an increased ultimate resistance above the ultimate flexural resistance. Compression membrane occurs at relatively low deflections, which are less than the component thickness, and tension membrane response occurs at much greater deflections. This is illustrated in Figure 4-14 in Section 4-1.2.2.1. Specific formulas for determining the ultimate resistance, stiffness, and critical deflections for reinforced concrete components with compression membrane are shown in Section 4-1.2.2.2. Similar formulas are shown for tension membrane response in Section 4-1.2.2.1.

5-7 REINFORCING STEEL DEVELOPMENT LENGTHS AND SPLICES

All tension laps and embedment lengths of steel reinforcement should be based on equations used for static reinforced concrete design, where the dynamic reinforcement yield strength and dynamic concrete compressive strength are used in place of corresponding static values. According to TM 5-1300, only contact splices that are staggered by a least the length of the splice are permitted for blast design. No splices of bundled bars or bars greater than 35 mm (1.4 inch) diameter are permitted. Any use of bundled bars is discouraged. It is recommended that all splices be placed in areas of low stress, such as inflection points in the moment diagram along the span. Due to stress reversals that occur during rebound, all splices at both faces of blast-loaded reinforced concrete components should be treated as tension splices. Welding of reinforcing steel should be avoided.

Mechanical splices that have test data showing they will develop the full ultimate strength of the reinforcing bars without reducing their ductility may be used according to TM 5-1300. Splices that develop the full ultimate strength of reinforcing steel have been used for precast concrete frame buildings in earthquake zones and are commercially available. Use of such splices can greatly reduce congestion at corners of reinforced concrete components, which can be a very serious problem for components that are designed to resist high blast loads. This is especially true for internal explosions, which cause combined tension and flexure in the wall and roof components. Also, the concrete plasticity during placement and maximum aggregate size must also be considered in such cases with congested reinforcement. The use of a maximum aggregate size of 6 mm (0.25 inches) is recommended.

5-8 REBOUND

Rebound causes a reversal of the component stresses (i.e., tension stress regions become compression regions and vice versa) and a reversal in the direction of connection forces (i.e., into the building and outward from the building) as discussed in Section 4-1.2.5. Stress reversals are a concern for conventionally reinforced concrete components because little or no steel is often designed for areas that are in compression under gravity loading. Therefore, rebound can cause tension in areas with insufficient steel reinforcement or no steel reinforcement. Also, it can cause tension in steel that is spliced assuming the surrounding concrete is in compression rather than tension. The SDOF response of reinforced concrete components in rebound is calculated in SBEDS with a similar approach as inbound response except that the flexural resistance is based on the input steel area for rebound, assuming this steel can develop its full dynamic tensile yield strength. Reinforced concrete components designed to resist blast load are typically symmetrically reinforced at both faces with all steel reinforcement splices designed assuming the splice is in tension.

The moment of inertia of reinforced concrete during rebound is not well understood, as discussed in Section 5-2.3. For lack of a better, validated approach, the moment inertia during rebound is assumed equal to that during inbound response in SBEDS.

5-9 CONNECTIONS

Reinforced concrete components can be cast-in-place or precast at an off-site location and then connected together at the building site. Cast-in-place reinforced concrete components have no exterior connections between intersecting components. The cross sections at the connections must have adequate strength to resist direct and diagonal tension shear forces. The connections must develop the forces from the ultimate dynamic moment capacity, if it is a moment connection, and the tension forces in tension steel used to resist any axial tension forces from connected components. Section 10.7 of UFC 3-340-01 has typical details for connections in monolithic blast-resistant concrete connections.

Traditionally, blast-resistant buildings have been constructed from cast-in-place reinforced concrete components, but it is also possible in many cases with larger scaled standoffs (i.e., greater than approximately 2 m/kg$^{1/3}$) to use well-connected precast components. Connections for precast components can be designed to resist the component's maximum equivalent static reaction force, as described in Section 4-7. Simple shear or bearing connections are usually be used to connect precast components to a supporting frame. However, bearing connections must also be designed for outward reaction forces that occur during rebound of the component, as shown in Figure 5-10a from ASCE (1997). Conservatively, the maximum rebound connection force is assumed equal to the maximum inbound connection force.

Alternatively, it may be based on an equivalent static reaction force for rebound response.

Figure 5-10 Example Connections at Top and Bottom of Precast Wall Panel (from ASCE)

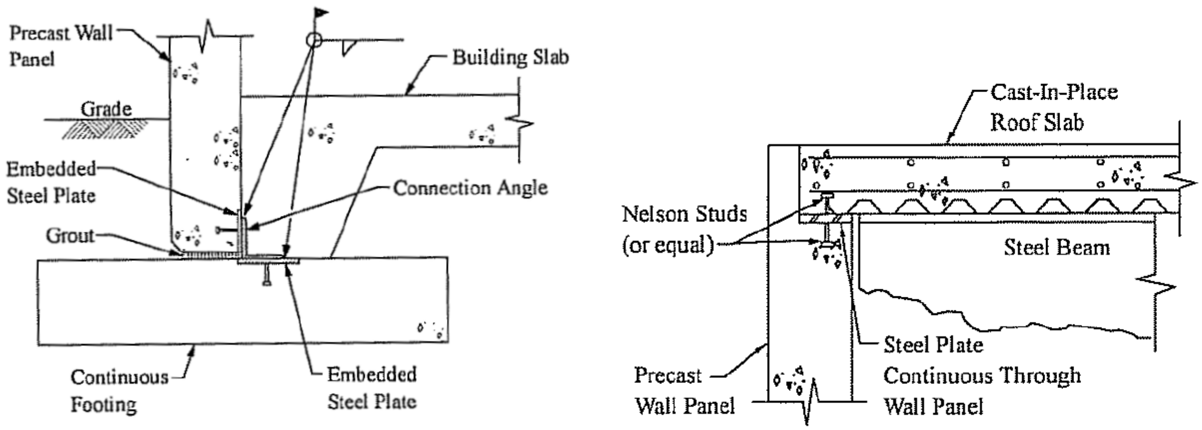

Bearing connection (tension during rebound)

Connection in shear and tension during rebound

It is very common for precast connections to be simultaneously subjected to several types of dynamic forces. Connections between precast components that both respond to blast load must typically be designed for combined shear and tension. An example of this is a roof component supported by a load-bearing precast concrete wall panel, as shown in Figure 5-10b from ASCE (1997). The connection between the components resists a dynamic tension or compression force from the roof and a shear reaction force from the wall. The worst case combination of tension force and shear force considering inbound and rebound response of the two components should be used for connection design. The connection shear force also includes out-of-plane shear, if the wall acts as a shear wall against lateral load applied to the perpendicular face of the building, based on the equivalent static reaction force from the wall along this face.

The connection in Figure 5-10a may be required to take upward shear in the plane of the wall against the rebound reaction force from a supported roof, and out-of-plane shear if the wall acts as a shear wall, in addition to tension during rebound. Shear forces acting in different directions can be combined into a resultant shear force. In a more detailed design, the relative timing of the different forces on a connection may be considered so that maximum values are not simultaneously assumed for all the forces. Precast walls are also connected together along their sides. If the walls are designed to act as together as a monolithic shear wall, heavy structural connections are normally required, as shown in Figure 5-11.

Figure 5-11 Example Connection Between Precast Concrete Wall Panels (from ASCE)

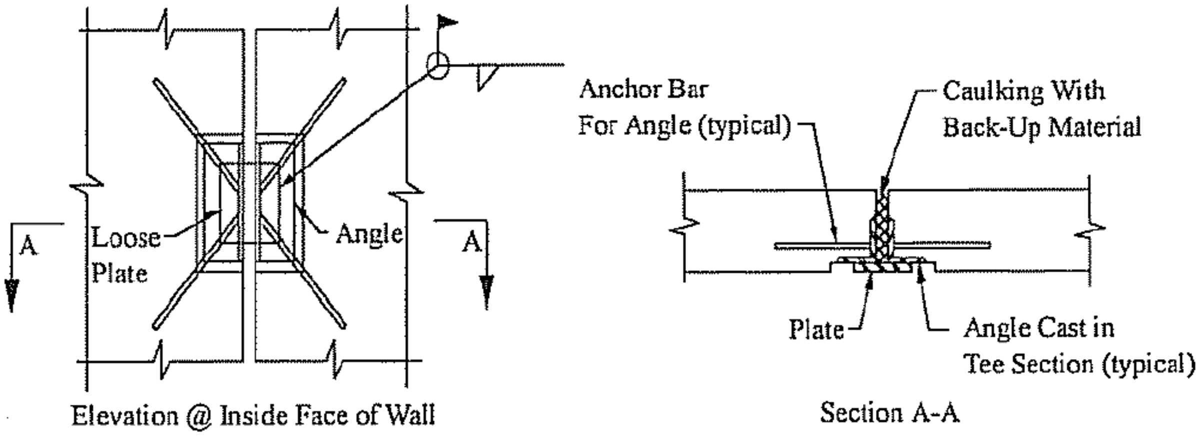

Moment-resisting connections have been used for precast reinforced concrete framing members used in high earthquake zones and therefore can be used between blast-loaded precast concrete members, if necessary. The connection must transfer a tension load based on the full dynamic yield strength of the flexural reinforcing steel in the precast component, as well as a shear reaction force based on the component's maximum equivalent static reaction force. The fact that full stress reversal may occur during rebound must also be considered. Ideally, any moment-resisting components between precast components should be placed at low stress locations. Moment-resisting precast concrete frames in high earthquake areas have been connected in this manner, where precast columns are cast with protruding tees that extend out to the inflection point in the moment distribution of the beam span. If this is not the case, the limited ductility of the connection may control the allowable support rotation for the component, rather than the ductility of the reinforced concrete cross section at maximum moment regions.

This page intentionally blank

CHAPTER 6 - STEEL AND ALUMINUM COMPONENTS

6-1 DYNAMIC MATERIAL PROPERTIES

Equation 6-1 shows the enhanced dynamic yield strength for structural steel and aluminum materials typically used for blast resistant design. The average strength increase factor, *a*, in Equation 6-1 accounts for the average ratio of the actual static strength of materials to the minimum specified strength. The dynamic increase factor, *c*, in Equation 6-1 accounts for the measured strength enhancement in steel and aluminum materials when they response at high strain-rates representative of those caused by blast loads.

Equation 6-1

$$f_{dy} = acf_y$$

where:

f_{dy} = dynamic design yield strength
f_y = minimum static yield strength
c = dynamic increase factor (DIF)
a = average static increase factor (SIF)
Note: a is also referred to as an average strength factor (ASF)

Figure 6-1 shows the empirical relationship between strain-rate and the dynamic increase factor (DIF) in Equation 6-1 for several structural steels. The strain-rate in Figure 6-1 should be based on a steel dynamic yield strain and the time to yield of the steel component caused by the blast load of interest. This involves an iterative process described in Section 4-6, because the time to yield and dynamic yield strain are based, in part, on an assumed value for the DIF. However, according to guidance in TM 5-1300 strain-rates of 0.01 sec^{-1} and 0.03 sec^{-1} can be assumed for secondary components (i.e., those directly subject to blast load) that are subject to far-range blast loads (i.e., scaled standoff > 1.2 $m/kg^{1/3}$) and close-in blast loads, respectively. A smaller strain-rate should be assumed in each case for components subject to a filtered dynamic load from the reactions of supported components (e.g., columns), as discussed in Section 5-1.1.

Table 6-1 shows recommended default values for the DIF based on an assumed strain-rate of 0.01 sec^{-1}, and the average static strength increase factor (SIF), for different types of structural steel components commonly used in building construction from TM 5-1300. As shown in Table 6-1, DIF and SIF values both reduce with increasing yield strength. This occurs because steel manufacturers minimize the additional strength provided over the minimum specified strength for more expensive high yield strength steels and testing shows that the DIF decreases with increasing yield strength, as shown in Figure 6-1. The use of cold-formed steel with a yield strength greater than 400 MPa (60,000 psi) is not recommended for blast design because the higher yield strength is usually attained by additional rolling and therefore more strain hardening of the steel, which significantly reduces its ductility.

Figure 6-1 Strain-Rate vs. Structural Steel Yield Strength

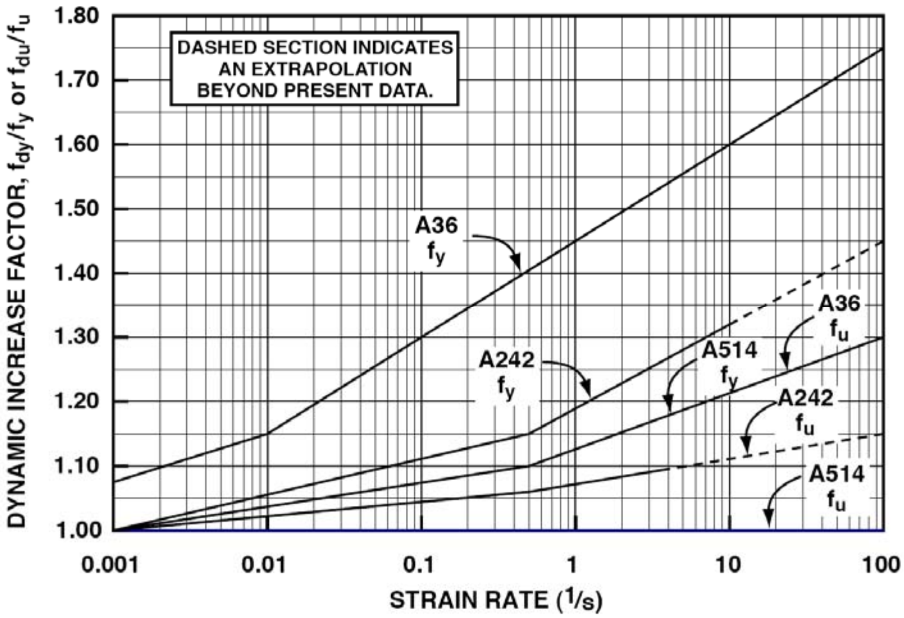

Table 6-1 Material Strength Increase Factors for Structural Steel

Material	Minimum Static Yield Strength	Average Strength Increase Factor (SIF)* (a)	Dynamic Strength Increase Factor (DIF) (c)
Cold Formed Panels, Beams	200 – 400 MPa (30,000 - 60,000 psi)	1.21	1.1
Steel	200 – 240 MPa (30,000 - 36,000 psi)	1.1	1.29
Steel	290 – 400 MPa (42,000 - 60,000 psi)	1.05	1.19
Steel	515 – 690 MPa (75,000 - 100,000 psi)	1.0	1.09
*Also referred to as an average strength factor (ASF)			

Table 6-2 shows recommended values for the SIF and DIF for different types of aluminum components commonly used in window frame construction. A great deal of research conducted on the strain-rate sensitivity of aluminum for aircraft and spacecraft research in the range of $1e^{-4}$ sec^{-1} up to 100 sec^{-1}indicates that the aluminum yield strength is essentially independent of strain-rate (DOE/TIC 11268, 1992). This is reflected in the very low value for the DIF in Table 6-2 from ASCE (1997). The values for the SIF in Table 6-2 were tabulated by dividing typical tensile yield strengths at 75^0F provided by the Aluminum Association (1993) by corresponding minimum specified yield strengths.

Table 6-2 Material Strength Increase Factors for Aluminum

Type of Aluminum	Yield Strength MPa	SIF (a)*	DIF (c)
6061 T6	241 (35,000 psi)	1.07	1.02
6063 T5	110 (16,000 psi)	1.16	1.02
6063 T6	172 (25,000 psi)	1.12	1.02
*Also referred to as an average strength factor (ASF)			

6-2 FLEXURAL RESPONSE OF STRUCTURAL STEEL COMPONENTS

Most blast-loaded steel and aluminum components respond to blast load primarily in flexure. Flexural response of blast-loaded components can be modeled with an equivalent SDOF system as discussed in Section 4-1.2.1. This requires determining the ultimate dynamic moment capacity of the component. The shear capacity must also be determined since it may also control the ultimate load capacity of the component, as discussed in Section 4-1.2.2.4.

6-2.1 ULTIMATE DYNAMIC MOMENT CAPACITY OF PLATES

The moment capacity of a ductile steel plate goes through a transition from the maximum elastic moment capacity to the fully plastic moment capacity. The moment capacity for a fully formed plastic hinge of a component with a rectangular cross section is 1.5 times the elastic moment capacity. A fully plastic moment capacity is developed when plate curvature at the hinge is about five times the curvature at initial elastic yielding, as shown in Figure 6-2 for a plate. Little error (< 3 percent) is obtained by assuming that the resisting moment increases linearly with curvature up to the full plastic moment and then stays constant with increasing curvature for plates and rectangular beams that have a ductility ratio at maximum response of at least 7.0. Thus, the ultimate dynamic moment capacity per unit width of a steel or aluminum plate is given by Equation 6-2.

The ultimate dynamic moment capacity of plates in SBEDS is always calculated conservatively using the average section modulus in the top formula in Equation 6-2. If a large ductility is calculated, the plate response in SBEDS can be recalculated with an extra factor of 1.2 applied to the input SIF, since the two moment capacity formulas in Equation 6-2 differ by a factor of 1.2 for a rectangular cross section.

High shears can have a significant effect on moment capacity of components with rectangular cross sections. When the applied shear does not exceed 55% of the ultimate dynamic shear capacity (i.e., $0.55V_{du}$), the effect of shear on moment capacity is less than 10 percent and can be ignored. The ultimate dynamic moment capacity for rectangular plate sections with an applied shear greater than $0.55V_{du}$ should be multiplied by the reduction factor K_{mv} in Equation 6-3. Equation 6-3 is not accounted for in SBEDS because it rarely applies for typical structural plates. For a plate with fixed ends (i.e., the most conservative case), the span-to-thickness ratio must be less than 6.0 for K_{mv} in Equation 6-3 to cause more than a 10% reduction in moment capacity. This is an unusual case for conventionally designed building components.

Figure 6-2 Typical Moment-Curvature Relationships for Steel Plates and Beams

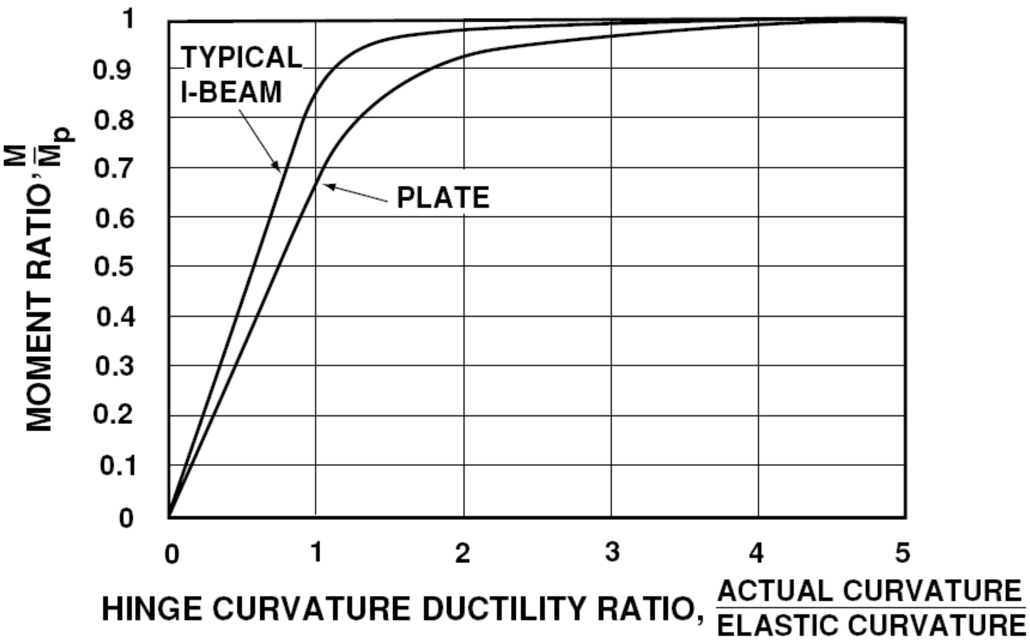

Equation 6-2

$$M_{du} = \begin{Bmatrix} f_{dy}\left(\frac{S+Z}{2}\right) & \mu \leq 7 \\ f_{dy} Z & \mu > 7 \end{Bmatrix}$$

where:

M_{du} = ultimate dynamic moment capacity per unit width
f_{dy} = dynamic yield strength of steel or aluminum plate
S =elastic section modulus per unit width
Z =plastic section modulus per unit width
μ= ductility ratio

Equation 6-3

$$K_{mv} = 1 - \left(\frac{V}{V_{du}}\right)^4$$

where:

K_{mv} = moment reduction factor for steel plates with high shear
V =applied shear force per unit width at the section in question (See equivalent static reaction load in Section 4-3.2)
V_{du} = dynamic ultimate shear capacity per unit width for steel plates (See 6-5)

6-2.2 ULTIMATE DYNAMIC MOMENT CAPACITY OF HOT ROLLED BEAMS

The AISC Manual of Steel Construction divides structural steel shapes into non-compact and compact sections based on the width-to-thickness ratios of the beam flanges and the height-to-thickness ratios of the beam web. Only compact sections are generally recommended for blast design. Almost all structural steel tube sections and I-beams with depths greater than 200 mm (8 inches) are compact members. Compact beams with well-braced compression flanges reach fully plastic moment capacity at lower ductilities than plates, as shown in Figure 6-2. Little error (< 3 percent) is obtained by assuming that the resisting moment increases linearly with curvature up to the full plastic moment and then stays constant with increasing curvature for I-beams, channels, and tube sections responding with a ductility ratio of least three. Thus, the ultimate dynamic moment capacity for well-braced, compact beams is given by Equation 6-4. A ductility ratio greater than 3 is almost always acceptable for design and typically implies limited blast damage. Therefore, the moment capacity for beams in SBEDS is always calculated with the plastic section modulus in Equation 6-4 assuming μ>3. The ratio between the two formulas for moment capacity in Equation 6-4 is less than 10% for most beam cross sections, based on a typical ratio of Z/S equal to 1.15.

Equation 6-4

$$M_{du} = \left\{ \begin{array}{cc} f_{dy}\left(\dfrac{S+Z}{2}\right) & \mu \le 3 \\ f_{dy}Z & \mu > 3 \end{array} \right\}$$

where:

M_{du} = ultimate dynamic moment capacity per unit width
f_{dy} = dynamic yield strength or steel or aluminum beam
S =elastic section modulus per unit width
Z =plastic section modulus per unit width
μ = ductility ratio

The compression flanges of beams must be braced adequately to resist lateral and torsional displacements at plastic hinge locations. Such lateral bracing should be provided at expected plastic hinge locations (i.e., maximum moment locations) and at adjacent points spaced at no more than the minimum unbraced length for the beam. According to UFC 3-340-01, points of zero moment (inflection points) may be considered as braced points for blast design. Spacing between lateral bracing points for beams bent about their strong axis should not exceed that given by Equation 6-5 in order for the full plastic moment capacity M_{du} to develop at the maximum moment region. There is no limit on distance between braced points for members with circular or tubular cross sections or for any beam bent about its weak axis. Equation 6-6 from TM 5-1300 calculates the reduced ultimate dynamic moment capacity, M_m, for beams with lateral bracing spaced at more than l_b in Equation 6-5.

Equation 6-5

$$l_b = \frac{17200 r_y}{f_{dy}}$$

where:

l_b = distance between cross sections braced against twist or lateral displacement of the compression flange, equal to the actual length for cantilevers braced only at the support (mm)

r_y = radius of gyration of the member about its weak axis (mm)

f_{dy} = steel dynamic yield stress (MPa)

SBEDS requires an input distance between laterally braced points of steel beams for inbound and rebound response, l_{bp}, which is used in Equation 6-6 to calculate M_m for inbound and for rebound response. M_m is used in SBEDS to calculate the ultimate flexural resistance of all I-beams and channels. SBEDS always calculates an ultimate dynamic moment capacity based on the plastic section modulus in Equation 6-4 for tubular cross sections and beams responding in the weak bending axis direction.

Equation 6-6

$$M_m = \left(1.07 - \frac{l_{bp}}{8300 r_y}\sqrt{f_{dy}}\right) M_{du} \leq M_{du}$$

where:

M_m = ultimate dynamic moment capacity accounting for effects of lateral bracing

l_{bp} = distance between lateral bracing points for compression flange provided to beam input separately in SBEDS for inbound and rebound response(mm)

r_y = radius of gyration of the member about its weak axis (mm)

f_{dy} = steel dynamic yield stress (MPa)

6-2.3 ULTIMATE DYNAMIC MOMENT CAPACITY OF COLD-FORMED COMPONENTS

Cold-formed steel beams and corrugated panels conforming to ASTM A446 are used in construction of many conventional industrial and office buildings. This ASTM standard covers three grades (A, B, and C) depending on the yield strength. Most panels are made of Grade A steel, which has a minimum static yield strength of 233 MPa (33,000 psi). Most cold-formed beams are made with Grade A or Grade B steel, with minimum static yield strengths of 233 MPa or 345 MPa (50,000 psi). Cold-formed components are thin enough (i.e., less than 3 mm) so they can be bent and formed from flat sheet with presses. This causes some strain-hardening in the bent regions. These components typically do not have compact cross sections, so that some local buckling occurs at maximum moment locations.

Ultimate design procedures, combined with the effective flange width concept to get cross sectional properties to account for some local buckling in the maximum moment region, are used to determine the ultimate moment capacity of cold-formed steel components. The effective section modulus at flexural yielding of the cross section and the value of moment of inertia at a service stress level of 140 MPa (20,000 psi) are provided for standard cold-formed steel component shapes. These properties can also be calculated based upon the relationships in the AISI Design Specification.
Equation 6-7 shows the ultimate dynamic moment capacity calculated in SBEDS for cold-formed steel beams, corrugated steel panels, and metal studs. These components typically do not maintain the ultimate moment capacity at deflections greater than the

yield deflection because of increased localized buckling over the whole compression area of the cross section with increasing post-yield deflection. This is characterized by "kinking" that occurs in the maximum moment regions on the compression face, as shown in Figure 6-3. However, typical connections and in-plane restraint for these components can allow a limited amount of tension membrane to develop that at least replaces the loss of flexural moment capacity caused by buckling in the compression flange out to post-yield deflections corresponding to high damage levels. This is more true for beams than panels, which is the reason for the 0.9 reduction factor on the ultimate moment capacity for panels in Equation 6-7.

Equation 6-7

$$M_{du} = S_e f_{dy} \qquad for \quad beams$$

$$M_{du} = 0.9 S_e f_{dy} \qquad for \quad panels$$

where:

M_{du} = ultimate dynamic moment capacity
S_e = effective section modulus accounting for localized buckling at from high stress in compressive face
f_{dy} = dynamic yield strength of cold-formed steel

Figure 6-3 Local Buckling in Maximum Moment Region of Cold-Formed Beams and Panels

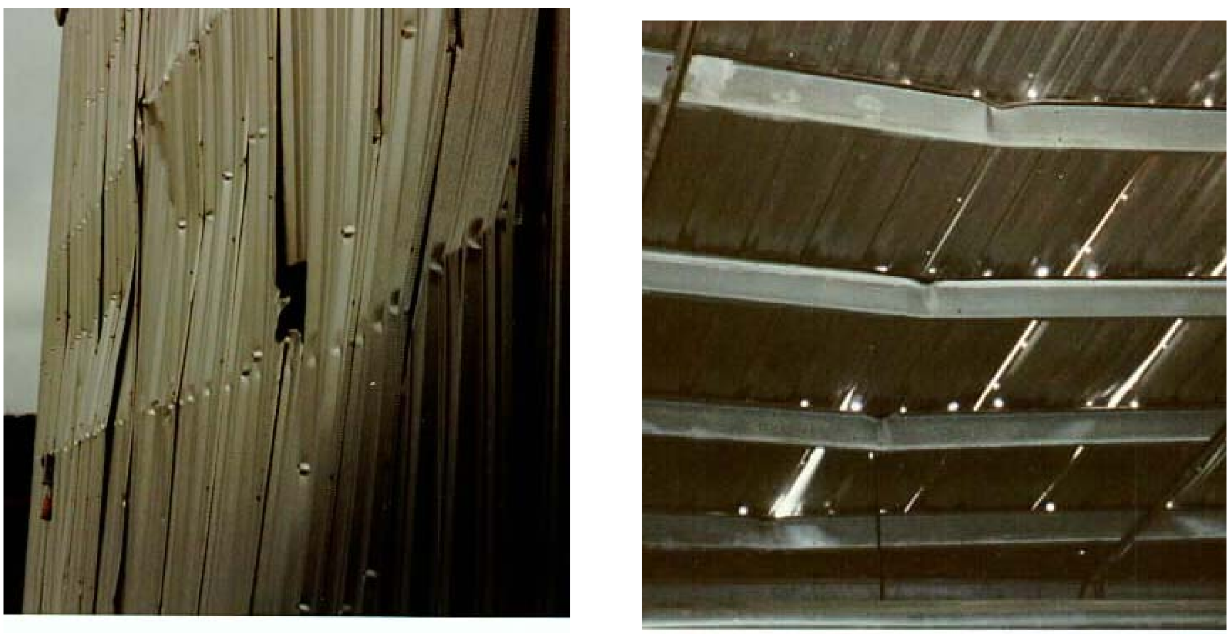

In cases where there is more significant tensile membrane restraint provided by connections and supports designed to provide this restraint, or cases where there is reason to analyze this effect more exactly, combined tension membrane and flexural response in cold-formed steel components can be modeled explicitly with SBEDS as described in Section 4-1.2.2.1.

6-3 METAL STUD WALLS

Metal stud walls consist of cold-formed steel sections, typically spaced at 400 mm (16 inch) centers, spanning vertically between floors,. Designated structural metal stud shapes are provided by the Steel Stud Manufacturer's Association (SSMA). The studs typically have web punch-outs to facilitate electrical conduit placement. Standard factory punch-outs have a minimum center-to-center spacing of 600 mm (24 inch), a maximum width equal to the lesser of one-half the member depth or 65 mm (2.5 inch), and a maximum length of 115 mm (4.5 inch). The minimum distance to the supports is 255 mm (10 inch). Punch-outs are assumed to reduce the critical axial section of the stud for compression and tension in SBEDS, but not the flexural or shear capacity. Therefore, the effective cross sectional area, A_e in Equation 6-8, is used in Equation 6-10 and Equation 4-11 to help determine the axial load capacity and controlling tension membrane force, respectively, in metal studs with web punch-outs.

Equation 6-8

$$A_e = A - w_{po} t$$

where:

A_e = effective cross sectional area
A = full member cross sectional area away from punch-out
w_{po} = width of punch-out (lesser of 65 mm of one-half member depth)
t = member thickness

The dynamic response of metal studs is calculated in a similar manner as any cold-formed steel beam in SBEDS. However, the combined response of a metal stud wall and a masonry veneer wall can also be considered in SBEDS. In this case, the veneer wall is assumed to deflect with the metal studs and to have the same span as the studs with simple boundary conditions. There is not available test data to show that the veneer wall deflects with the studs during blast loading, but significant ties are required between the veneer wall and studs for conventional design and very little deflection occurs during blast loading before the low-strength veneer wall yields in a brittle manner and the studs provide almost all additional strength. The resistance-deflection relationship for the veneer wall and metal stud wall are superimposed to get the relationship for the combined wall system. The veneer wall is assumed to have brittle flexural response and axial load arching from self-weight, as explained in Section 4-1.2.2.3.

The metal studs are assumed to respond in ductile flexural response. The first part of the combined resistance-deflection relationship is typically dominated by the veneer wall response, since it is much stiffer than the metal studs. After the veneer wall reaches maximum flexural resistance and responds in axial load arching from self-weight, the combined resistance-deflection relationship is usually dominated by the metal stud response. Typically, veneer walls are relatively thin, weak, and brittle and therefore do not add much blast capacity to the combined wall system (less than 20%). If the masonry veneer wall fully yields in flexure (i.e., cracks) during inbound response, only the metal stud wall response is considered by SBEDS during rebound.

6-4 STEEL BEAM-COLUMNS WITH COMBINED FLEXURE AND COMPRESSIVE AXIAL LOAD

The moment capacity for beam-columns is calculated in SBEDS based on the interaction formula for combined lateral and axial load from the AISC ASD Design Specification, Chapter N, Plastic Design, with the dynamic yield strength substituted for the static yield strength. The same interaction equations are in Chapter 5 of TM 5-1300. These interaction equations are set equal to 1.0 and solved to determine the available moment capacity considering simultaneous axial compressive load in Equation 6-9. The ultimate dynamic moment including axial effects, M_{duA}, in Equation 6-9 is used in SBEDS to determine the ultimate flexural resistance for all beams with input axial load. The term $(1-P/P_e)/C_m$ in Equation 6-9 is assumed equal to 1.0 in SBEDS because second order P-delta effects are accounted for directly in SBEDS with an equivalent lateral load, as described in Section 4-4.1. The moment capacity for metal studs in SBEDS is only based on the interaction equation that considers column slenderness, which is consistent with static design for these members.

Equation 6-9

$$M_{duA1} = M_m\left(1-\frac{P}{P_{cr}}\right)\left[\frac{1}{C_m}\left(1-\frac{P}{P_e}\right)\right] \quad where \quad \frac{1}{C_m}\left(1-\frac{P}{P_e}\right)=1 \quad in \quad SBEDS$$

$$M_{duA2} = 1.18M_{du}\left(1-\frac{P}{P_y}\right) \le M_{du}$$

$$M_{duA} = MIN\left(M_{duA1}, M_{duA2}\right)$$

***Note**: $M_{duA} = M_{duA1}$ for metal studs*

Equation 6-10

$$P_{cr} = 0.658^{\lambda_c^2} f_{dy}A \quad if \quad \lambda_c \le 1.5 \quad where \quad \lambda_c = \frac{KL}{r\pi}\sqrt{\frac{f_{dy}}{E}}$$

$$P_{cr} = \frac{0.877}{\lambda_c^2} f_{dy}A \quad if \quad \lambda_c > 1.5$$

where:

- M_{duA} = ultimate dynamic moment capacity accounting for axial compressive load
- P = applied axial compression load including input static load and peak dynamic axial load
- P_e = Euler buckling load
- P_{cr} = axial load capacity accounting for column slenderness (see Equation 6-10)
- P_y = axial load capacity for short column based on beam-column cross section area = $f_{dy}A$
- A = cross sectional area
- M_m = moment capacity accounting for bracing to compression flange in weak axis direction (see Equation 6-6)
- M_{du} = moment capacity accounting for fully braced component $=f_{dy}Z$ (see

Equation 6-4)

C_m = coefficient applied to bending term in moment-axial load interaction formula and dependent upon column curvature caused by applied moments (see AISC Design Specification)

E = Young's modulus

KL/r = larger slenderness ratio considering strong and weak bending axes where L = unbraced length, K= effective length factor based on boundary conditions, and r = radius of gyration about each axis. K assumed =1.0 in weak bending axis. Critical KL/r is calculated for inbound response and also used for rebound response in SBEDS.

6-5 SHEAR CAPACITY OF PLATES, PANELS, AND BEAMS

The dynamic shear strength of steel and aluminum components is calculated in SBEDS with Equation 6-11 for cases where web slenderness criteria, as defined by the web height to thickness (h/t) ratio, does not control shear strength. This is the case for all plates and for all beam and panel components that meet the h/t criterion in Equation 6-11. Equation 6-12 through Equation 6-14 are used for all beam and panel components where the h/t criterion in Equation 6-11 is not met, except panels with fixed supports. SBEDS calculates the shear strength for these components using Table 6-3.

Equation 6-11

$$f_{dv} = 0.55 f_{dy} \qquad for \quad \frac{h}{t} \le 2.45\sqrt{\frac{E}{f_{dy}}}$$

where:

f_{dv} = dynamic shear strength of steel or aluminum
f_{dy} = dynamic yield strength of steel or aluminum
A_v = shear area of component (i.e., beam web area)
h = height of beam web
t = web thickness
E = Young's modulus

Equation 6-12

For f_y= 227 MPa (33,000 psi)

$$\text{If } \left(\frac{h}{t}\right) \le 83, \text{ then} \qquad f_{dv} = \frac{8.7x10^3}{(h/t)}\ \text{MPa}$$

$$\text{If } 83 < \left(\frac{h}{t}\right) \le 150, \text{ then} \qquad f_{dv} = \frac{7.4x10^5}{(h/t)^2}\ \text{MPa}$$

Equation 6-13

For f_y= 345 MPa (50,000 psi)

$$\text{If } \left(\frac{h}{t}\right) \le 67, \text{ then} \qquad f_{dv} = \frac{10.6x10^3}{(h/t)} \text{ MPa}$$

$$\text{If } 67 < \left(\frac{h}{t}\right) \le 150, \text{ then} \qquad f_{dv} = \frac{7.4x10^5}{(h/t)^2} \text{ MPa}$$

Equation 6-14

For f_y = 550 MPa (80,000 psi)

$$\text{If } \left(\frac{h}{t}\right) \le 58, \text{ then} \qquad f_{dv} = \frac{12.3x10^3}{(h/t)} \text{ MPa}$$

$$\text{If } 58 < \left(\frac{h}{t}\right) \le 150, \text{ then} \qquad f_{dv} = \frac{7.4x10^5}{(h/t)^2} \text{ MPa}$$

Table 6-3 Dynamic Shear Strengths for Cold-Formed Steel Panels at Fixed Interior Supports (Combined Bending and Shear)

Web Height to Thickness Ratio (h/t)	f_y = 227 MPa	f_y = 345 MPa	f_y = 550 MPa
20	75	113	149
30	75	112	145
40	74	110	138
50	73	109	130
60	72	103	121
70	70	98	110
80	68	90	99
90	66	81	86
100	62	72	74
110	57	60	61
120	51	51	51

The shear capacity of components not meeting the h/t criterion in Equation 6-11 is dictated by web instability due to shear stresses, including elastic buckling for large values of h/t and inelastic buckling for intermediate h/t values. Equation 6-12 through Equation 6-14 from TM 5-1300 account for the effects of web instability on shear strength based on criteria from AISI (American Iron and Steel Institute) LRFD design, where the dynamic yield strength is substituted for the minimum static yield strength. If the input yield strength does not exactly match any of the minimum specified static yield strengths shown for each of these equations, the equation for the closest matching yield strength is used.

Web instability of corrugated steel panels is controlled by combined bending and shearing stresses at fixed supports, where both loadings are present. Compression stresses in the web from high bending moments, such as those occurring then the corrugated panels yield at negative moment regions, combine with shear stresses to cause more severe web instability conditions that those from shear forces alone. TM 5-1300 provides shear strengths for this case that are shown in Table 6-3. These stresses are based on an interaction formula for shear and moment stresses presented in the AISI ASD design manual and increased to represent ultimate dynamic shear strengths. They are shown in tabular form for materials with three static yield strength levels due to the complexity of the interaction formula.

6-6 STEEL COMPONENTS WITH TENSION MEMBRANE RESPONSE

Tension membrane response increases the resistance of steel components at relatively large deflections, as shown in Figure 4-11 in Section 4-1.2.2.1. It can be considered in combination with flexural response for corrugated steel panel, steel plate, steel beam, and metal stud components in SBEDS, although it is recommended primarily for cold-formed steel beam components. The connections and framing for these components are typically strong and rigid enough to develop a significant amount of tension membrane resistance compared to their relatively low ultimate flexural resistance.

Table 6-4 summarizes guidance on including tension membrane response in SBEDS analyses for different types of steel components. In all cases, tension membrane response should only be considered if it provides significant increase in the overall component resistance and strain energy compared to the ultimate flexural resistance. The tension membrane force in the component is usually limited by the in-plane tension capacity of the connections or the in-plane load capacity of the surrounding framing. The lesser of these two forces is an input into SBEDS. This input is compared in SBEDS to the dynamic tensile capacity of the component cross section, subtracting the area of any utility punch-outs in metal studs, and the lesser of these two forces is used as the maximum tension force that can develop in the component. The maximum tension force is used to calculate the tension membrane stiffness with Equation 4-11 in SBEDS.

6-7 OPEN WEB STEEL JOISTS

Open-web steel joists (OWSJ) are commonly used to support roof panels and floor decks in buildings. The design of joists for conventional loads is covered by the "Standard Specifications, Load Tables, and Weight Tables for Steel Joists and Joist Girders", adopted by the Steel Joist Institute (SJI). H and K Series joists are composed of chord members with 345 MPa (50,000 psi) steel in the chord members and either 248 MPa (36,000 psi) or 345 MPa steel for the web sections. LH Series, DLH Series and joist girders are composed of chords or web sections with a yield strength of at least 248 MPa, but not greater than 345 MPa. All OWSJ can be constructed from hot-rolled or cold-formed steel members.

Standard load tables are available from the SJI for simply supported, uniformly loaded joists with the top chord continuously braced by steel deck. The load capacity of a particular joist may be governed by either flexure or shear (maximum end reaction or buckling of compression web member), where flexure controls for longer spans and shear controls for shorter spans. At typical spans, the load capacity of most joists is controlled by flexural response. The governing response mode is not explicitly stated in current load tables, but it can be inferred if the allowable load changes with the square of span length (flexure control) or linearly with span length (shear control). At very short spans, the allowable load capacity becomes constant with span. It is preferable in blast applications to select a member whose capacity is controlled by flexure rather than shear, since shear is a less ductile response mode.

Table 6-4 Guidance on Including Tension Membrane Response in SBEDS Calculations

Steel Component	Tension Membrane Guidance
Corrugated steel panels	Tension membrane response is almost always limited by the in-plane force that can be developed by the connections and the in-plane load capacity of supporting beams. Usually, the available tension membrane force causes only enough tension membrane resistance to make up for loss in moment capacity after yield from local buckling in the maximum moment area and no separate input of tension membrane response is generally recommended.
Steel plates	Very significant tension membrane capacity can be developed by structural steel plates that are welded or bolted to supporting members. The available in-plane tension force is usually limited by the in-plane load capacity of supporting beams or columns.
Hot-rolled beams	Tension membrane resistance is usually limited by the in-plane force that can be provided by the connections or the in-plane load capacity of supporting girders or columns. Usually, the available tension membrane resistance is less than approximately 25% of the beam ultimate flexural resistance at typical allowable design deflections. In this case, no input of tension membrane resistance is recommended.
Cold-formed beams	Tension membrane forces are usually limited by the capacity of the beam connections. Tension membrane input is typically recommended to determine the damage level of existing cold-formed beams, since tension membrane resistance can significantly increase the relatively low flexural resistance for these components at larger deflections. Conservatively, consideration of tension membrane response is not typically recommended for design of new components.
Metal studs	Tension membrane forces are usually limited by the in-plane capacity of the stud connections of the framing. The connection is very weak. Therefore, tension membrane input is only recommended for cases where the stud to framing connection is designed to develop significant tensile forces.
Open web steel joist	Significant tension membrane can develop in the top chord, depending on the restraint provided by welded connections to the surrounding building and the restraint provided by the building walls or framing. Conservatively, no tension membrane input is allowed for open web steel joists in SBEDS. Tension membrane response of the top chord can be considered an extra degree of redundancy to account for possible brittle response modes, such as buckling of compression web or chord members.

The ultimate flexural resistance of an OWSJ with a span L may be calculated from the published allowable load capacity for the joist type and span length of interest using Equation 6-15 from TM 5-1300. This formula does not differentiate between a load capacity based on shear or flexure because both the joist shear and flexural capacity are assumed to increase by the same static and dynamic strength increase factors. The values for the SIF and DIF in

Equation 6-15 are conservatively based on the values in Table 6-1 for the highest possible steel yield strength in the joist of 345 MPa (50,000 psi). After shear failure or during flexural response with large deflections, the top chord of the joist will act as a tension element between supports and some tension membrane resistance will develop.

Equation 6-15

$$r_{uf} = 1.7ac\left(\frac{w_{dL}}{b}\right) = 2.12\frac{w_{dL}}{b}$$

where:

r_{uf} = ultimate flexural resistance per unit area of joist for span L
w_{dL} = allowable load per unit length for joist with span L from SJI load tables
b = joist spacing
a = applicable static increase factor (SIF) from Table 6-1 (assumed 1.05)
c = applicable dynamic increase factor (DIF) from Table 6-1 (assumed 1.19)

Significant tension membrane resistance was noted in blast tests sponsored by the U.S. government on OSWJ designed to represent typical industrial building construction, with standard welded connections to base plates embedded in walls of a reinforced concrete test building (Coltharp et al, 1999). SBEDS conservatively does not account for any tension membrane response in OWSJ. However, tension membrane response provides an additional level of redundancy to help maintain the resistance of OWSJ governed by brittle response at larger deflections.

The flexural stiffness of an OWSJ can be calculated from the published load causing deflection equal to L/360, where L is the span length, for the joist type and span length of interest, as shown in
Equation 6-16. Values for w_{LL} in
Equation 6-16 are published for each joist type and span length in the standard SJI load tables.

Equation 6-16

$$K = \frac{360w_{LL}}{bL}$$

where:

K = flexural stiffness in units of pressure/length
w_{LL} = load per unit length for joist with span L causing L/360 deflection from Manufacturer's load tables or SJI load tables

Values for w_{dL} and w_{LL} in the standard SJI load tables for each K series and LH series joist type at various span lengths were used to back-calculate an average allowable moment capacity and flexural stiffness (i.e., EI) for each joist type assuming uniformly loaded, simply supported spans. These moment capacities and flexural stiffnesses are stored in a data table in SBEDS, along with the maximum allowable load for each joist type that controls at short span lengths. The allowable moment capacity for the input joist type and the input span length are used to calculate w_{dL} from Equation 6-15 in SBEDS, which is not allowed to exceed the maximum allowable load from the SJI load tables for the joist type. The flexural stiffness of the input joist and the input span length are used to calculate w_{LL} from Equation 6-16 in SBEDS, which is used to calculate the spring stiffness K of the equivalent SDOF system. The use of back-calculated moment capacity and bending stiffness values for each joist type in SBEDS precludes the need to enter the entire load tables with data for all spans of interest for each joist type into a look-up data table.

6-8 REBOUND

Rebound causes a reversal of connection forces and component stresses (i.e., tension regions become compression regions and vice versa), as discussed in Section 4-1.2.5. The tension flange or tension chord of steel components is not normally provided with sufficient lateral bracing to develop full compression yield strength during rebound. This can be accounted for in SBEDS for steel beams by inputting separate unbraced lengths for inbound and rebound response. In each case, the ultimate moment capacity considering the unbraced length, M_m, is calculated with Equation 6-6.
Tension membrane response provides resistance at large rebound deflections for beams that loose flexural capacity because they undergo lateral torsional buckling in rebound due to insufficient lateral bracing of the tension flange. This is particularly true for cold-formed beams because the tension membrane resistance is a larger percentage of the low flexural resistances of these components and these components customarily have relatively light bracing on the tension flange and an unsymmetrical cross section that is more susceptible to twisting. There have been many observed cases of severely twisted cold-formed beams that are still attached to industrial buildings after accidental explosions. Therefore, total failure of steel beams in rebound is very uncommon in blast tests and explosion events. It is possible to see some beams that apparently were damaged more during rebound than during inbound response.

Unlike steel beams, there is no separate input of rebound properties in SBEDS for open web steel joists. Joists are usually only designed with lateral bracing on the bottom chord to develop 20 psf to 40 psf in uplift pressure, depending on the design wind load, which is less than the rebound resistance necessary to respond to most blast loads. However, limited blast testing has shown that the top chord can develop sufficient tension membrane response after the bottom chord buckles during rebound response to prevent failure, even when bottom chord buckling during rebound was severe enough to cause plastic deformation (Coltharp et al, 1999). The limited duration of rebound response also helps limit damage.

These observations, combined with the fact that cross sectional properties and bracing for the lower chord of joists are often difficult to obtain without a site inspection, are reasons why no rebound input for open web steel joists is included in SBEDS. The inbound and rebound ultimate flexural resistances of open web steel joists are always simplistically assumed equal, where top chord tension membrane is implicitly assumed to make up for any lower flexural resistance available during rebound. Open web steel joists that are designed to resist blast load should ideally have adequate lower chord bracing to develop the full compression yield strength of the bottom flange, or at least to develop the bottom flange stress based on the maximum calculated rebound resistance of component.

Plates, corrugated steel panels, and beams with closed cross sections or are in bending about the weak axis typically do not require lateral bracing to develop full compressive yield stress in flexure. Therefore, these components have equal inbound and rebound ultimate flexural strength.

6-9 CONNECTIONS

Steel connections are designed to resist the equivalent static reaction force from the component, as described in Section 4-7. The strengths of simple shear or bearing connections can be determined based on LRFD connection strengths or manufacturers' allowable connection strengths, as described in Section 4-7. Any bearing connections normally must also be designed for tension from reaction forces occurring during component rebound, unless outward failure of the component is acceptable (e.g., cold-formed steel panels). The connection strength of cold-formed steel components is often controlled by material bearing failure or tear-out around bolts and screws. The connection strength can be improved for these cases by using washers to distribute material stresses around screws and screwing additional gage thickness steel plate or beam sections to beams near bolted connections. Conservatively, the maximum rebound connection force is assumed equal to the maximum inbound connection force, or it may be based on the equivalent static reaction force from the peak rebound resistance. Rebound is discussed in more detail in Section 4-1.2.5.

Moment resisting steel connections require special attention to detail to help ensure they can rotate adequately without a reduction in moment capacity at large component deflections. Ideally, the connection should have a greater capacity than the maximum dynamic flexural and shear loads that are delivered by the connected components. This can be accomplished by using a connection with a reduced beam flange or by using other proprietary and non-proprietary connections that have been developed and tested by the researchers after the Northridge earthquake for seismic steel beam-column connections. As a minimum, connections should include stiffeners that will help transfer tension and compression forces from the flanges of connected components through the connection. Bolted connections and connections where fillet welds are kept in shear are more ductile, and therefore preferable, to welded connections that are in tension or compression.

The web area within the boundaries a moment resisting connection should meet the shear stress requirements of Section 6-5. If the web area is unsatisfactory, diagonal stiffeners or web doubler plates should be provided. Web crippling must also be checked at points of load application, such as beam-girder intersections. In these cases, the requirements of AISC LRFD (2001) should be considered.

Figure 6-4 shows an example of a moment resisting beam connection designed to undergo large rotations from blast loading adapted from TM 5-1300.

Figure 6-4 Moment Resisting Steel Beam Connections Designed for Large Rotations (from TM 5-1300)

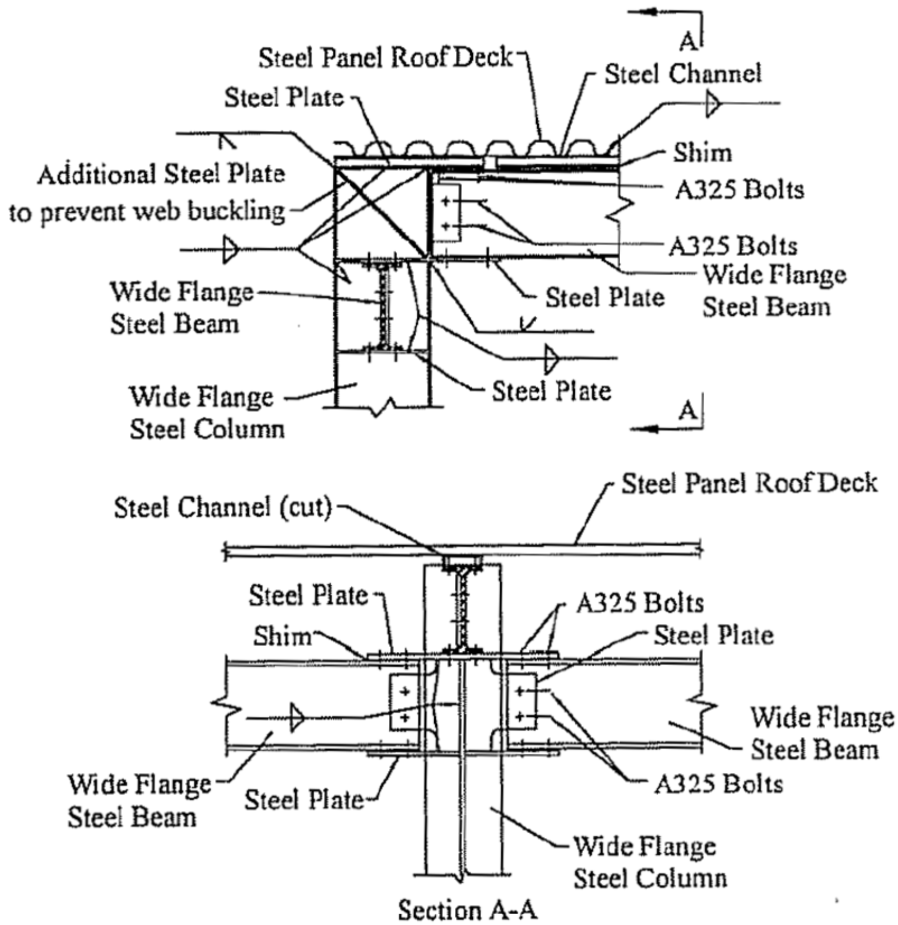

Much research on steel frames response to earthquakes has been performed because of many cases of observed damage to steel frames from earthquakes. There have not been known cases where moment resisting connections in steel frames have failed during blast loading, but there has been very few of these types of structures that have been subject to blast tests or severe loads from accidental explosions. There have been cases where significant local buckling of flanges on built-up girders in pre-engineered buildings occurred without causing overall frame failure. Seismic criteria for connections of moment resisting steel frames subject to blast loads is probably conservative due to the much shorter duration of blast induced stresses. However, these criteria are the best available design criteria for steel frames.

UFC 4-023-03 *Design of Buildings to Resist Progressive Collapse* (2003) and *Progressive Collapse Analysis and Design Guidelines for New Federal Office Buildings and Major Modernization Projects* (GSA, 2003) both have maximum ductility ratio and support rotation criteria for design of moment-resisting steel frames against progressive collapse that is based on earthquake design criteria. Separate criteria are given for components and connections in moment-resisting frames, where the connection criteria almost always control. These criteria can conservatively be used for blast design. Less conservative support rotation and ductility ratio criteria for blast design and analysis of steel frames are given in ASCE (1997) that are intended primarily for one or two-story steel frame buildings.

CHAPTER 7 - MASONRY COMPONENTS

7-1 TYPES OF MASONRY WALLS

Masonry is a broad category of materials including stone, brick, clay tile, clay block, concrete masonry units (CMU), and adobe. These materials are manufactured or cut into individual units, such as blocks, and mortared together to create a structural component. They have relatively high compressive strengths and low tensile strengths. Figure 7-1 shows typical shapes for different types of masonry units. Masonry construction in the U.S. and Canada consists primarily of brick and CMU, with some clay tile construction. Modern European masonry construction consists primarily of insulated clay brick and block, which have many small voids that help improve bonding with the mortar, reduce weight, and improve insulating properties. Older European masonry construction often consists of solid brick walls or mortared stone covered with plaster. Generally, a masonry unit is described based on its type and its nominal dimension in the direction of the wall thickness (i.e., Figure 7-1 shows a standard 8 inch CMU block). The actual overall dimensions of manufactured masonry units are 9.5 mm (3/8 inch) less than nominal dimensions to allow for the mortar thickness and thickness of interior wall material (i.e., gypsum board).

Table 7-1 provides information for the most common types of masonry units that are available in SBEDS. European insulated block has variable properties; the values shown in Table 7-1are average values based on limited available information. Table 7-1 also includes several weights of CMU. CMU manufacturing depends in part on locally available materials, but most CMU used in modern U.S. construction is lightweight CMU. This has become increasingly true over the last 20 to 30 years due to advances in CMU materials that has allowed lightweight CMU to meet ASTM strength requirements. Heavier weight CMU has been used more in older construction and cold weather climates. Unfortunately, it is very hard to determine the weight of CMU block, without sampling some block and measuring the specific gravity, if it is not noted in construction drawings or specifications. It is usually conservative to assume lightweight CMU for blast design or analysis because this will result in the least calculated mass and corresponding inertial resisting force.

Table 7-2 shows cross sectional property information used in SBEDS for each masonry type. This table includes a parameter for the percentage of solid thickness through the webs, as illustrated in Figure 7-2. The parameter is used to determine the shear strength, as discussed in 7-5. SBEDS also considers grouted CMU block, where the areal wall weight, moment of inertia area, and percentage of solid thickness through the webs of grouted CMU block are calculated as shown in Equation 7-1. The uncracked section modulus of grouted CMU is equal to the moment of inertia divided by one-half the thickness.

Figure 7-1 Typical Masonry Unit Shapes

Various Brick Shapes

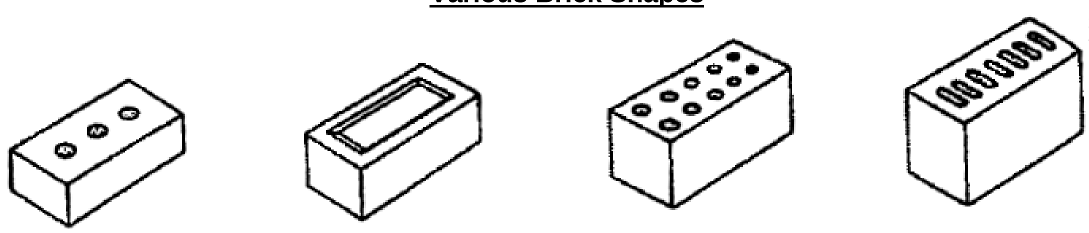

Various Clay Tile Shapes

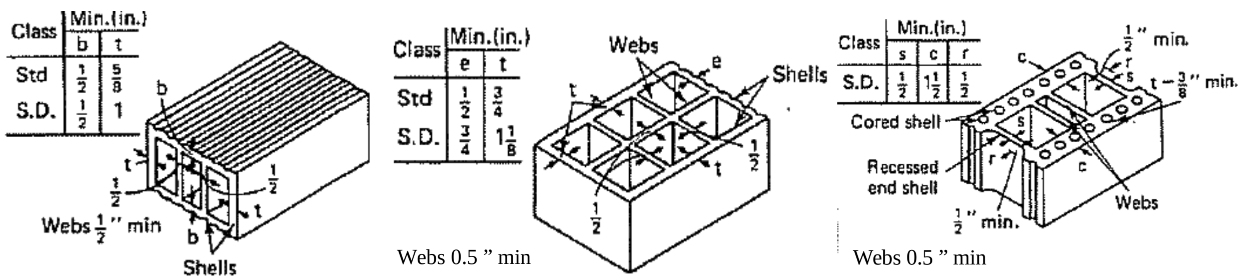

Standard 8”x8”x16” CMU Block and Bond Beam Block

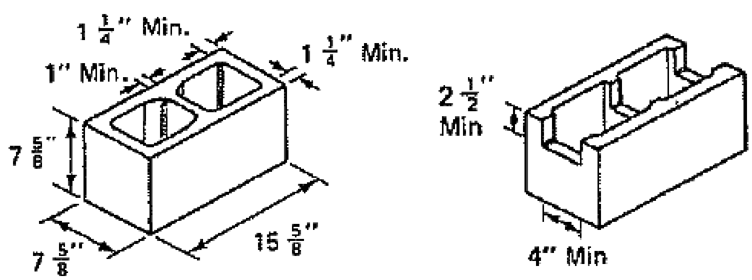

European Insulated Clay Brick and Clay Block

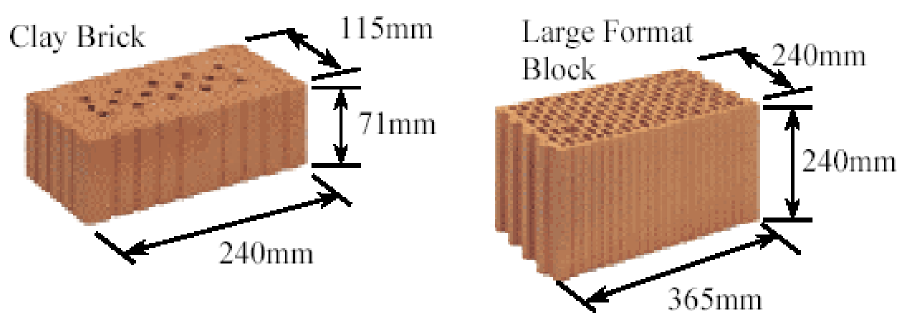

Methodology Manual TOC

Table 7-1 Masonry Block Information

Type	Density kg/m^3 (pcf)	Percentage Solid Cross Section (%)	Solid Thickness Through Webs[1] (%)	Moment of Inertia (per unit width)[2]	Section Modulus (per unit width)[2]
Solid Brick	1925 (120)	100	100	$t^3/12$	$t^2/6$
European Insulated Block[3,4]	962-1925 (60-120)	50	50	$0.3(t^3/12)$	$0.3(t^2/6)$
Heavy Weight CMU	2165 (135)	See Table 7-2			
Light Weight CMU	1524 (95)				
Medium Weight CMU	1925 (120)				

Note 1: See Figure 7-2.
Note 2: "t" is block or brick thickness.
Note 3: A density of 1395 kg/m^3 (87 pcf) is used in SBEDS. Based on comparisons of available manufacturers' values to solid block values, the area is assumed equal to 50% of the solid area and the section modulus and moment of inertia is assumed equal to 30% of the solid section values for insulated blocks in Figure 7-1.

Table 7-2 Assumed Cross Section Parameters for CMU Blocks

Nominal Block Thickness mm (in)	Face Shell Thickness mm (in)	Web Thickness mm (in)	Solid Cross Sectional Area (%)	Solid Thickness Through Webs (%)	Moment of Inertia mm^4/mm (in^4/in)	Section Modulus mm^3/mm (in^3/in)
102 (4)	19 (0.75)	19 (0.75)	50	14	53750 (3.3)	1168 (1.8)
152 (6)	32 (1.25)	25 (1)	55	19	209263 (12.8)	2928 (4.5)
203 (8)	32 (1.25)	32 (1.25)	49	23	464656 (28.4)	121877 (7.4)
254 (10)	32 (1.25)	32 (1.25)	43	23	840578 (51.3)	6873 (10.7)
305 (12)	32 (1.25)	32 (1.25)	40	23	1350950 (82.4)	9151 (14.2)

Figure 7-2 Percent Solid Thickness Through Web of CMU Cross Section

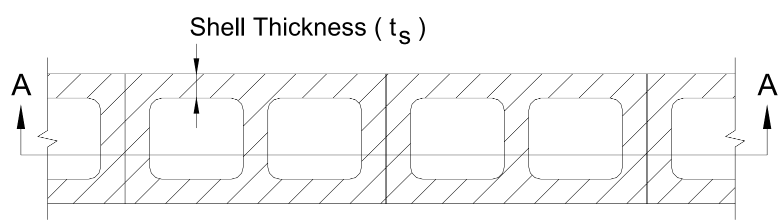

Percent Solid Thickness Through Web =100 x (width of solid space through block along A-A)/(block width)

Equation 7-1

$$w = \left(A_{fs}\rho_m + (1 - A_{fs})\frac{V}{100}\rho_g \right) t$$

$$I = I_m + \frac{(t - 2t_s)^3}{12}\frac{V}{100}\left(1 - \frac{\psi_m}{100}\right)$$

$$\psi = \psi_m + \frac{V}{100}(100 - \psi_m)$$

where:

Methodology Manual TOC

w = areal weight of grouted cross section
I = moment of inertia of grouted CMU
Ψ = percentage of solid thickness through webs and grout of CMU
A_{fs} = fraction of cross sectional area that is solid CMU (see Table 7-2)
r_m = density of CMU (see Table 7-2)
r_g = density of grout (equal to 120 pcf or 1922 kg/m^3 in SBEDS)
t_s =CMU shell thickness (see Table 7-2)
t = masonry thickness
V = percent of voids that are grouted
I_m = moment of inertia of CMU not considering grout (see Table 7-2)
Ψ_m = percentage of solid thickness through webs of CMU

***Note**: Brick and European Block do not include consideration of any grouted area*

Table 7-3 shows information on mortars used for masonry construction. The voids of CMU walls are filled with grout if they have vertical reinforcement. Usually, unreinforced voids are not grouted. Grout, which is very similar to concrete without any large aggregate, generally has compression strengths near 20 MPA (3000 psi). It must have sufficient slump, or plasticity, and must be vibrated during placement in the CMU voids to avoid voids, or honeycombing in the grout. Excessive mortar squeezed into the void space of CMU block, or falling off into the void space, inhibits good placement of grout and may compromise composite action of the vertical reinforcement with the surrounding CMU wall.

Table 7-3 Information on Mortar Used for Masonry

Mortar	Type	Portland Cement or Blended Cements	Masonry Cement or Mortar Cement			Hydrated Lime or Lime Putty	Aggregate Ratio (measured in Damp, Loose Conditions
			M	S	N		
Cement-Lime	M	1	—	—	—	¼	Not less than 2¼ and not more than 3 times the sum of the separate volumes of cementitious materials
	S	1	—	—	—	over ¼ to ½	
	N	1	—	—	—	over ½ to 1¼	
	O	1	—	—	—	over 1¼ to 2½	
Masonry Cement or Mortar Cement	M	1	—	—	1	—	
	M	—	1	—	—	—	
	S	½	—	—	½	—	
	S	—	—	1	—	—	
	N	—	—	—	1	—	
	O	—	—	—	1	—	

Masonry walls can be constructed as a single, monolithic wall with one or more units through the thickness, or as multi-wythe cavity walls consisting of multiple, closely spaced walls with an air gap or insulation between walls. Almost all modern masonry walls in the northern part of the United States and Canada are multi-wythe cavity walls, which are necessary to provide required insulation. They are also becoming more common in the other parts of the U.S. for buildings where insulation is a primary concern. Figure 7-3 shows a cavity wall constructed with brick and CMU. Cavity walls

Methodology Manual TOC

can also be constructed with other types of masonry. All cavity walls are typically connected together across the gap between walls with joint reinforcement, as shown in Figure 7-3, or with steel ties or tabs that cause both walls to deflect together when lateral loads are applied to the outer wall.

Figure 7-3 Double Wythe Cavity Wall with Brick and CMU

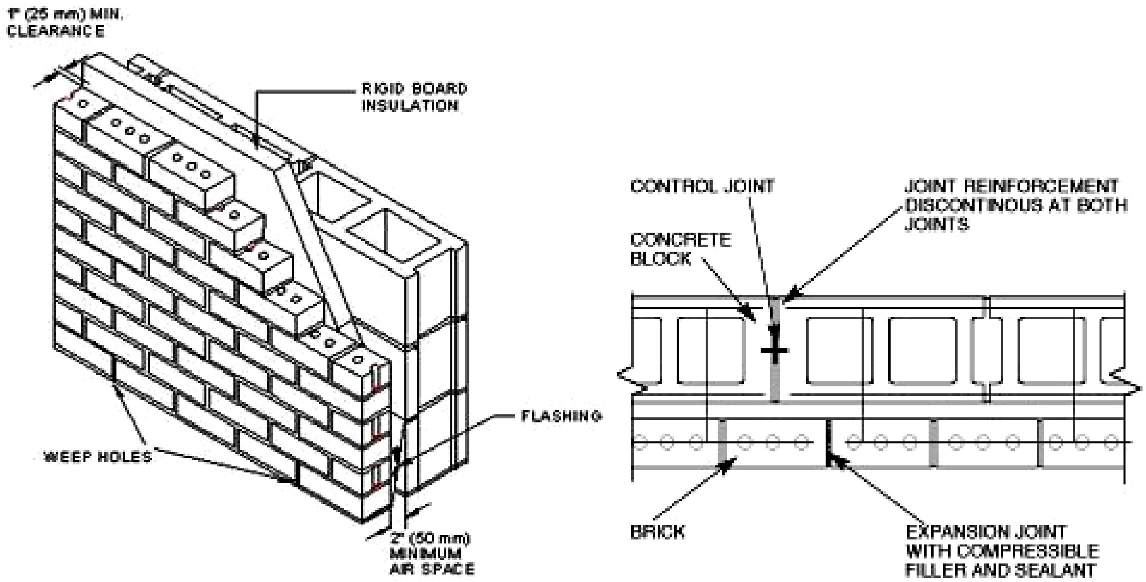

7-2 DYNAMIC MASONRY PROPERTIES

Masonry compressive strength is usually expressed in terms of the prism compression strength (f'_m), which is the compressive strength of a short column of masonry material that is mortared together in a manner representative of the wall construction. The prism strength is typically less than the compression strengths of the masonry material and mortar. If no test data is available, Table 7-4 shows conservative values for f'_m of CMU and brick material from TM 5-1300. Note that f'_m of European insulated block is assumed to represent the crushing load for the prism divided by the gross cross sectional area of the block, rather than the net area, in SBEDS. This allows compressive resisting forces for the block to be analyzed as if the block is solid. CMU, clay tile, and other masonry with concentrated area of voids symmetric about the midthickness are input into SBEDS based on their net area and the compressive strength of the net area. However, f'_m for CMU, clay tile, and other masonry with concentrated areas of voids symmetric about the midthickness should be input into SBEDS based on the compressive strength of the net area. SBEDS is programmed to account for the large void space in CMU and clay tile. This approach is also consistent with conventional design.

The dynamic masonry compressive strength can be calculated as shown in Equation 7-2. There is no high strain-rate testing available for masonry. Therefore, the recommended dynamic increase factor (DIF) in Equation 7-2 is 1.19, which is the same as the default value for concrete with a strain-rate of 0.1 sec^{-1} from TM 5-1300. The modulus of elasticity (E_m) of masonry units is given by Equation 7-3.

Table 7-4. Recommended Conservative Values for Static Masonry Prism Compressive Strength

Type of Masonry Unit	Compressive Strength[1] (f'_m)
Ungrouted CMU	1350 psi
Fully Grouted CMU	1500 psi
Brick or Solid Masonry or European Insulated Block	1800 psi
Note 1: SBEDS assumes that f'_m is based on the prism crushing load divided by gross cross sectional area of block with small uniformly distributed voids, such as European insulated block. However, f'_m is based on the crushing load divided by net area of masonry with large voids, such as CMU or clay tile.	

Equation 7-2

$$f'_{dm} = f'_m \left(DIF\right)$$

where:

f'_{dm} = masonry dynamic compression stress
f'_m = static masonry prism compression strength
DIF = dynamic increase factor (equal to 1.19)

Equation 7-3

$$E_m = 1000 f'_m$$

where:

E_m = masonry modulus of elasticity
f'_m = masonry prism compression strength

The flexural tensile strength of masonry walls is controlled by the adhesion between the mortar and masonry units. It can be measured with wallettes, which are short unreinforced masonry wall sections that are tested in three-point bending. The tension strength is determined from the breaking load and the section modulus of the masonry unit. Measured static flexural strengths vary significantly because of variables that affect the mortar adhesion to the masonry, including mix proportions of the mortar and absorption of moisture from the mortar by the masonry block. The static flexural tension strength for a vertically spanning ungrouted CMU wall, which cracks in the maximum moment region within a single horizontal mortar joint, is in the range of 0.2 MPa (30 psi) to 0.35 MPa (50 psi). The flexural tension strength for a horizontally spanning ungrouted CMU wall with a running bond masonry placement, which cracks in the maximum moment region through the mortar in a stair-stepping pattern around the masonry units or through the masonry units, is in the range of 0.69 MPa (100 psi) to 1.0 MPa (150 psi) (Hamid and Drysdale, 1988). Grouted block and solid block have somewhat higher tensile strengths.

7-3 MASONRY REINFORCEMENT

Masonry walls can be reinforced with vertical and/or horizontal reinforcement. Vertical reinforcement is placed in the grouted voids of CMU block and in a grouted gap between multi-wythe brick or insulated block walls. The grout causes the reinforcement to act compositely with the masonry. The vertical reinforcement is the same deformed bars used to reinforce concrete, with diameters usually between 12.5 mm (0.5 inch) and 19 mm (0.75 inch).

Horizontal wall reinforcement is usually non-structural steel wire reinforcement with shapes shown in Figure 7-4 that is placed in horizontal “bed” mortar joints of walls. It helps distribute any concentrated loads, reduce crack widths, and act as a tie between multi-wythe walls. The ladder and truss type horizontal reinforcement in Figure 7-4 are the most commonly used shapes. It typically has a wire size of W1.7 [No. 9 gage, (0.148 in.) (3.8 mm)] or W2.8, [3/16 in. (4.8 mm)] in diameter, and is usually placed at 405 mm (16 in) on center in every other bed joint. Horizontal joint reinforcement is rarely used as structural reinforcing because this implies that dynamic reactions from the wall are transferred into the columns, which must also resist axial forces associated with blast loading on the roof.

Figure 7-4 Horizontal Joint Reinforcement

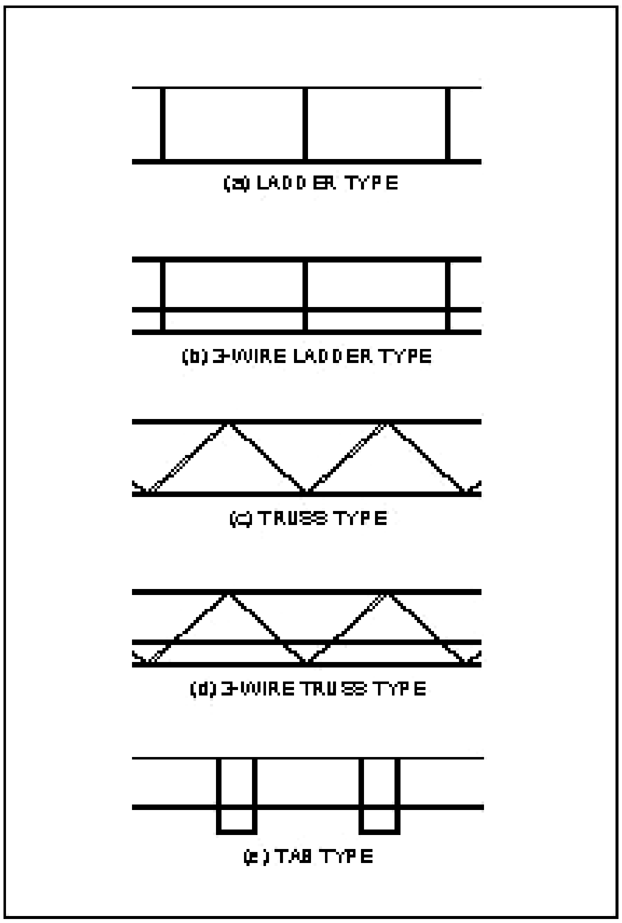

Usually, masonry walls are built continuous in front of steel columns, with a gap between the wall and column, or between concrete columns, with an expansion gap between the wall and columns. In both cases there are usually only light metal ties attaching the walls to the columns that cannot transfer the equivalent static reaction load from the wall spanning horizontally between columns. If the gap between the wall and adjacent concrete columns is small enough, the wall can develop some bearing support in the horizontal direction as it deflects or rotates into the column.

7-4 FLEXURAL RESPONSE OF MASONRY

The flexural response of masonry is analyzed differently in SBEDS depending on whether it is structurally reinforced and whether the masonry is part of a multi-wythe wall system. Unlike concrete, masonry is constructed both with and without steel reinforcement. Masonry walls designed to resist blast load always have structural reinforcement. Conventional low-rise buildings subject to blast load can be constructed with either reinforced or unreinforced masonry walls. Masonry walls are usually not analyzed for two-way flexural response because of a weak connection between the wall and adjacent columns and because the vertical span is often much less than the horizontal span (i.e., by approximately one-half the horizontal span) so that most of the wall strength and stiffness is provided by the vertical span. An exception to this in some cases is unreinforced masonry walls that bear on interior masonry walls. Reinforced masonry almost always have the predominant amount of reinforcing steel in the vertical direction, so that they are analyzed as one-way spanning components.

Another issue affecting flexural response of masonry walls is the assumed support condition between the bottom of the wall and the foundation. It seems reasonable to assume that unreinforced walls with dowels extending from the foundation are fixed at the bottom of the wall. However, these dowels almost never extend into the wall sufficiently to provide a full tension splice as required in ASCE 530-02 for reinforced masonry. In this case, the wall will only act fixed at the base for a short time until the splice fails and it is conservative to analyze the wall assuming a simple support at the base. If the dowels do have a necessary splice length, the wall can be assumed fixed at the foundation if the rigidity of the foundation against rotation is adequate. This is often the case considering the very short duration of blast load response. Unreinforced walls without dowels should typically be assumed pinned at the base because of the unknown adhesion between the mortar and the foundation material.

7-4.1 FLEXURAL RESPONSE OF UNREINFORCED MASONRY

Two flexural response options are available for unreinforced masonry in SBEDS, ductile flexural response and brittle flexural response with axial load arching. The latter option is generally recommended since available static test data clearly shows unreinforced masonry does not exhibit any significant resistance at deflections larger than the yield deflection. This approach has also been incorporated into SDOF analyses used to develop scaled pressure-impulse (P-i) diagrams that generally compare well with scaled damage data from blast-loaded unreinforced masonry walls (Oswald, 2005). The assumption of ductile flexural response for blast-loaded unreinforced masonry walls is only included in SBEDS since it has been used in the past, primarily because previous brittle flexural analyses without axial load arching significantly over predicted observed response of unreinforced masonry test walls. The use of ductile flexural response for unreinforced masonry walls in SBEDS is not generally recommended.

Brittle flexural response of an unreinforced masonry wall is based on the wall moment capacity, which is controlled by the flexural tensile strength between masonry units. As discussed in Section 7-2, there is no available test data on the dynamic flexural tensile strength of masonry walls. If no better information is available, a value of 1.38 MPa (200 psi) is recommended based on use of this assumed value in SDOF analyses that approximately matched measured unreinforced masonry wall response from a number of high explosive tests (Oswald, 2005). If f'_{dm} exceeds 1380 MPa, a value of 10% of f'_{dm} may also be used provided that it does not exceed 1.75 MPa (250 psi). Equation 7-4 shows the ultimate dynamic moment capacity of unreinforced masonry walls based on the dynamic tensile strength of the wall and the elastic section modulus of the masonry unit. Values for the elastic section modulus of solid blocks and European insulated blocks that are assumed in SBEDS are shown in Table 7-1. Values for CMU that are assumed in SBEDS are shown in Table 7-2.

Equation 7-4

$$M_{du} = Sf_{dt}$$

where:

M_{du} = ultimate dynamic moment capacity
f_{dt} = dynamic tensile strength of masonry wall
S = elastic section modulus of masonry unit

The dynamic moment capacity in Equation 7-4 is used to determine the ultimate flexural resistance of an unreinforced masonry wall based on the boundary conditions as described in Section 4-1.2.1. In the case of ductile flexural response, this resistance is assumed to remain constant with increased deflection beyond the yield deflection. However, the recommended approach is to assume brittle flexural response, where the flexural resistance is zero at deflections beyond the yield deflection and axial load arching resistance occurs between the flexural yield deflection and the wall thickness. Axial load arching is discussed in Section 4-1.2.2.3.

7-4.2 FLEXURAL RESPONSE OF REINFORCED MASONRY WALLS

Masonry walls are most commonly reinforced using vertical steel bars placed in grouted cells of CMU or in a grouted section between wythes of brick or block masonry, where the grout causes the vertical steel reinforcement to act compositely with the surrounding masonry. Vertical steel bars in CMU are spaced at increments of 200 mm (8 in), corresponding to the center-to-center spacing between cells, up to 812 mm (32 in). Walls with a steel reinforcement spacing of 1220 mm (48 in), or more, are usually considered unreinforced. The reinforcing bars are usually placed at the center of CMU unit cells. If the CMU is at least 250 mm (10 in) nominal thickness, separate bars may be placed in the voids near each face rather than a single bar at the center.

Ductile flexural response is always assumed in SBEDS for steel reinforced masonry walls. The ultimate dynamic moment capacity is calculated using Equation 7-5 from TM 5-1300. This equation assumes that reinforced masonry will respond in essentially the same manner to blast load as reinforced concrete. The applicability of this assumption has been demonstrated in numerous static tests (Heeringa et al, 1989) (Hamid et al, 1992). It is also consistent with data from a series of twenty-one shock tube tests on reinforced masonry CMU walls that were subject to inspection and material testing during construction, as required in the International Building Code and ASCE 530-02 (Oswald and Holgado, 2004).

However, the deflections calculated with SDOF analyses based on a moment capacity from Equation 7-5 were approximately 30% to 40% lower than measured deflections in twenty-two reinforced CMU walls from three different test series in the CMUDS database (Wesevich et al, 2002) where no quality assurance (QA) inspection or materials testing was performed during test wall construction (Polcyn et al, 2004). Therefore, Equation 7-5 was non-conservative for these cases assuming that the difference between measured and calculated deflections was due to a reduced moment capacity in the test walls caused by poor composite action of the masonry and reinforcing steel as it was stressed near its dynamic yield strength. Poor composite action in reinforced CMU walls is caused by grout that is not well consolidated during placement due to insufficient vibrating or rodding or mortar after it is placed in the cells, mortar protrusion and drippings in the cells, or insufficient plasticity due to incorrect proportioning and mixing of materials used to make the grout.

Equation 7-5

$$M_{du} = \frac{A_s f_{dy}}{b}\left(d - \frac{A_s f_{dy}}{1.7bf'_{dm}}\right)$$

where:

M_{du} = dynamic ultimate moment capacity per unit width
A_s = area of tension reinforcement in width, b
f_{dy} = dynamic design stress
d =effective depth (distance from the extreme compression fiber to the centroid of the tension reinforcement)
b = spacing between reinforcement
f'_{dm} = masonry prism dynamic compressive strength

This indicates that QA during construction as required in the IBC and ACI 350-02 is very important for ensuring the applicability of Equation 7-5 for reinforced masonry walls subject to blast loads. If no such QA is performed, the ultimate dynamic moment capacity in Equation 7-5 should be reduced by a factor of approximately 60%, which would cause the previously sited twenty-two walls from the CMUDS database to have calculated deflections approximately equal, on the average, to measured values. This is consistent with similar guidance for static design of reinforced masonry walls from the Uniform Building Code (UBC, 1997), which recommended that only one-half the theoretical wall design strength should be assumed for uninspected reinforced masonry walls. The applicability of Equation 7-5 also depends on proper splicing of reinforcing steel in accordance with ACI 530-02 and splicing only small bars in maximum moment regions. Based on recent shock tube testing, only small spliced bars with a diameter no larger than 12 mm (0.5 in) maintained their full dynamic yield strength in the maximum moment region without slipping at large rotations (i.e., greater than 2 degrees), when spliced according to the ACI requirements (Oswald and Holgado, 2004).

SBEDS provides a user option to analyze reinforced masonry components assuming the moment capacity transitions from a Type I to a Type II cross section for support rotations greater than 2 degrees. SBEDS uses the same approach for this as described for reinforced concrete components in Section 5-2.1. Type II cross sections must be used for blast design of DoD buildings according to UFC 3-340-01 and TM 5-1300 for response with a support rotation greater than 2 degrees.

Masonry can also be reinforced with fiber reinforced plastics (FRP) that are attached with epoxy on the exterior surfaces of the walls. The FRP can be placed as a large sheet or in separate strips that are continuous over the wall span. The tension strength provided by the fibers significantly increases the flexural strength of masonry, but do not add very much ductility. The fibers do not significantly increase the strength of the masonry compression block in the maximum moment region or the masonry shear strength. Therefore, the strength of masonry walls reinforced with FRP must be checked for possible failure in these response modes.

FRP reinforcement must be placed on both sides of walls to avoid failure during rebound response. Regardless of the controlling response mode, the flexural response of walls reinforced with FRP is usually not very ductile. Because steel reinforcement provides both increased ductility and strength, it is usually used to reinforce new masonry walls designed to resist blast loads. However, FRP may be a practical option for reinforcing existing unreinforced masonry walls, as discussed in UFC 04-023-02. No options are provided for input of FRP reinforcement in the current version of SBEDS (SBEDS V3.0), although FRP reinforcement can be input for a Reinforced Masonry component with the user input option for material properties.

7-4.3 MOMENT OF INERTIA OF MASONRY WALLS

The moment of inertia for an unreinforced masonry wall in SBEDS is equal to the gross moment of inertia based on the net section of the masonry units in the wall. Values for the gross moment of inertia of solid blocks and European insulated blocks that are assumed in SBEDS are shown in Table 7-1. Assumed values for CMU are shown in Table 7-2.

The moment of inertia for reinforced masonry walls in the elastic and elastoplastic range is complicated by increasing cracking along the masonry wall span as the wall deflects. It is recommended in TM 5-1300 that the flexural stiffness in the elastic and elastoplastic range be based on an average moment of inertia calculated with Equation 7-6. This formula is based on a singly reinforced wall with a 0.1% reinforcement ratio, which is a lower bound on commonly used reinforcement ratios. However, even tripling the value of I_c in Equation 7-6 typically has little effect on I_a, which is dominated by the gross moment of inertia term. SBEDS calculates the moment of inertia for reinforced masonry walls as I_a in Equation 7-6.

Equation 7-6

$$I_a = \frac{I_n + I_c}{2}$$

$$I_c = 0.005 d^3$$

where:

I_a = average moment of inertia per unit width used to determine flexural stiffness for equivalent SDOF system of a reinforced masonry wall

I_n = gross moment of inertia per unit width based on net section of masonry units in wall

I_c = cracked moment of inertia per unit width

d = effective depth (distance from the extreme compression fiber to the centroid of the tension reinforcement)

7-5 SHEAR STRENGTH OF MASONRY

The dynamic shear strength of unreinforced masonry is calculated in SBEDS using Equation 7-7. This equation is based on the assumption that masonry has the same static and dynamic shear strength as concrete. There is a variation in recommended shear strengths for masonry in the literature. Paulay and Priestly (1992) recommend a masonry shear strength of $0.16f'_m{}^{0.5}$ MPa ($2\ f'_c{}^{0.5}$ psi) for reinforced masonry walls subject to out-of-plane earthquake loads, which is consistent with Equation 7-7, except in potential hinge regions. In these regions, a large reduction of 70% is conservatively recommended based on limited available test data. Separate shear strengths are defined for unreinforced and reinforced masonry in ACI 530-02. The shear strength for plain unreinforced masonry is defined by the least value from five different equations, but for typical ungrouted CMU the shear strength is about $0.13f'_m{}^{0.5}$. Higher values apply for grouted CMU or solid masonry. The masonry shear strength in reinforced masonry walls in ACI 530-02 depends on the ratio of the moment to shear at the critical cross section and is always greater than $0.19f'_m{}^{0.5}$. An assumed masonry shear strength based on a coefficient of 0.16 is therefore within the range of values available in the literature.

Equation 7-7

$$V_m = 0.16\sqrt{f'_{dm}}\,d\,\frac{\psi}{100}$$

where:

V_m = dynamic shear force per unit width along wall resisted by masonry (MPa/mm)

f'_{dm} = masonry prism dynamic compressive strength (MPa)

d = effective depth of flexural reinforcement (distance from the extreme compression fiber to the centroid of the tension reinforcement) (mm)
Note: d= overall wall thickness for unreinforced masonry

ψ = percent solid thickness through web - equal to 100 for solid masonry, see Table 7-1 for European insulated block and Table 7-2 and Equation 7-1 for CMU

Closed stirrups similar to those used in reinforced concrete beams can be placed along the horizontal bed joints near the support where the equivalent static reaction load exceeds V_m from Equation 7-7. In this case, the shear strength is the sum of V_m from Equation 7-7, which represents the shear force resisted by the masonry, and V_s from Equation 7-8, which represents the shear force resisted by shear reinforcing steel placed perpendicular to the flexural steel. However, the shear reinforcement must be placed at a maximum spacing along the span equal to the depth of flexural reinforcing steel from the compression face, d, divided by 2 (i.e., d/2) to be effective. This is almost impossible to do for most reinforced masonry walls, since the reinforcement is often placed at midthickness and the bed joints are always 200 mm (8 inches) apart. For this reason, stirrups are only practical for a pilaster. If necessary, steel plates can be through-bolted on both sides of a wall in the high shear area where the bolts act as shear reinforcement. Fortunately, the equivalent static reaction force is less than V_m for most practical cases.

Equation 7-8

$$V_s = \frac{A_v f_{dy} d}{bs}$$

where:

- V_s = dynamic shear force per unit width along wall resisted by reinforcing steel
- A_v = area of shear reinforcement placed perpendicular to the flexural steel
- b = spacing along wall between stirrups with area A_v
- s = spacing along span length between stirrups with area A_v
- d = effective depth of flexural reinforcement (distance from the extreme compression fiber to the centroid of the tension reinforcement)
- f_{dy} = dynamic yield stress of the shear reinforcement

7-6 COMPRESSION MEMBRANE RESPONSE BETWEEN RIGID SUPPORTS AND AXIAL LOAD ARCHING IN MASONRY WALLS

The resistance-deflection relationship for compression membrane response between rigid boundaries is described in Section 4-1.2.2.2, including summary information in Table 4-6. Note that separate approaches are used in SBEDS for calculating the peak compression membrane resistance of non-solid masonry components depending on whether there are large central voids, such as CMU block, or uniformly distributed voids through the thickness, such as European insulated block. The presence of large voids is explicitly considered in SBEDS, whereas the effect of small uniformly distributed voids is accounted for by assuming the compression strength is relative to the gross cross sectional area. Also, the initial flexural response of unreinforced masonry components is ignored in SBEDS when compression membrane response between rigid boundaries occurs.

The resistance-deflection relationship for unreinforced masonry components with axial load arching is described in Section 4-1.2.2.3. Separate approaches depending on the voids are not needed for calculating the resistance of components with arching from axial load because it is assumed that typical axial line loads applied along masonry walls in buildings can be resisted by a small thickness of masonry along the compression face of the block near midspan, regardless of the presence of voids.

7-7 DOUBLE WYTHE UNREINFORCED MASONRY WALLS

Figure 7-3 shows an unreinforced double wythe masonry wall, which is also known as a cavity wall. As shown in the figure, horizontal joint reinforcement is used to connect the two wythes together. Thin steel tabs and ties are also used for this purpose. Only non-composite double wythe unreinforced walls, where the walls are connected by ties or joint reinforcement that cause the walls to deflect together, are considered in SBEDS.

Composite multi-wythe walls should be input in SBEDS as monolithic single walls so that composite action will be considered.

Non-composite double wythe walls are assumed in SBEDS to respond to lateral blast load as two springs in parallel, so that they deflect equally, have a flexural stiffness equal to the summed stiffness of both walls, and resist the applied blast load in proportion to their relative flexural stiffnesses. This is consistent with the approach recommended in ACI 530-02. The two walls are assumed to resist lateral load in flexure together in this manner until one of the walls yields at its dynamic tensile stress at all maximum moment locations. The combined resistance of the two wall system when this occurs is the ultimate flexural resistance.

If brittle flexural response with axial load arching is input for the walls, all resistance is assumed to occur only due to axial load arching at deflections greater than the ultimate flexural yield deflection of the wall yielding first. The peak resistance from axial load arching is calculated separately for each wall and summed to get the peak axial load arching resistance for the double wall system. The axial load arching resistance is assumed to decay linearly to zero resistance at a deflection equal to the thickness of the wall providing the larger axial load arching resistance. If ductile flexural response is selected, the ultimate flexural resistance of the two-wall system is assumed to remain constant with increasing deflections.

The maximum flexural resistance of a double wythe wall system, R_u, is determined in SBEDS as shown in

Equation 7-9 based on the assumptions that the walls have equal midspan deflection, Δ, due to ties between the walls, and equal span (L) and boundary conditions. For indeterminate walls,

Equation 7-9 is used to define both the maximum elastic resistance and ultimate resistance of the two-wall system in terms of the corresponding resistances of each wall. It is illustrative to consider a few examples. For the case where Wall 2 is identical to Wall 1 except that it has one-half the thickness, Wall 1 will have a moment of inertia eight times greater than Wall 2 and a section modulus four times greater. Based on

Equation 7-9, Wall 1 will yield first and, since K_1/K_2 equals eight, the value of R_u for the two-wall system will only be 1.125 times greater than R_u of the thicker wall, R_1. This contrasts sharply with the case where both walls are equal thickness, where the value of R_u for the combined wall system is 2.0 times R_1. The stiffness of the double wythe wall system is shown in Equation 7-10. This equation is assumed to apply to both the elastic and elastic-plastic stiffnesses of indeterminate multi-wythe walls.

The shear capacity of the two-wall system, V_u, is based on the combined maximum resisting shear forces of the two walls when the first wall yields in shear, as shown in

Equation 7-11. Again, it is assumed that both walls have the same boundary conditions and span. The shear capacity is compared to equivalent static reaction forces from the double wythe wall system that are calculated based on the ultimate flexural resistance of the two-wall system (R_u from

Equation 7-9) and the span and boundary conditions of the two-wall system using the procedures in Section 4-3.2.

Equation 7-9

$$R_1 = K_1\Delta \qquad R_2 = K_2\Delta \qquad \textit{therefore} \quad \frac{R_1}{R_2} = \frac{K_1}{K_2} \textit{and} \quad K_i \propto \frac{C_K E_i I_i}{L^4} \quad \textit{so} \quad \frac{R_1}{R_2} = \frac{K_1}{K_2} = \frac{E_1 I_1}{E_2 I_2}$$

$$R_i \propto \frac{C_m M_i}{L^2} \qquad \textit{therefore} \quad \frac{R_1}{R_2} = \frac{M_1}{M_2} = \frac{\sigma_1 S_1}{\sigma_2 S_2} \quad \textit{and} \quad \frac{\sigma_1}{\sigma_2} = \frac{R_1 S_2}{R_2 S_1} = \frac{E_1 I_1 S_2}{E_2 I_2 S_1} = \sigma_r\,, Let \quad \sigma_{ry} = \frac{\sigma_{1y}}{\sigma_{2y}}$$

If $\dfrac{\sigma_r}{\sigma_{ry}} \geq 1$, Wall 1 yields first and $R_u = R_{1u} + R_2 = R_{1u}\left(1 + \dfrac{E_2 I_2}{E_1 I_1}\right)$,

Else, $R_u = R_{2u} + R_1 = R_{2u}\left(1 + \frac{E_1 I_1}{E_2 I_2}\right)$

Note: R_u is also bounded where: Max(R_{1u}, R_{2u}) $\leq R_u \leq$ (R_{1u}+R_{2u})

Equation 7-10

$$K = K_1 + K_2$$

where:

i =1 for inner wall and 2 for outer wall
R_i = resistance i^th wall
R_{iu} = ultimate or maximum resistance of i^th wall
R_u = ultimate or maximum resistance of two-wall system
K_i = flexural stiffness of i^th wall
K = flexural stiffness of two-wall system
E_i = Young's modulus of walls
I_i = moment of inertia of i^th wall
S_i = section modulus of i^th wall
Δ = equal midpan deflections of both walls
L = equal spans of both walls
σ_i = maximum flexural stress in walls
M_i = maximum moment capacity of i^th wall
σ_{iy} = yield stress of i^th wall
C_m = moment constants dependent on boundary conditions - same for each wall
C_K = stiffness constants dependent on boundary conditions - same for each wall

Equation 7-11

$$V_i \propto \frac{C_v R_i}{L} \qquad \textit{therefore} \quad \frac{V_1}{V_2} = \frac{R_1}{R_2} = \frac{K_1}{K_2} = \frac{E_1 I_1}{E_2 I_2}$$

$$\frac{V_1}{V_2} = \frac{v_1 A_1}{v_2 A_2} \quad \textit{let} \quad v_r = \frac{v_1}{v_2} = \frac{A_2 R_1}{A_1 R_2} = \frac{A_2 K_1}{A_1 K_2} \quad \textit{and} \quad v_{yr} = \frac{v_{y1}}{v_{y2}}$$

If $\frac{v_r}{v_{ry}} \geq 1$, then Wall 1 yields first and $V_u = V_{1u} + V_2 = V_{1u}\left(1 + \frac{E_2 I_2}{E_1 I_1}\right)$

Else, Wall 2 yields first and $V_u = V_{2u} + V_1 = V_{2u}\left(1 + \frac{E_1 I_1}{E_2 I_2}\right)$

where:

i =1 for inner wall and 2 for outer wall
V_i = shear force on of i^{th} wall
V_{iu} = ultimate resisting shear force of i^{th} wall
V_u = ultimate resisting shear force of two wall system
K_i = flexural stiffness of walls
A_i = shear area of i^{th} wall
L = equal spans of both walls
v_i = maximum shear stress in i^{th} wall
v_{yi} = yield shear stress of i^{th} wall from Equation 7-7
C_v = shear force constants dependent on boundary conditions - same for each wall

Compression membrane of a double wythe wall between rigid supports is assumed in SBEDS to occur only for the inner wall. It is very unusual in construction to have a double wythe wall system where both walls have rigid supports that can cause compression membrane. The resistance-deflection relationship for the double wall system with compression membrane between rigid supports is based entirely the inner wall response as described in Section 4-1.2.2.2 and the outer wall is always treated as a non-structural wall that only affects the system mass.

7-8 REBOUND RESPONSE

Reinforced masonry walls are assumed to have equal flexural resistances and stiffnesses in both inbound and rebound response in SBEDS because these walls are almost always symmetrically reinforced, usually with a single layer of reinforcement at midthickness. An unreinforced masonry wall with ductile flexural response is also assumed to have equal flexural resistances and stiffnesses in inbound and rebound response. An unreinforced masonry component with a brittle flexure and arching from axial load is not assumed to have any flexural resistance during rebound if it has reached its ultimate resistance during initial inbound response. This implies the wall has cracked all the way through the thickness and no flexural resistance is available during any subsequent response. Flexural response will occur in rebound in SBEDS if there has not been cracking during inbound response. Compression membrane response in rebound does not occur in SBEDS until the component has negative deflection. If there was cracking during inbound response, SBEDS assumes zero resistance until there is negative deflection. Section 4-1.2.3 contains more information on the resistance-deflection relationship during rebound for components with compression membrane response between rigid boundaries and brittle flexural response with axial load arching.

Connections between masonry walls and steel or reinforced concrete framing are sometimes weak in rebound, especially for double wythe walls. These connections may only be sized for suction wind pressures, which can be much less than the ultimate flexural resistance of the wall during rebound. In this case, the walls can collapse outward during rebound response to blast loads. This is especially hazardous for load bearing walls.

This page intentionally blank

CHAPTER 8 - WOOD COMPONENTS

8-1 WOOD COMPONENT TYPES

Even though wood is not typically used for blast resistant design, existing wood buildings can be subject to blast loads. Common wood components include plywood cladding, wall studs and roof purlins, posts and beams, laminated wood sections used for girders and long span main framing members, and roof trusses. Wood studs, beams, and posts are typically cut from a single larger piece of wood with nominal cross sectional dimensions ranging from 2 inches to 12 inches. The actual dimensions of studs and laminated cross sections are 12.5 mm (0.5 in) less than the nominal dimensions, unless they are more than approximately 40 years old. In this case, the actual dimensions may be closer to the nominal dimensions. Glue-laminated or glulam wood cross sections are manufactured by attaching several layers of wood together with structural adhesive. Roof purlins often span between wood trusses, which are manufactured with studs, beams, or laminated cross sections that are attached together to form large triangular trusses. Plywood is typically used as cladding between wall studs and roof purlins in wood buildings It is manufactured from thin laminated panels of wood, where the grain direction of adjacent panels are cross oriented relative to each other so that plywood has relatively equal strength in two perpendicular directions. Plywood typically has thicknesses ranging from 9.5 mm (3/8 in) to 16 mm (5/8 in).

8-2 WOOD MATERIAL PROPERTIES

The most important wood properties affecting response to blast load are wood density, modulus of elasticity, and flexural tension strength. The compression strength of wood is significantly greater than the tension strength so it is unusual for wood building components to be controlled in flexure by compression capacity. Also, shear strength perpendicular to the grain (i.e., perpendicular to the span) almost never controls member load capacity for typical design cases. The connection strength, however, can be critical. Blast analysis almost always focuses on flexural response of wood components because this is the dominant response mode for the critical components (usually studs and purlins) that are most susceptible to blast damage.

Wood properties are affected by many factors including the wood type, grade, size, load duration, and moisture content. The grade is usually based on visual inspection and accounts for the effects of knots, checks, shakes, splits, and slope of grain, which can all decrease strength properties.

Figure 8-1 shows a typical flexural tension stress-strain relationship for wood, which indicates that wood can have a limited amount of plasticity. Numerous national design code bodies and manufacturers associations, including the National Design Specification (NDS) and the International Building Code (IBC), issue tables of wood properties with the flexural tensile strength and modulus of elasticity for various wood types, grades, and common sizes. Tables are available showing both allowable strengths and ultimate strengths, although allowable strength values are more commonly available. The published strength values are intended for loads with a given duration and factors are applied for design loads with shorter or longer durations.

Figure 8-1 Typical Static Stress-Strain Relationship for Wood in Flexure

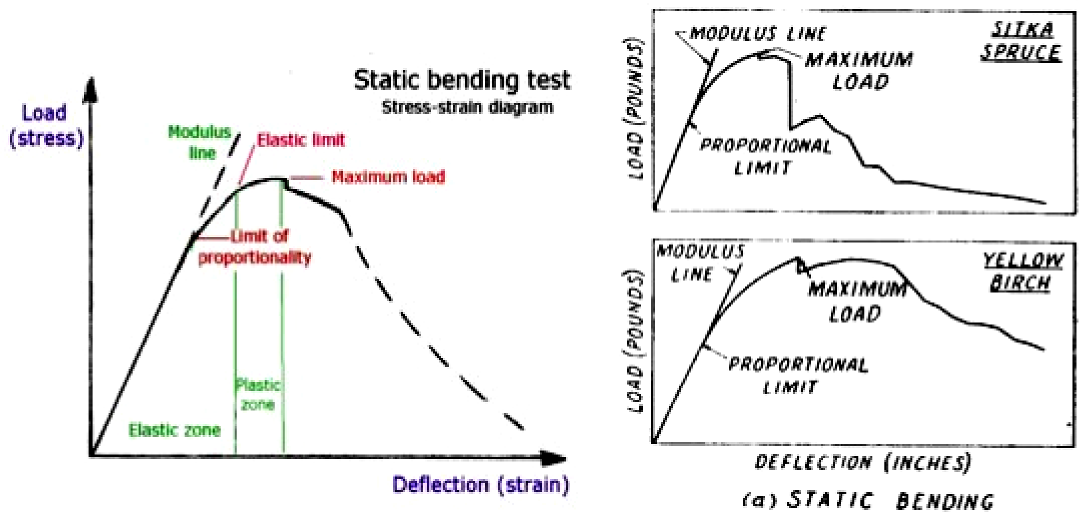

Published allowable design flexural strengths for wood are intended for loads with approximately 10 year durations. A strength increase factor of up to 2.0 can be applied to these strengths for impact loads. The ultimate strength of wood can be assumed equal to 2.5 times the allowable strength, so the available strength to resist stresses from short duration loads is approximately five times greater than the allowable design stress. For example, the measured static failure load was 5 to 10 times greater than the allowable load based on NDS flexural strength information in recent static tests with durations of several minutes on wood stud wall systems at Penn State University (Starr and Krauthammer, 2005). The walls were constructed with 2”x6” No. 2 grade Southern Pine.

The only available testing on the relationship between wood strength and strain-rate is for the crushing strength of wood (DOE/TIC 11268. 1992). This testing indicates that between a slow loading rate, where yielding occurs in approximately 7 minutes (strain-rate of $1e^{-5}$ sec^{-1}), and a very fast loading rate, where yielding occurs in approximately 50 ms (strain-rate of $1e^{-1}$ sec^{-1}), the crushing strength increases by a factor of 1.3 to 1.5. There was no significant change in the modulus of elasticity. Even though this information is for compression, it indicates that high strain-rates caused by blast loads may cause some increase in wood flexural strength. However, no additional strain-rate effect on yield strength, other than the impact factor of 2.0, is typically used for blast analysis.

Table 8-1 and Table 8-2 show allowable static design strengths and moduli of elasticity for various wood species and grades in SBEDS from the NDS. SBEDS calculates a dynamic flexural strength for a user selected wood species and grade by multiplying the allowable bending strength in Table 8-1 by a factor of 5.0 to represent the ultimate strength under blast loading. SBEDS uses the static moduli of elasticity in Table 8-2 without any modifications to calculate the wood beam stiffness.

Table 8-1 Allowable Bending Stresses for Wood Species from NDS

Species	Allowable Bending Strength - psi (MPa)							
	Select Structural	No. 1	No. 2	No. 3	Stud	Construction	Standard	Utility
ALASKA CEDAR	1150 (7.93)	975 (6.72)	800 (5.52)	450 (3.1)	625 (4.31)	900 (6.21)	500 (3.45)	250 (1.72)
ALASKA HEMLOCK	1300 (8.96)	900 (6.21)	825 (5.69)	475 (3.28)	650 (4.48)	950 (6.55)	525 (3.62)	250 (1.72)
ALASKA SPRUCE	1400 (9.65)	950 (6.55)	875 (6.03)	500 (3.45)	675 (4.65)	1000 (6.89)	550 (3.79)	275 (1.9)
ALASKA YELLOW CEDAR	1350 (9.31)	900 (6.21)	800 (5.52)	475 (3.28)	625 (4.31)	925 (6.38)	500 (3.45)	250 (1.72)
ASPEN	875 (6.03)	625 (4.31)	600 (4.14)	350 (2.41)	475 (3.28)	700 (4.83)	375 (2.59)	175 (1.21)
BALDCYPRESS	1200 (8.27)	1000 (6.89)	825 (5.69)	475 (3.28)	650 (4.48)	925 (6.38)	525 (3.62)	250 (1.72)
BEECH-BIRCH-HICKORY	1450 (10)	1050 (7.24)	1000 (6.89)	575 (3.96)	775 (5.34)	1150 (7.93)	650 (4.48)	300 (2.07)
COAST SITKA SPRUCE	1300 (8.96)	925 (6.38)	925 (6.38)	525 (3.62)	725 (5)	1050 (7.24)	600 (4.14)	275 (1.9)
COTTONWOOD	875 (6.03)	625 (4.31)	625 (4.31)	350 (2.41)	475 (3.28)	700 (4.83)	400 (2.76)	175 (1.21)
DOUGLAS FIR-LARCH	1500 (10.34)	1000 (6.89)	900 (6.21)	525 (3.62)	700 (4.83)	1000 (6.89)	575 (3.96)	275 (1.9)
DOUG. FIR-LARCH (NORTH)	1350 (9.31)	850 (5.86)	850 (5.86)	475 (3.28)	650 (4.48)	950 (6.55)	525 (3.62)	250 (1.72)
DOUGLAS FIR-SOUTH	1350 (9.31)	925 (6.38)	850 (5.86)	500 (3.45)	675 (4.65)	975 (6.72)	550 (3.79)	250 (1.72)
EAST. HEMLOCK-BALSAM FIR	1250 (8.62)	775 (5.34)	575 (3.96)	350 (2.41)	450 (3.1)	675 (4.65)	375 (2.59)	175 (1.21)
EAST. HEMLOCK-TAMARACK	1250 (8.62)	775 (5.34)	575 (3.96)	350 (2.41)	450 (3.1)	675 (4.65)	375 (2.59)	175 (1.21)
EASTERN SOFTWOODS	1250 (8.62)	775 (5.34)	575 (3.96)	350 (2.41)	450 (3.1)	675 (4.65)	375 (2.59)	175 (1.21)
EASTERN WHITE PINE	1250 (8.62)	775 (5.34)	575 (3.96)	350 (2.41)	450 (3.1)	675 (4.65)	375 (2.59)	175 (1.21)
HEM-FIR	1400 (9.65)	975 (6.72)	850 (5.86)	500 (3.45)	675 (4.65)	975 (6.72)	550 (3.79)	250 (1.72)
HEM-FIR (NORTH)	1300 (8.96)	1000 (6.89)	1000 (6.89)	575 (3.96)	775 (5.34)	1150 (7.93)	650 (4.48)	300 (2.07)
MIXED MAPLE	1000 (6.89)	725 (5)	700 (4.83)	400 (2.76)	550 (3.79)	800 (5.52)	450 (3.1)	225 (1.55)
MIXED OAK	1150 (7.93)	825 (5.69)	800 (5.52)	475 (3.28)	625 (4.31)	925 (6.38)	525 (3.62)	250 (1.72)
NORTHERN RED OAK	1400 (9.65)	1000 (6.89)	975 (6.72)	550 (3.79)	750 (5.17)	1100 (7.58)	625 (4.31)	300 (2.07)
NORTHERN SPECIES	975 (6.72)	625 (4.31)	625 (4.31)	350 (2.41)	475 (3.28)	700 (4.83)	400 (2.76)	175 (1.21)
NORTHERN WHITE CEDAR	775 (5.34)	575 (3.96)	550 (3.79)	325 (2.24)	425 (2.93)	625 (4.31)	350 (2.41)	175 (1.21)
RED MAPLE	1300 (8.96)	925 (6.38)	900 (6.21)	525 (3.62)	700 (4.83)	1050 (7.24)	575 (3.96)	275 (1.9)
RED OAK	1150 (7.93)	825 (5.69)	800 (5.52)	475 (3.28)	625 (4.31)	925 (6.38)	525 (3.62)	250 (1.72)
Species	**Allowable Bending Strength psi (MPa)**							

	Select Structural	No. 1	No. 2	No. 3	Stud	Construction	Standard	Utility
REDWOOD	1350 (9.31)	975 (6.72)	925 (6.38)	525 (3.62)	575 (3.96)	825 (5.69)	450 (3.1)	225 (1.55)
SOUTHERN PINE	2850 (19.65)	1850 (12.76)	1500 (10.34)	850 (5.86)	850 (5.86)	1100 (7.58)	625 (4.31)	300 (2.07)
SOUTHERN PINE (MIXED)	2050 (14.13)	1450 (10)	1300 (8.96)	750 (5.17)	750 (5.17)	1000 (6.89)	550 (3.79)	275 (1.9)
SPRUCE-PINE-FIR	1250 (8.62)	875 (6.03)	875 (6.03)	500 (3.45)	675 (4.65)	1000 (6.89)	550 (3.79)	275 (1.9)
SPRUCE-PINE-FIR (SOUTH)	1300 (8.96)	875 (6.03)	775 (5.34)	450 (3.1)	600 (4.14)	875 (6.03)	500 (3.45)	225 (1.55)
WESTERN CEDARS	1000 (6.89)	725 (5)	700 (4.83)	400 (2.76)	550 (3.79)	800 (5.52)	450 (3.1)	225 (1.55)
WESTERN WOODS	900 (6.21)	675 (4.65)	675 (4.65)	375 (2.59)	525 (3.62)	775 (5.34)	425 (2.93)	200 (1.38)
WHITE OAK	1200 (8.27)	875 (6.03)	850 (5.86)	475 (3.28)	650 (4.48)	950 (6.55)	525 (3.62)	250 (1.72)
YELLOW CEDAR	1200 (8.27)	800 (5.52)	800 (5.52)	475 (3.28)	625 (4.31)	925 (6.38)	525 (3.62)	250 (1.72)
YELLOW POPLAR	1000 (6.89)	725 (5)	700 (4.83)	400 (2.76)	550 (3.79)	800 (5.52)	450 (3.1)	200 (1.38)

Table 8-2 Modulus of Elasticity for Wood Species from NDS

Species	Modulus of Elasticity - psi (MPa)							
	Select Structural	No. 1	No. 2	No. 3	Stud	Construction	Standard	Utility
ALASKA CEDAR	1.4x10^6 (9653)	1.3x10^6 (8963)	1.2x10^6 (8274)	1.1x10^6 (7584)	1.1x10^6 (7584)	1.2x10^6 (8274)	1.1x10^6 (7584)	1.0x10^6 (6895)
ALASKA HEMLOCK	1.7x10^6 (11721)	1.6x10^6 (11032)	1.5x10^6 (10342)	1.4x10^6 (9653)	1.4x10^6 (9653)	1.4x10^6 (9653)	1.3x10^6 (8963)	1.2x10^6 (8274)
ALASKA SPRUCE	1.6x10^6 (11032)	1.5x10^6 (10342)	1.4x10^6 (9653)	1.3x10^6 (8963)	1.3x10^6 (8963)	1.3x10^6 (8963)	1.2x10^6 (8274)	1.1x10^6 (7584)
ALASKA YELLOW CEDAR	1.5x10^6 (10342)	1.4x10^6 (9653)	1.3x10^6 (8963)	1.2x10^6 (8274)	1.2x10^6 (8274)	1.3x10^6 (8963)	1.1x10^6 (7584)	1.1x10^6 (7584)
ASPEN	1.1x10^6 (7584)	1.1x10^6 (7584)	1.0x10^6 (6895)	0.9x10^6 (6205)	0.9x10^6 (6205)	0.9x10^6 (6205)	0.9x10^6 (6205)	0.8x10^6 (5516)
BALDCYPRESS	1.4x10^6 (9653)	1.4x10^6 (9653)	1.3x10^6 (8963)	1.2x10^6 (8274)	1.2x10^6 (8274)	1.2x10^6 (8274)	1.1x10^6 (7584)	1.0x10^6 (6895)
BEECH-BIRCH-HICKORY	1.7x10^6 (11721)	1.6x10^6 (11032)	1.5x10^6 (10342)	1.3x10^6 (8963)	1.3x10^6 (8963)	1.4x10^6 (9653)	1.3x10^6 (8963)	1.2x10^6 (8274)
COAST SITKA SPRUCE	1.7x10^6 (11721)	1.5x10^6 (10342)	1.5x10^6 (10342)	1.4x10^6 (9653)	1.4x10^6 (9653)	1.4x10^6 (9653)	1.3x10^6 (8963)	1.2x10^6 (8274)
COTTONWOOD	1.2x10^6 (8274)	1.2x10^6 (8274)	1.1x10^6 (7584)	1.0x10^6 (6895)	1.0x10^6 (6895)	1.0x10^6 (6895)	0.9x10^6 (6205)	0.9x10^6 (6205)
DOUGLAS FIR-LARCH	1.9x10^6 (13100)	1.7x10^6 (11721)	1.6x10^6 (11032)	1.4x10^6 (9653)	1.4x10^6 (9653)	1.5x10^6 (10342)	1.4x10^6 (9653)	1.3x10^6 (8963)
DOUG. FIR-LARCH (NORTH)	1.9x10^6 (13100)	1.6x10^6 (11032)	1.6x10^6 (11032)	1.4x10^6 (9653)	1.4x10^6 (9653)	1.5x10^6 (10342)	1.4x10^6 (9653)	1.3x10^6 (8963)
DOUGLAS FIR-SOUTH	1.4x10^6 (9653)	1.3x10^6 (8963)	1.2x10^6 (8274)	1.1x10^6 (7584)	1.1x10^6 (7584)	1.2x10^6 (8274)	1.1x10^6 (7584)	1.0x10^6 (6895)
Species	Modulus of Elasticity - psi (MPa)							

	Select Structural	No. 1	No. 2	No. 3	Stud	Construction	Standard	Utility
EAST. HEMLOCK-BALSAM FIR	1.2×10^6 (8274)	1.1×10^6 (7584)	1.1×10^6 (7584)	0.9×10^6 (6205)	0.9×10^6 (6205)	1.0×10^6 (6895)	0.9×10^6 (6205)	0.8×10^6 (5516)
EAST. HEMLOCK-TAMARACK	1.2×10^6 (8274)	1.1×10^6 (7584)	1.1×10^6 (7584)	0.9×10^6 (6205)	0.9×10^6 (6205)	1.0×10^6 (6895)	0.9×10^6 (6205)	0.8×10^6 (5516)
EASTERN SOFTWOODS	1.2×10^6 (8274)	1.1×10^6 (7584)	1.1×10^6 (7584)	0.9×10^6 (6205)	0.9×10^6 (6205)	1.0×10^6 (6895)	0.9×10^6 (6205)	0.8×10^6 (5516)
EASTERN WHITE PINE	1.2×10^6 (8274)	1.1×10^6 (7584)	1.1×10^6 (7584)	0.9×10^6 (6205)	0.9×10^6 (6205)	1.0×10^6 (6895)	0.9×10^6 (6205)	0.8×10^6 (5516)
HEM-FIR	1.6×10^6 (11032)	1.5×10^6 (10342)	1.3×10^6 (8963)	1.2×10^6 (8274)	1.2×10^6 (8274)	1.3×10^6 (8963)	1.2×10^6 (8274)	1.1×10^6 (7584)
HEM-FIR (NORTH)	1.7×10^6 (11721)	1.6×10^6 (11032)	1.6×10^6 (11032)	1.4×10^6 (9653)	1.4×10^6 (9653)	1.5×10^6 (10342)	1.4×10^6 (9653)	1.3×10^6 (8963)
MIXED MAPLE	1.3×10^6 (8963)	1.2×10^6 (8274)	1.1×10^6 (7584)	1.0×10^6 (6895)	1.0×10^6 (6895)	1.1×10^6 (7584)	1.0×10^6 (6895)	0.9×10^6 (6205)
MIXED OAK	1.1×10^6 (7584)	1.0×10^6 (6895)	0.9×10^6 (6205)	0.8×10^6 (5516)	0.8×10^6 (5516)	0.9×10^6 (6205)	0.8×10^6 (5516)	0.8×10^6 (5516)
NORTHERN RED OAK	1.4×10^6 (9653)	1.4×10^6 (9653)	1.3×10^6 (8963)	1.2×10^6 (8274)	1.2×10^6 (8274)	1.2×10^6 (8274)	1.1×10^6 (7584)	1.0×10^6 (6895)
NORTHERN SPECIES	1.1×10^6 (7584)	1.1×10^6 (7584)	1.1×10^6 (7584)	1.0×10^6 (6895)	1.0×10^6 (6895)	1.0×10^6 (6895)	0.9×10^6 (6205)	0.9×10^6 (6205)
NORTHERN WHITE CEDAR	0.8×10^6 (5516)	0.7×10^6 (4826)	0.7×10^6 (4826)	0.6×10^6 (4137)	0.6×10^6 (4137)	0.7×10^6 (4826)	0.6×10^6 (4137)	0.6×10^6 (4137)
RED MAPLE	1.7×10^6 (11721)	1.6×10^6 (11032)	1.5×10^6 (10342)	1.3×10^6 (8963)	1.3×10^6 (8963)	1.4×10^6 (9653)	1.3×10^6 (8963)	1.2×10^6 (8274)
RED OAK	1.4×10^6 (9653)	1.3×10^6 (8963)	1.2×10^6 (8274)	1.1×10^6 (7584)	1.1×10^6 (7584)	1.2×10^6 (8274)	1.1×10^6 (7584)	1.0×10^6 (6895)
REDWOOD	1.4×10^6 (9653)	1.3×10^6 (8963)	1.2×10^6 (8274)	1.1×10^6 (7584)	0.9×10^6 (6205)	0.9×10^6 (6205)	0.9×10^6 (6205)	0.8×10^6 (5516)
SOUTHERN PINE	1.8×10^6 (12411)	1.7×10^6 (11721)	1.6×10^6 (11032)	1.4×10^6 (9653)	1.4×10^6 (9653)	1.5×10^6(10342)	1.3×10^6 (8963)	1.3×10^6(8963)
SOUTHERN PINE (MIXED)	1.6×10^6 (11032)	1.5×10^6 (10342)	1.4×10^6 (9653)	1.2×10^6 (8274)	1.2×10^6 (8274)	1.3×10^6(8963)	1.2×10^6 (8274)	1.1×10^6(7584)
SPRUCE-PINE-FIR	1.5×10^6 (10342)	1.4×10^6 (9653)	1.4×10^6 (9653)	1.2×10^6 (8274)	1.2×10^6 (8274)	1.3×10^6 (8963)	1.2×10^6 (8274)	1.1×10^6 (7584)
SPRUCE-PINE-FIR (SOUTH)	1.3×10^6 (8963)	1.2×10^6 (8274)	1.1×10^6 (7584)	1.0×10^6 (6895)	1.0×10^6 (6895)	1.0×10^6 (6895)	0.9×10^6 (6205)	0.9×10^6 (6205)
WESTERN CEDARS	1.1×10^6 (7584)	1.0×10^6 (6895)	1.0×10^6 (6895)	0.9×10^6 (6205)	0.9×10^6 (6205)	0.9×10^6 (6205)	0.8×10^6 (5516)	0.8×10^6 (5516)
WESTERN WOODS	1.2×10^6 (8274)	1.1×10^6 (7584)	1.0×10^6 (6895)	0.9×10^6 (6205)	0.9×10^6 (6205)	1.0×10^6 (6895)	0.9×10^6 (6205)	0.8×10^6 (5516)
WHITE OAK	1.1×10^6 (7584)	1.0×10^6 (6895)	0.9×10^6 (6205)	0.8×10^6 (5516)	0.8×10^6 (5516)	0.9×10^6 (6205)	0.8×10^6 (5516)	0.8×10^6 (5516)
YELLOW CEDAR	1.6×10^6 (11032)	1.4×10^6 (9653)	1.4×10^6 (9653)	1.2×10^6 (8274)	1.2×10^6 (8274)	1.3×10^6 (8963)	1.2×10^6 (8274)	1.1×10^6 (7584)
YELLOW POPLAR	1.5×10^6 (10342)	1.4×10^6 (9653)	1.3×10^6 (8963)	1.2×10^6 (8274)	1.2×10^6 (8274)	1.3×10^6 (8963)	1.1×10^6 (7584)	1.1×10^6 (7584)

8-3 SDOF ANALYSIS OF WOOD BUILDING COMPONENTS

Analysis of wood building response to blast load is complicated by the many different types of wood and grades of wood, as well as a lack of data on dynamic flexural properties. Also, wood components often function in more than one capacity in buildings (i.e., walls resisting lateral load and functioning as load bearing and shear walls), which can complicate the analysis. Many fewer blast tests have been performed on wood components than the other materials discussed in this manual. Therefore, there is much less design information and guidance available. It is only possible to summarize available information and make limited recommendations based on this information.

8-3.1 BLAST TESTS ON WOOD BUILDINGS

There have been two relatively large blast test programs on wood buildings and a very limited test series in a shock tube on wood wall components. These tests are discussed from a general standpoint in this section. SDOF analyses related to wood wall tests are discussed in the next section. In the first test series, a number of one and two-story wood houses were tested against very large, far-range charge weights of high explosive simulating nuclear blast loading threats in the 1960s. The test results are summarized in Table 8-3. These buildings were probably stronger than similar modern wood buildings because of different construction practices. There were no overall failures of building lateral load resisting systems in any of the houses even when all the walls had failed, as indicated in Figure 8-2. The windows in these buildings failed, allowing interior blast loads that significantly reduced the net impulse applied on the building walls.

Table 8-3 House Damage from Very Long Duration Blast Loads

House Type	Peak Free-Field Pressure MPa (psi)	Observed Damage
Two-story house and one-story house	11.7 to 13(1.7 to 1.9)	Minimal damage except failed windows and doors
One-story house	18.5 (2.7)	60% damage to roof framing and surface, 20% damage to exterior sheathing and framing
Two-story house and one-story house	34 (5.0)	Total failure

The BAIT (Blast and Airman Injury Tests) test series was conducted in 2001 on SEA Huts, which are small wood buildings with light wood construction and no windows (Marchand, 2002). These huts had 50 mm x 100 mm (2 in x 4 in) wood wall studs and roof purlins supporting 9.5 mm (5/8 in) plywood. The purlins were supported by wood trusses, which were supported by the walls. Blast loads were applied from high explosive charge weights modeling large vehicle bomb threats at typical distances between military outpost boundaries and base housing. These blast loads had much shorter durations than those in the 1960s test series modeling nuclear explosions. Damage to the SEA Huts was characterized by damage and failure of the reflected wall studs at lower blast loads followed by damage and failure of side-on wall studs and roof purlins at higher blast loads. The wood roof truss systems on the SEA Hut tests were not seriously damaged in the tests. Also, there were no overall failures of building lateral load resisting systems, indicating that the wood stud shear walls were able to resist the applied side-on blast loads and shear loads transferred from blastward wood stud walls through the roof diaphragm system.

Figure 8-2 Wood Frame Building After Long Duration Blast Load with 34 KPa (5 psi) Peak Overpressure

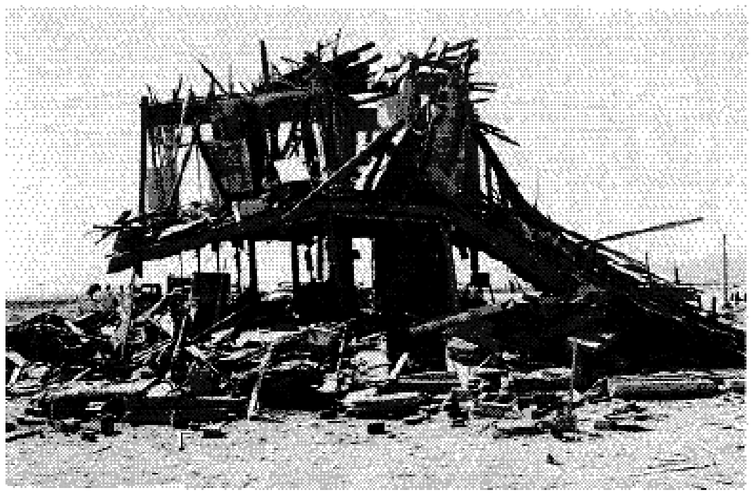

The results from these test series on two different types of wood construction with very long and short duration blast loads both indicate that the wall studs and roof purlins were the weak part of the overall wood building system against blast load. These components typically did not transfer large enough dynamic reaction loads into supporting roof trusses, framing members, or building lateral load resisting system to cause failure of these systems. Overall roof failure occurred when the blast loads were large enough to catastrophically fail load-bearing walls. This information is helpful for SDOF analysis of wood buildings because it indicates that typically such analyses can focus on the wood studs and roof purlins, since damage to these components will tend to control the overall building damage.

8-3.2 SDOF ANALYSES OF WOOD COMPONENTS SUBJECTED TO BLAST LOADS

Limited SDOF-based analysis was performed during development of the CEDAW blast damage assessment methodology for the wood stud walls on the reflected faces of the BAITS SEA Huts and wood stud walls tested in a large shock tube at Wilfred Baker Engineering, Inc. (Oswald, 2005). In both tests, an allowable static flexural yield strength for the wood studs of 1300 psi was assumed based on the published allowable strength for the No. 2 Grade Southern Pine studs used for the shock tube tests. No specific wood type or grade information was available for the BAITS tests. This allowable flexural tension strength was multiplied by 2.5 to calculate an ultimate flexural yield strength and then by 2.0 for short duration loading to obtain a dynamic flexural tension strength of 6500 psi. The dynamic moment capacity was based on this tensile strength and the elastic section modulus of the studs, ignoring any composite action with the wall cladding. Wood studs with observed medium damage in the tests had calculated ductility ratios from the SDOF analysis between 1 and 2. Wood studs that failed had calculated ductility ratios of 3 and greater.

Therefore, the calculated ductility ratios are consistent with the observed damage for a relatively brittle material like wood. This consistency gives credence to the assumed dynamic flexural tensile strength used in the SDOF analyses. A modulus of elasticity of $1.4e^6$ psi and density of 35 lb/ft^2 were also assumed. More details of these analyses are provided in the CEDAW Methodology Report (Oswald, 2005). No SDOF analyses were performed of the wood houses from the first test series discussed in the previous section because fill pressures inside the building complicate the applied net load on the walls.

8-4 DYNAMIC MOMENT CAPACITY OF WOOD COMPONENTS

The dynamic moment capacity of wood components is calculated in SBEDS using Equation 8-1. The dynamic flexural tension strength, f_{dt}, includes any effects from high-strain rate loading. As stated previously, there is no high strain-rate testing available to help define the DIF. Therefore, f_{dt} can be taken as five times the allowable design flexural tensile strength as described in Section 8-2 and 8-3.2. The dynamic moment capacity is based only on the elastic section modulus because wood is not assumed to yield plastically through the cross section due to its limited ductility.

Equation 8-1

$$M_{du} = Sf_{dt}$$

where:

M_{du} = ultimate dynamic moment capacity
f_{dt} = dynamic tensile strength of wood component
S = elastic section modulus ignoring any composite action with attached material

Based on available static and shock tube test data, the section modulus should not be increased to account for composite action with any attached material. Strain measurements in static tests on wood studs in wood wall systems and on 12.5 mm (0.5 in) plywood connected to the studs with nails showed that only limited composite action occurred between the plywood and studs (Starr and Krauthammer, 2005). Much higher strains were measured when the plywood was also attached with adhesive, indicating much more composite response prior to peak load capacity. However, no difference in load capacity was measured between walls where the plywood was only nailed to the studs and where it was nailed and attached with adhesive.

The wood stud walls used for the shock tube tests described in Section 8-3.2 had 12.5 mm (0.5 in) thick plywood cladding nailed on one face or two faces with nails as close as 3 inches on center. The measured peak dynamic reactions were consistent with an ultimate resistance calculated with a moment capacity equal to the section modulus of only the studs and a dynamic yield strength equal to five times the allowable design flexural strength. Also, similar peak dynamic reaction forces were measured when the plywood was cut horizontally at midspan so that it could not contribute to the overall flexural capacity of the wall system and when the cladding was very well nailed to one and two sides of the studs (Oswald, 2005)

8-5 WOOD CONNECTIONS

Wood components can be directly nailed together or attached with many different types of metal straps and plates. Figure 8-3 shows hanger straps that are used with nails to attach wood studs to sill and header boards that form the top and bottom framing for a wood stud wall. The studs can also be directly nailed to the sill and header boards. Main framing members and truss members are almost always attached with metal plates that span across the connected members and are nailed into each member. Allowable load capacity information for connections with hanger straps and metal plates are provided by manufacturers.

Figure 8-3 Wood Stud Hanger Connections

This page intentionally blank

CHAPTER 9 - PRESSURE-IMPULSE AND CHARGE WEIGHT-STANDOFF DIAGRAMS

9-1 PRESSURE-IMPULSE DIAGRAMS

Figure 9-1 shows a pressure-impulse (P-i) curve, which is a curve of points representing the peak positive phase pressure and the positive phase impulse of all blast loads causing a given maximum dynamic deflection to a given component. Typically, P-i curves are based on SDOF analyses of the equivalent spring-mass system for the given component. SBEDS plots several P-i curves on the P-i_Diagram worksheet for maximum deflections, or target deflections, input in terms of a target ductility ratio or support rotation for the component on the Input worksheet. If a target ductility ratio and support rotation are both input, SBEDS will plot the P-i curve based on the smaller target deflection considering both criteria. Note that SBEDS will generate P-i diagrams based on the current values for the SDOF parameters, and other relevant parameters on the Input sheet.

Figure 9-1 Illustration of P-i Diagram For Positive Phase Blast Load Showing Three Regions of Response

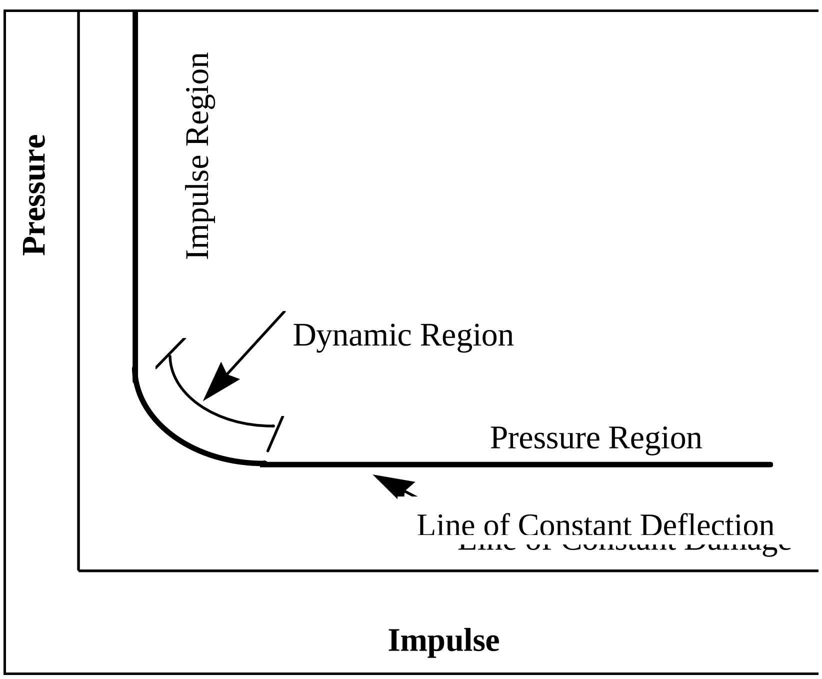

P-i diagrams with up to four P-i curves can be generated in SBEDS for blast loads with positive phase blast load only and blast loads with positive and negative phase blast load. In the case of positive phase blast load only, the blast load histories have a simplified right triangular shape as shown in Figure 2-3. In the case of positive and negative phase blast loads, the blast load histories are calculated with charge weight-standoff combinations and have a shape similar to Equation 2-1. In some cases involving negative phase blast load, the absolute value of the maximum deflection during rebound response can exceed that during inbound response. However, P-i diagrams in SBEDS are always based the inbound maximum deflection.

SBEDS creates the P-i curves by performing repeated SDOF analyses, iterating on the peak pressure or charge weight depending if the P-i diagram blast loads include negative phase blast load or not, until the trial SDOF analysis has a maximum deflection equal to the target maximum deflection within a small tolerance. The peak pressure and impulse of the blast load from this trial SDOF analysis defines a point on the P-i diagram. This process is repeated with a different blast load duration or standoff and the new peak pressure or charge weight causing the target maximum deflection in trial SDOF analyses is determined until sufficient blast load points are created to form a full P-i curve. All maximum deflections calculated within this iteration routine in SBEDS use the same SDOF solver routine used for the Run SDOF function on the Input worksheet. The only exception is that all cases involving charge weight-standoff combinations do not consider any clearing of the blast wave and the blast load is either side-on or fully reflected, depending on user input.

The P-i curve in Figure 9-1 is for the case of positive phase blast load only. It is characterized by three response regions, known as the impulsive, dynamic, and pressure sensitive regions. In the impulsive region, the applied impulse causing the target deflection is constant regardless of the peak pressure. This implies that component response to blast loads in the impulsive region is only sensitive to the impulse in the blast loads. In the pressure region, the applied peak pressure causing the target deflection is constant regardless of the impulse. Component response to blast loads in the pressure region is only sensitive to the peak pressure in the blast loads. In the dynamic region, the target deflection is sensitive to both the peak pressure and the impulse in the applied blast load. As a rule of thumb, a structural component is sensitive only to the impulse in the blast load if its natural period is at least three times greater than the blast load duration (t_d) and a structural component is sensitive only to the peak pressure of the blast load when t_d is at least 10 times greater than the natural period (T_n). The structural component is sensitive to both the peak pressure and impulse when $1/3 < t_d/T_n < 10$. The natural period is defined in Equation 4-22.

9-1.1 P-I DIAGRAMS FOR BLAST LOADS WITH POSITIVE PHASE LOAD ONLY

The P-i diagram in Figure 9-2 from SBEDS shows all the peak pressures and impulses of blast load histories with only positive phase load that cause a given target deflection (i.e., 3.49 inches) for a given component on the Input worksheet. The positive phase blast loads histories are all assumed to have a simplified right triangular shape shown in Figure 2-3. The P-i curves are based on 15 points where the blast load duration ranges from 0.05 to 60 times the natural period of the component. SBEDS iterates on the peak pressure for each duration, calculating the maximum deflection for each trial peak pressure, until the maximum deflection for a given trial peak pressure equals the target maximum deflection within a small tolerance. This peak pressure and the impulse from this peak pressure and the current blast load duration define a point on the P-i diagram. Some error may occur in the pressure region shown in Figure 9-1, which is characterized by long duration blast loads, because small changes in peak pressure can cause relatively large changes in maximum deflection and this can cause convergence problems for the iteration algorithm in SBEDS.

Figure 9-2 P-i Diagram for Positive Phase Blast Load Only

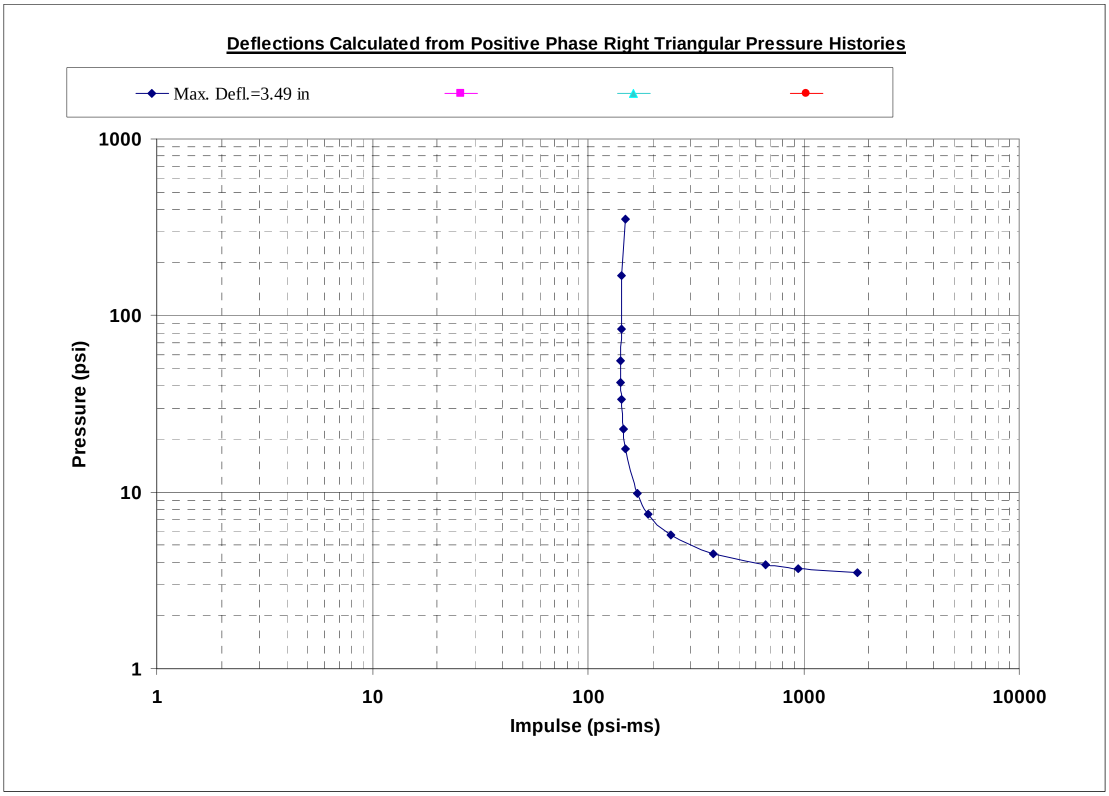

9-1.2 P-I DIAGRAMS FOR BLAST LOADS WITH POSITIVE AND NEGATIVE PHASE LOAD

P-i diagrams in SBEDS can also be based on blast load histories with positive and negative phase blast loads, as shown in Figure 9-3. In this case, the blast load points represent fully reflected blast loads determined for up to twenty-five charge weight-standoff combinations with standoffs starting at 1.5 m (5 ft). For these cases, SBEDS determines each blast load point on the P-i curve based on a standoff and for each standoff iterates on the charge weight, calculating the maximum deflection for the full positive and negative phase blast load from each trial charge weight until the maximum deflection equals the target maximum deflection within a small tolerance. The positive phase peak pressure and positive phase impulse from this trial charge weight-standoff combination define a point on the P-i diagram. The blast load history calculated for all charge weight-standoff combinations has the shape shown in Figure 2-1 and Figure 2-2 if negative phase is included.

No charge-weight standoffs causing a positive phase blast load with an equivalent triangular duration exceeding 60 times the component's natural period are considered since the P-i curve calculations are terminated. Also, the negative phase peak pressure and impulse, which affect the calculated maximum deflection for many of the blast load points on the P-I curve, are not included in the peak pressure or impulse values of the blast load points. The effect of negative phase blast loading is only included implicitly in the P-I curve since larger positive phase blast loads are necessary to cause the target deflection when the they are from blast loads that also include negative phase loading.

Figure 9-3 P-i Diagram for Positive and Negative Phase Blast Load

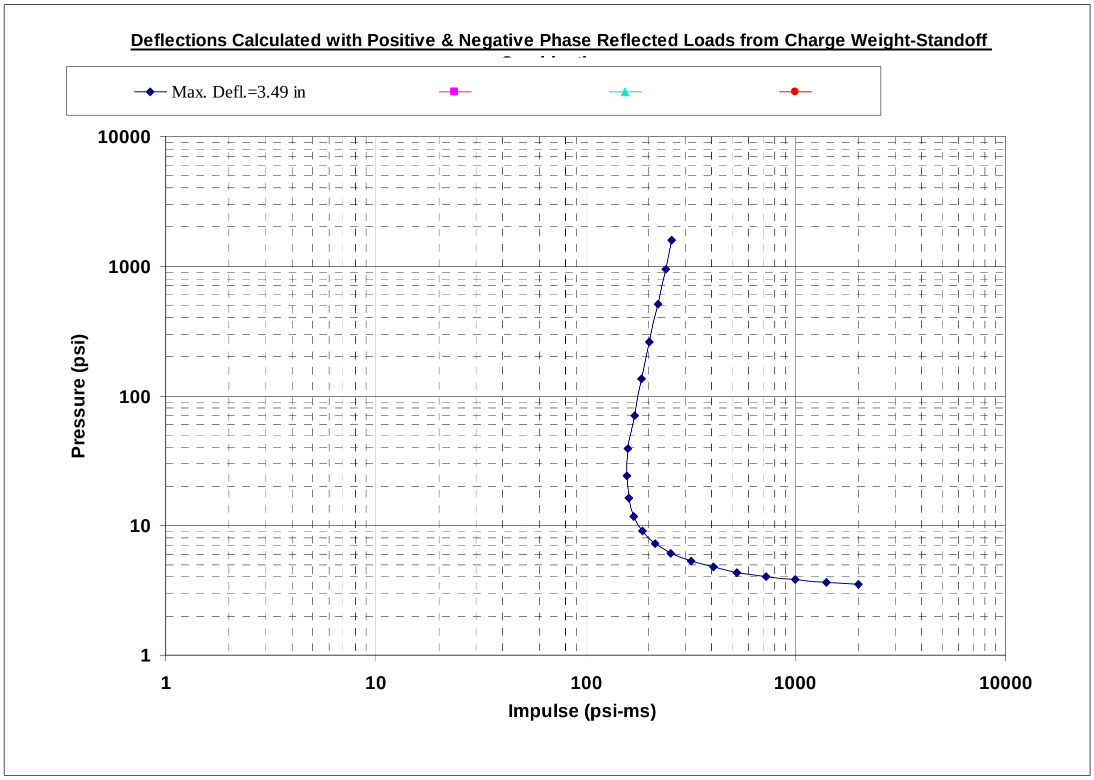

Comparison of Figure 9-2 and Figure 9-3, which were both generated for the same target deflection in the same structural component with positive phase blast load only and with positive and negative blast load, shows that they have the same pressure asymptote, but different blast loads in the dynamic and impulsive region. Blast loads with significantly greater positive phase impulse are required in Figure 9-3 to cause the target deflection in these two regions of the P-i curve when negative phase blast load is included. The negative phase blast load reduces the maximum deflection from a given positive phase blast load if it occurs before the component reaches its maximum deflection, as is the case in the dynamic and impulsive regions of Figure 9-3. Therefore, more positive phase impulse is needed to cause the same deflection when the negative phase blast load is included in the SDOF analysis.

Blast load durations are not shown on P-i curves, but the positive phase duration for any blast load point can be approximated as twice the impulse divided by the peak pressure (this is the exact duration if the blast load has the shape of a right triangle). The points nearer the top of the impulsive region of P-i curves have the shortest durations, so that negative phase blast load affects the component response most for these cases. This causes this P-i curve in Figure 9-3 to curve to the right in the impulsive region. This does not occur in Figure 9-2, which is asymptotic in the impulsive region, because no negative phase blast load is considered. At a short enough duration, P-i curves for blast loads with positive and negative phase blast load will also become asymptotic in the impulsive region because both the positive and negative phase blast load will occur within a time less than one-third of the natural period of the component. However, blast

Methodology Manual TOC

loads with these durations are outside the realm of cases considered in SBEDS if they correspond to standoffs less than 1.5 m.

The negative phase blast load can also occur in-phase with the rebound response of the component for some blast load points on a P-i curve, so that the maximum inbound deflection occurs during the second inbound phase rather than during initial inbound response. In this case, the negative phase blast load increases the component maximum deflection, rather than decreasing it. An example of this is shown in Figure 9-4, where the highlighted blast loads cause the maximum inbound deflections to occur during the second inbound response cycle as shown in Figure 9-5. This case can occur in the dynamic region of P-i diagrams with positive and negative phase blast load, although it is relatively unusual.

Figure 9-4 P-i Diagram with Positive and Negative Phase Blast Load with Points from Maximum Deflection During Second Inbound Response

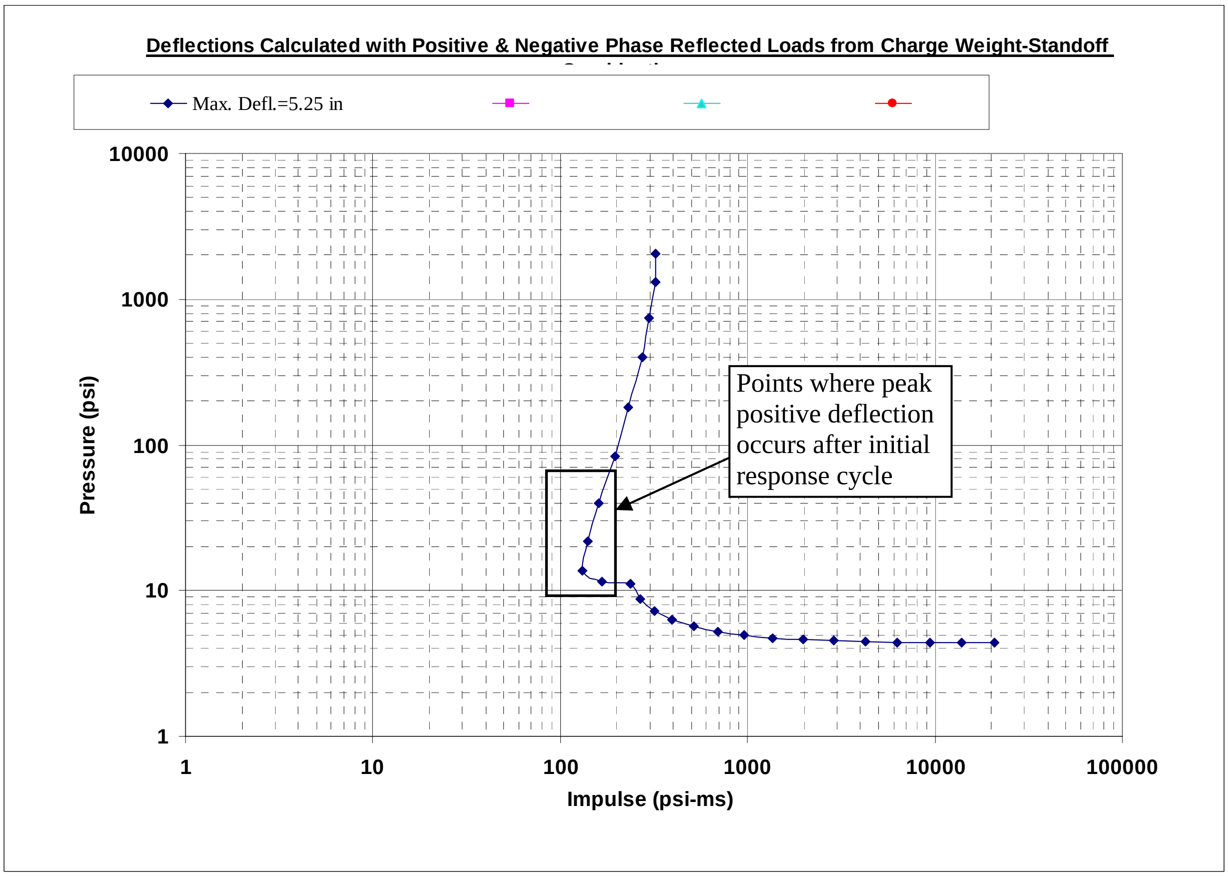

Figure 9-5 Representative SDOF Output for Highlighted Cases in Figure 9-4

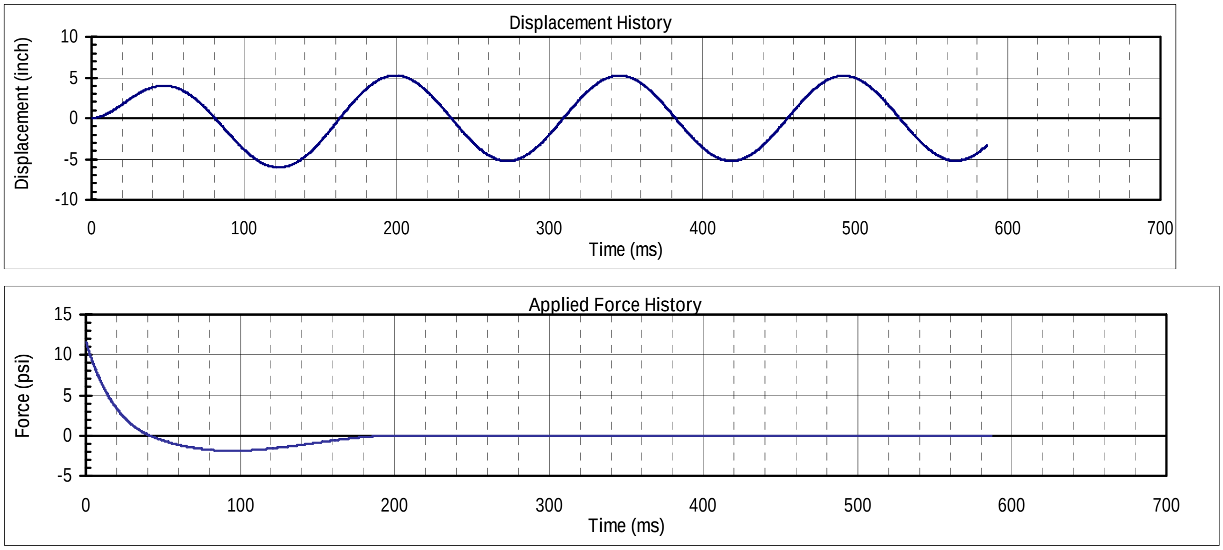

9-2 CHARGE WEIGHT-STANDOFF DIAGRAMS

The charge weight-standoffs used to determine peak pressure and impulse points in Figure 9-3 can be plotted directly as a charge weight-standoff (W-R) diagram, as shown in Figure 9-6. The charge weight-standoff curve in Figure 9-6 shows all charge weight-standoff combinations that cause a given maximum deflection (i.e., 3.49 in) in a given component defined on the Input worksheet in SBEDS up to a user defined maximum charge weight, based on positive and negative phase blast load. If no maximum charge weight is defined, a default value of 226,800 kg (500,000 lb) is used. SBEDS generates charge weight-standoff diagrams for fully reflected and side-on blast loads considering positive phase load only and positive and negative phase blast load. Reflected blast loads do not include any clearing effects. Note that SBEDS will generate W-R diagrams based on the current values for the SDOF parameters, and other relevant parameters on the Input sheet.

The blast load histories for charge weight-standoff combinations with positive phase blast load only have an exponential decay shape, as shown in Figure 2-1, rather than a right triangular shape. Otherwise, SBEDS uses the same iteration process and blast load shapes described previously for P-i diagrams to generate charge weight-standoff diagrams. SBEDS iterates to find charge weights causing the target inbound maximum deflection for standoffs starting at 1.5 m for up to twenty-five charge weight-standoff combinations or until the duration of the equivalent triangular positive phase blast load is greater than 60 times the natural period of the component. Charge weight-standoff curves for positive and negative phase blast load where some charge weight-standoff combinations cause the target maximum inbound deflection during the second response cycle will have a “hump” in the overall shape of the curve, similar to the hump in the P-i curve in Figure 9-4.

9-3 LIMITATIONS OF PRESSURE-IMPULSE AND CHARGE-WEIGHT STANDOFF DIAGRAMS

P-i diagrams and charge-weight standoff diagrams are both determined using very similar algorithms. Since these diagrams are based on SDOF analyses, they are subject to all the limitations of SDOF analyses discussed in Section 4-8. Also, P-i diagrams are only applicable for blast load histories with the assumed shapes discussed previously in this section. For example, P-i diagrams generated in SBEDS are not valid for blast loads with a finite rise time to peak pressure. However, they are conservative for this case (particularly in the pressure region) because the blast loads with an immediate rise to peak pressure used to generate P-i diagrams in SBEDS cause equal or greater response than a blast load with the same peak pressure and impulse and a finite rise time.

Figure 9-6 Charge Weight-Standoff Diagram for Positive and Negative Phase Blast Load

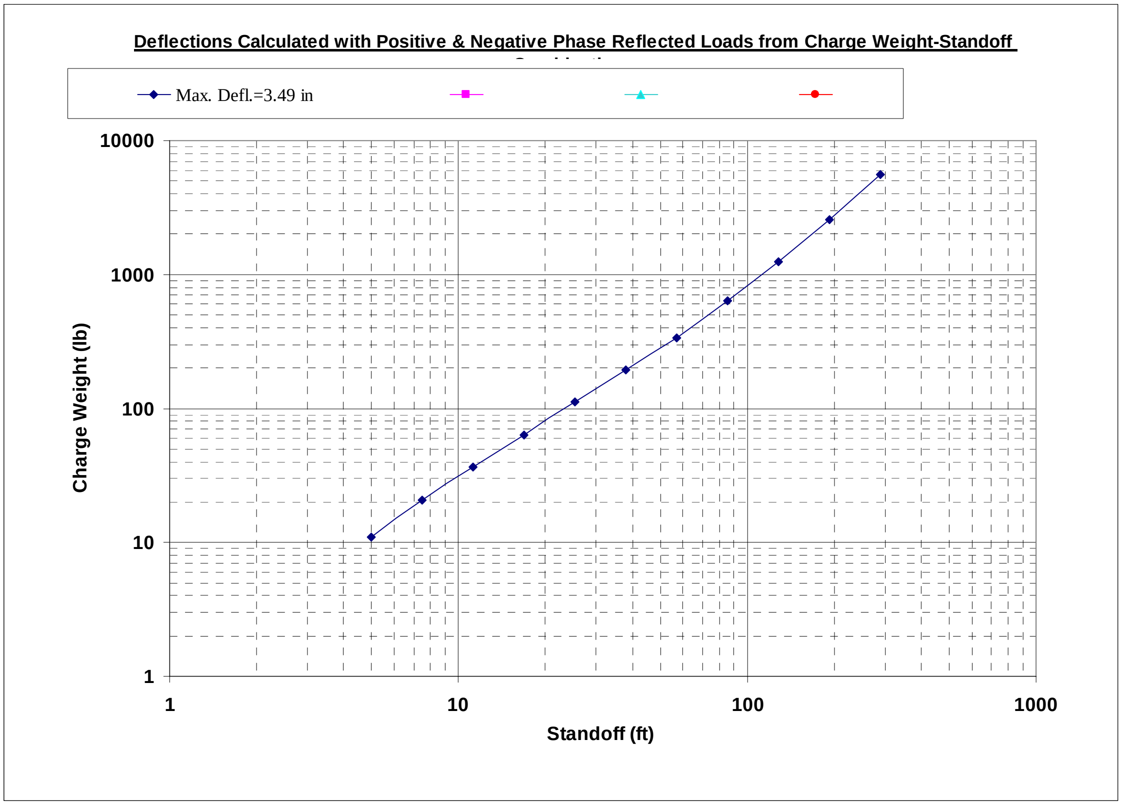

P-i diagrams for positive phase blast load only, which are generated assuming the blast load has the shape of a right triangle, are conservative for positive phase blast loads with an exponential decay to ambient pressures. P-i diagrams for positive and negative phase blast load are only valid for cases where the blast load is calculated from high explosives as described in Chapter 2. They are generated in SBEDS assuming fully reflected blast loads and therefore there may be some inaccuracy if they are applied for cases with side-on blast loads. Charge weight-standoff diagrams can be determined for side-on blast loads, including negative phase load if designated. All charge weight-standoff diagrams for reflected blast loads are fully reflected blast loads without any clearing effects.

Additionally, P-i diagrams and charge-weight standoff diagrams are subject to error from any incorrect convergence in the iteration method in SBEDS to determine the peak pressure or charge weight causing the target deflection. Errors occur when a time step

Methodology Manual TOC

is too small for the SDOF analyses used in the iteration process to reach maximum deflection and when the time step is too large compared to the duration of a positive phase blast load. SBEDS uses logic that is intended to prevent both types of time step problems, but it is not always possible for some blast load points and input components. An error message will be displayed if the time step used in the SDOF analysis to determine a point on the P-i or Charge Weight-Standoff diagrams is less than 10% of the equivalent triangular duration of the blast load. An error message will also be displayed if there is no calculated rebound deflections in the SDOF analysis used to determine a point on the diagrams, indicating that the time step was too small to allow the maximum deflection to be calculated. Convergence error can also occur occasionally when the iteration routine gets stuck oscillating about the target maximum deflection, rather than converging on it. A maximum of twelve iteration cycles is performed for any blast load point, after which iteration is terminated and the last peak pressure or charge weight from the final iteration is used to determine the point on the diagram. A ratio of the actual calculated deflection in the iteration routine to the target deflection is displayed for each blast load point in SBEDS to the right of the plots on the P-i_Diagram worksheet.

Points on a P-i diagram or charge weight-standoff diagram that do not lie along a smooth curve defined by surrounding points may be in error. In these cases, the curve can be smoothed to obtain a corrected curve by ignoring outlying points. Any point on a P-i diagram or charge weight-standoff diagram can be verified by inputting the load corresponding to that point on the Input worksheet for exactly the same component that the diagram was developed for, using the Runs SDOF button to determine the maximum inbound deflection, and comparing it to the target deflection. It is important to use the same type of load (i.e., with or without negative phase load and fully reflected without clearing or side-on for a charge-weight standoff diagram) as specified for the P-i or charge weight-standoff diagram when it was generated.

Charge weight-standoff input should be used on the Input worksheet if the point in question was generated for a charge weight-standoff diagram or for a P-i diagram that included negative phase load. The charge weight and standoff corresponding to all blast load points that include negative phase blast load are shown to the right of the P-i diagram on the *P-i_diagram* worksheet. A manually input pressure-time history with a right triangular shape and a peak pressure and impulse corresponding to the point in question should be used on the Input worksheet if the point in question was generated for a P-i diagram with positive phase blast load only. In all cases, the calculated maximum positive deflection for the blast load on the Input worksheet corresponding to the point of interest should be within approximately five percent of the target deflection for the P-i or charge weight-standoff curve.

Also, charge weight-standoff diagrams for side-on blast load can have an unusual shape at small standoffs caused by the shape of the side-on blast in Figure 2-9 at small scaled standoffs. The side-on impulse remains constant with decreasing scaled standoff, and even decreases somewhat, at scaled standoffs between approximately 0.2 and 1.0 m/kg$^{0.33}$ (0.5 and 1.5 ft/lb$^{0.33}$) rather than increasing monotonically with decreasing standoff as it does for all other scaled standoffs, as shown in Figure 2-9.

Methodology Manual TOC

This can cause a relatively flat region in the charge weight-standoff diagram at small scaled standoffs.

9-4 SCALED PRESSURE-IMPULSE DIAGRAMS

The P-i diagrams plotted in SBEDS apply only for the component on the Input sheet. They are plotted in terms of dimensional blast load terms (i.e., pressure and impulse), and are therefore referred to as dimensional P-i diagrams. More general P-i curves plotted in terms of non-dimensional pressure and impulse terms (i.e., Pbar and Ibar terms) can be developed for constant levels of component response in terms of a non-dimensional response criterion, such as ductility ratio or support rotation, instead of deflection, that are applicable to all components of a given component-type. These are referred to as scaled P-i curves. The non-dimensional Pbar and Ibar terms are scaled peak pressure and impulse values, where the peak pressure and positive phase impulse are divided by component properties generally related to the mass, stiffness, and ultimate resistance of the component. The Pbar and Ibar terms are developed using a conservation of energy approach, where applied energy from blast load is described in terms of work energy to develop the Pbar term, and in terms of kinetic energy to develop the Ibar term, and set equal to the strain energy under a representative resistance-deflection relationship for the component type of interest out to the maximum component deflection (Baker et al, 1983).

Figure 9-7 shows a scaled P-i diagram for reinforced concrete slabs, where the dimensionless Pbar and Ibar terms are defined in Equation 9-1. It has P-i curves showing all Pbar and Ibar values causing support rotations of 2, 5, and 10 degrees in a reinforced concrete slab. The Y factor in Equation 9-1 accounts for the effect of negative phase loading. If the peak positive phase pressure and impulse for a blast load and all the properties of the equivalent SDOF system for the component in Equation 9-1 are known, then Pbar and Ibar terms for the blast loaded component can be calculated and the support rotation of the component can be determined based on the location of the (Pbar, Ibar) point in Figure 9-7 relative the P-i curves for the three support rotations. For example, if the (Pbar, Ibar) point lies halfway between the P-i curves for 2 and 5 degrees of support rotation, then the deflection of the component from the blast load has a 3.5 degree support rotation. This can be verified by a SDOF analysis.

Scaled P-i diagrams, such as that in Figure 9-7, have been developed for many common building types in the CEDAW (Component Explosive Damage Assessment Workbook) methodology developed for the U.S. Army Corps of Engineers (Oswald, 2005). In the first step of the development process, conservation of energy equations that transform the peak pressure and positive phase impulse into the scaled blast load terms Pbar and Ibar, respectively, were developed. The energy equations were based on strain energy from the dominant response modes that affects given component types, including flexure, tension membrane, and arching from axial load, and the non-dimensional response terms that best correlates component response to damage (i.e., ductility ratio or support rotation). Essentially, the Pbar and Ibar terms normalize the applied blast load on a component by properties of that component so that two different components with the same non-dimensional response to separate blast loads lie along the same scaled P-i curve.

Figure 9-7 Scaled P-i Curve-fits vs. Scaled SDOF Points in Terms of Support Rotation for Flexural Response of Reinforced Concrete Slabs

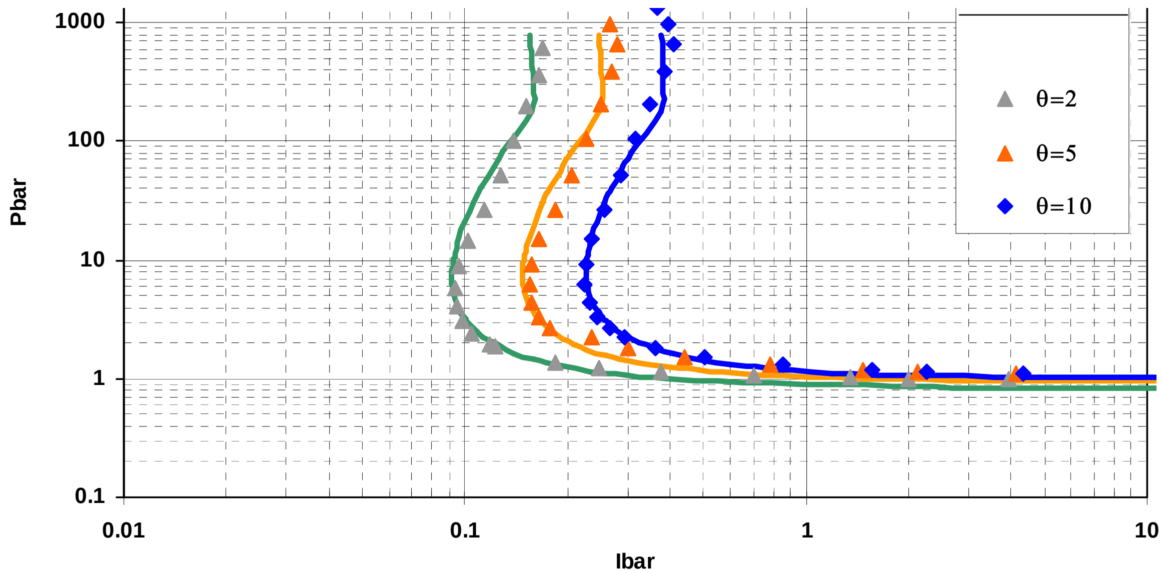

Equation 9-1

$$Pbar = \frac{P}{R_u} \qquad Ibar = i\sqrt{\frac{1}{K_{LM}\, m R_u L}}\,Y \qquad Y = \frac{Pbar^{\left(0.5-0.39\,Rbar^{-0.127}\right)}}{2.59\,Rbar^{0.067}}$$

where:

P = peak positive phase pressure
i = applied positive phase impulse
m = mass of equivalent SDOF system for component
K_{LM} = load-mass factor of equivalent SDOF system for component
R_u = component ultimate flexural resistance
L = component span length
Rbar = R_u/P_a
P_a = atmospheric pressure

After the equations for Pbar and Ibar terms were developed, these terms were used to scale the blast loads with a wide range of durations that all caused a given value of a non-dimensional response parameter in SDOF analyses of a representative component of the given component type. The positive phase peak pressure and impulse from each of these blast loads were divided by properties of the component used in the SDOF analyses to calculate Pbar and Ibar values, which defined points on a P-i diagram that were connected to form a P-i curve for the given value of the nondimensional response parameter. For example, each point along a curve in Figure 9-7 represents a scaled blast load causing the given support rotation (θ) to any reinforced concrete component with a blast load and component properties such that Pbar and Ibar for the blast-loaded component lie on the curve. If the Pbar and Ibar terms are calculated correctly, peak pressures and impulses acting on many different components of the given component type that all cause component response with the same value of the given non-dimensional response parameter for which the Pbar and Ibar terms were developed, can be scaled using the Pbar and Ibar terms and these Pbar and Ibar points will all lie along a single response curve on a scaled P-i diagram.

A scaled P-I diagram can be developed using blast loads either with, or without negative phase blast load. The P-I diagram in Figure 9-7 was developed for blast loads including negative phase. Scaled P-i curves that include the effect of the negative phase blast load have the same basic shape as dimensional P-i curves that include the effect of the negative phase blast load, as discussed in Section 9-1.2 . The inclusion of negative phase must be considered in the development of the Pbar and/or Ibar terms. This effect was included in the Ibar value for CEDAW using a curve-fitting approach to develop a factor, Y, which is applied to the Ibar term. Y is a function of Pbar, and causes the Ibar term to increase at high Pbar values relative to the ultimate resistance of the component, which is the region of the P-i curve affected by negative phase blast load.

The scaled P-i diagrams in CEDAW have P-i curves that define upper and lower bounds to given damage levels. Test data was used to establish the support rotation and ductility ratio values for scaled upper and lower bound P-i curves for each damage level. More information on the development of the scaled P-i curves and the use of test data to establish scaled P-i curves bounding different damage levels for CEDAW is described elsewhere (Oswald, 2005), (Oswald and Nebuda, 2006). Scaled P-i diagrams were also developed to predict blast damage to conventional building components for the Facility and Component Explosive Damage Assessment Program (FACEDAP) computer program, which was developed for the U.S. Army Corps of Engineers in the early 1990’s (Oswald, 1993). However, these scaled P-i diagrams involved empirical modifications to match data, where whole P-i curves were moved from their theoretically derived locations to match available scaled data points. Fortunately, this was not necessary for the CEDAW P-i diagrams due to more carefully developed Pbar and Ibar terms that include strain energy from varying response modes, the inclusion of negative phase loading effects, and the consideration of response in terms of support rotation where applicable.

This page intentionally blank

CHAPTER 10 - REFERENCES

GOVERNMENT PUBLICATIONS:

1. Department of Defense Washington, DC	UFC 3-340-01 Design and Analysis of Hardened Structures to Conventional Weapons Effects 2002
2. Department of Defense Washington, DC	UFC 4-010-01 DoD Minimum Antiterrorism Standards for Buildings 2002
3. Departments of the Army, the Navy and the Air Force	Army Technical Manual TM 5-1300, Department of the Navy Publication NAVFAC P-397, Department of the Air Force Manual AFM 88-22, Structures to Resist the Effects of Accidental Explosions, November 1990
4. Department of Defense Washington, DC	UFC 4-012-03 Design of Buildings to Resist Progressive Collapse 2003
5. U.S. General Services Administration (GSA)	Progressive Collapse Analysis and Design Guidelines for New Federal Office Buildings and Major Modernization Projects June 2003
6. U.S. Army Corps of Engineers, Protective Design Center	PDC-TR 06-08 Rev 1 Single Degree of Freedom Structural Response Limits for Antiterrorism Design, January 2008.

NON-GOVERNMENT PUBLICATIONS:

1. American Concrete Institute P.O. Box 9094 Farmington Hills, MI 48333-9094	ACI 318-02, Building Code Requirements for Structural Concrete 2002
2. American Concrete Institute P.O. Box 9094	ACI 530-02 Building Code Requirements for Masonry Structures

	Farmington Hills, MI 48333-9094	2002
3.	American Institute of Steel Construction One E. Wacker Dr., Suite 3100 Chicago, IL 60601-2000	AISC Manual of Steel Construction, Load and Resistance Factor Design (LRFD) 2001
4.	American Iron and Steel Institute 1101 Seventeenth Street NW Suite 1300 Washington, DC 20036-4700	AISI Standard North American Specification for the Design of Cold-Formed Steel Structural Members 2002
5.	The Aluminum Association 900 19th Street, N.W. Washington, DC 20006	Aluminum Standards and Data 1993
6.	American Society of Civil Engineers 345 East 47th Street New York, NY 10017	Design of Blast Resistant Buildings for Petrochemical Facilities 1997
9.	U.S. Department of Energy Albuquerque Operations Office	A Manual for the Prediction of Blast and Fragment Loadings on Structures, DOE/TIC 11268, July 1992

REFERENCED PAPERS AND JOURNAL ARTICLES

Baker, W. E., Cox, P. A., Westine, P. S., Kulesz, J. J., and Strehlow, R. A., *Explosion Hazards and Evaluation*, Elsevier Scientific Publishing Company, New York, NY, ISBN 0-444-42094-0, 1983.

Britt, J. R., Ranta, D.E., and Joachim, C.E., "BLASTX Code, Version 4.2, User's Manual", Report ERDC/GSL TR-01-2 Distributed by U.S Army Engineer Research and Development Center, Vicksburg, MS, March, 2001.

Coltharp, D.R., Simmons, L., and Bogosian, D.D., “Blast Response Evaluation of a Lightweight Steel Roof,” Proceedings of the 9th International Symposium on Interaction of the Effects of Munitions with Structures, Berlin-Strausberg, Federal Republic of Germany, May, 1999.

ConWep Version 2.1.0.3, Developed by USAE Engineering and Development Center ,Geotechnical/Structures Laboratory (Contact: David Hyde), Vicksburg, MS.

Granstrom, S.A., “Loading Characteristics of Air Blasts from Detonating Charges,” Report No. 100, Transactions of the Royal Institute of Technology, Stockholm, Sweden, 1956.

Hamid, A.A. and Drysdale, R.G., “Flexural Tension Strength of Concrete Block Masonry,” Journal of Structural Engineering, Vol. 144, No. 1, January, 1988.

Hamid, A.A. Chia-Calabria, C., and Harris, H.G., “*Flexural Behaviour of Joint Reinforced Block Masonry Wall*,” ACI Structural Journal, January-February 1992.

Heeringa, R.L. and McLean, D. I, “*Ultimate Strength Flexural Behaviour of Reinforced Concrete Masonry Walls*,” The Masonry Society Journal, July-December 1989.

Ketchum, D.E., Oswald, C.J., and Clutter, J.K, “The Applicability of Cr_{α} Blast Pressure Estimates to Structural Analysis,” Proceedings from the 28th DDESB Seminar, Orlando, FL, August, 1998.

Thomas, J.T., Geng, J., and Hallgarth, A.D. “Evaluation of Door Blast Shields,” Proceedings from the 31rst DDESB Seminar, San Antonio, TX, August, 2004.

Coltharp, D.R. and Mosher, R. L., “Blast Loading of a Full-Scale, Five-Story Building,” Proceedings of the 9th International Symposium on Interaction of the Effects of Munitions with Structures, Berlin-Strausberg, Federal Republic of Germany, May 1999.

Marchand, K. A., “*BAIT, BASS & RODS Testing Results,*” Prepared for the USAF Force Protection Battlelab by Applied Research Associates, Report within 12-CD set issued by The Technical Support Working Group (TSWG) and Defense Threat Reduction Agency (DTRA), April, 2002.

Morison, C., "Dynamic Response of Walls and Slabs by Single-degree-of-freedom Analysis - A Critical Review and Revision", Intl. J. Imp. Engrg. 32 (2006) 1214-1247.

Needam, C.E., and Witttwer, L.A., “Low Altitude Multiple Burst Model, S-Cubed Report No. 84-6402, 1977.

Oswald, C.J., "Facility And Component Explosive Damage Assessment Program (FACEDAP) User's Manual," Prepared by Southwest Research Institute for the Department of the Army, Corps of Engineers, Omaha District, CEMRO-ED-ST, Contract No. DACA 45-91-D-0019, April, 1993.

Oswald, C.J., " Component Explosive Damage Assessment Workbook (CEDAW)," Prepared by Baker Engineering and Risk Consultants for the U.S.

Army Corps of Engineers Protective Design Center, Contract No. DACA45-01-D-0007-0013, May, 2005.

Oswald, C.J., Holgado, D., "Shock Tube Testing on Reinforced Masonry Walls," Prepared for Protective Design Center, U.S. Army Corps of Engineers, Omaha District by Wilfred Baker Engineering, Inc., WBE Report No. 0724-001, August, 2004.

Oswald, C.J. and Nebuda, D, "SBEDS (Single degree of freedom Blast Effects Design Spreadsheets)," Proceedings from the 31st DoD Explosives Safety Seminar, San Antonio, Texas, August, 2004.

Park and Gamble, *Reinforced Concrete Slabs*, John Wiley and Sons, New York, NY, 2000.

Polcyn, Michael A., Oswald, Charles J., and Conrath, Edward J., "Response Limits for Masonry and Cold-Formed Steel Structural Components," presented at the Thirty-First United States Department of Defense Explosives Safety Seminar, August, 2004.

Salim, H.A., Dinan, R., Kiger, S.A., Townsend, P.T., and Shull, J., "Blast-Retrofit Wall Systems Using Cold-Formed Steel Studs," 16th ASCE Engineering Mechanics Conference, University of Washington, Seattle, July 16-18, 2003.

Tedesco, J.W., McDougal, W.G., and Ross, C.A., *Structural Dynamics,* Published by Addison Wesley, Menlo Park, CA, 1999.

Uniform Building Code (UBC), Published by the International Conference of Building Officials, Whittier, CA, 1997.

Wesevich, J.W., Oswald, C. J., Edel, M.T., Lowak, M. J., Alaoui, S. S., "Compile and Enhance Blast Related CMU Wall Test Database (CMUDS)," Prepared for the Office of Special Technology by Baker Engineering and Risk Consultants, Inc., Contract No. 41756-00-C-0900, September 6, 2002.

Starr, C. M., and Krauthammer, T., "Evaluation of Wood Framed Structures subjected to Static and Dynamic Pressure Loads," Prepared by The Protective Technology Center at Pennsylvania State University for the Protective Design Center, U.S. Army Corps of Engineers, Omaha District, April, 2005.

\\

This page intentionally blank

DISTRIBUTION STATEMENT A: Approved for Public Release; Distribution is unlimited.

Methodology Manual TOC